Development of new late transition metal catalysts for the oligomerisation of ethene

A thesis submitted to the

University of Cape Town

In partial fulfillment of the requirements for the degree of

Doctor of Philosophy

By

Matthew James Overett

Department of Chemistry

University of Cape Town

Rondebosch, 7701,

Cape Town, South Africa

May 2003

Development of new late transition metal catalysts for the oligomerisation of ethene

Matthew James Overett

University of Cape Town

May 2003

To Rosalie

whose presence was my inspiration

whose absence was my motivation

and who makes the future smile

Abstract

The oligomerisation of ethene to linear 1-alkenes is an important industrial process. The recent discovery of iron and cobalt bisiminopyridyl and nickel and palladium α-diimine catalysts for the polymerisation and oligomerisation of 1-alkenes has stimulated interest in the use of late transition metals as catalysts for these processes.

An investigation of the chemistry of *cis*-$Os(CO)_4Me_2$ was carried out. *fac*-$Os(CO)_3(NCMe)Me_2$ was prepared, and its reactions with monodentate and bidentate ligands as well as CPh_3PF_6 have been explored. The reactions of *fac*-$Os(CO)_3(NCMe)Me_2$ with the bidentate ligands L^L (L^L = 2,2'-bipyridyl, bis(diphenylphosphino)methane and bis(diphenylphosphino)ethane) give the novel alkyl, acyl osmium compounds $Os(CO)_2(L^L)(COMe)Me$ in good yield, and the X-ray crystal structure of $Os(CO)_2$(dppm)(COMe)Me (dppm = bis(diphenylphosphino)methane) has been determined. Treatment of *fac*-$Os(CO)_3(NCMe)Me_2$ with CPh_3PF_6 results in the abstraction of a methyl group. The resulting 16-electron cationic complex $[Os(CO)_3(NCMe)Me]PF_6$ is unstable and decomposes immediately. However this complex may be trapped *in situ* by MeCN to give the 18-electron species $[Os(CO)_3(NCMe)_2Me]PF_6$, which has been isolated and characterised. The isoelectronic alkyl ethene complex $[Os(CO)_3(NCMe)(CH_2{=}CH_2)Me]PF_6$ could be a model for a catalytic intermediate in the oligomerisation of ethene by iron bisiminopyridyl complexes; however the synthesis of this compound by the same route was unsuccessful. Reactions explored in this investigation, such as ligand substitution, decarbonylation, alkyl migration onto carbonyl and alkyl abstraction, are of fundamental importance in organometallic chemistry and homogeneous catalysis.

The use of carbosilane dendrimers and dendritic wedges in homogeneous catalysis has been the subject of much study. To this end, a series of novel carbosilane dendritic wedges (generation 0 to 2) with bromobutyl core functionality has been prepared, and the reactivity of these compounds investigated. A series of carbosilane dendrimers (generation 1 to 3) with 4, 12 and 36 terminal bromobutyl groups has also been prepared, and the reactivity of the dendrimers investigated. These dendrimers may be synthetically useful, as the reactivity of their terminal groups will likely be greater than that of previously reported (chloromethyl)dimethylsilyl functionalised dendrimers, in which the silicon deactivates the adjacent chloromethyl for nucleophilic reactions.

A series of bisiminopyridyl iron complexes (fig A) with substitution in the *para* position (R_3) of the ligands' aryl groups has been prepared. Previous research on this class of ethene oligomerisation/polymerisation catalysts has focused on substitution in the *ortho* position (R_1, R_2) , which has been shown to have a profound impact on catalytic activity and the molecular weight of the products. Complexes with substitution by dendritic

wedges, including both poly(benzylphenylether) (generation 0, 1 and 2) and carbosilane (generation 0 and 1) wedges, and by electron donating (OEt, Me) and electron withdrawing (Br, NO_2) groups have been prepared.

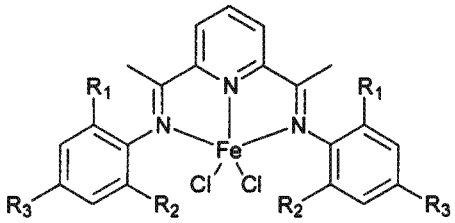

R_1, R_2 = Me, H
R_3 = H, OR_{wedge}, OEt, Me, Br, NO_2
(R_{wedge} = generation 0, 1, 2 poly(benzylphenylether) wedge
generation 0, 1 carbosilane wedge)

Fig. A: New para-substituted bisiminopyridyl iron complexes

Ethene oligomerisation experiments have been carried out. It was found that most of the new *para*-substituted bisiminopyridyl complexes were active oligomerisation catalysts when activated with MAO. Substitution by poly(benzylphenylether) dendritic wedges increases both the propagation constant, α, and the catalytic activity compared with an unsubstituted literature catalyst (R_1 = Me, R_2, R_3 = H). The increased α-value is ascribed to the influence of the ether linkage between the aryl ring and the wedge, and does not appear to be dependent on the size of the wedge. The increased activity is tentatively ascribed to intermolecular interactions between the attached wedges and either the catalytic centre or the aluminium co-catalyst. This is supported by the unexpected observation that addition of two equivalents of an unattached first generation poly(benzylphenylether) dendritic wedge as a co-catalyst with the literature iron catalyst results in an increase in activity of close to 100%.

Substitution of bisiminopyridyl catalysts with more electron withdrawing groups in the *para* position results in an increase in catalytic activity but not α. The observed turnover numbers increase approximately linearly with increased σ_p, the Hammett parameter for the substituent. *Para* substitution by NO_2 increased the activity by almost 50% relative to the literature catalyst. The exception to this trend occurred with the ethoxy substituted complex, for which the activity was higher than expected. This is ascribed to Lewis acid-base interactions between the ethoxy group and the aluminium co-catalyst, which reduce the electron donating ability of the ethoxy substituent.

List of abbreviations

bipy	bipyridyl
Bu (^{n}Bu) (^{t}Bu)	butyl (normal butyl) (tertiary butyl)
cs	carbosilane
COD	1,5-cyclooctadiene
Cp	cyclopentadienyl (η-C_5H_5)
cs	carbosilane
dppe	bis(diphenylphosphino)ethane
dppm	bis(diphenylphosphino)methane
dppp	bis(diphenylphosphino)propane
EI	electron impact
EPR	electron paramagnetic resonance
Et	ethyl
FAB	fast atom bombardment
GC	gas chromatography
IR	infrared
M^+	molecular ion
MAO	methylaluminoxane –$(AlMeO)_n$- in toluene
Me	methyl
m.p.	melting point
m/z	mass to charge ratio (mass spectrometry)
NMR	nuclear magnetic resonance
pbpe	poly(benzylphenylether)
Ph	phenyl
^{i}Pr	isopropyl
R	general alkyl group
R_f	ratio of movement of solute to solvent in TLC
SHOP	Shell Higher Olefin Process
tetraglyme	tetraethylene glycol dimethyl ether
THF	tetrahydrofuran
TLC	thin layer chromatography
TON	turnover number (moles of substrate reacted per mole of catalyst per hour)
TMEDA	N,N,N',N'-tetramethylethylenediamine

Abbreviations used in the reporting of NMR data

(italics in a molecular formula indicates the atom or group assigned to the signal under discussion)

Ar	aryl
d	doublet
dd	doublet of doublets
^{n}J(XY)	coupling constant between atoms X and Y over n bonds
m	multiplet
ppm	parts per million
py	pyridyl
q	quartet
qn	quintet
t	triplet
td	triplet of doublets

Table of Contents

Chapter 1:

A review on late transition metal cationic oligomerisation and polymerisation catalysts

1.1 Industrial importance of alkene polymerisation and oligomerisation processes

Since the early discoveries by Ziegler[1] and Natta[2] of the polymerisations of ethene and propene, the polymerisation of 1-alkenes has developed into a vast industry, with worldwide production of more than 70 million tons per year.[3] Polymers are mainly produced by heterogeneous titanium-based Ziegler catalysts or chromium-based catalysts (e.g. the Philips process)[4], although the older free radical process is still utilised industrially.[5] In 40 years of development, these catalytic processes have become highly efficient, both in activity and stereocontrol of polypropenes and higher poly(alkenes).[6]

Oligomerisation of ethene to produce linear 1-alkenes in the C_6- C_{20+} range is also an important industrial process. These higher alkenes have a wide range of applications including the manufacture of detergents, as fuel additives for enhancing octane number and as co-monomers in polymerisation processes.[7,8] The Shell Higher Olefin Process (SHOP) and Dimersol® processes are the most important examples of industrial production of alkenes by oligomerisation of ethene.[7]

1.2 Other classes of homogeneous catalysts

Although they do not fall under the subject of this review, two classes of homogeneous catalysts must be mentioned in passing, as they relate to the development of the new cationic late transition metal catalysts here reviewed. The discovery that early transition metal metallocenes could polymerise 1-alkenes when co-catalysed by partially hydrolysed aluminium alkyls such as methylaluminoxane (MAO) lead to an explosion of research in this field.[4] Of particular significance here is that the mechanism developed for metallocene catalysts and the use of co-catalysts such as MAO are equally important in the cationic late transition metal catalysts which are the subject of this review. The accepted mechanism involves formation of a cationic, coordinatively unsaturated, electron deficient catalytic centre with a metal alkyl bond, and propagation proceeds by successive coordinations of alkene to the metal and insertions into the metal alkyl bond. The exact role of MAO is still not clearly established. MAO is an ill-defined polymeric substance with approximate formulation $-[MeAlO]_n-$, and it is generally believed that it both alkylates the catalytic centre and abstracts an alkyl group to give the cationic coordinatively unsaturated active catalyst, with a poorly defined bulky counterion [MAO-alkyl]$^-$ (Fig. 1-1).[4]

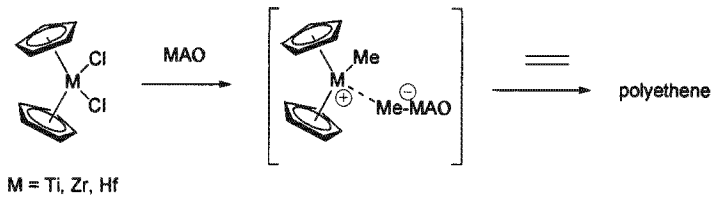

Fig. 1-1: Activation of a group 4 metallocene by MAO to give an active catalyst for polymerising ethene

The other class of homogeneous catalysts worthy of comment are the neutral late transition metal catalysts for the oligomerisation of ethene to higher alkenes. The oligomers are produced with a Schultz-Flory distribution of chain length.[9] Nickel complexes with chelating P,O ligands form the basis of the SHOP process (Fig.1-2).[8] Very high linearity (up to 99%) and selectivity to 1-alkenes (>95%) can be achieved, and the reaction may be tuned by modifications of the chelate P,O ligand and the phosphine ancillary ligand.[8] The mechanism again involves coordination of ethene to the metal centre and insertion into the metal-carbon bond. As is typical with late transition metals[3], chain transfer by β-hydride elimination is competitive with propagation by insertion, and this determines the selectivity to oligomers rather than polymers.

Fig. 1-2: A SHOP-type catalyst for the oligomerisation of ethene to linear 1-alkenes

1.3 Initial reports: polymerisation by late transition metal α-diimine and bisiminopyridyl catalysts

Because late transition metals generally exhibit lower rates of alkene insertion relative to β-hydride elimination than early transition metals, it was thought that late transition metals were unsuited to the polymerisation of alkenes.[3] Until the mid 1990's, few reports of late transition metal polymerisation catalysts had been published.

The breakthrough came with the parallel discoveries by Brookhart and Gibson of nickel and palladium systems with α-diimine ligands and iron and cobalt systems with bisiminopyridyl ligands. For example, in Brookhart's earliest report, the complex $[N_2MMe(OEt_2)]^+BAr'_4^-$ (N_2 = α-diimine ligand; M = Ni, Pd; Ar' = 3,5-$C_6H_3(CF_3)_2$) was prepared by treatment of N_2MMe_2 with $H^+(OEt_2)_2BAr'_4^-$ and was found to be highly active for the polymerisation of ethene and other 1-alkenes (propene and 1-hexene) (Fig. 1-3).[10] The key feature responsible for the high molecular weight products was reported to be the bulky *ortho* substituents on the aryl rings. The palladium derived polymers are highly branched and amorphous, whereas the nickel

catalysts give polymers with low to moderate branching by mainly methyl groups. Mechanistic studies were carried out by low temperature NMR (see section 1.6).

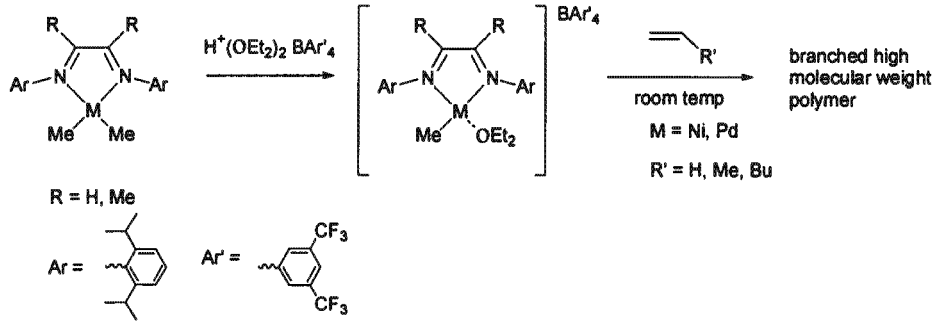

Fig. 1-3: Alkene polymerisation and mechanistic studies with Ni and Pd α-diimine complexes

Active catalysts may be generated more conveniently *in situ* by treatment of the corresponding N_2NiBr_2 complexes with MAO (Fig. 1-4), and the resulting systems achieve polymerisation activity comparable with early transition metal metallocene catalysts.[10]

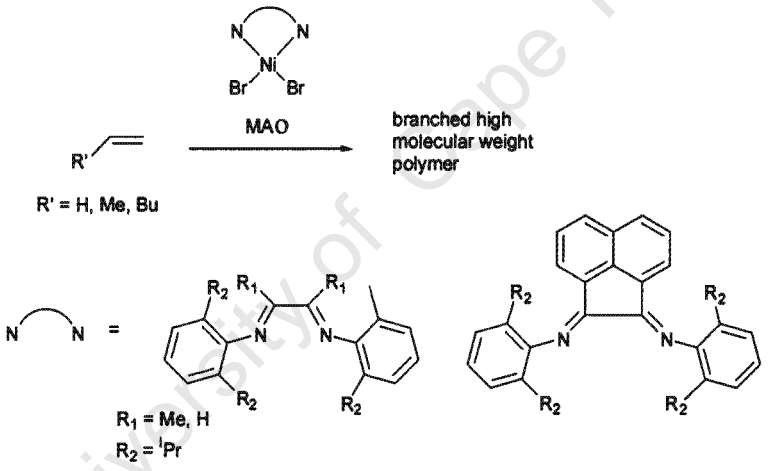

Fig. 1-4: Polymerisation of 1-alkenes by nickel α-diimine complexes / MAO

The branched polymers formed in this new catalytic process are of industrial significance, as branched polymers are typically produced by a co-polymerisation of ethene and 1-alkenes. The new system achieves a similar result with a single monomer.

A similar catalytic system based on iron and cobalt bisiminopyridyl complexes was independently reported by Gibson[11,12] and Brookhart[13] in 1998. The active species is generated *in situ* by using MAO as a co-catalyst, and the resulting activities for the polymerisation of ethene and other 1-alkenes are comparable with metallocene catalysts (Fig. 1-5). The polyethene formed is highly linear and has properties similar to commercially available high density polyethene.[14] The average molecular weight is dependent on the ligand (bulkier *ortho* substituents on the aryl rings, R in Fig. 1-5, give higher molecular weights), on the metal (iron gives higher molecular weights than cobalt) and on the relative concentration of MAO (greater

Al:catalyst ratios lead to bimodal molecular weight distributions and lower average molecular weights).[12,13] The catalytic activity is dependent on ethene pressure for the iron systems. Under conditions where a unimodal distribution of molecular weight polymer was obtained, the polymer yield is linearly dependent on ethene pressure.[12] The iron catalytic activities are in general an order of magnitude greater than the cobalt analogues.[13] The ketimine catalysts (R' = Me) are more active than the equivalent aldimine catalysts (R' = H).[12] Fe(III) complexes (complexes of $FeCl_3$) appeared to give similar catalytic results to the Fe(II) complexes.[12] An increase in reaction temperature (from 35°C to 70°C) reduces both the activity of the catalyst and the molecular weight of the polymeric product.[12] End group analysis of the polymers produced from the iron systems indicated both saturated and unsaturated functionality, suggesting that several chain transfer mechanisms are in operation. The cobalt systems appeared to give exclusively unsaturated polymer end groups.

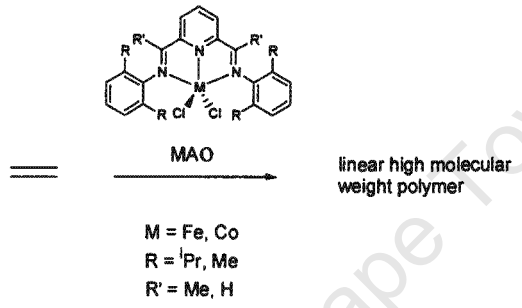

Fig. 1-5: Polymerisation of ethene by iron and cobalt bisiminopyridyl complexes / MAO

1.4 Initial reports: oligomerisation

Following the reports of late transition metal catalysts for the polymerisation of 1-alkenes, in which the presence of two bulky *ortho* substituents on the ligand aryl rings mediates the high polymer molecular weights, it was subsequently reported that similar complexes with a single *ortho* alkyl substituent on the aryl ring are efficient catalysts for the oligomerisation of ethene.[15-17]

Nickel α-diimine complexes with one or no *ortho* aryl substituents were active for oligomerisation of ethene to $C_4 - C_{20+}$ alkenes when activated by MAO (Fig. 1-6).[15,16] The activities were reported to be an order of magnitude greater than neutral SHOP type catalysts.[16]

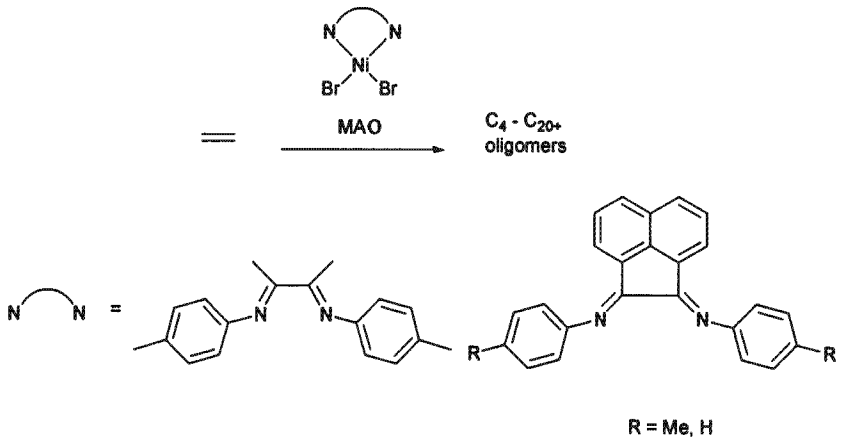

Fig. 1-6: Oligomerisation of ethene by nickel α-diimine complexes / MAO

A Schultz-Flory distribution[9] of oligomers was observed. This means that the rate of chain propagation relative to chain transfer remains constant, which may be represented by a propagation constant, α, expressed as:

$$\alpha = \frac{\text{rate of propagation}}{\text{rate of propagation} + \text{rate of chain transfer}} = \frac{\text{moles of } C_{n+2}}{\text{moles of } C_n}$$

A larger α value thus leads to higher molecular weight oligomers.

The oligomers produced were primarily linear 1-alkenes, with a small amount of 2-alkenes also present as a result of β-hydride elimination of the alkyl chain and reverse reinsertion.[15] After long reaction times, small amounts of branched products were observed due to reincorporation of lower oligomers. An increase in ethene pressure results in higher α values, greater selectivity to 1-alkenes (chain transfer, but not chain isomerisation, being dependent on monomer concentration) and higher activities (up to 30 atmospheres; at greater pressures, a decrease in activity is observed).[15] An increase in temperature causes a decrease in both 1-alkene selectivity and α values. These effects can possibly be assigned to decreased solubility of ethene in the solvent at higher temperature. Higher activities were observed at higher temperatures, although this is offset by significant catalyst decomposition above 55°C.[15] The lifetime of the catalysts was monitored by following the ethene uptake in the reaction. There is a significant drop in activity of the catalysts over time, with MAO activated systems showing a drop in ethene uptake after 20 minutes. After three hours, the catalysts were almost completely inactive. The catalyst lifetimes were found to be dependent on the choice of co-catalyst and the Al:Ni ratio.[15]

As with the polymerisation catalysts, a similar system for alkene oligomerisation may be generated from iron bisiminopyridyl complexes co-catalysed by an aluminoxane such as MAO (Fig. 1-7).[17,18] The use of a single *ortho* substituent (Me, Et, ^{i}Pr) on the aryl rings (instead of two) is responsible for the selectivity to oligomers (rather than polymers). A Schultz-Flory chain length distribution was again observed, and higher

α-values were reported for bulkier *ortho* substituents. The activity was found to be dependent on ethene pressure, whereas the Schultz-Flory α-values appear to be independent of ethene pressure, which differs from the nickel catalysts. This suggests that the rates of both chain propagation and chain transfer are first order in monomer. An increase in temperature reduces the α-value and increases the catalytic activity. The selectivity for 1-alkenes is greater than 99%, and at very high activities and conversions, some branched products due to reincorporation of oligomers were detected.[17]

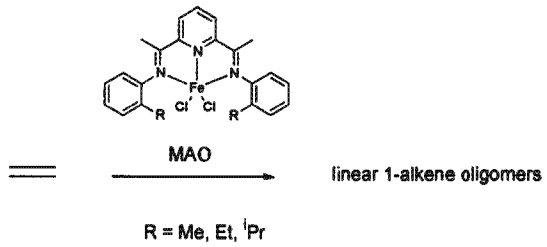

Fig. 1-7: Oligomerisation of ethene with iron bisiminopyridyl complexes / MAO

1.5 Mechanistic considerations

The active catalytic species in these polymerisation and oligomerisation reactions are believed to be cationic, coordinatively unsaturated, electron deficient metal alkyl or metal hydride species. It has been assumed that the active catalysts are in the 2+ oxidation state, although recent evidence suggests that this may not be true for the iron and cobalt catalysts (see section 1.7) A schematic representation of some of the important mechanistic processes is shown in Fig. 1-8.

The general propagation mechanism involves a rapid coordination of alkene to the metal centre, and a slower rate determining insertion of alkene into the metal alkyl bond.[16] This Cossee-Arlman propagation mechanism[19] is characteristic of Ziegler-Natta, metallocene and SHOP catalytic processes as well. Alkene insertion is reported to be first order in monomer concentration (ethene pressure) for the iron systems[12], which suggests that the insertion is a bimolecular process mediated by the new coordinating monomer, but zero order for the palladium systems[20], suggesting a unimolecular process. Thus it is observed that the iron activities increase linearly with increased ethene pressure[12] (although this is offset by increased chain transfer to aluminium co-catalyst under some conditions). The pressure dependence is less pronounced in the nickel systems, and both increases[21] and decreases[22] in activity at higher ethene pressures have been reported.

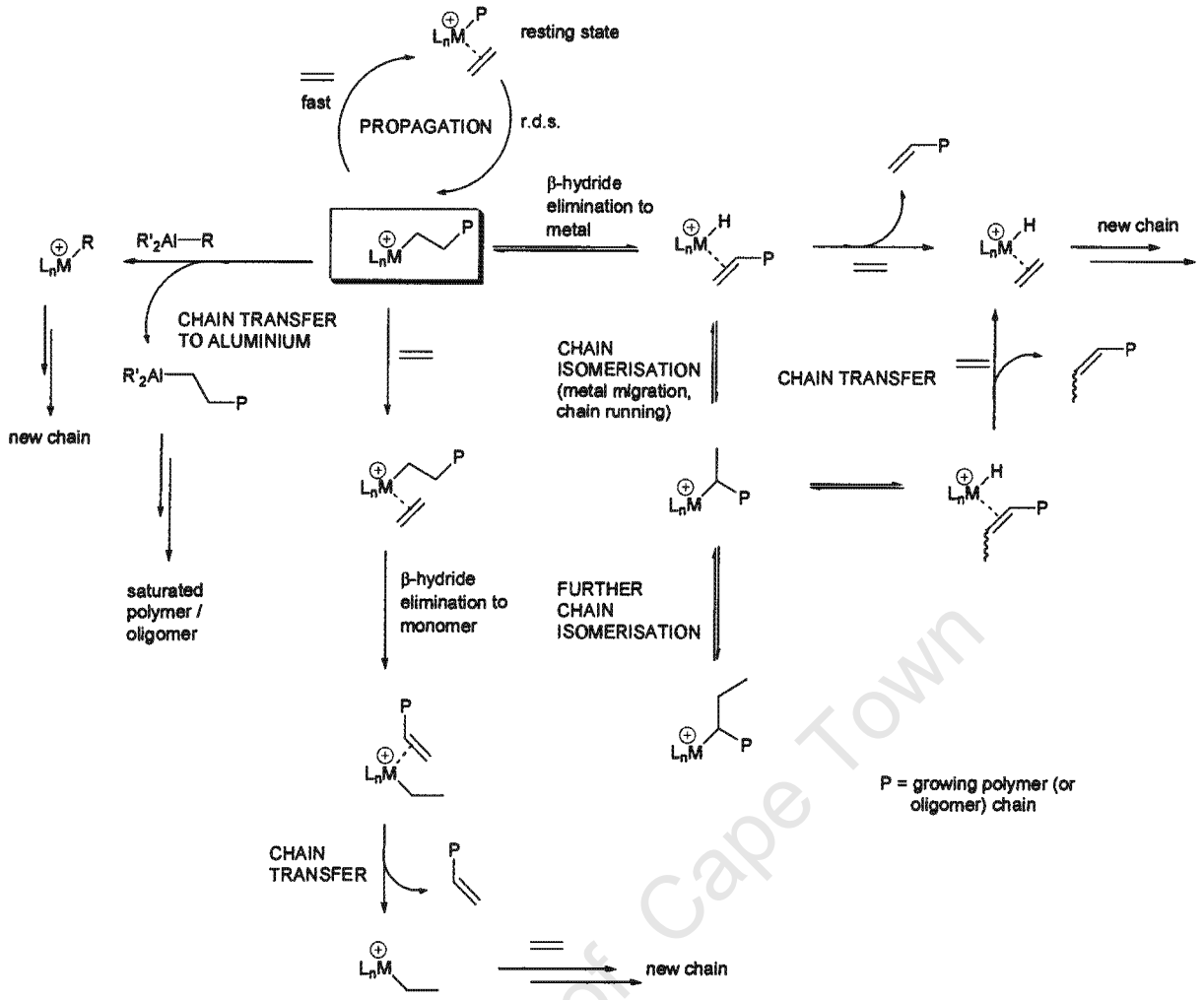

Fig. 1-8: A schematic representation of some of the proposed propagation, chain transfer and isomerisation mechanisms in the polymerisation and oligomerisation of ethene

The barrier to alkene insertion in the rate determining propagation step appears to be reduced by the introduction of bulky *ortho* substituents on the aryl rings, which destabilise the alkene complexed catalytic resting state $[L_nM(alkene)P]^+$ (P = growing polymer chain) by steric hindrance of the axial coordination sites. This is supported by experimental observations[20] and theoretical investigations.[23] The resulting enhanced rate of propagation relative to chain transfer is part of the reason why the catalytic systems with two bulky *ortho* substituents give high molecular weight polymers whereas two less bulky substituents, and systems with only one *ortho* substituent, give lower molecular weight polymers and oligomers respectively. In both the bisiminopyridyl iron and the α-diimine nickel systems the molecular weight of the polyethene is largely independent of ethene pressure[12,21], but is reduced at higher temperatures.

The branching in polymers produced by the nickel and palladium catalysts[10] is caused by the facile process of metal migration along the alkyl chain. With the nickel catalysts, primarily methyl branches are observed, whereas with the palladium catalysts, longer branches and even branched branches are found. The metal migration ('chain running') occurs by repeated and reversible β-hydride eliminations and reinsertions with

the reverse stereochemistry (Fig. 1-8).[10,20] The discrete alkene hydride intermediate has not been directly observed, and theoretical evidence suggests that the metal migration may take place via a concerted mechanism.[23] Low temperature NMR studies have been used to observe Pd-alkyl isomerisations for the α-diimine palladium catalytic system, both directly and with trapping by Lewis-bases.[20,24] The degree of branching is dependent on the bulk of the *ortho* substituents on the aryl rings: greater bulk leads to a higher degree of branching.[21,25] This is because the metal alkyl catalytic species is shielded from incoming monomer, thus allowing for more isomerisation steps before further insertions. The degree of branching is also decreased by an increase in ethene pressure.[21,22] Chain running occurs with the naked metal alkyl intermediate $[L_nMP]^+$ and not with the alkene complexed resting state $[L_nM(alkene)P]^+$ (Fig. 1-8). An increase in ethene pressure reduces the lifetime of $[L_nMP]^+$ before it reverts to the resting state, thereby reducing the rates of isomerisation relative to propagation.[21] Branching is observed to increase with increased temperature.[21,22]

The lack of branching in the polymers produced by the iron and cobalt systems[11-13] demonstrates that the isomerisation (metal migration on the alkyl chain) process is not competitive with propagation and chain transfer. This is supported by the extremely high selectivity of the iron oligomerisation catalysts to 1-alkenes; the nickel and palladium oligomerisation catalysts by contrast produce significant quantities of 2-alkenes due to isomerisation.[15] However, moderately branched polymers (methyl and ethyl branching) have been reported for the iron systems when pyrenyl- and naphthylimino ligands are used.[26]

Chain transfer (termination) may take place by several different mechanisms (Fig. 1-8). In the first proposed mechanism, β-hydride transfer to the metal is followed by an associative displacement of the polymeric/oligomeric alkene by monomer. If this displacement is rate determining, the process is bimolecular and the rate is first order in monomer concentration; if it is faster than the β-hydride transfer, the process is unimolecular and the rate of chain transfer is independent of (zero order in) monomer concentration.[12] A second proposed chain transfer mechanism involves β-hydride transfer to monomer (Fig. 1-8). This has previously been proposed for metallocene catalysts and is implicated as the probable chain transfer mechanism in the nickel systems on the basis of theoretical studies.[23, 27] This mechanism gives the same products and is similarly rate dependent on monomer concentration as the bimolecular β-hydride transfer to metal mechanism. A final possible termination mechanism involves chain transfer to the aluminium alkyl co-catalyst (Fig. 1-8). This mechanism results in the formation of saturated polymer end groups, as has been observed with the iron polymerisation catalysts.[11] Strong evidence for this competing mechanism was obtained when polymerisations were carried out at high Al:catalyst ratios. A bimodal molecular weight distribution of polymer was observed, and the lower molecular weight fraction was found to have almost exclusively saturated end groups.[12] It thus appears that this fraction is formed by chain transfer to aluminium whereas the high molecular weight fragment is formed by a β-hydride elimination process.

It has already been mentioned that the rate of chain propagation is enhanced by the effect of the bulky *ortho* substituents in the late transition metal polymerisation systems. A second effect of these substituents is to slow the rate of chain transfer. Assuming chain transfer is primarily occurring through β-hydride transfer to the metal and associative displacement of the coordinated alkene end group by monomer to give $[L_nM(alkene)H]^+$, the bulky substituents block the axial positions on the metal centre (which is now coordinatively saturated) and thereby hinder the association of the incoming monomer. This has been observed by low temperature NMR studies of the exchange rates of bound and free ethene in α-diimine palladium methyl ethene complexes with different substituents at the *ortho* positions.[20] Alternatively, if the chain transfer mechanism involving β-hydride transfer to monomer is accepted, theoretical calculations have indicated an increase in the barrier to this process with greater bulk of the *ortho* substituents.[23,27] In either event, the effect is to retard the rate of chain transfer, which favours the formation of high molecular polymers.

1.6 Low temperature NMR studies on Pd- and Ni α-diimine catalysts

The propagation steps of ethene coordination and insertion may be monitored directly by low temperature NMR studies of both the palladium and the nickel systems. The complexes $[N_2MMe(OEt_2)]^+BAr'_4^-$ (N_2 = α-diimine ligand; M = Ni, Pd; Ar' = 3,5-$C_6H_3(CF_3)_2$) were prepared by treatment of N_2MMe_2 with $H^+(OEt_2)_2BAr'_4^-$.[10,28] At very low temperatures, ethene displaces the labile ether, to form a metal methyl ethene complex (Fig. 1-9). Upon warming, alkene insertion into the metal-alkyl bond is observed, and a series of alkyl alkene complexes with increasing chain length is observed (Fig. 1-9).

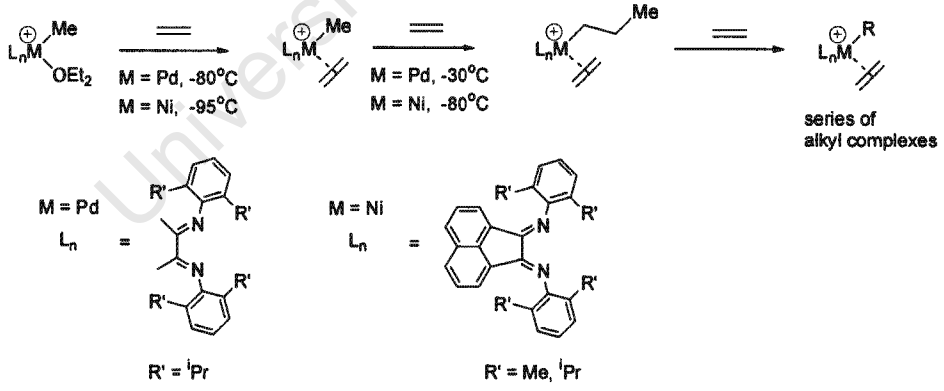

Fig. 1-9: Low temperature NMR observations of initial propagation steps in the polymerisation of ethene

These observations establish that the catalytic resting species are the metal alkyl alkene complexes and that the rate determining step is alkene insertion. Kinetic analysis indicated that the insertions are zero order in ethene. A comparison of the nickel and palladium systems indicated that the barrier to insertion is lower by ca. 4-5 kcal/mol for the nickel complexes, and calculations for theoretical turnover frequency (TOF) correspond to observed experimental activities.[28] In the nickel complexes, the barrier to ethene insertion is

ca. 0.4 kcal/mol lower for the system with isopropyl *ortho* substituents than for the system with methyl substituents, which supports the claim that bulky *ortho* substituents facilitate high molecular weight polymers in part because of an enhanced rate of chain propagation relative to transfer.[28] Similar results are reported for palladium analogues.[20]

Similar studies with propene suggests that 2,1-insertion of propylene is favoured in the palladium system whereas both 2,1- and 1,2- insertion products are observed for the nickel analogues[28]. For the nickel system, the resting states are not alkyl propene complexes but β-agostic alkyl complexes[10], while with palladium, the expected alkyl propene complexes are observed.[10,28]

The isomerisation of Pd-alkyl species by β-hydride transfer and reinsertion has also been observed by low temperature NMR studies (Fig. 1-10).[20,24,29] The alkyl complexes are β-agostic. Both chain isomerisation and rotation about the C_α-C_β bond may be observed by trapping experiments and by coalescence of different signals upon warming, and kinetic data for these processes were ascertained.

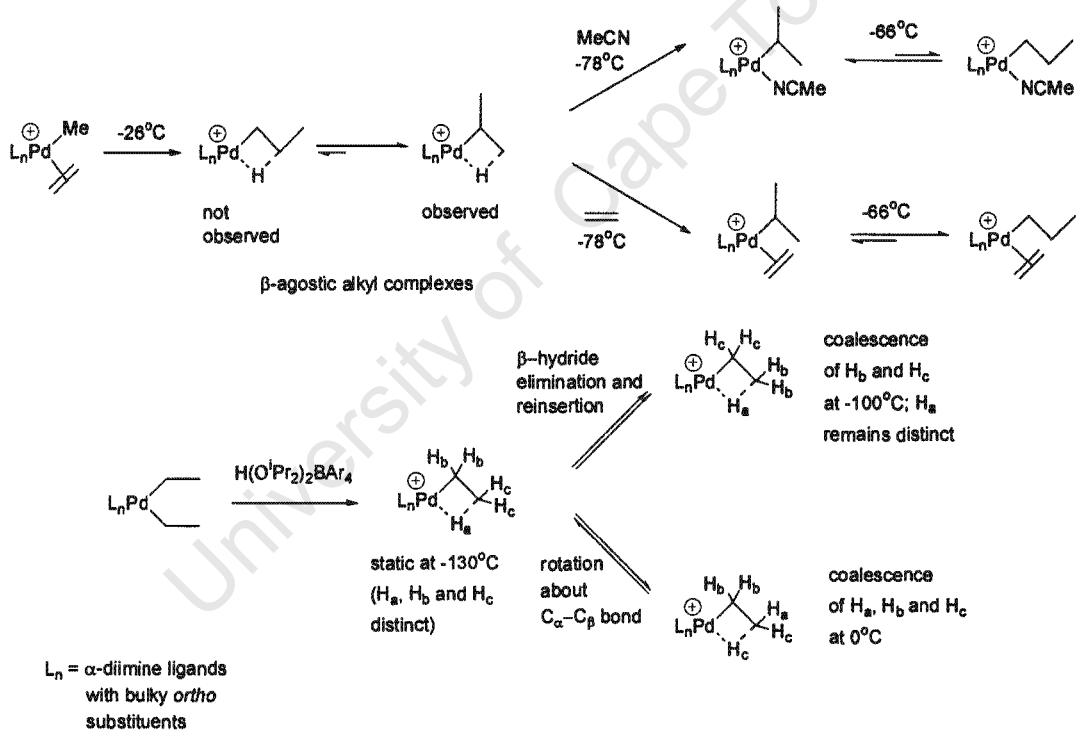

Fig. 1-10: Low temperature NMR studies of the isomerisation process in sterically hindered α-diimine Pd cationic alkyl species

1.7 Mechanistic studies of the Co- and Fe bisiminopyridyl catalysts

Gibson and Gal have independently published reports suggesting the involvement of Co(I) and possibly Co(III) species in the formation of the active catalyst from the cobalt system N_3CoCl_2 (N_3 = 2,6-bis-[1-(2,6-diisopropylphenylimino)ethyl]pyridine).[30,31] Treatment of N_3CoCl_2 with an alkylating reagent such as

MeLi, MeMgBr or Et_2Zn leads first to the reduction from Co(II) to Co(I): N_3CoCl was isolated[30], and this may be selectively alkylated to give N_3CoR (R = Me, CH_2Ph, CH_2SiMe_3) (Fig. 1-11).[30,31] It was further observed that treatment of N_3CoCl_2 with a few equivalents of MAO similarly leads to the sequential formation of N_3CoCl and N_3CoMe.[30] N_3CoMe is itself not active for polymerisation of ethene. However, activation by $B(C_6F_5)_3$ gives a cationic Co(I) species with no metal alkyl bond which binds dinitrogen or a single equivalent of ethene (Fig. 1-11). Crucially, treatment of this species with excess ethene gives polymer with similar properties to the MAO activated process, although with lower activity.[31] The nature of the active species is not clear, although it is postulated that it could be a Co(III) species, possibly formed by C-H activation of the bound ethene to form a cationic vinyl hydride species. Although the active catalyst was not identified, the studies establish the intermediacy of Co(I) in the activation process and raise questions as to whether the assumption of a Co(II) active species is correct.

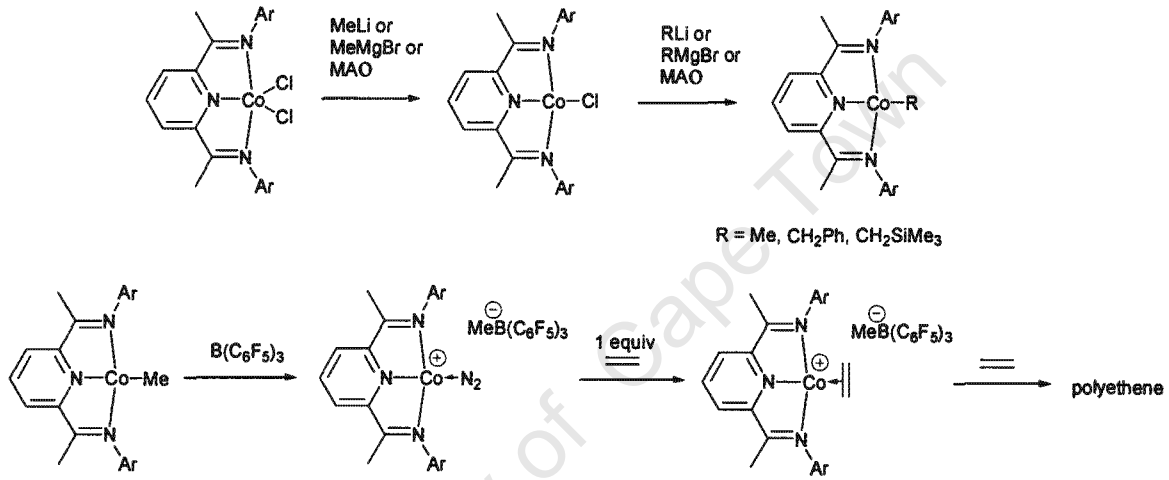

Fig. 1-11: Reduction of a Co(II) complex to Co(I) by MAO, and borane activation to form an active ethene polymerisation catalyst

A similar system has been used to model the proposed chain transfer mechanism and establish if β-hydride elimination to metal or monomer is in operation.[32] $N_3CoCH_2CH_2R$ (R = Me, Et) reacts with ethene to give N_3CoEt with loss of $RCH{=}CH_2$. This reaction was observed to be zero order in ethene. The reaction of N_3CoBu with propene has the same rate as the reaction with ethene. Both of these results suggest that the rate determining step involves β-hydride transfer to metal, and not formation of a concerted transition state involving β-hydride transfer to the ethene/propene.

Similar studies on bisiminopyridyl Fe(II) alkyl complexes have been frustrated due to the poor stability of these compounds. In particular, N_3FeR_2 and $[N_3Fe\text{-}R]^+$ complexes could not be prepared.[33] In order to obtain mechanistic information about the active species, Mössbauer and electron paramagnetic resonance (EPR) studies have been carried out.[14] Fe(II) and Fe(III) precatalysts N_3FeCl_2 and N_3FeCl_3 (which have been shown to produce catalytic systems with similar activities and polymer properties[13]) were treated with 100 equivalents of MAO, and Mössbauer spectra were obtained for the untreated complexes and the

MAO treated complexes under inert conditions. The isomer shifts (δ) for the precatalysts are typical of high spin Fe(II) and Fe(III) complexes respectively. However, after treatment with MAO, the two catalysts show essentially identical Mössbauer spectra, and the δ value lies within the range of high spin Fe(III) species. These results are confirmed by EPR studies. Fe(II) species are EPR inactive whereas Fe(III) are EPR active. The MAO treated precatalysts both showed EPR resonances typical of a Fe(III) species, while, as expected, the untreated Fe(II) precatalyst showed no resonance. These results suggest that the active catalytic species in the iron bisiminopyridyl polymerisation systems are not cationic Fe(II) alkyl species, but involve as yet undetermined Fe(III) species.

1.8 Ligand modifications

The effect of the number and steric bulk of *ortho* substituents on the aryl rings of both Ni/Pd α-diimine and Fe/Co bisiminopyridyl systems has already been discussed. An additional ligand effect worthy of comment is the effect of substitution on the backbone at the imino carbons (Fig. 1-12 a). In both systems, R_1 = Me results in more active catalysts and higher molecular weight products than R_1 = H (where in both cases R_2 = isopropyl).[12,22] It is believed that non-hydrogen R_1 substitution results in increased crowding of the metal centre by the bulky R_2 group, thereby enhancing the preference for high molecular weights and activities already described.[22]

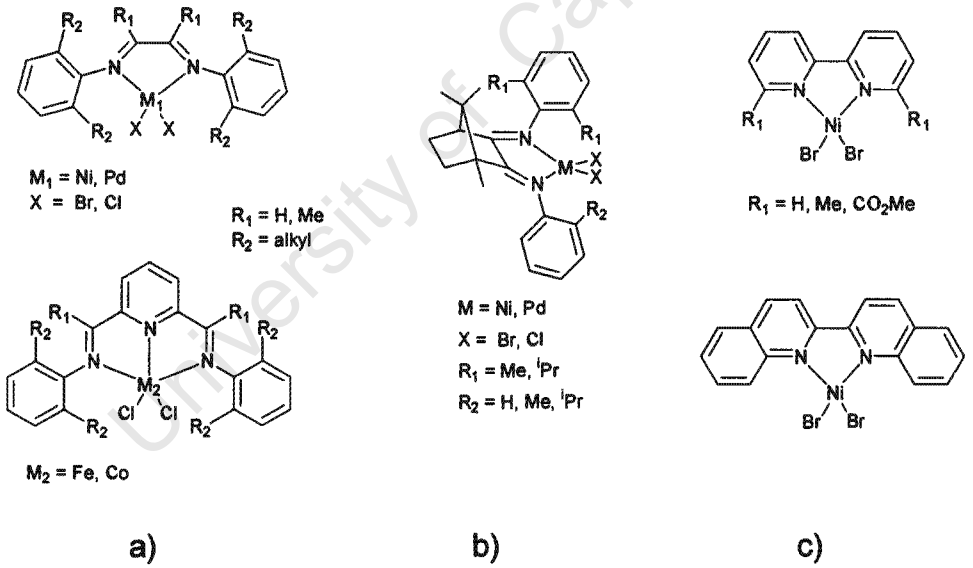

Fig.1-12: Variations in backbone substitution R_1 affect the catalytic activity and selectivity

Other reported backbone variations include optically active camphor-derived diimine ligands with unsymmetrical imino substitution (Fig. 1-12 b).[34] Although the nickel complexes of these ligands are active for ethene polymerisation, no comparative studies of catalytic activities and polymer properties with other α-diimine systems have been reported yet. A series of nickel complexes with substituted 2,2'-bipyridine and 2,2'-biquinoline ligands were also active for ethene polymerisation to high density polyethene (Fig. 1-12 c).[35] Substitution in the 6,6'-positions by methoxycarbonyl groups increased activity in accordance with

the expected increase in steric demand at the metal centre, although it was also suggested that the electron withdrawing ester substituents may stabilise the cationic active species, thereby improving activity. Overall, however, the catalysts had lower activity than the α-diimine catalysts with bulky aryl groups.

Modification of bisiminopyridyl ligands by replacing the *ortho* substituted imino aryls by naphthyl and pyrenyl groups has been reported (Fig. 1-13 a).[26] Although the effect on activity is not clear from the report, the polymers produced display a degree of methyl and ethyl branching which is not apparent in polymers produced under the same conditions by a catalyst with a single *ortho* benzyl substitute on the imino-aryl ring.

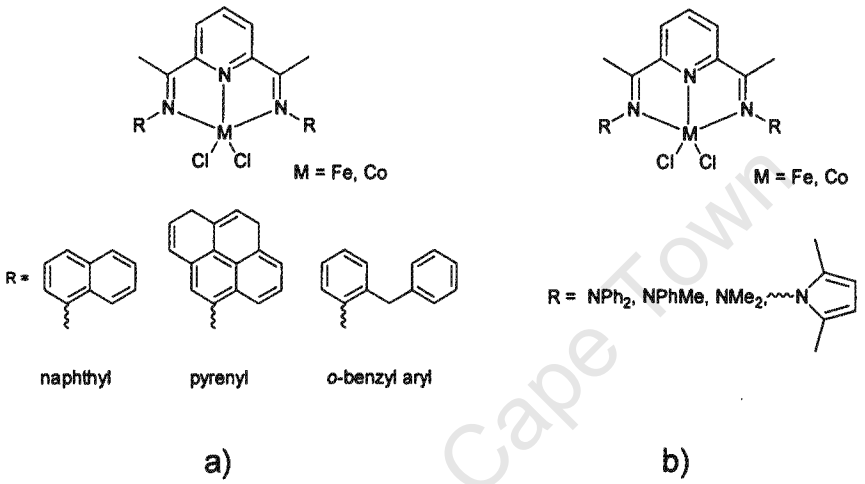

Fig. 1-13: Replacement of o-substituted iminoaryl groups by other functionalities

Replacement of the aryl rings by amines to give bis(hydrazone)pyridyl ligands has also been described (Fig. 1-13 b).[36] Diphenyl amine and 2,5-dimethylpyrrole substituted systems gave low molecular weight polyethene at 10bar ethene pressure, while the methylphenylamine and dimethylamine analogues produce exclusively toluene soluble oligomers with a Schultz-Flory distribution. This is ascribed to the usual steric affects. The activities are substantially reduced for the diphenyl-, methylphenyl- and dimethylamine systems, possibly due to lone pair donation to the imine nitrogen or interactions with the aluminium co-catalyst, and the catalysts degrade rapidly over time as well. The 2,5-dimethylpyrrole systems (in which the pyrrole nitrogen lone pair is involved in bonding in the pseudo-aromatic ring) are longer lasting and more active, though the activities are still lower than for the 2,6-dimethylphenylimino analogue under the same conditions. It is noteworthy that the molecular weight of polymer produced by the 2,5-dimethylpyrrole systems is substantially lower (M_w = 900) than for the sterically similar 2,6-dimethylphenylimino analogue (M_w = 242000), which implicates some electronic mediation of the rates of chain propagation and transfer. As expected, the cobalt systems exhibited lower activity than the iron systems.

Ligand modification may also be accomplished by changing the nature of the donor atoms chelating to the metal centre. 2-Iminoalkyl-6-aminoalkylpyridyl and 2,6-bisaminoalkyl ligands have been synthesised, their

$FeCl_2$ complexes prepared (Fig. 1-14 a) and the ethene polymerisation behaviour studied and compared with analogous 2,6-bisiminopyridyl systems.[37] When treated with MAO, active catalysts are generated from the new systems; however the activities are several orders of magnitude lower than for the bisiminopyridyl analogues. The 2-iminoalkyl-6-aminoalkylpyridyl systems were more active than the 2,6-bisaminoalkyl The usual trends relating to the effects of aryl (R_2) and imino (R_1) substitution were observed. Possible reasons for the lower activities of the aminoalkylpyridyl iron systems are weak amino-iron interactions leading to dissociation, lack of conjugation or difference in the orientation of the bulky aryl groups.

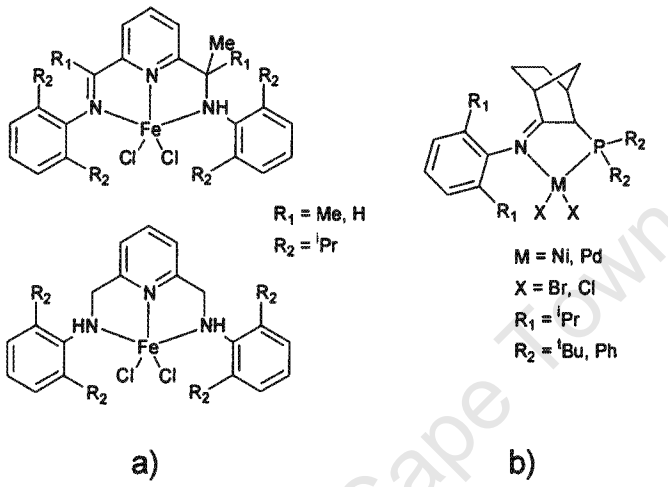

Fig. 1-14: Reported modifications to the nature of the chelating donor atoms

Mixed N,P nickel and palladium complexes have been prepared in which one of the two imine groups has been replaced by a bulky phosphine (Fig. 1-14 b).[38] While the palladium systems are inactive, the nickel complexes polymerise ethene when activated with MAO. The diphenylphosphine precatalysts are more active than the di^{t}butylphosphines because of greater electron donation from alkylphosphines than from arylphosphine. The di^{t}butylphosphine system, however, produced polymers with higher molecular weight because of the greater steric bulk of the ^{t}Bu groups. The activities and molecular weights of the new systems do not compare favourably with the α-diimine catalysts; however the degree of branching is higher (50-60 branches per thousand atoms compared to about 20 for the diimine catalyst). The chief advantage of these iminophosphine catalysts is their greater thermal stability. Catalysts remain active above 70°C after 7 hours; under these conditions, α-diimine catalysts are typically inactive after half an hour.

An extensive range of unsymmetrical iminopyridyl, iminoquinoline, iminobipyridyl and iminophenanthroline complexes have been described (Fig. 1-15) [39-42]

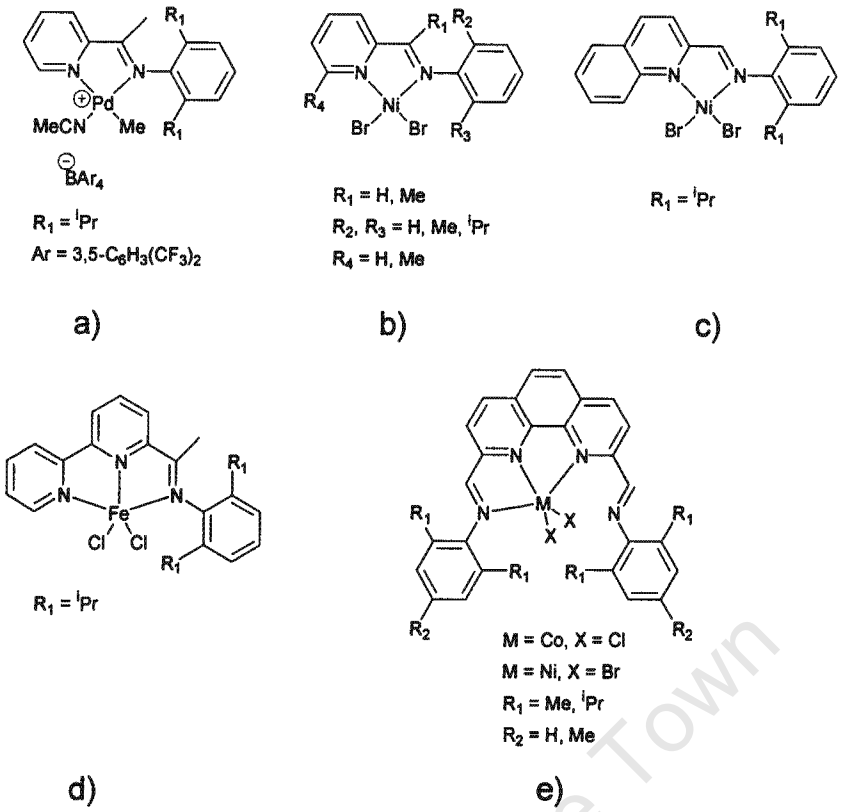

Fig. 1-15: Iminopyridine, -quinoline,- bipyridine and phenanthroline complexes active in ethene oligomerisations or polymerisations

Monoiminopyridyl palladium and nickel complexes have been reported as active in the oligomerisation of ethene. Both isolable cationic species with non-coordinating borane counterions[39] (Fig. 1-15 a) and dihalide complexes activated by MAO (Fig. 1-15 b, R_4 = H)[40] demonstrate this catalytic behaviour. Significant branching (due to chain running and reincorporation of lower oligomers) was observed and mainly internal double bonds were seen in the oligomeric products.[39] Methyl substituted iminopyridine (Fig. 1-15 b: R_4 = Me) and iminoquinoline (Fig. 1-15 c) systems appear to produce lower molecular weight products (oligomers) than corresponding unsubstituted iminopyridyls (fig 1-15 b: R_4 = H), which under the conditions reported, produced very low molecular weight polymers / high molecular weigh oligomers.[42] The additional methyl or quinolyl component is in the plane of the chelating nitrogens and nickel centre, and thus does not inhibit the β-hydride elimination. An iron iminobipyridyl complex (Fig. 1-15 d) formed low molecular weight oligomers (mainly butenes and hexenes) under MAO co-catalysed conditions.[42] Despite the bulky iminoaryl functionality, the absence of steric demand on the opposite side means that chain transfer is not hindered and even lower weight oligomers are obtained than with the 2,6-bis[-1-(2-methylphenylimino)ethyl]pyridine oligomerisation catalyst. Tridentate cobalt and nickel complexes of potentially tetradentate bisiminophenanthroline ligands (Fig. 1-15 e) were inactive at 1 bar ethene; at 10 bar they displayed moderate activity for low molecular weight oligomers. Iron complexes of the same ligands were generally found to be inactive.[41]

1.9 Electronic effects

A large proportion of research activity on the new late transition metal α-diimine and bisiminopyridyl catalysts has focused on structural and steric modifications of the ligands. Relatively little work has been done on understanding the electronic effects that increasing or reducing electron density on the metal centre may have.

In a study of various factors affecting the oligomerisation of ethene with nickel diimine catalysts, complexes with electron withdrawing (Fig. 1-16 a) and electron donating (Fig. 1-16 b) substituents on the *para* aryl positions were prepared.[15] The electron withdrawing -CF_3 substituent results, as expected, in higher activity relative to unsubstituted catalysts due to increased electrophilicity of the metal centre and consequent higher rate of ethene insertion. However, the electron donating -OMe substituent does not conversely reduce activity. This was tentatively ascribed to Lewis acid-base interactions of methoxy with the aluminium co-catalyst, which reduce the electron donation by this group. A similar increase in activity for *ortho*-CF_3 (Fig. 1-16 c) over *ortho*-Me substituted α-diimine catalysts has been noted[21], and the tendency for electron withdrawing groups (such as halogens) to increase nickel α-diimine[43] and cobalt bisiminopyridyl[44] polymerisation activities has been described elsewhere. However, no significant effect due to halogen substitution was found in iron bisiminopyridyl catalytic systems.[44]

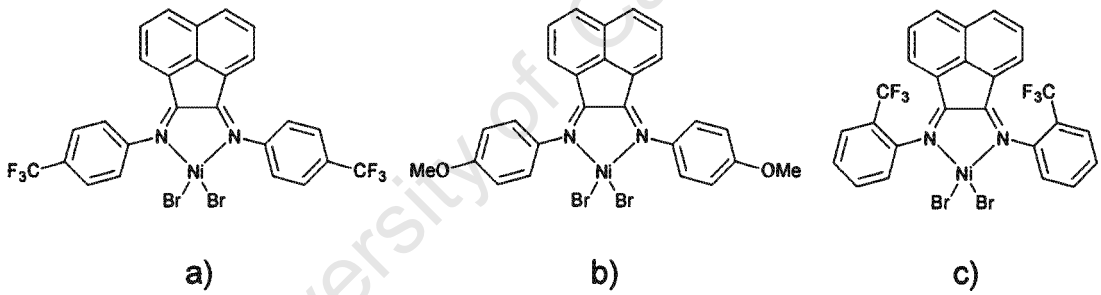

Fig. 1-16: Complexes with electron withdrawing and electron donating groups

1.10 Other metals

Most reports of alkene polymerisation/oligomerisation catalysts with imine type ligands have focused on the metals Ni, Pd, Fe and Co. However, in ongoing efforts to expand the range of catalytic systems with these and similar ligands, other metals have been studied.

MAO activated α-diimine copper(II) complexes, [Ar-N=(Me)C-C(Me)=N-Ar]$CuCl_2$ (Ar = 2,6-$C_6H_3Ph_2$ and 2,6-$C_6H_3{}^iPr_2$) have been shown to be active as ethene polymerisation catalysts.[45] Bulky *ortho* substituents (Ph, ^iPr) were again important in stabilising the active centre and facilitating high molecular weight polymers. The activities were low relative to nickel systems. The *ortho*-phenyl substituted complexes were substantially more active than the sterically similar *ortho*-isopropyl analogue, which was

ascribed to a weak stabilisation interaction of the phenyl with the metal centre. The polymer molecular weights were found to be extremely high (> $5x10^6$ $gmol^{-1}$).

Bisiminopyridyl vanadium(III) complexes were active for polymerisation of ethene when co-catalysed by excess MAO.[46,47] The activity was found to be high, though lower than for the Fe analogues, and the polymer showed high polydispersity, suggesting that several active species were in operation. Stoichiometrically controlled activation experiments with MAO and MeLi indicated a series of unusual reactions involving alkylation of the pyridyl ring to give a formally anionic ligand with reduced coordination around the vanadium centre and loss of aromaticity of the pyridyl ring (Fig. 1-17).[46] This is presumed to be precursor to the active catalytic species. Upon further alkylation by a strong alkylating reagent such as MAO, reduction to V(I) occurs, which was assumed to be the pathway for catalytic deactivation, as these species were catalytically inactive.

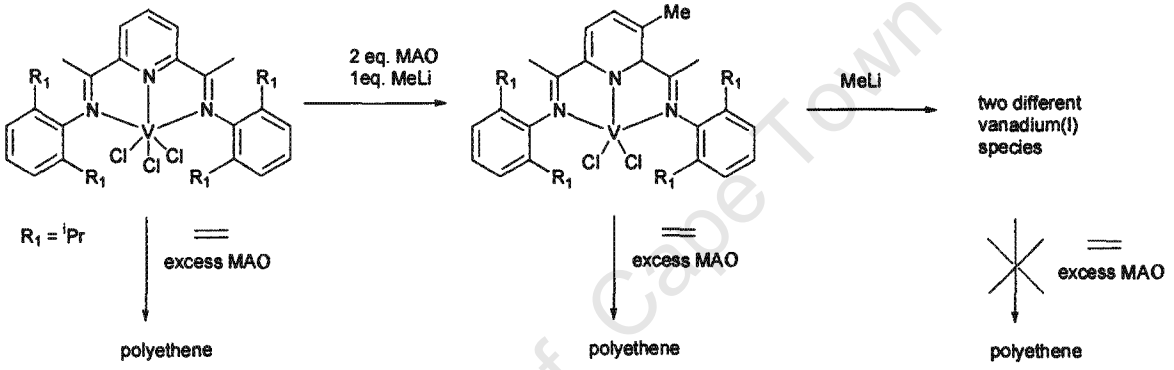

Fig. 1-17: Polymerisation of ethene by a vanadium complex, showing an unusual initial activation by MAO involving alkylation of the ligand and a possible deactivation mechanism

A similar bisiminopyridyl complex of $MnCl_2$ proved to be completely inactive as a polymerisation catalyst when activated with MAO and other co-catalysts.[48] Treatment with stoichiometric MeLi and $LiCH_2SiMe_3$ was shown to reduce the complex to Mn(I) and Mn(0) alkyl species respectively.

Aluminium co-catalysts are typically important in the activation of late transition metal precatalysts. However, it has recently been shown by two groups that aluminium complexes can themselves be activated by, for example, borane compounds to form active catalysts for ethene polymerisation. Treatment of known bisiminopyridyl ligands with $AlMe_3$ affords aminoamidopyridyl aluminium complexes with consequent alkylation of the ligand (Fig. 1-18 a).[49] Upon activation with $B(C_6F_5)_3$, cationic alkyl complexes are formed which are moderately active as ethene polymerisation catalysts. A similar two coordinate imino-amido $AlMe_2$ complex has been prepared and activated by $B(C_6F_5)_3$ to polymerise ethene with low activity (Fig. 1-18 b).[50]

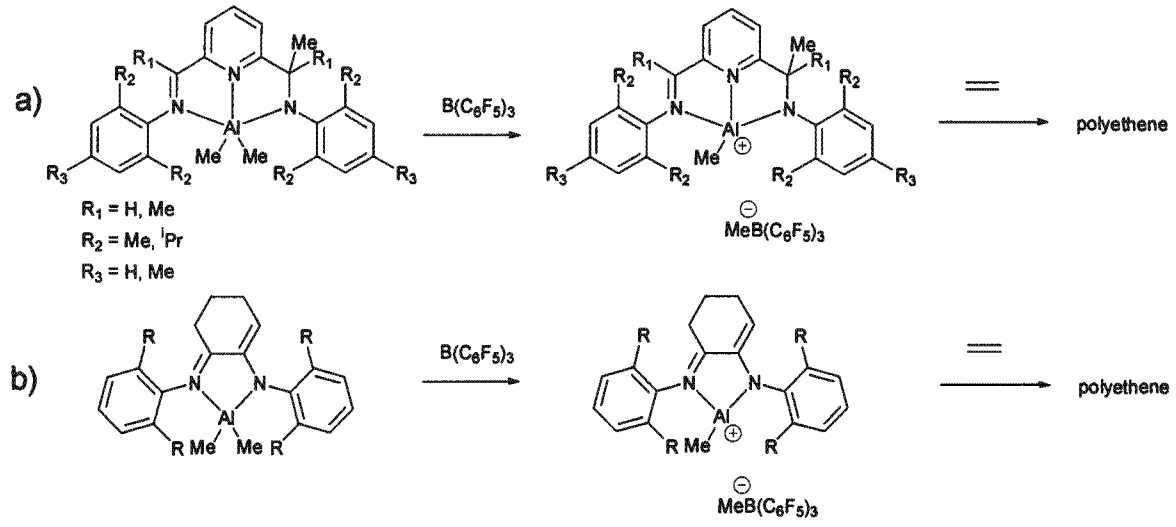

Fig. 1-18: Polymerisation of ethene with aluminium complexes

Following on from the success of the iron bisiminopyridyl system for ethene polymerisation and oligomerisation, the activity and chemistry of similar complexes of ruthenium, the 4d congener of iron, were investigated.[51] Isoelectronic rhodium(III) complexes were also investigated. Stable cationic alkyl Ru(II) and Rh(III) complexes with coordinated ethene may be prepared (Fig. 1-19). These complexes showed very high stability against alkene insertion at room temperature, and were thus found to be inactive for polymerisation of ethene. It was suggested that the lack of activity may be due to the octahedral geometry of the complexes (as opposed to the iron analogues' square pyramidal structure, see Fig. 1-21). This is supported by theoretical studies.

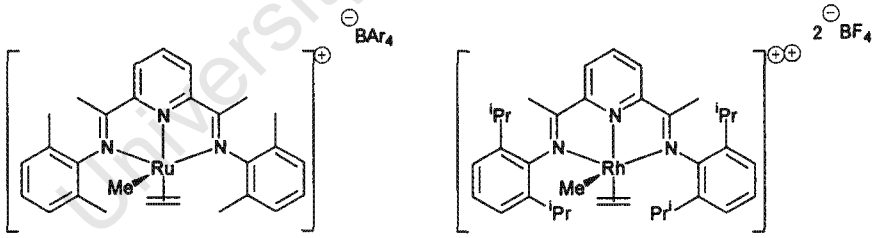

Fig. 1-19: Ruthenium(II) and rhodium(III) bisiminopyridyl complexes with octahedral geometry.

1.11 Co-polymerisations with polar monomers

Co-polymerisations of ethene with functionalised alkenes such as methyl (meth)acrylate, (meth)acrylic acid and vinyl acetate are important industrial processes.[3] Crosslinking interactions between polar groups on the polymer chain leads to beneficial properties, including toughness and enhanced compatibility with other substances. Unfortunately the high oxophilicity of early transition metals means that catalysts based on these metals (titanium, zirconium, chromium) are poisoned by polar co-monomers, and co-polymers are typically produced industrially by extremely high pressure free radical processes.[3] Late transition metals

are known to be less oxophilic than early transition metals. For example, polymerisation of ethene by a cationic α-diimine palladium complex in water has been reported.[52] Therefore, the possibility of developing catalysts for co-polymerisations with polar co-monomers under mild conditions is one of the main driving forces for the current interest in late transition metal catalysts.[5]

The first report of such co-polymerisations with cationic late transition metal catalysts was by Brookhart and co-workers in 1996.[53] High molecular weight, highly branched co-polymers of ethene and methyl acrylate (MA) were formed by the previously reported α-diimine palladium complexes. The activities were substantially lower than for ethene homopolymerisation. The MA units were randomly distributed through the polymeric structure with a proportion dependent on the relative concentrations of the two monomers, and were found predominantly at the end of branches. Low temperature NMR studies were used to elucidate the mechanism of co-polymerisation. The catalytic resting state was found to be a six-member π-acrylate chelate complex (Fig. 1-20) formed by 2,1-insertion of MA into the growing chain and subsequent rearrangements by β-hydride elimination and reinsertion. Reversible carbonyl/ethene coordinative substitution (carbonyl:ethene coordination ratio = 1000:1) is the rate determining step, which explains the reduced activity. Rapid propagation by repeated ethene insertions and branching by chain running proceeds until the next insertion of MA.

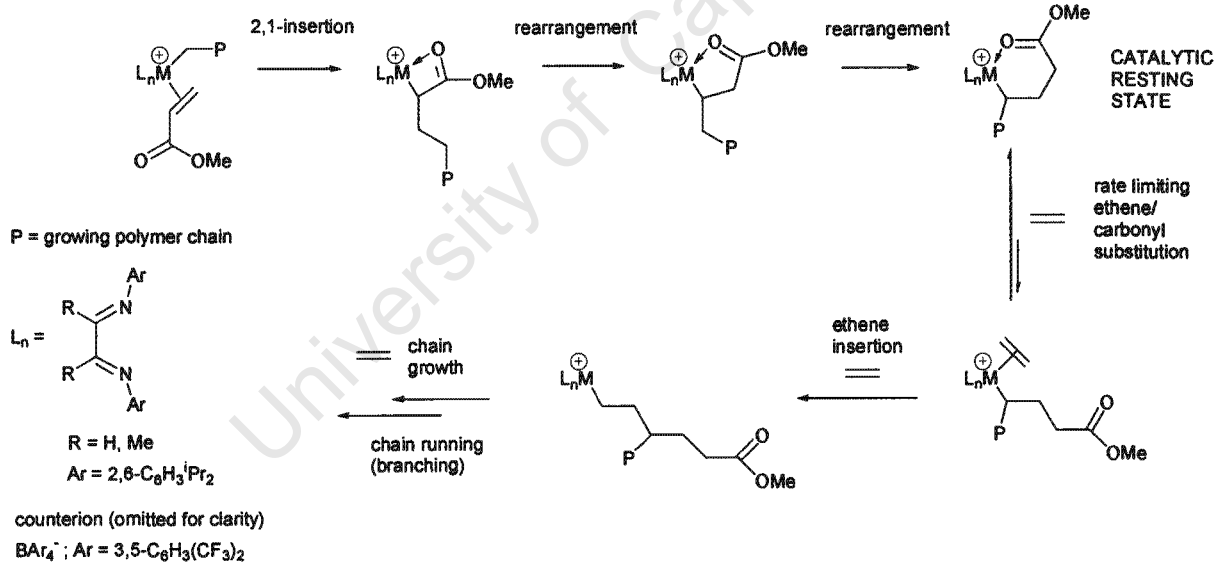

Fig. 1-20: Mechanism for the copolymerisation of ethene and methyl acrylate

Utilising the α-diimine catalysts, a wide range of other polar monomers has been incorporated in co-polymerisations with ethene and other 1-alkenes, although the reports have largely been restricted to the patent literature. Examples include acrylates, carboxylates, ketones, CO, crotonaldehyde, carbonate esters, sulfones, ethers and epoxides.[3] There is a general trend to lower activity for more polar functionalities. Very polar functionalities may be successfully incorporated provided the polar group is sufficiently removed from the double bond (e.g. 10-undecenol) or if chain running towards the polar moiety is blocked

by non-hydride substituents on the chain, which prevents β-hydride elimination (e.g. 2,2-dimethyl-4-pentenol).[3] Nitrile, amine and amide functionality typically inhibit polymerisation.

Co-polymerisation reactions have also been attempted with the well-known iron bisiminopyridyl complexes. When activated with MAO, and in the presence of ethene (1atm) and 1000 equivalents of methyl (meth)acrylate, styrene or 2-vinyl-1,3-dioxalane, polymer was produced with varying levels of activity. However, analysis of the polymers indicated that a mixture of ethene homopolymer and small amounts of polar homopolymers (probably formed by a free radical mechanism[3]) had been formed in each case.[33] Co-monomers such as vinyl acetate, acrolein and acrylonitrile completely deactivated the catalysts. As such, these results simply establish the stability of the late transition metal catalysts in the presence of some polar functionalities, and no co-polymerisation activity was observed.

Incorporation of deuterated vinyl chloride and vinyl acetate in ethene oligomers produced by a MAO activated bisiminopyridyl iron complex has been reported.[54] However, the incorporation effectively terminates chain growth due to rapid β-chloride or β-acetate transfer to the metal, and thus the reaction cannot be thought of as a true co-oligomerisation. Similar results have been reported for palladium α-diimine systems.[55]

1.12 Non-polar alkene monomers other than ethene: selected features

Several reports primarily detailing late transition metal catalysts for the polymerisation or oligomerisation of ethene have also described the polymerisation or oligomerisation of propene and higher 1-alkenes under similar conditions.[10,28,39] Internal alkenes may also be polymerised using late transition metal catalysts. Reports of addition polymerisations of cyclopentene[56,57] and *trans*-2-butene[58] with α-diimine nickel or palladium catalysts have been published.

A series of bisiminopyridyl iron complexes, including complexes of unsymmetrically substituted ligands, has been prepared, and the polymerisation activity with propene at low temperature (-20°C) investigated (Fig. 1-21).[59] It is well-established from studies of metallocene catalysts that the tacticity of polypropene may be controlled by modifications to the symmetry of the catalysts (by 'site-control', in which the geometry of the ancilliary ligands controls the stereochemistry of the insertions). Certain metallocenes with C_2 or C_1 symmetry have been shown to produce isotactic polymers, while other metallocenes with C_s symmetry are selective for syndiotactic polymers.[6] The bisiminopyridyl complexes studied (in which NMR evidence indicates that free rotation around the N-Ar bonds is inhibited by two bulky *ortho* substituents and the imino-methyl) included complexes with C_1, C_{2v}, C_s and C_2 / C_s (by rotation around the N-Ar bond) symmetry (Fig. 1-21).

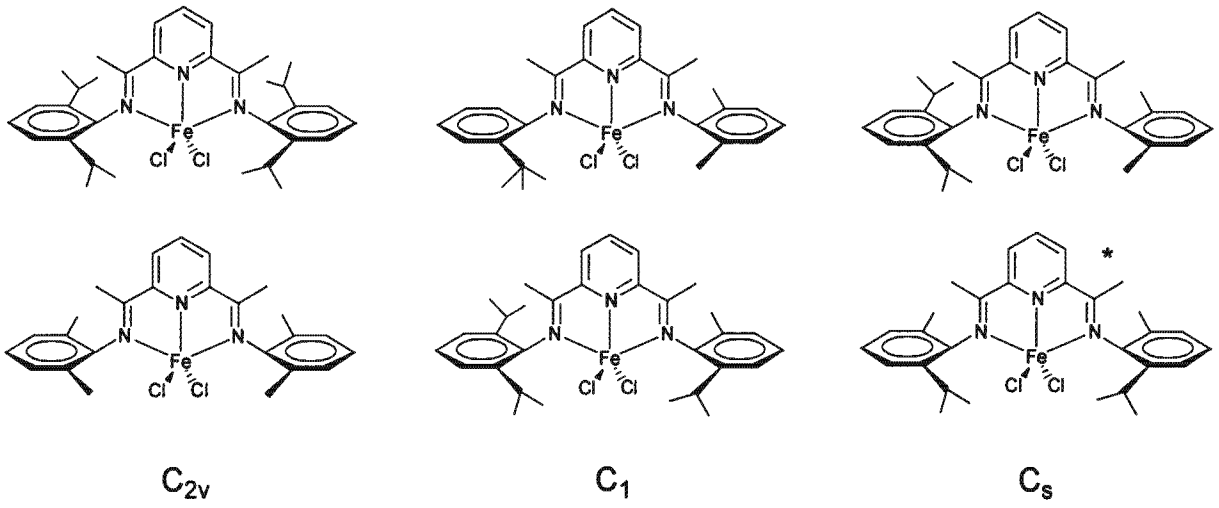

*Fig 1-21: Bisiminopyridyl ligands with different symmetry (complex marked * is conformationally locked, as indicated by NMR and crystal structure)*

As expected, the bulkiness of the *ortho* substituents on the aryl ring has a significant effect on polymer molecular weight and catalyst lifetime. In addition, bulkier substituents cause propene addition to the growing polymer be highly regioselective (2,1-insertions), with no head-to-head insertions or 1,3-enchainment observed. Of greater interest was the tacticity of the resulting polypropenes, and in all cases the polypropene was found to be moderately isotactic. However, analysis of the errors in tacticity indicated that stereospecificity is 'chain-end controlled'. This means that the stereospecificity of the insertion is dictated by the stereospecificity of the previously inserted monomer, and not by the geometry of the ligands. Similar chain-end controlled isotacticity has been previously observed with metallocene catalysts.[60]

Interestingly, polypropene produced by nickel and palladium α-diimine catalysts has a very different microstructure to that produced by the iron systems.[61] Although the microstructure varies greatly with catalytic conditions and choice of ligand, key features include regioirregular additions (both 2,1- and 1,2-insertions, with 1,2 insertions predominating), 'chain straightening' (by 1,3-enchainment) to give 7 or more consecutive unbranched methylenes, atactic stereoselectivity and long branches including branches on branches.

Dimerisation of 1-alkenes is an important industrial process, and the production of linear dimers is particularly desirable.[56] This can only be achieved by a head-to-head regioselective dimerisation, in which the primary insertion into the M-H bond takes place in a 1,2-fashion, and the second insertion by the opposite 2,1-process (Fig. 1-22). Other regio-additions lead to vinylidene and branched products, and completing side reactions include alkene isomerisations and formation of trimers and higher oligomers (Fig. 1-22). Most dimerisation processes previously reported therefore suffer from a lack of selectivity due to multiple reaction pathways.[56]

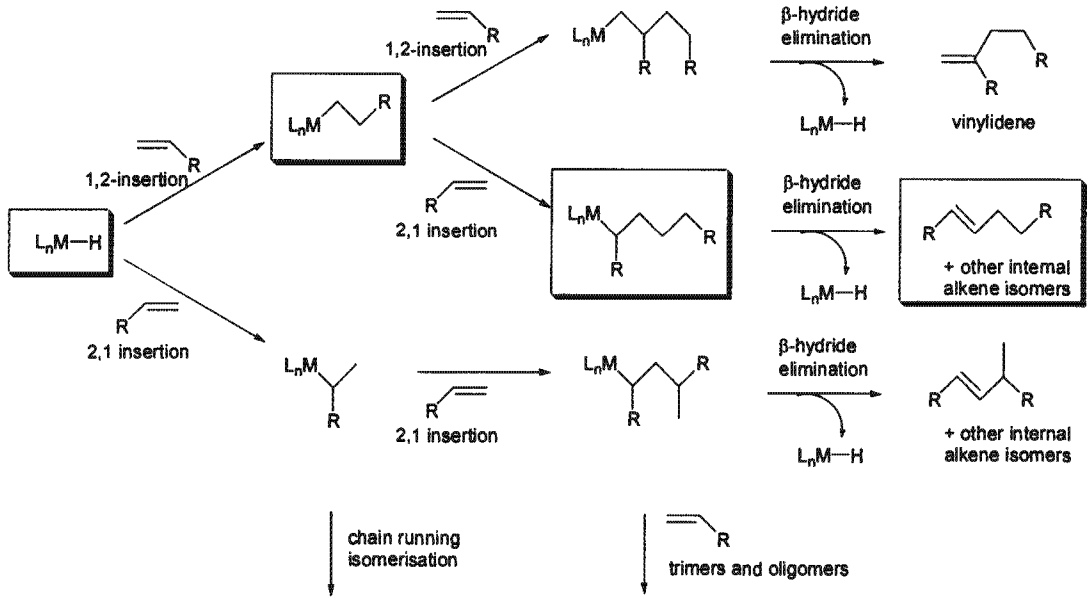

Fig. 1-22: Mechanisms for the dimerisation of 1-alkenes, the pathway for linear dimers highlighted

Bisiminopyridyl iron complexes with only one or no *ortho* aryl substituents (which have been previously shown to oligomerise ethene[17,18]) were found to dimerise higher 1-alkenes ($C_5 - C_{24}$) with conversion rates of over 70% in some instances (Fig. 1-22).[56] Selectivity to dimers is in the order of 85-95% and selectivity of up to 81% for linear products was reported. The selectivity for preferential 1,2-insertion into M-H and 2,1-insertion into M-R in bisiminopyridyl iron systems has been noted elsewhere.[59] The high activities observed are also surprising, as very little reincorporation of lower oligomeric products in oligomerisation reactions of ethene using these catalysts is observed.[15] This activity was ascribed to the fact that half the insertions take place into the reactive primary M-H bonds. Higher temperature increases the catalytic activity but reduces the catalyst lifetime and the selectivity to linear dimers.

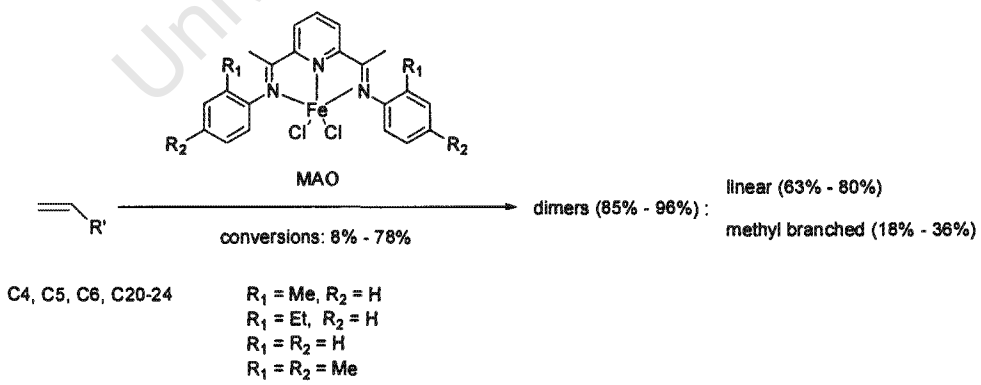

Fig. 1-22: Dimerisation of 1-alkenes to form predominantly linear internal alkenes

1.13 Living polymerisations and block co-polymers

Living polymerisations are polymerisation reactions in which chain transfer reactions are effectively suppressed. Upon consumption of the monomer, the growing chain remains attached to the still-active metal centre until further monomer is added, when chain growth resumes. Living polymerisations are characterised by very narrow polymer polydispersities. It has been reported that at low temperatures (-10°C) and low monomer concentrations, nickel α-diimine catalysts produce poly(1-alkenes) with polydispersities characteristic of living systems.[62,63] Furthermore, the molecular weight of the polymers was observed to increase linearly with time, with no significant increase in polydispersity. The living nature of the polymerisations under these conditions enables the synthesis of diblock and triblock polymers. Sequential addition of propene and 1-hexene to a MAO activated nickel catalyst results in clean formation of a polypropene-poly(1-hexene) A-B diblock polymer.[62] GPC analysis clearly established that a diblock polymer (and not a mixture of propene and 1-hexene homopolymers) had been formed. Similarly, low polydispersity A-B-A triblock polymers such as poly(1-octene)-polypropene-poly(1-octene) may be prepared. Such polymers with semicrystalline (polyoctene) and amorphous (polypropene) blocks have unusual properties, including high elasticity.

1.14 Objectives of the research in this thesis

The development of catalysts for alkene polymerisations and oligomerisations is clearly a 'hot' topic in current catalytic chemistry. We were specifically interested in catalysts for oligomerisation of ethene and 1-alkenes, and the newer cationic late transition metal catalysts seemed an attractive starting point, rather than the more mature (and heavily patented) neutral systems. A few areas of general interest were apparent to us, and became objectives of the research described in this thesis:

- Organometallic chemistry models for the key reaction steps in the mechanism using more stable systems, in which relevant reactions may lead to isolable intermediates under ambient conditions. Some of this work is described in chapter 2.

- The synthesis of novel carbosilane dendritic wedges and dendrimers, with previously unreported haloalkyl core and terminal functionality. The new wedges in particular were prepared specifically for incorporation as components of catalytic ligands (see below), and the synthetic route to the haloalkyl periphery-functionalised dendrimers arose as a result of the work on the dendritic wedges. This work is described in chapter 3.

- An investigation of the effect of dendritic wedges attached to the aryl rings. Our group is interested in dendrimers and dendritic wedges and in their properties as new materials and applications in catalysis. Functionalisation with dendritic wedges may have interesting effects on the activity, steric control and product distribution (possible non-Schultz-Flory distribution) of oligomerisation

catalysts. Dendritically functionalised catalysts may bridge the gap between homogeneous catalysis and heterogeneous catalysis by enabling catalyst recovery by ultrafiltration techniques. This work is described in chapters 4 (synthesis) and 6 (catalysis)

- An investigation of the effect of electron withdrawing and donating groups on catalytic activity is reported in chapter 5 (synthesis) and chapter 6 (catalysis).

- Efforts toward the synthesis of carbosilane dendrimers with terminal bis(diphenylphosphino)methane functionality are described in chapter 7.

Chapter 2:

Osmium carbonyl compounds as models of late transition metal catalysts for the polymerisation/oligomerisation of 1-alkenes

2.1 Introduction and rationale

As discussed in Chapter 1, early transition metal metallocene and late transition metal bisiminopyridyl and α-diimine systems are examples of successful cationic catalysts for 1-alkene oligomerisations/polymerisations. The active catalytic species in all these systems (Fig. 2-1) have the following key properties:

- cationic 14-electron complex
- coordinatively unsaturated allowing for alkene coordination
- a metal-carbon bond into which a coordinated alkene may insert
- bulky and non-coordinating counterion

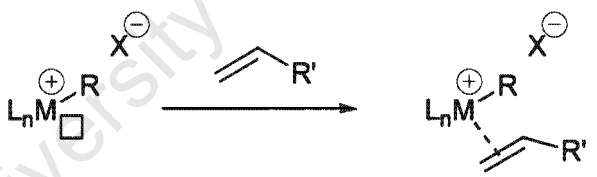

14-electron 16-electron

L_n = non-participating ligand system
M = metal centre
R = growing alkyl chain
X^- = counterion
R' = generalised substituent on alkene
□ = vacant coordination site

Fig. 2-1: Representation of the active catalytic species in the cationic oligomerisation / polymerisation of alkenes showing coordination of an alkene in the vacant coordination site

Since transition metal catalysed homogeneous reactions can be thought of as a series of organometallic reactions with fast kinetics, the principles of organometallic chemistry may be useful in shedding light on

the mechanism of such catalytic reactions. In many homogeneous catalytic processes, such classical organometallic reactions as oxidative addition, reductive elimination, migratory insertions and extrusions, π-coordination and disassociation and attack on metal-coordinated ligands form the basis for the accepted catalytic cycle.[64,65]

Homogeneous catalytic reactions are typically most successful with first and second row transition metals, as these metals display faster kinetics than third row transition metals. Thus organometallic species, which in first and second row transition metal catalytic cycles are transient intermediates, are often stable and isolable in the case of the third row congeners. In this way, the organometallic chemistry of third row transition metals can provide mechanistic information about the catalytic processes of the first and second row metals in the same group.

Since we were interested in late transition metal catalysts for the oligomerisation of 1-alkenes, of which the bisiminopyridyl iron complexes developed by Gibson and Brookhart are the most successful recent examples[17,18], we decided to look at fundamental organometallic chemistry of the iron/ruthenium/osmium group of transition metals. Osmium, as the third row member of this group, is the natural choice for a study of individual catalytically relevant reactions which in iron and ruthenium may lead to kinetically unstable products.

The chemistry of *cis*-$Os(CO)_4Me_2$ (hereafter referred to as $Os(CO)_4Me_2$) has received relatively little attention in the literature, and it seemed that that a study of the reactivity of this fundamentally important organometallic compound would provide an interesting window on the chemistry of alkyl-substituted iron group metals. The carbonyl ligands, while electronically and sterically different from the ligands in a bisiminopyridyl iron complex, provide a useful observational handle for monitoring reactions: IR spectroscopy is particularly informative for the reactions of metal carbonyl compounds.[66] In addition, the chemistry of other metal carbonyl systems has been extensively studied[67], and similar reactions may be anticipated in the case of $Os(CO)_4Me_2$. The carbonyl ligand system may be modified by decarbonylation, substitution and carbonyl insertion reactions[64], which would allow for some control over the electronic and steric environment of the metal centre.

The alkyl substituents may be reactive as well, and in particular it was hoped that a methyl abstraction through the use of CPh_3X (X = non-coordinating counterion) or $B(C_6F_5)_3$ may lead to the formation of a 16-electron, cationic and coordinatively unsaturated species (Fig. 2-2). If the carbonyl ligand framework was modified to include a labile ligand (such as MeCN, THF or Et_2O), the disassociation of this ligand could result in the desired 14-electron species that could be a model for the catalytic species in the oligomerisation reaction (Fig. 2-2).

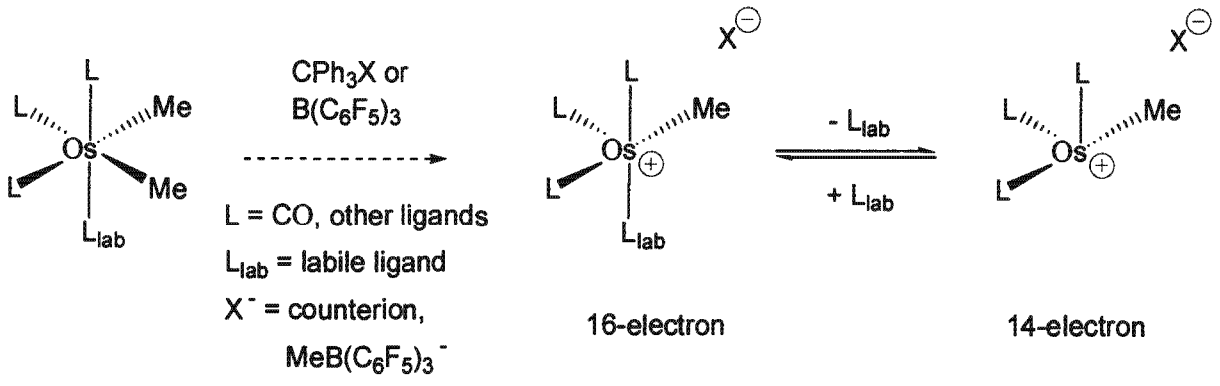

Fig. 2-2: Proposed methyl abstraction and ligand dissociation to give a 14-electron coordinatively unsaturated cationic species

While such speculative reaction schemes may or may not shed light on the mechanism of the alkene oligomerisation reaction, a study of this organometallic system is worthy in its own right. Whereas the chemistry of other simple transition metal carbonyl alkyl systems such as $Mn(CO)_5R$ or $Re(CO)_5R$ has been extensively studied [68,69], few reactions of $Os(CO)_4Me_2$ are described in the literature (see Fig. 2-3).

Substitution of CO by PPh_3 in $Os(CO)_4Me_2$ was reported by thermal[70] and oxidative[71] decarbonylation to form *fac*-$Os(CO)_3(PPh_3)Me_2$. Formation of $Os(CO)_3(PPh_3)_2$ has also been observed upon thermal reaction with excess PPh_3.[72] Treatment of $Os(CO)_4Me_2$ with Br_2 cleaves one Os-Me bond to give $Os(CO)_4MeBr$.[73] Under high CO pressures (130 atm) and at elevated temperature (120°C), $Os(CO)_4Me_2$ is converted to $Os(CO)_5$ with accompanying release of ethane.[73] The same reaction is achieved under milder conditions using laser pyrolysis.[74] Treatment of $Os(CO)_4Me_2$ with cyclooctatetraene (COT) in refluxing octane gives a complicated mixture of products, from which the binuclear complex η-(1,1,1-tricarbonyl-1-osmainden-1-yl)tricarbonylosmium was isolated as the major component.[75]. Thermolysis of $Os(CO)_4Me_2$ (162.5°C) resulted in the formation of CH_4 as the primary organic decomposition product, and various labelling studies were carried out to determine the mechanism of this decomposition.[72,76] Formation of ethane was not observed under the conditions described. $Os(CO)_4Me_2$ reacts with hydrido-osmium complexes such as $Os(CO)_4H_2$ or $Os(CO)_4MeH$ to form binuclear compounds $HOs_2(CO)_8Me$ and a mixture of $MeOs_2(CO)_8Me$ and $HOs_2(CO)_8Me$ respectively.[71] Finally, $Os(CO)_4Me_2$ reacts with anhydrous HF to form *cis*-$Os(CO)_4F_2$, which cannot be isolated and partially dimerises in solution.[77]

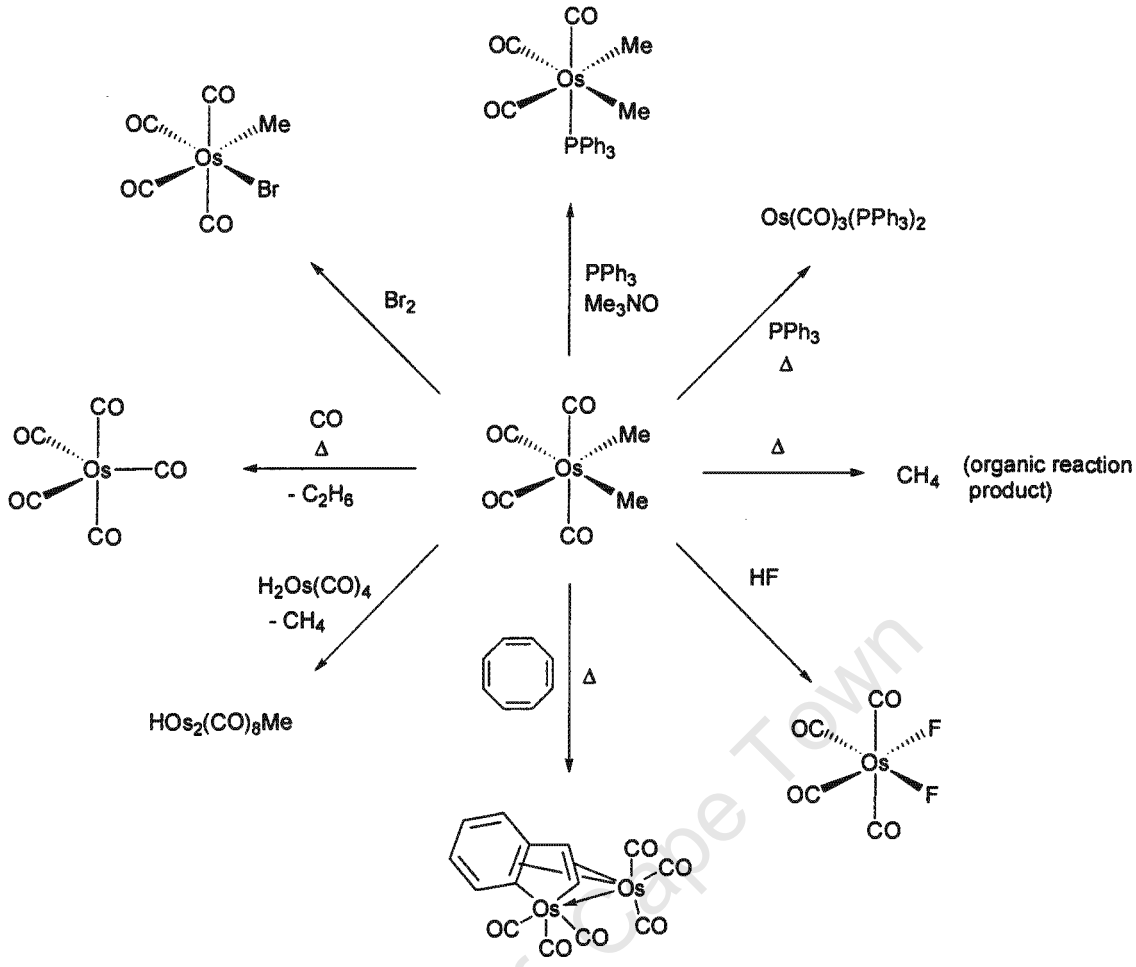

Fig. 2-3: Literature reactions of cis-Os(CO)$_4$Me$_2$

2.2 Synthesis of osmium carbonyl dimethyl compounds

2.2.1 Synthesis of Os(CO)$_4$Me$_2$ (1)

Several preparations of Os(CO)$_4$Me$_2$ have been reported in the literature.[71,73,78] All preparations involve the initial reduction of Os$_3$(CO)$_{12}$ in liquid ammonia by Na to form Na$_2$Os(CO)$_4$. This salt can then be isolated and reacted with MeI in an ethereal solvent such as THF.[73] In one preparation, Na$_2$Os(CO)$_4$ was treated with methyl tosylate in tetraglyme; the use of the involatile methylation reagent and solvent allows the volatile Os(CO)$_4$Me$_2$ to be isolated by high vacuum techniques.[71] In our case it was more convenient to react the freshly prepared Na$_2$Os(CO)$_4$ with MeI directly in the liquid ammonia (Fig. 2-4).[78] The reaction even at this low temperature (-78°C) is instantaneous, as can be seen by the immediate dissolution of the suspended Na$_2$Os(CO)$_4$. After removing the liquid ammonia by warming to room temperature, the Os(CO)$_4$Me$_2$ (**1**) is recovered by sublimation at 60°C under vacuum (c.a. 1mm).

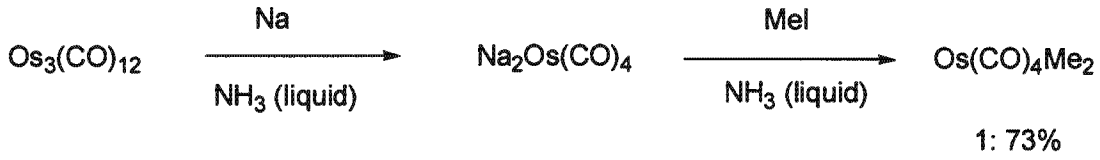

Fig. 2-4: Synthesis of $Os(CO)_4Me_2$ (1)

2.2.2 Synthesis of $Os(CO)_3(L_{labile})Me_2$ (L_{labile} = MeCN, THF)

Substitution of one or more carbonyl ligands from a metal carbonyl compound can be achieved in certain cases by treatment with the decarbonylation reagent Me_3NO in the presence of a suitable ligand.[79-81] The carbonyl ligand is oxidised by Me_3NO to form CO_2 which disassociates from the metal centre. NMe_3 weakly coordinates in its place and is then displaced by the incoming ligand (Fig. 2-5).

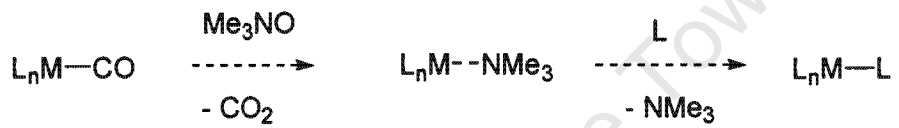

Fig. 2-5: Decarbonylation reaction with Me_3NO

For example, $Os_3(CO)_{12}$ may be decarbonylated by treatment with the appropriate amount of Me_3NO in MeCN to give $Os_3(CO)_{11}(NCMe)$ or $Os_3(CO)_{10}(NCMe)_2$.[82] These complexes may be substituted with a wide range of other donor ligands by displacement of the labile MeCN ligand(s), and are thus very important reaction intermediates in osmium cluster chemistry.

Me_3NO mediated decarbonylation is dependent on the electronic environment of the metal carbonyl system.[83] The M-CO bond must be sufficiently weak for decarbonylation to take place; in other words, the coordinated carbonyl must be sufficiently electrophilic to react with the Me_3NO. This means that strong electron donating ligands such as phosphines deactivate the carbonyls for oxidative decarbonylations in metal carbonyl systems. An empirical observation is that only CO ligands with IR absorptions above $2000cm^{-1}$ are susceptible to Me_3NO mediated decarbonylation.[79,80] Exceptions to this rule of thumb have been reported.[83]

Me_3NO mediated decarbonylation of $Os(CO)_4Me_2$ has been reported in one instance in the literature. Treatment of $Os(CO)_4Me_2$ with Me_3NO in the presence of PPh_3 results in formation of *fac*-$Os(CO)_3(PPh_3)Me_2$.[71] The reaction was carried out with a mixture of MeCN and CH_2Cl_2 as the solvent, and it is not clear if the reaction proceeds via the acetonitrile adduct or directly to the triphenylphosphine complex. In any event, $Os(CO)_3(NCMe)Me_2$ was not isolated.

Our interest in the incorporation of a labile ligand into the system led us to attempt the synthesis of $Os(CO)_3(L_{labile})Me_2$ (where L_{labile} = MeCN, THF) by decarbonylation of $Os(CO)_4Me_2$. *Fac*-$Os(CO)_3(NCMe)Me_2$ (**2**, hereafter $Os(CO)_3(NCMe)Me_2$) was prepared by reaction of $Os(CO)_4Me_2$ with an excess of Me_3NO in acetonitrile (Fig. 2-6). The reaction may be followed by IR spectroscopy, with new υ_{CO} bands characteristic of a *fac*-tricarbonyl developing at 2072s and 1980vs cm^{-1}. Excess Me_3NO did not result in a second decarbonylation, and the *fac* isomer of the products was exclusively obtained in good yield. $Os(CO)_3(NCMe)Me_2$ is a white, involatile crystalline compound, m.p. 104-107°C. In the solid form the compound is stable in air for long periods of time. It is apparent that the MeCN ligand is quite strongly coordinated to the metal centre.

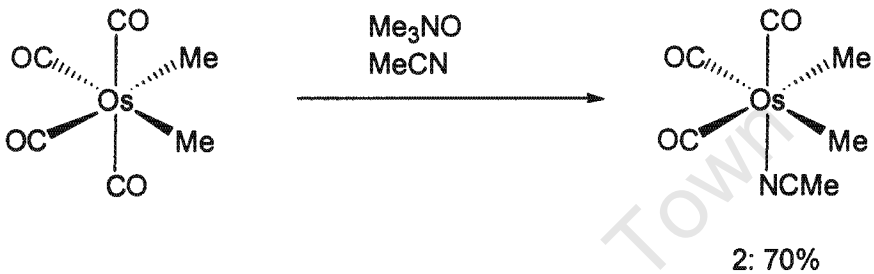

Fig. 2-6: Preparation of $Os(CO)_3(NCMe)Me_2$ (2)

The ^1H NMR spectra of $Os(CO)_3(NCMe)Me_2$ in both $CDCl_3$ and C_6D_6 are shown below (Fig. 2-7). The interest in the comparison lies in the shift in the Os-NC*Me* singlet from 2.45ppm to 0.27ppm and of the Os-*Me* peak from 0.06 to 0.58. This is definitely due to NMR environment and not irreversible reaction with solvent, as the same sample may be run consecutively in the two different solvents, and the same spectrum is obtained. The reason for this enormous shift is possibly due to the π-stacking effects in the deutero-benzene solvent. This is also apparent in the observed fine structure of the methyl signals in the C_6D_6 spectrum, where barriers to rotation on an NMR time-scale imposed by π-stacking in the solvent renders the methyl protons non-equivalent.

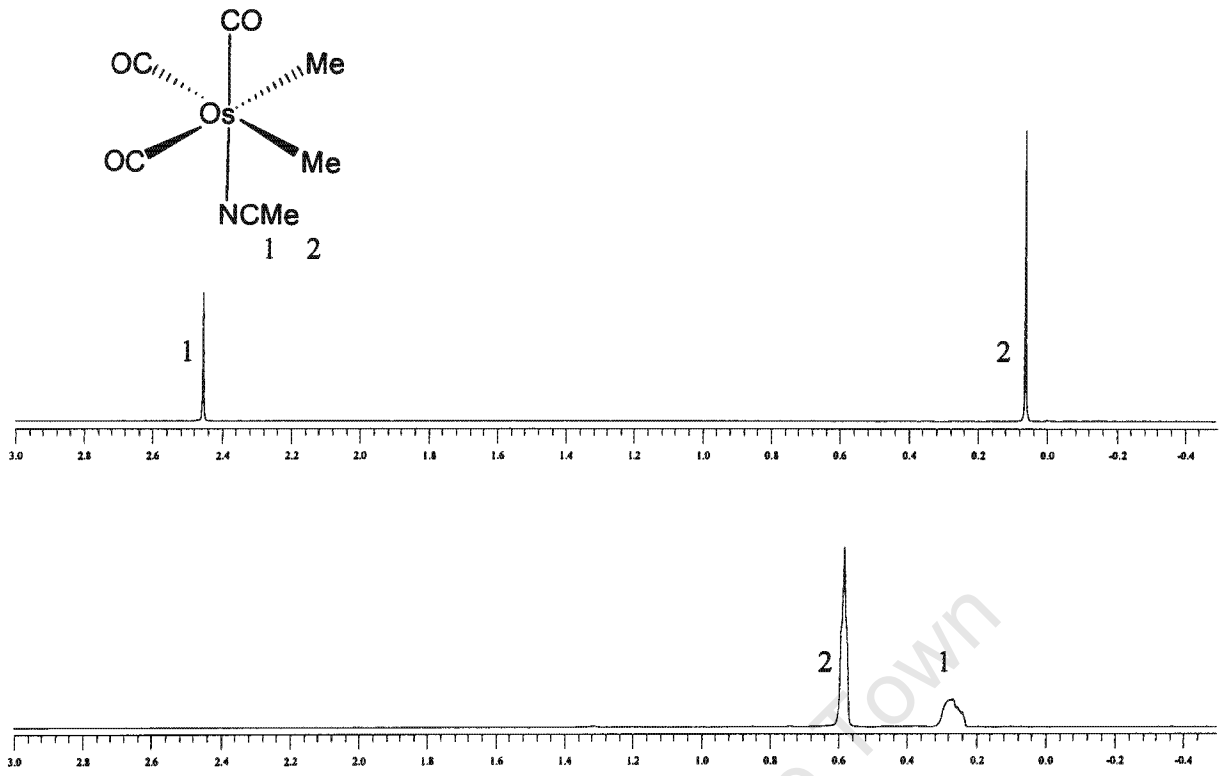

Fig. 2-7: ^1H NMR spectra of $Os(CO)_3(NCMe)Me_2$ in $CDCl_3$ (top) and C_6D_6 (bottom)

$Os(CO)_3(THF)Me_2$ (**3**) was prepared similarly to $Os(CO)_3(NCMe)Me_2$. Upon treatment of $Os(CO)_4Me_2$ with excess Me_3NO in THF, IR spectroscopy indicated the clean formation of a new *fac*-tricarbonyl in solution (υ_{CO} = 2068s, 1979vs cm^{-1}). However attempts at isolation failed as the product decomposes within a few minutes under vacuum. This is presumably because the THF ligand is so labile that it freely dissociates and is removed under vacuum, leaving the unstable 16-electron complex, $Os(CO)_3Me_2$. Nevertheless, $Os(CO)_3(THF)Me_2$ is stable as a THF solution, and it may be adequately characterised by its IR spectrum and by its analogous reactivity to $Os(CO)_3(NCMe)Me_2$ (see sections 2.2.3 and 2.3.1).

2.2.3 Substitutions with PPh_3: the limits of Me_3NO mediated decarbonylation

The previously reported[71] compound *fac*-$Os(CO)_3(PPh_3)Me_2$ (**4**, hereafter $Os(CO)_3(PPh_3)Me_2$) was prepared in a new synthesis by displacement of the MeCN ligand in $Os(CO)_3(NCMe)Me_2$ by PPh_3 (Fig. 2-8). The reaction took place slowly and at 50°C in toluene required 5 days before completion, as indicated by monitoring the reaction with IR spectroscopy. At 75°C the reaction was completed in 48h. $Os(CO)_3(PPh_3)Me_2$ was obtained as a pure crystalline product, m.p. 119-122°C, in 77% yield after column chromatography. Its characterisation data was in agreement with the literature[71], and unreported data such as the melting point and ^{13}C and ^{31}P NMR spectra were obtained. $Os(CO)_3(PPh_3)Me_2$ may similarly be prepared by treatment of a freshly prepared THF solution of $Os(CO)_3(THF)Me_2$ (see section 2.2.2) with PPh_3, and this reaction serves as characterisation for the non-isolable $Os(CO)_3(THF)Me_2$.

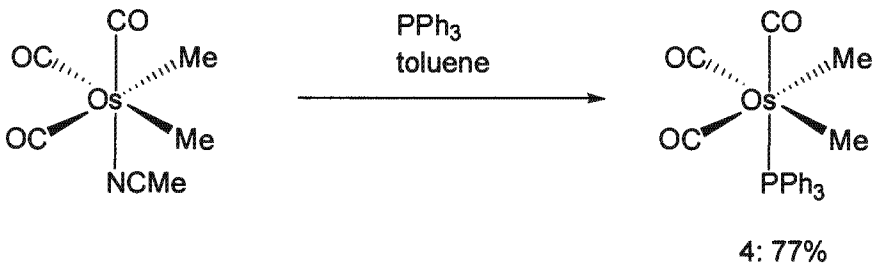

4: 77%

Fig. 2-8: Preparation of $Os(CO)_3(PPh_3)Me_2$ (4)

A further decarbonylation of $Os(CO)_3(PPh_3)Me_2$ was found to be possible. *cis,cis*-$Os(CO)_2(PPh_3)(NCMe)Me_2$ (**5**) was prepared by reaction of $Os(CO)_3(PPh_3)Me_2$ with an excess of Me_3NO in acetonitrile (Fig. 2-9). The reaction is slower than the analogous reaction of $Os(CO)_4Me_2$ with Me_3NO in acetonitrile. The product is obtained as a white powder in 67% yield after column chromatography.

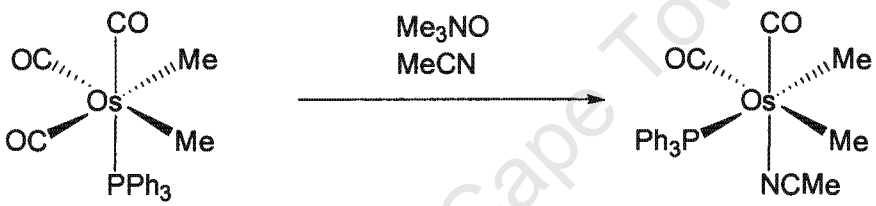

5: 67%

Fig. 2-9: Synthesis of $Os(CO)_2(PPh_3)(NCMe)Me_2$ (5)

The solid is unstable and significant decomposition is observed within a few hours of isolation of the solid. The poorer π-accepting phosphine ligand increases electron density on the metal centre, thereby decreasing the strength of the coordination between osmium and MeCN. Full characterisation was not possible, but IR, ^1H and ^{31}P NMR and mass spectrometry confirm the presence of the desired product.

The stereochemistry of *cis,cis*-$Os(CO)_2(PPh_3)(NCMe)Me_2$ is noteworthy. From the ^1H NMR evidence (the spectrum was run in C_6D_6), and in particular the significant difference in the chemical shifts and $^3J(PH)$ coupling constants of the methyl signals (Fig. 2-10), the complex has been assigned a stereochemistry with the MeCN ligand *cis* to the two methyls and the PPh_3 ligand *trans* to a methyl (Fig. 2-10). The methyl *trans* to PPh_3 is located upfield (0.49ppm) and has a greater $^3J(PH)$ coupling (8Hz) than the methyl *cis* to PPh_3 (1.25ppm, $^3J(PH)$ 4Hz). The expected configuration with the PPh_3 remaining *cis* to both methyls would result in similar chemical shifts and particularly similar $^3J(PH)$ coupling constants for the two methyl signals. The position of the Os-NC*Me* signal at 0.26ppm is consistent with the same signal in the ^1H NMR spectrum of $Os(CO)_3(NCMe)Me_2$ (0.20ppm) when run in C_6D_6 (Fig. 2-10), and a small $^5J(PH)$ coupling is observed (1.5Hz).

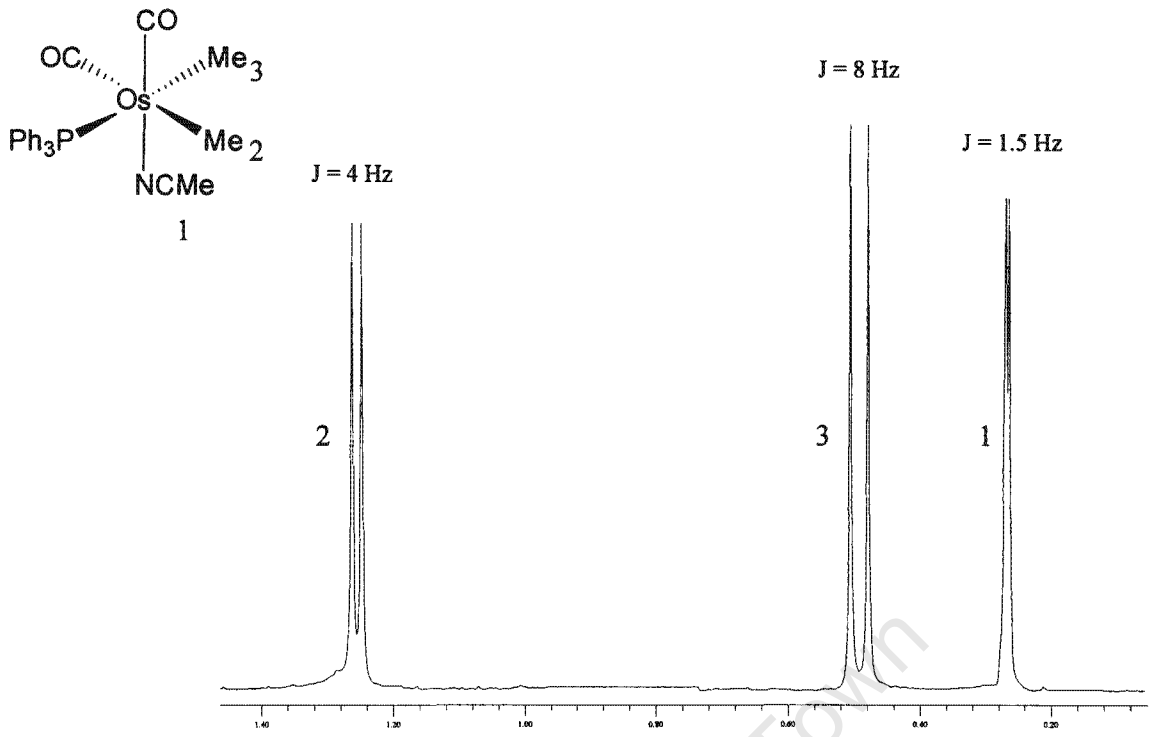

Fig. 2-10: ^1H NMR spectrum of $Os(CO)_2(PPh_3)(NCMe)Me_2$ (5)

This stereochemistry of the reaction may be rationalised by assuming a pentacoordinate 16 electron intermediate $[Os(CO)_2(PPh_3)Me_2]$ which loses its octahedral configuration (Fig. 2-11). The incoming acetonitrile then coordinates to the metal centre, re-establishing the octahedral centre with a stereochemistry not dictated directly by the initial octahedral arrangement. It is not immediately clear why the reaction gives the single isomer so selectively. One possibility is that a kinetic mixture of isomers is initially formed, but because of the lability of the acetonitrile, isomerisation to the thermodynamically favoured isomer subsequently takes place.

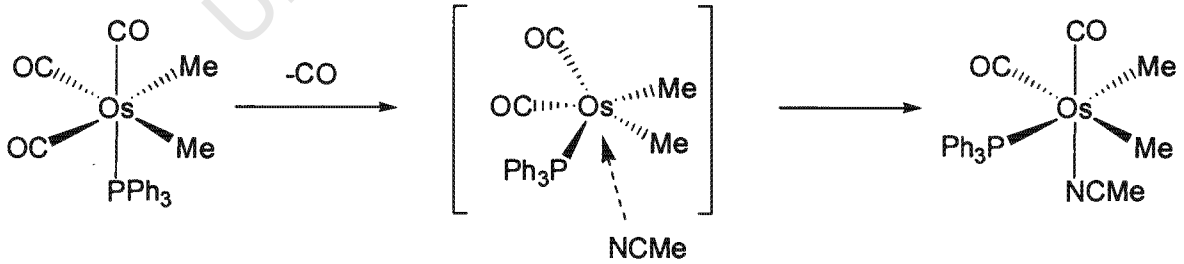

Fig. 2-11: Formation of $Os(CO)_2(PPh_3)(NCMe)Me_2$ showing the postulated pentacoordinate intermediate and the orthogonally directed attack of the incoming MeCN ligand

Substitution of the MeCN ligand in $Os(CO)_2(PPh_3)(NCMe)Me_2$ by a second PPh_3 would be expected to be a facile reaction given the lability of the MeCN. The reaction with PPh_3 is usefully observed by IR spectroscopy, and it is apparent that after 1h at 60°C in toluene the substitution of MeCN by PPh_3 is

complete (new bands characteristic of a *cis*-dicarbonyl at 2006 and 1915cm^{-1}). However, after 3h, an isomerisation is observed, with the bands at 2006 and 1915cm^{-1} being replaced by new bands at 1985 and 1912cm^{-1}. After 16h, IR spectroscopy indicates that this isomerisation is complete. Upon isolation of the product, the expected compound $Os(CO)_2(PPh_3)_2Me_2$ is indeed obtained (Fig. 2-12), although an interesting stereochemical isomerisation has taken place. Substitution of the MeCN by PPh_3 gives the IR observed intermediate (υ_{CO} = 2006, 1915cm^{-1}) with similar stereochemistry to the starting material (Fig. 2-12). However, isomerisation results in a shift of the PPh_3 *trans* to the methyl to the *cis* position, such that the two PPh_3 ligands are *trans* to each other (Fig. 2-12). This isomerisation is presumably sterically directed, with the bulky PPh_3 ligands favouring a *trans* configuration, giving *cis,trans*-$Os(CO)_2(PPh_3)_2Me_2$ (**6**) as the exclusively isolated stereoisomer.

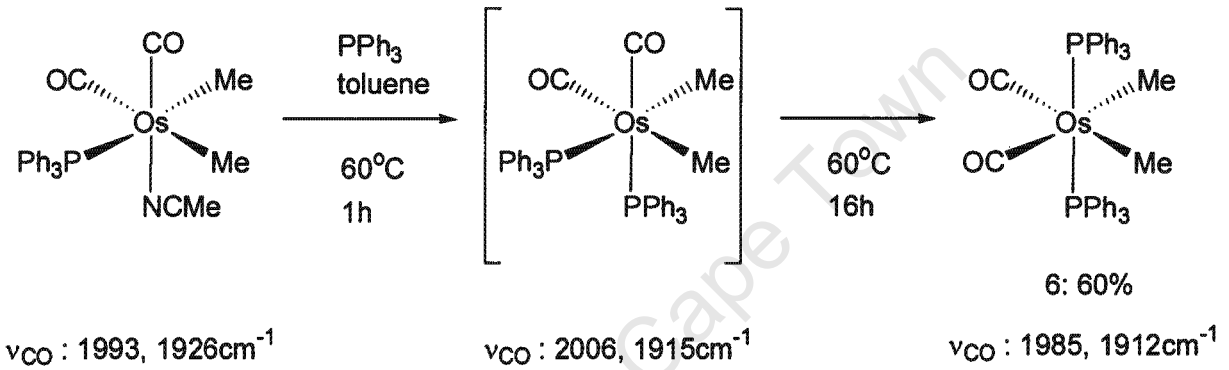

Fig. 2-12: The reaction of $Os(CO)_2(PPh_3)(NCMe)Me_2$ with PPh_3

The NMR evidence is again extremely powerful in assigning the stereochemistry (Fig. 2-13). In the ^{1}H NMR spectrum of **6**, a single signal for the two methyl ligands is observed. This signal is observed as a triplet (^3J(PH) 8Hz) as a result of coupling to two equivalent phosphorus nuclei. One singlet is observed in the ^{31}P NMR spectrum (Fig. 2-13, inset). This indicates that the two phosphines are chemically equivalent. Non-equivalent phosphines would obviously have signals at different chemical shifts, and would also show a large ^2J(PP) coupling, as can be seen with other diphosphine osmium complexes discussed in section 2.3.

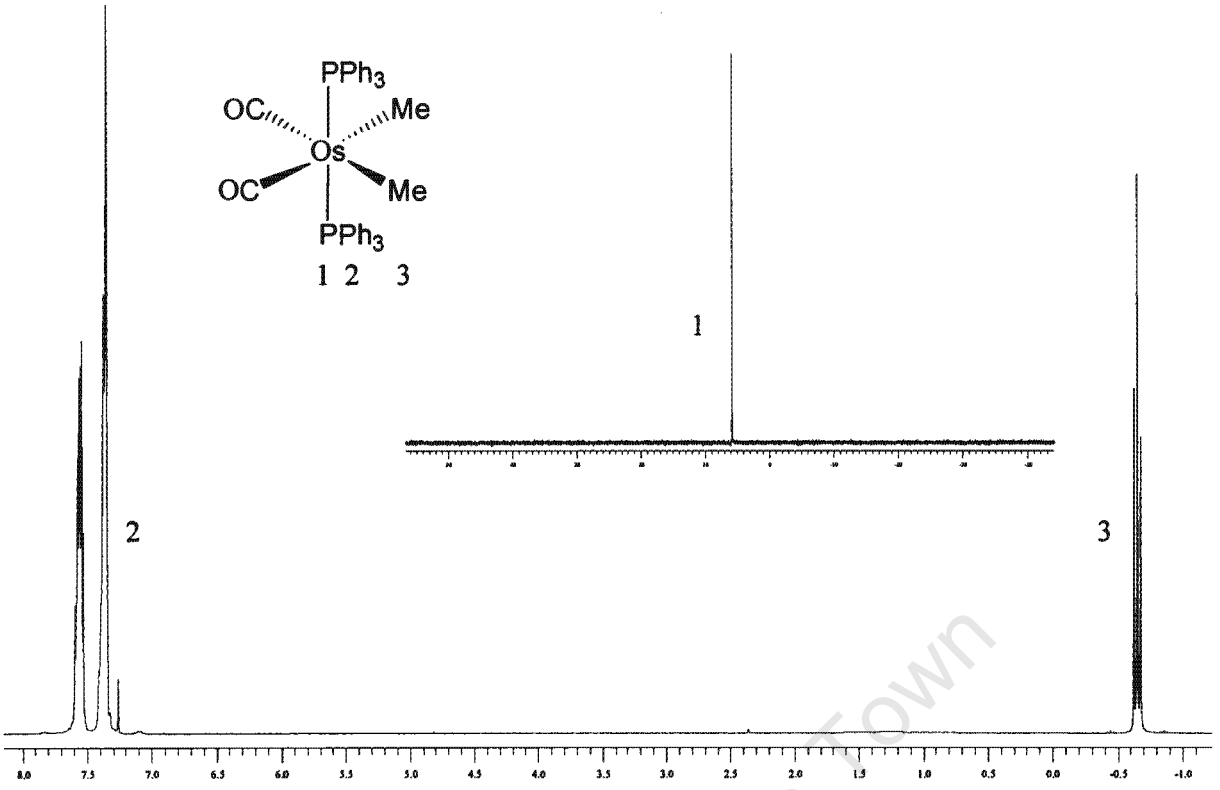

Fig. 2-13: ^{1}H and ^{31}P (inset) NMR spectra of cis,trans-$Os(CO)_2(PPh_3)Me_2$ (6)

A similar compound with the same stereochemistry, *cis,trans*-$Os(CO)_2(PMe_3)Me_2$, has reportedly been prepared by a different route.[84] Treatment of *fac*-$[Os(CO)_3(PMe_2)Me]BPh_4$ (derived from *cis,trans*-$Os(CO)_2(PPh_3)_2MeI$[85]) with MeLi gives *cis,trans*-$Os(CO)_2(PMe_3)Me_2$ in 54% yield. Direct treatment of *cis,trans*-$Os(CO)_2(PPh_3)_2MeI$ with MeLi does not give quantitative conversion to *cis,trans*-$Os(CO)_2(PMe_3)Me_2$, even when excess MeLi is used.[84]

Further reaction of $Os(CO)_2(PPh_3)Me_2$ with Me_3NO proved impossible under the conditions attempted (Fig. 2-14). Even after refluxing in MeCN with a large excess of Me_3NO for 72h, no observable decarbonylation reaction was detected by IR spectroscopy, and the sparingly soluble starting material persisted. This is due to the increased electron density on the osmium centre introduced by the phosphine ligands. This renders the carbonyls less electrophilic and thus unreactive towards Me_3NO. The rule of thumb that only carbonyls with CO stretches above $2000cm^{-1}$ are susceptible to Me_3NO mediated decarbonylation[79,80] applies here ($Os(CO)_2(PPh_3)_2Me_2$: υ_{CO} = 1985, $1912cm^{-1}$).

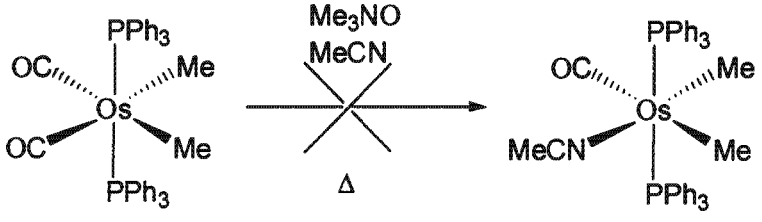

Fig. 2-14: Attempted reaction of $Os(CO)_2(PPh_3)Me_2$ with Me_3NO / MeCN

2.3 Reactions of $Os(CO)_3(L_{labile})Me_2$ with bidentate ligands

2.3.1 Reactions of $Os(CO)_3(L_{labile})Me_2$ (L_{labile} = MeCN, THF) with 2,2'-bipyridyl (bipy), bis(diphenylphosphino)methane (dppm) and bis(diphenylphosphino)ethane (dppe)

The electronic effect of different ligands on the reactivity of the Os-Me bonds is likely to be significant. Carbonyl ligands withdraw electron density from the metal centre through back-bonding; thus strengthening the Os-Me bonds and reducing their reactivity. It is therefore desirable in order to obtain a degree of control over the reactivity of the Os-Me bonds to introduce more electron donating ligands such as phosphine and nitrogen containing ligands. In section 2.2, the modification of the $Os(CO)_4Me_2$ system with monodentate ligands such as PPh_3 and MeCN was investigated. Our attention now turned to bidentate ligands, because of the stability that their chelating ability confers and the interesting chemistry that may result.

It was initially anticipated that reaction of $Os(CO)_3(L_{labile})Me_2$ (L_{labile} = MeCN, THF) with a bidentate ligand (L^L) might result in the formation of the product $Os(CO)_2(L^L)Me_2$ by displacement of the labile ligand by one coordination site and subsequent thermally induced decarbonylation and chelation by the second coordination site (Fig. 2-15).

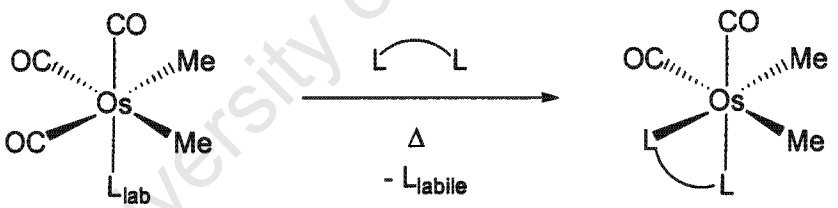

Fig. 2-15: Anticipated reaction of $Os(CO)_3(L_{labile})Me_2$ with bidentate ligands

The first such reaction attempted was between $Os(CO)_3(NCMe)Me_2$ and 2,2'-bipyridyl. Stoichiometric equivalents of the two reagents were stirred together in toluene at 50°C for 5 days. A bright orange solution suggested the formation of a bipy complex. The reaction was monitored by IR spectroscopy, and development of new bands at 1992 and 1916cm^{-1}, consistent with the presence of a *cis*-dicarbonyl, suggested the formation of the expected product. However, upon isolation of the bright orange crystalline product, a different structure was elucidated (Fig. 2-16). The labile MeCN is indeed displaced by the 2,2'bipyridyl; however a methyl migration onto carbonyl and not a decarbonylation accompanies chelation. The resulting product, $Os(CO)_2$(2,2'-bipy)(COMe)Me (7) has an acyl as well as a methyl substituent.

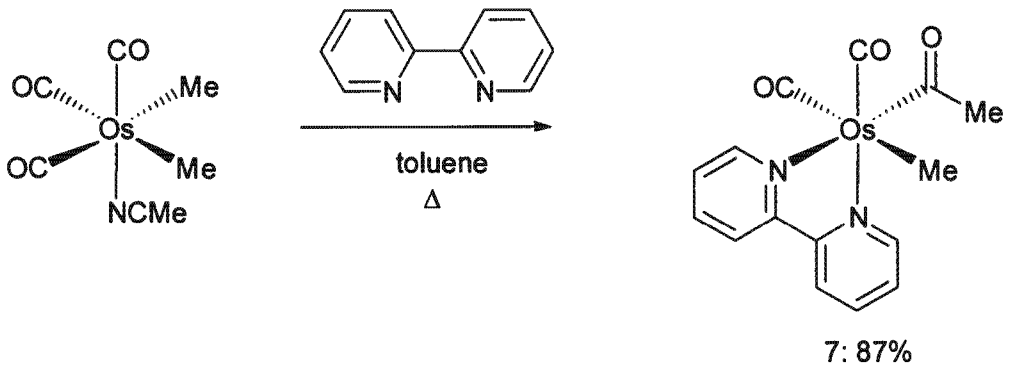

Fig. 2-16: The reaction between $Os(CO)_3(NCMe)Me_2$ and 2,2'-bipyridyl to give 7

Characterisation of this novel compound was carried out by elemental analysis, NMR and IR spectroscopy and mass spectrometry. Upon closer examination of the IR spectrum, the acyl band at 1584cm^{-1} is observed. In the ^{1}H NMR spectrum, the two methyl signals (Os-CO*Me* and Os-*Me*) can be seen as singlets at 3.15 and -0.01ppm respectively. The molecular ion (less a proton) at 461amu is observed in the mass spectrum under electron ionisation conditions. The observed fragmentation pattern is consistent with the loss of Me and CO fragments from the parent ion. Some dimerisation under the ionisation conditions is also observed in the mass spectrum.

The stereochemistry of this compound (COMe *trans* to bipy, Me *trans* to CO) is assigned by analogy to a similar compound prepared with dppm (see below), where couplings to phosphorus in the ^{1}H NMR and a crystal structure confirm the stereochemistry.

$Os(CO)_2$(2,2'-bipy)(COMe)Me may also be prepared by treatment of a freshly prepared THF solution of $Os(CO)_3(THF)Me_2$ with 2,2'-bipyridyl. After reflux for 48h, the orange product was isolated and identified by spectroscopic means as $Os(CO)_2$(2,2'-bipy)(COMe)Me.

Further decarbonylation of $Os(CO)_2$(2,2'-bipy)(COMe)Me using Me_3NO was found to be impossible. Despite stirring for an extended period of time at elevated temperature with a large excess of Me_3NO in MeCN, no reaction was observed, as indicated by monitoring the reaction with IR spectroscopy. This is to be expected, as the υ_{CO} bands of $Os(CO)_2$(2,2'-bipy)(COMe)Me (1992, 1916cm^{-1}) are below 2000cm^{-1}.[79,80]

The reactions between $Os(CO)_3(NCMe)Me_2$ and bis(diphenylphosphino)methane (dppm) or 1,2-bis(diphenylphosphino)ethane (dppe) proceed in a similar way to the reaction with 2,2'-bipyridyl (Fig. 2-17).

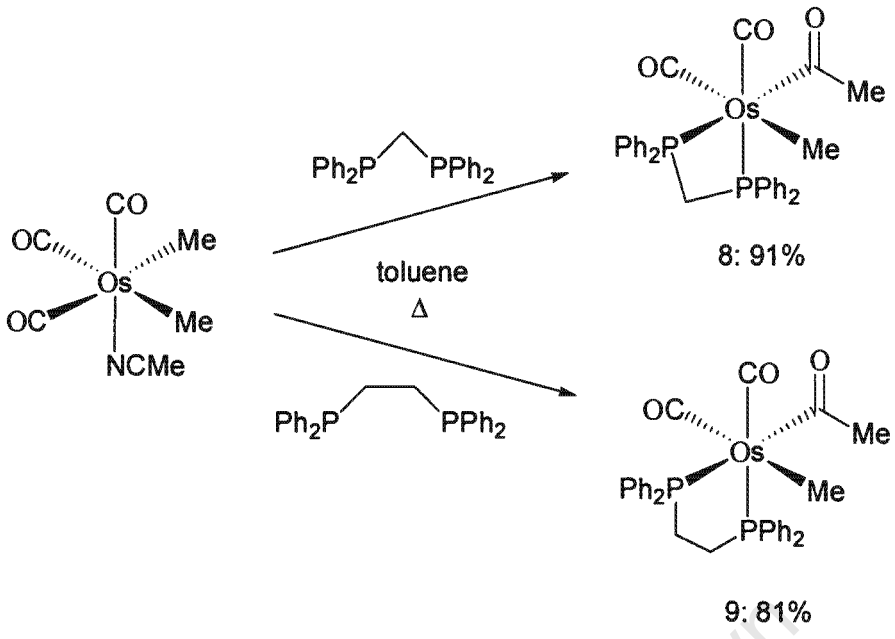

*Fig. 2-17: Reactions of $Os(CO)_3(NCMe)Me_2$ with dppm and dppe to give **8** and **9***

The reactions again proceed selectively in toluene at 70°C to form $Os(CO)_2$(dppm)(COMe)Me (**8**) and $Os(CO)_2$(dppe)(COMe)Me (**9**) in excellent yield. These new complexes were fully characterised by elemental analysis, NMR and IR spectroscopy and mass spectrometry. The ^1H and ^{31}P NMR spectra of $Os(CO)_2$(dppm)(COMe)Me are shown in Fig. 2-18 and Fig. 2-19 respectively. (The displayed spectra were run in C_6D_6, so the observed chemical shifts are different from those reported in the experimental system. The shifts as observed in $CDCl_3$ are reported in the experimental section in order to be consistent with other osmium compounds run in $CDCl_3$.) In the ^1H NMR spectrum (Fig. 2-18), the difference in chemical environment of the two methyl signals is clearly illustrated by their chemical shifts and multiplicities. The acyl methyl (Os-CO*Me*) appears as a singlet at 2.87ppm, whereas the alkyl methyl (Os-*Me*) appears as a triplet at 0.34ppm as a result of ^3J(PH) coupling to two phosphorus atoms. This multiplicity also confirms the assigned stereochemistry of the complex, with both phosphine coordination sites *cis* to the methyl group. Although the phosphines are chemically non-equivalent, the ^3J(PH) couplings are identical (10Hz), giving rise to a triplet, which conforms their *cis* orientation to the methyl.

The two protons on the bridging methylene of the dppm moiety are chemically non-equivalent as a result of their fixed spacial arrangements, and can be seen as doublets of triplets (^2J(HH) 16Hz, ^2J(PH) 9 and 10Hz) at 4.37 and 4.16ppm (Fig. 2-18). Second order distortion as a result of the relatively large ^2J(HH) coupling (16Hz) relative to the difference in chemical shifts of the two protons (82Hz) explains the greater intensities of the 'inner' peaks.[86] As a rule of thumb, in cases where the coupling is greater than 10% of the difference in chemical shifts, these distortions are commonly observed.[87]

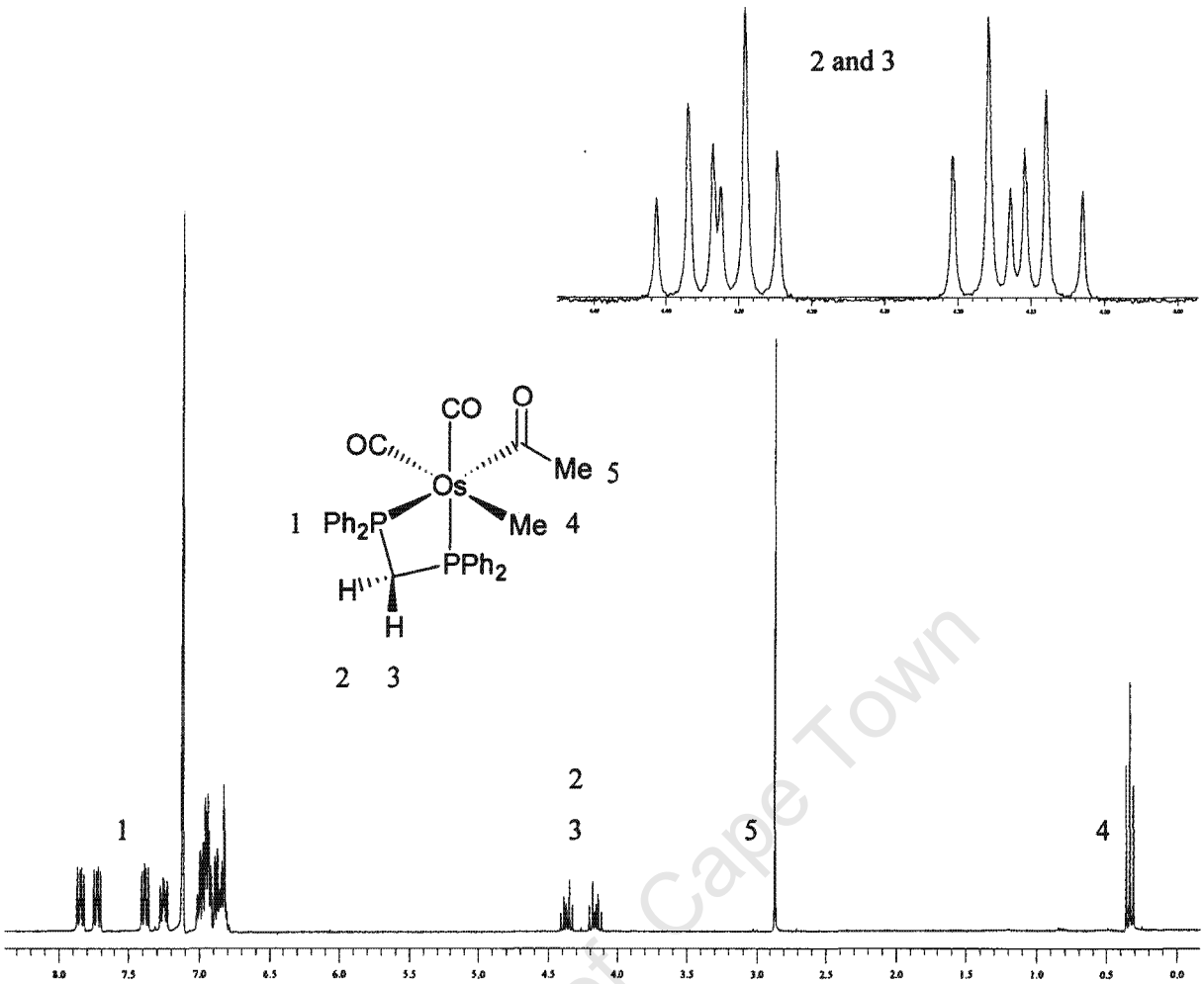

Fig. 2-18: ^{1}H NMR spectrum of $Os(CO)_2(dppm)(COMe)Me$, showing an expansion of the bridging methylene protons from the dppm

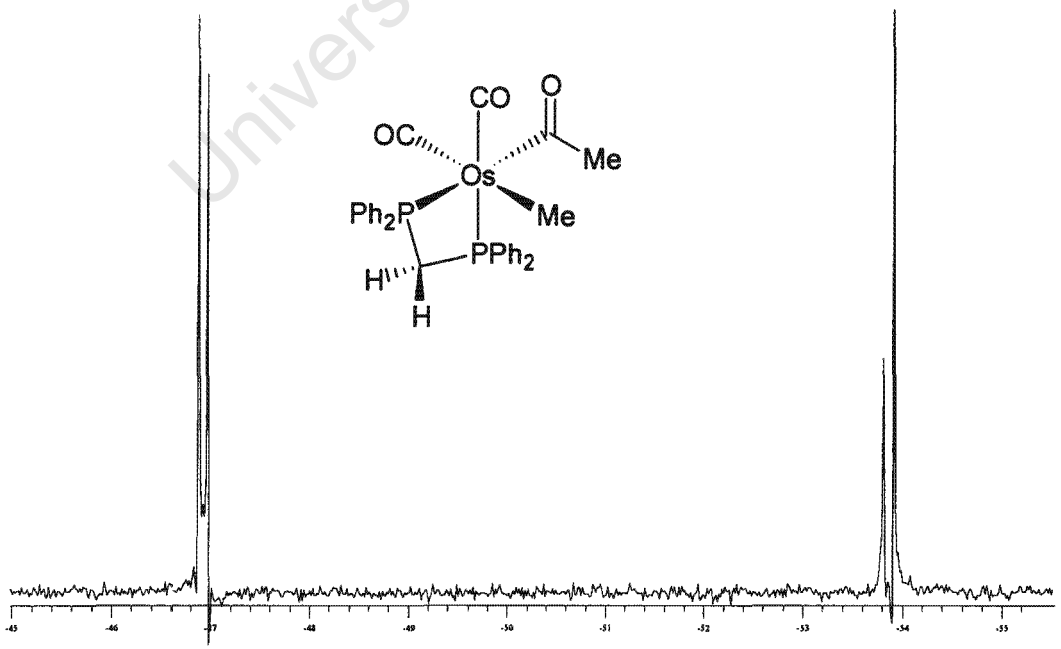

Fig. 2-19: ^{31}P NMR spectrum of $Os(CO)_2(dppm)(COMe)Me$ (the poor phasing apparent in this spectrum is due to a software problem for ^{31}P NMR spectra; despite appearances, the signals are both 1:1 doublets)

The ^{31}P NMR spectrum of $Os(CO)_2(dppm)(COMe)Me$ (Fig. 2-19) shows two signals at different chemical shifts (-46.9 and -53.9ppm), and the $^2J(PP)$ coupling (11Hz) is clearly observed.

Alkyl migrations onto metal carbonyls are extremely well established in organometallic chemistry and are important in catalysis. These reactions have been the subject of several reviews[88,89] and theoretical studies[90] In many systems such as $Mn(CO)_5R$ and $CpFe(CO)_2R$ (R = alkyl), reactions with ligands such as phosphines demonstrate that alkyl migration onto CO is preferred over carbonyl displacement (although the resulting acyl species may decarbonylate as a second step after the carbonyl insertion).

The reactions of chelating ligands (for example diphosphines) with $Mn(CO)_5Me$ have been studied.[91,92] The resulting products, $Mn(CO)_3(L\hat{}L)(COMe)$, are reported to be formed by a two step mechanism, involving a first step in which monosubstitution by one phosphine causes a methyl migration onto CO, and a second step in which chelation by the second phosphine displaces a second CO.[92] The order of these two steps establishes the preference for methyl migration onto CO over CO displacement.

Methyl migrations usually result in the incoming ligand coordinating *cis* to the newly formed acyl group.[93,94] The migration takes place onto a *cis*-CO, leaving a vacant coordination site *cis* to the acyl into which the incoming ligand may coordinate (Fig. 2-20).[90] However exceptions to this have been reported in the case of some octahedral complexes of Fe, Ru, Rh, Ir and Mn, in which the incoming ligand coordinates *trans* to the acyl.[93,95-99]

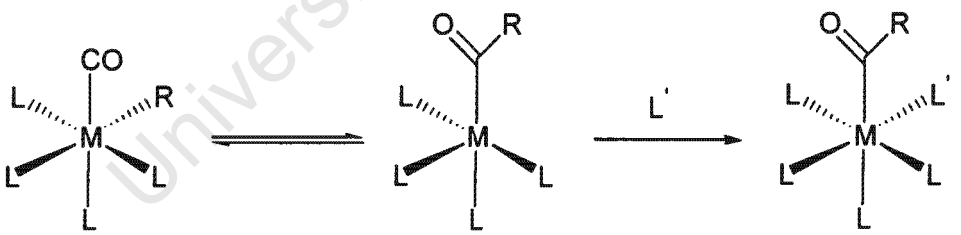

Fig. 2-20: Mechanism of the alkyl migration resulting in cis orientation of incoming ligand (L') to the acyl

Some comments on the mechanism of formation and stereochemistry of $Os(CO)_2(L\hat{}L)(COMe)Me$ can be made. It is believed that the first step is displacement of the labile MeCN ligand (Fig. 2-21). This is surmised by IR evidence from the reaction of $Os(CO)_3(NCMe)Me_2$ with dppp (see section 2.3.3), in which the monosubstituted intermediate can be clearly observed, and also by the reaction of $Os(CO)_3(NCMe)Me_2$ with PPh_3 (Fig. 2-8), in which the MeCN-substituted product $Os(CO)_3(PPh_3)Me_2$ (**4**) and not the carbonyl-insertion product $Os(CO)_2(PPh_3)(NCMe)(COMe)Me$ is exclusively formed. The second step is methyl migration onto the carbonyl *trans* to coordinated phosphine, and chelation by the second phosphine into the vacant coordination site *cis* to the newly formed acyl (Fig. 2-21).

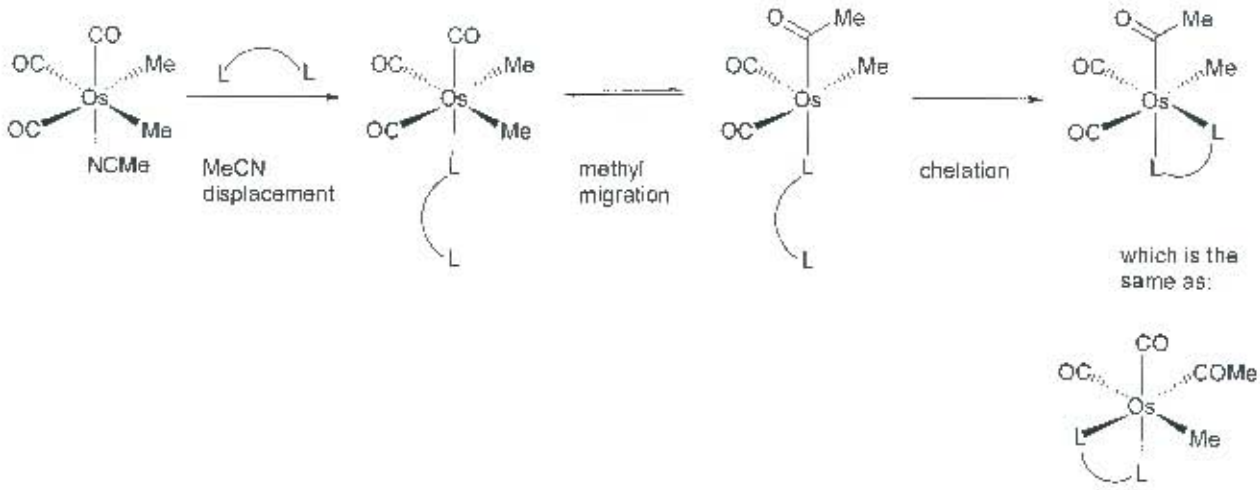

Fig. 2-21: Mechanism and stereochemistry of the formation of $Os(CO)_2(L^{\wedge}L)(COMe)Me$

To the best of our knowledge, the compounds $Os(CO)_2(L^{\wedge}L)(COMe)Me$ ($L^{\wedge}L$ = bipy, dppm, dppe) are the first isolated osmium complexes with both alkyl and acyl ligands. The osmium(VI) compound $Os(=NMe)(COMe)Me_3$ was spectroscopically observed, although not isolated.[100] Iron (spectroscopically observed) and ruthenium (isolated) complexes with acyl and alkyl ligands have also been reported.[84,101-105]

In this regard, the literature reaction of *fac*-$[Os(CO)_3(PMe_3)_2Me]BPh_4$ with MeLi to give *cis,trans*-$Os(CO)_2(PMe_3)_2Me_2$ (Fig. 2-22) is particularly interesting.[84] The postulated reaction mechanism involves the formation of the intermediate *cis,trans*-$Os(CO)_2(PMe_3)_2(COMe)Me$ by nucleophilic attack by Me^- at the carbonyl (Fig. 2-22). However this proposed intermediate decarbonylates immediately to form the dimethyl compound, and is neither isolated nor observed spectroscopically. It is interesting that this proposed acyl intermediate is so much less stable than the compounds $Os(CO)_2(L^{\wedge}L)(COMe)Me$ ($L^{\wedge}L$ – bipy, dppm, dppe) described above. In these compounds, the presence of the electron donating ligand *trans* to the acyl group may stabilise the acyl species so that decarbonylation is only achieved under harsh thermolytic conditions (see section 2.3.3).

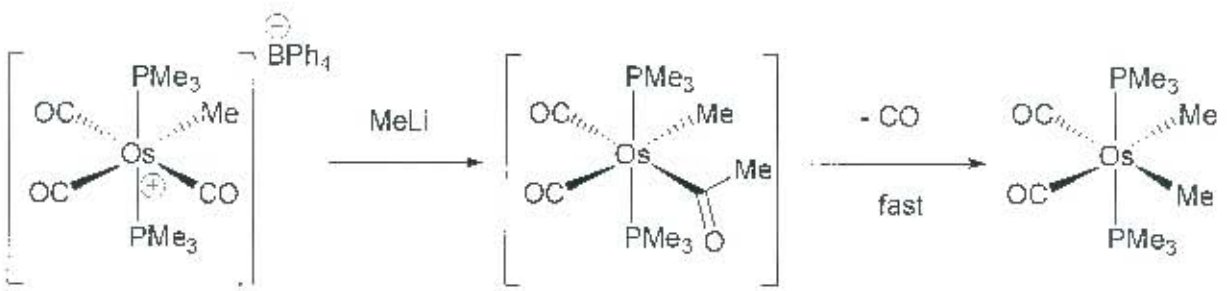

Fig. 2-22: Literature reaction of $[Os(CO)_3(PMe_3)_2Me]BPh_4$ with MeLi to form $Os(CO)_2(PMe_3)_2Me_2$ via a transient osmium alkyl/acyl intermediate[84]

2.3.2 The crystal structure of $Os(CO)_2(dppm)(COMe)Me$ (8)

X-ray quality single crystals of $Os(CO)_2(dppm)(COMe)Me$ (**8**) were grown by layering hexane on a concentrated dichloromethane solution of this compound, and slowly cooling to -15°C overnight. The colourless crystals grew as thin needles. **8** crystallises in the monoclinic crystal system with a C2/c space group and 8 repeating units per unit cell. The compound exists as a racemate. The molecular structure is shown in Fig. 2-23, and some selected bond angles and distances are shown in Table 2-1 below. All the data pertaining to the structure, including a full list of bond angles and distances, is presented in appendix B.

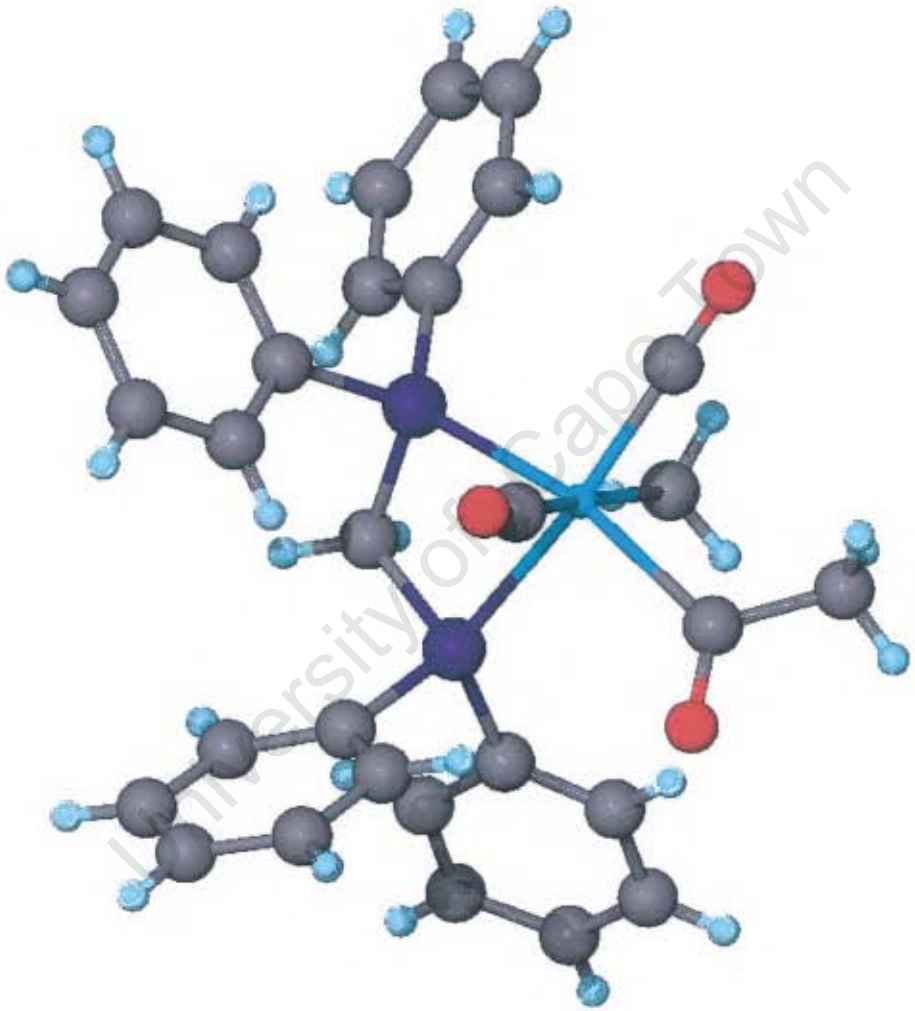

Fig. 2-23: The crystal structure of ***8***

Table 2-1: Selected bond angles and distances for the crystal structure of 8

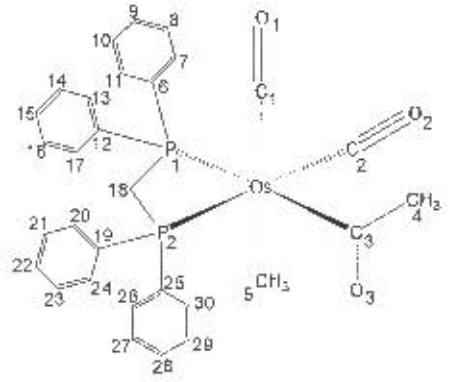

Bond distances (Å)		Bond angles (°)	
Os–C_5	2.24	P_1–Os–P_2	70.0
Os–C_3	2.12	C_3–Os–C_5	87.8
Os–C_1	1.90	C_1–Os–C_2	90.9
Os–C_2	1.92	C_1–Os–P_1	98.8
Os–P_2	2.42	C_1–Os–P_2	97.2
Os–P_1	2.41	C_5–Os–P_1	85.5
C_1–O_1	1.14	C_5–Os–P_2	85.3
C_2≡O_2	1.10	C_3–Os–P_2	94.2
C_3=O_3	1.19	C_2–Os–P_1	100.6
C_3–C_4	1.53	Os–C_3–C_4	120.0
		P_1–C_{18}–P_2	97.2

The osmium atom has a distorted octahedral geometry, as a result of the narrow bite angle of the dppm ligand. The P-Os-P angle was found to be 70.0°; substantially less than the perfect octahedral angle of 90°. The *trans* effect of the phosphine ligands can be seen in the differences in the carbonyl bond distances. The CO *trans* to P has a shorter Os-C bond (1.918Å) and longer C-O bond (1.096Å) than the CO *trans* to Me (1.895Å and 1.143Å) because of the competitive electron π-accepting ability of the phosphine which reduces the strength of the *trans* Os-CO bond. As expected, the acyl C-O bond is longer (1.193Å) than the C-O bond length in the CO ligands.

A packing diagram of the unit cell with the 8 repeating units (4 of each mirror image) is shown in Fig. 2-24. The cell is viewed down the a axis.

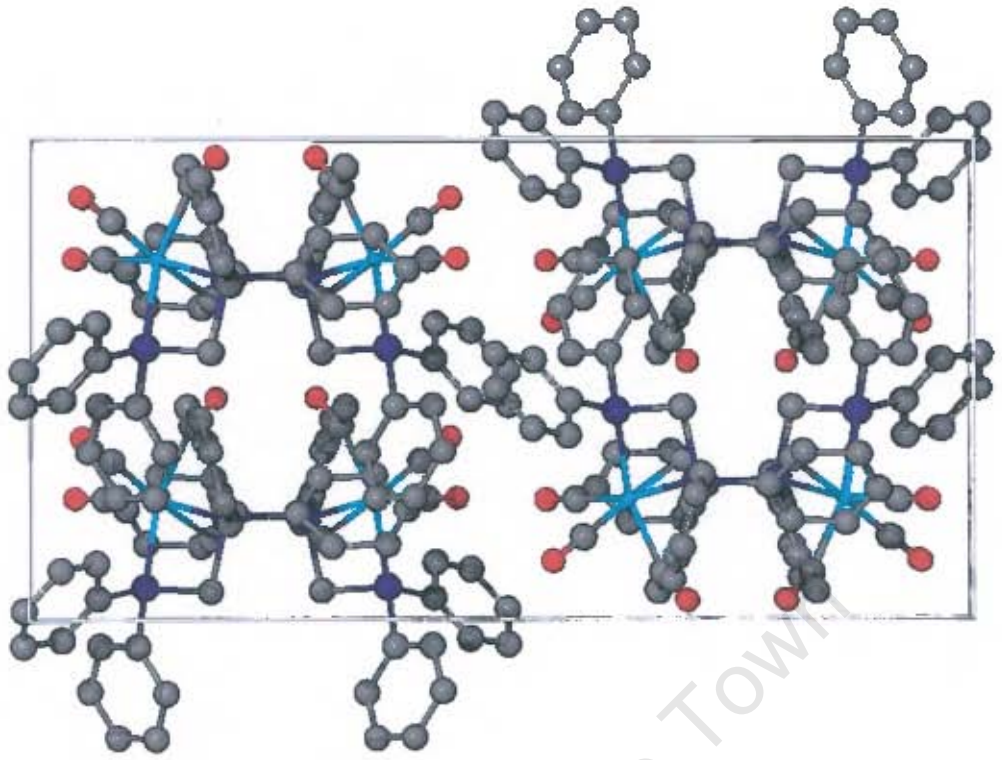

Fig. 2-24: The unit cell of the lattice of ***8*** *(viewed down the a axis) showing the 8 repeating units*

2.3.3 The reactions of $Os(CO)_3(NCMe)Me_2$ with bis(diphenylphosphino)propane (dppp)

It was anticipated that the reaction of $Os(CO)_3(NCMe)Me_2$ with dppp would proceed in a similar way to the reactions with dppm and dppe (Fig. 2-17). Stoichiometric equivalents of $Os(CO)_3(NCMe)Me_2$ and dppp were stirred together in toluene, and the reaction was monitored by IR spectroscopy. After 16h at 70°C, the starting material bands had been replaced by new bands, characteristic of a *fac*-tricarbonyl, at 2068, 1993 and 1960cm^{-1}. This new species is assigned as the 'dangling' or pendant diphosphine compound $Os(CO)_3(dppp)Me_2$ (Fig. 2-25). This is convincingly demonstrated by comparison of the IR bands with those of $Os(CO)_3(PPh_3)Me_2$ at 2068, 1994 and 1960cm^{-1}. Over 72h further reaction time at 70°C, new bands at 2013 and 1949 grew slowly relative to the bands at 2068, 1993 and 1960cm^{-1}. It is assumed that these absorptions are characteristic of the expected reaction product $Os(CO)_2(dppp)(COMe)Me$ (Fig. 2-25) by comparison with the absorptions of $Os(CO)_2(dppm)(COMe)Me$ at 2002 and 1942cm^{-1}. However, the reaction was extremely slow, and upon refluxing the reaction mixture (110°C), a third new species (initially present in solution with both $Os(CO)_3(dppp)Me_2$ and $Os(CO)_2(dppp)(COMe)Me$) was detected by the development of new bands at 2005 and 1929cm^{-1}. After four days reflux (which resulted in significant decomposition in solution), the reaction was judged to be complete. Upon isolation in low yield, the complex $Os(CO)_2(dppp)Me_2$ (**10**) was identified as the reaction product.

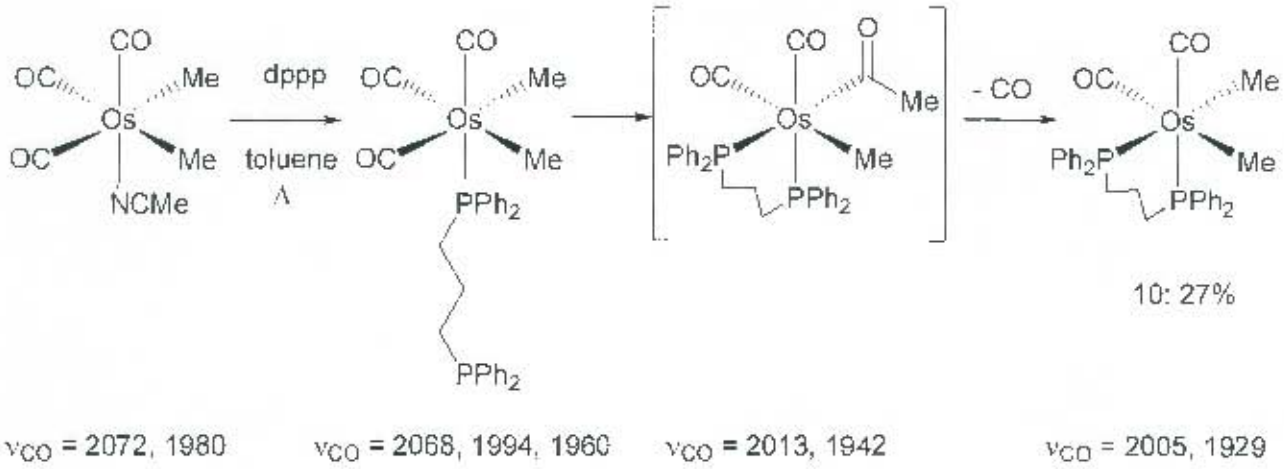

Fig. 2-25: The synthesis of $Os(CO)_2(dppp)Me_2$ showing the IR-observed pendant diphosphine and chelated acyl intermediates

$Os(CO)_2(dppm)Me_2$ was characterised by elemental analysis, NMR spectroscopy and mass spectrometry. As usual, the NMR is particularly useful in elucidating structure. The ^1H NMR is shown in Fig. 2-26.

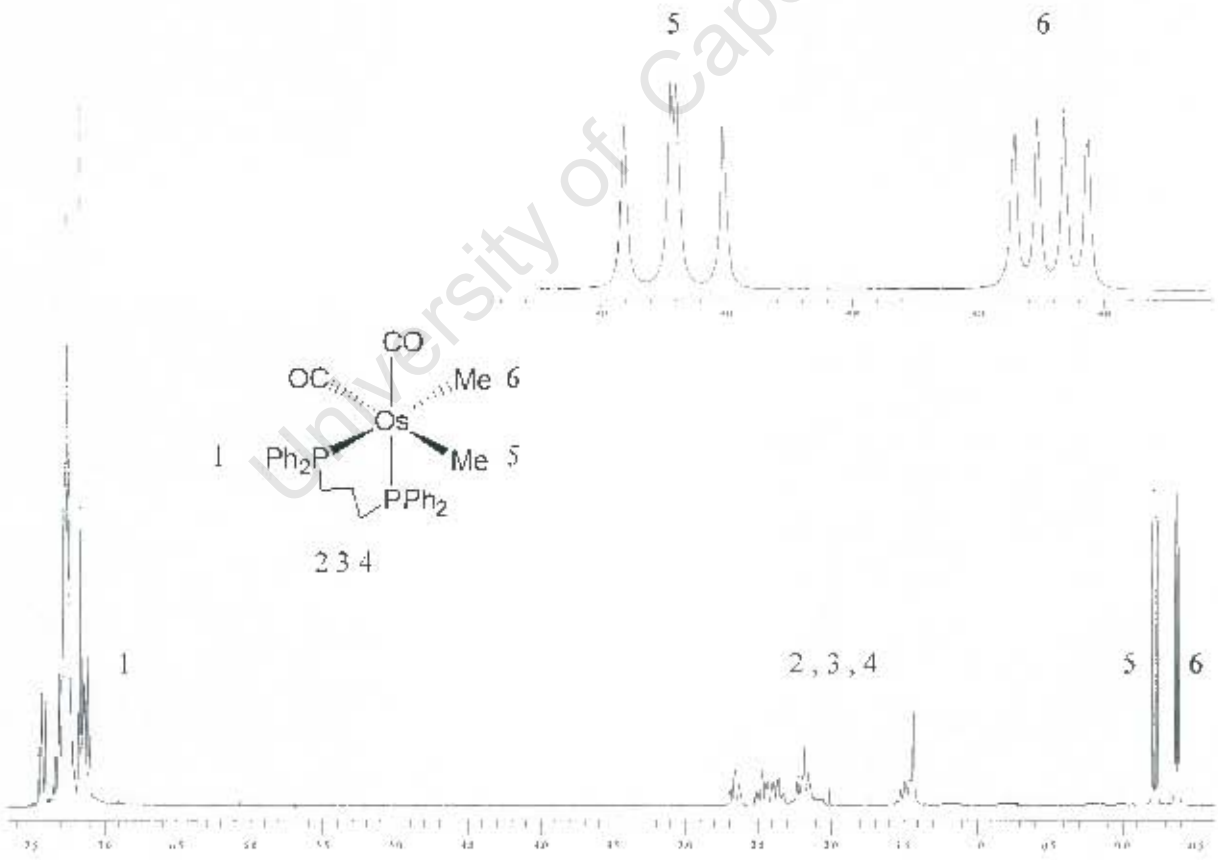

Fig. 2-26: ^1H NMR spectrum of $Os(CO)_2(dppp)Me_2$ showing an expansion of the Os-Me signals

The two methyl signals appear as doublets of doublets due to coupling to two different phosphorus atoms (see expansion in Fig. 2-26). Os-*Me trans* to P (-0.29ppm) displays significantly different *trans* (8Hz) and

cis (4Hz) ^3J(PH) couplings as expected. The Os-*Me trans* to CO has two *cis* ^3J(PH) couplings of similar size (8 and 7Hz). These *cis* coupling are much larger than that for the other methyl. The reason for this is not clear; however a similar *cis* ^3J(PH) coupling (8Hz) is observed in *fac*-$Os(CO)_3(PPh_3)Me_2$.[71] The methylene protons of the dppp bridge appear as a complex array of multiplets. This is due to the non-equivalence of the geminal protons due to structural rigidity imposed by the chelation.

In order to obtain confirmation for the proposed mechanism and intermediates, the reaction between $Os(CO)_3(NCMe)Me_2$ and dppp was performed in an NMR tube in C_6D_6, and the reaction was monitored by ^1H and ^{31}P NMR spectroscopy. A mixture of the two reagents was dissolved in C_6D_6 and heated to 50°C in the NMR tube for 16h. The NMR spectra confirm the presence in solution of both the proposed intermediates. In the ^1H NMR, a doublet at 0.10ppm (^3J(PH) 8Hz) is assigned to $Os(CO)_3(dppp)Me_2$, the pendant diphosphine intermediate. A triplet at 0.53ppm (^3J(PH) 8Hz) and a singlet at 2.45ppm correspond to $Os(CO)_2(dppm)(COMe)Me$. The ^{31}P NMR spectrum (Fig. 2-27) provides further evidence of these two intermediates as well. Two singlets for the coordinated (-6.5ppm) and uncoordinated phosphines (-17.4ppm) in the pendant intermediate, as well as two doublets (-24.0ppm and -24.8ppm, ^2J(PP) 26Hz) for the chelated acyl intermediate are apparent.

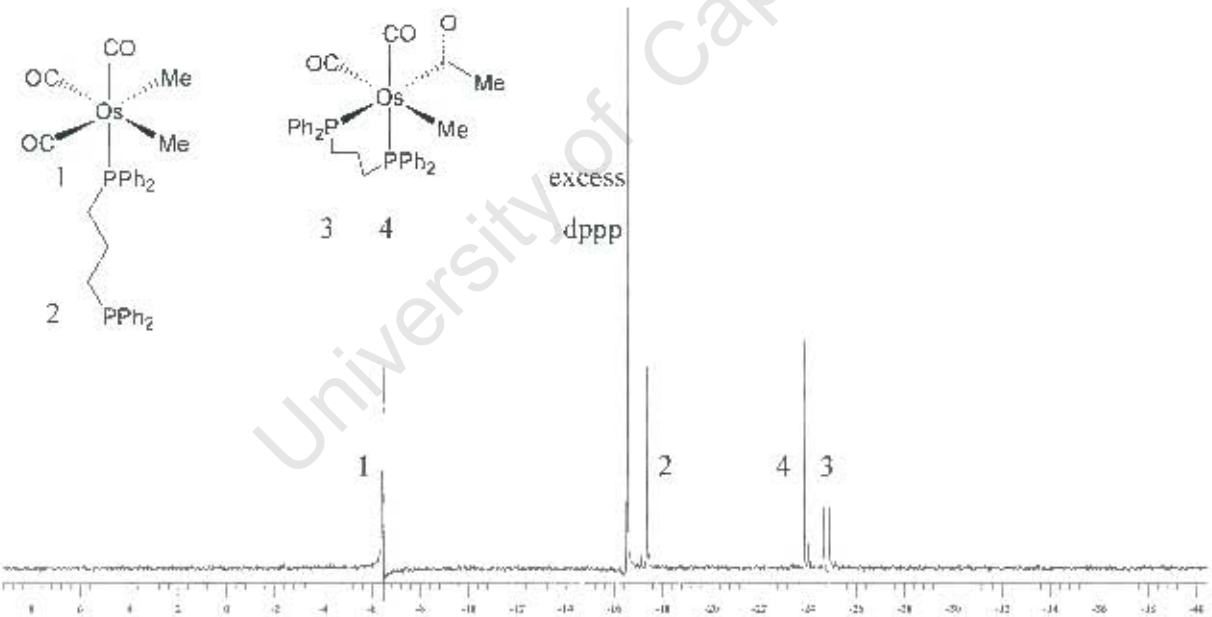

Fig. 2-27: ^{31}P NMR spectrum monitoring the reaction of $Os(CO)_3(NCMe)Me_2$ with dppp

It is clear that the effect of the spacer length n between the two phosphines in $Ph_2P(CH_2)_nPPh_2$ is important when considering the propensity of the ligand to chelate. The reactions of $Os(CO)_3(NCMe)Me_2$ with dppm (n = 1) and dppe (n = 2) proceed selectively and relatively quickly to form the acyl products $Os(CO)_2$(diphosphine)(COMe)Me. This takes place by displacement of the labile MeCN by the first phosphine and rapid chelation by the second phosphine due to the proximity to the metal centre. It is known that chelation by dppe to an octahedral centre, resulting in a stable 5 atom ring, is the most favoured

from the series $Ph_2P(CH_2)_nPPh_2$.[106] In the case of dppp, the initial displacement of the MeCN is easily accomplished, but chelation is a less favourable process than with dppm and dppe, as a result of the greater distance of the second phosphine from the metal centre. In order to drive the chelation to completion, higher temperatures and longer reaction times are necessary. Under these reaction conditions, decarbonylation of the acyl substituent occurs, resulting in the formation of $Os(CO)_2(dppp)Me_2$.

It is clear that in the equimolar reaction between $Os(CO)_3(NCMe)Me_2$ and dppp, the initial displacement of MeCN takes place faster than subsequent methyl migration and chelation. It thus appeared probable that if these two reagents were reacted in a 2:1 ratio, a binuclear osmium compound with bridging dppp would be the most likely product (Fig. 2-28). The reaction in toluene at 70°C was monitored by IR spectroscopy, and new absorptions at 2069, 1993 and 1961cm^{-1} consistent with a *fac*-tricarbonyl indicated the formation of the expected product, $CH_2[CH_2PPh_2Os(CO)_3Me_2]_2$ (11), (*c.f.* $Os(CO)_3(PPh_3)Me_2$ 2068, 1994 and 1960cm^{-1}). Characterisation by elemental analysis, NMR and IR spectroscopy and mass spectrometry confirmed the structure of the complex.

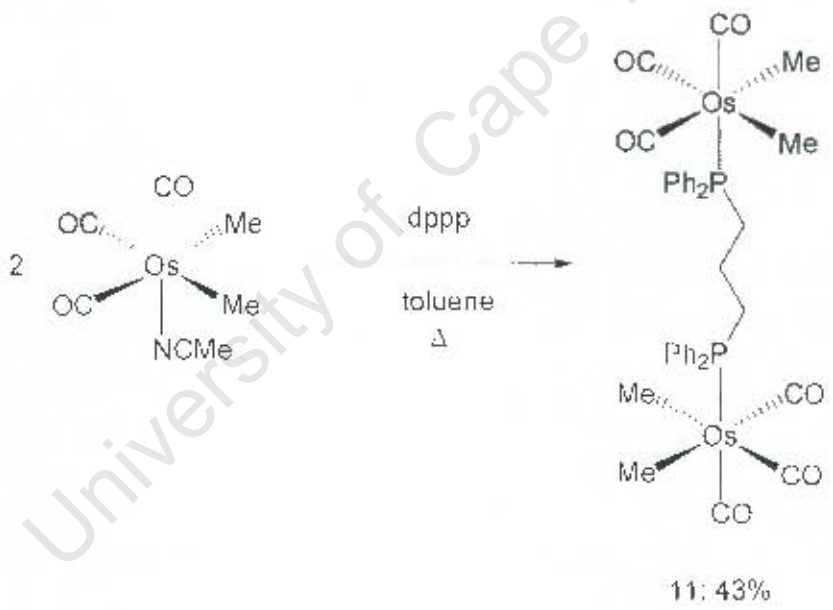

Fig. 2-28: Reaction of 2 equivalents of $Os(CO)_3(NCMe)Me_2$ with dppp to form a binuclear osmium complex with bridging dppp

2.4 Methyl abstractions from osmium compounds using trityl salts

2.4.1 Methyl abstraction reactions with CPh_3PF_6 and $B(C_6F_5)_3$

The use of trityl (CPh_3^+) salts as reagents for the abstraction of alkyl species and hydrides is well known in organometallic chemistry. In many late transition metal systems, a β-hydride is abstracted from a metal-

coordinated alkyl group to form η^2-coordinated alkene complexes (Fig. 2-29).[107-109] In some cases, α-hydride abstraction occurs, and alkylidene (carbene) complexes are formed (Fig. 2-29).[110,111] This may occur preferentially even when a β-hydride is available.[112,113] In still other cases, Me^- rather than H^- is abstracted (Fig. 2-29).[114] This is particularly common in early transition metal systems such as Cp_2ZrMe_2[115] in which case the abstraction of methyl activates the metallocene for the polymerisation of ethene.

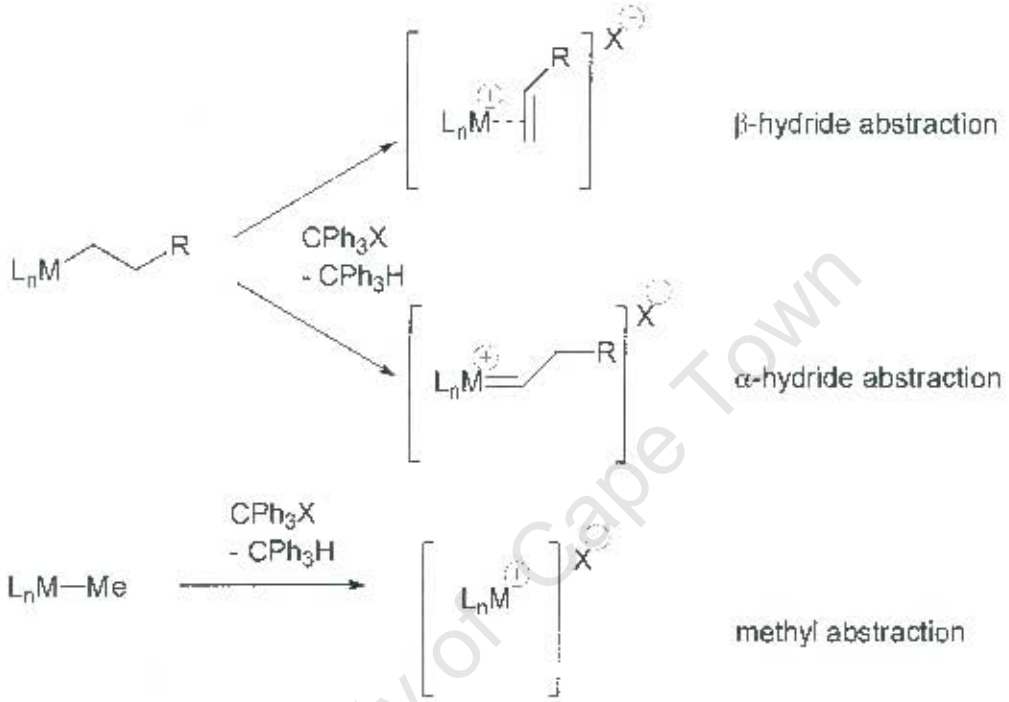

Fig. 2-29: Some known reactions of metal alkyl compounds with trityl salts

The choice of the counterion is important. Counterions such as BF_4^-, PF_6^- or ClO_4^- may interact strongly with the cationic metal centre[115], whereas bulky counterions such as BPh_4^- [115] and especially bulky perfluorated counterions like $B(C_6F_5)_4^-$ have been found to be unreactive and non-coordinating to the metal centre. This is particularly important in catalytic applications, where interactions between the counterion and the catalytic centre can deactivate the catalyst.

Methyl abstractions from organometallic compounds have also been successful with neutral borane compounds such as $B(C_6F_5)_3$ (Fig. 2-30).

Fig. 2-30: Methyl abstraction reactions with $B(C_6F_5)_3$

This has found application in early transition metal metallocenes catalysis, where $B(C_6F_5)_3$ activates Cp_2ZrMe_2 for the polymerisation of alkenes.[116,117] However, $B(C_6F_5)_3$ has also been reported to abstract a methyl from late transition metal complexes, for example Pt(dbbipy)Me_2 (dbbipy = 4,4'-di-*tert*-butyl-2,2'bipyridine).[118]

2.4.2 Reactions between $Os(CO)_3(L)Me_2$ (L = CO, NCMe, PPh_3) and CPh_3PF_6

Abstraction of a methyl from $Os(CO)_4Me_2$ was not possible with either CPh_3PF_6 or $B(C_6F_5)_3$ under the conditions attempted (Fig. 2-31). An excess of CPh_3PF_6 was added to a solution of $Os(CO)_4Me_2$ in dichloromethane, and monitoring of the reaction by IR spectroscopy over five days indicated that the $Os(CO)_4Me_2$ remained unchanged in solution. The reaction with $B(C_6F_5)_3$ was attempted in an NMR tube in C_6D_6, and again, no formation of a cationic species by methyl abstraction was apparent. The Os-Me bonds in $Os(CO)_4Me_2$ are very unreactive due to the electron withdrawing carbonyl ligands.

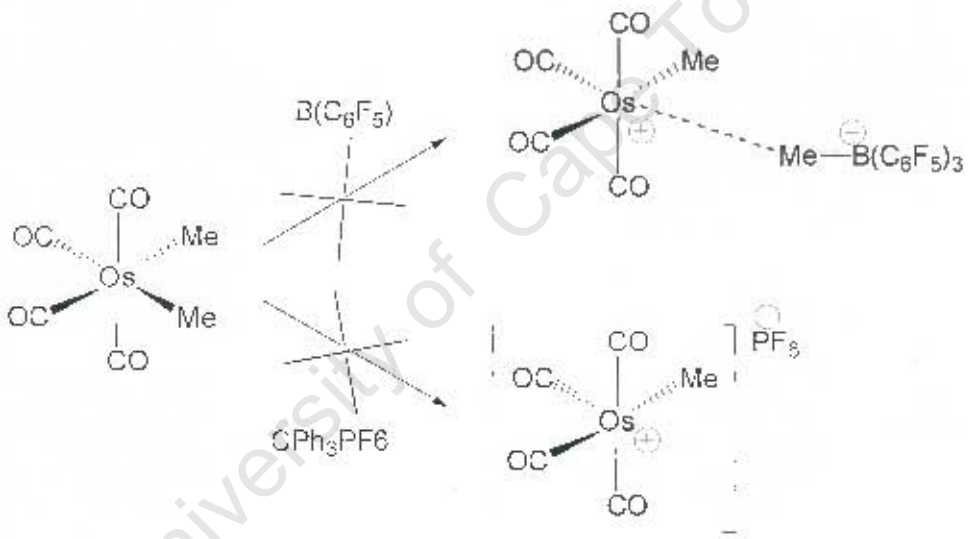

Fig. 2-31: Attempted methyl abstraction reactions from $Os(CO)_4Me_2$

It was hoped that methyl abstraction from $Os(CO)_3(NCMe)Me_2$ might give the target system described in section 2.1: a 16-electron, cationic and coordinatively unsaturated complex with a labile ligand and a metal-alkyl bond (Fig. 2-32).

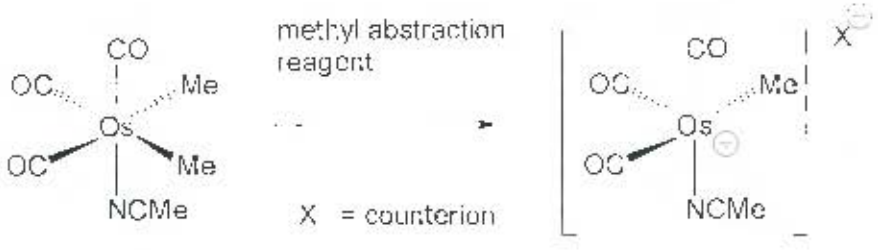

Fig. 2-32: Expected reaction between $Os(CO)_3(NCMe)Me_2$ and a methyl abstraction reagent

$B(C_6F_5)_3$ was again found to be unreactive towards $Os(CO)_3(NCMe)Me_2$ in an NMR observed experiment. The trityl salt CPh_3PF_6, however, did react with $Os(CO)_3(NCMe)Me_2$. One equivalent of CPh_3PF_6 was added to a solution of $Os(CO)_3(NCMe)Me_2$ in dichloromethane. The reaction was monitored by IR spectroscopy. The carbonyl stretching bands of the starting material (2072, 1981 cm^{-1}) were gradually replaced by three new bands (2114, 2040, 2013 cm^{-1}) over a period of 16h. The shift to higher wavenumber and the retention of the *fac*-tricarbonyl pattern of carbonyl stretches is consistent with the abstraction of a methyl or hydride to form a cationic tricarbonyl. However, upon removal of the volatiles and washing the CPh_3Me or CPh_3H by-product out with pentane, a complex mixture of products which could not be identified was observed in the ^1H NMR spectrum.

In an effort to obtain some information about the reaction, several attempts were made to perform the reaction in an NMR tube and to follow the reaction by ^1H NMR spectroscopy. A solution of $Os(CO)_3(NCMe)Me_2$ and excess CPh_3PF_6 in $CDCl_3$ (the reaction was also attempted in the less reactive solvent CD_2Cl_2) was transferred in the glovebox into a Teflon-valved NMR tube and an ^1H NMR spectrum was run immediately. The emergence of a singlet at 2.19ppm corresponds to CPh_3Me.[119] After 2 hours another spectrum was run. $Os(CO)_3(NCMe)Me_2$ had been completely consumed and one equivalent of CPh_3Me had been formed (as approximated by comparison of the integration with the total integration of the aryl signals, which will not change through the course of the reaction). It was clear, however, that the reaction was complex, with an array of new signals which could not be usefully interpreted.

The formation of one equivalent of CPh_3Me and the observed IR spectroscopic results confirm the abstraction of a single methyl from $Os(CO)_3(NCMe)Me_2$. It was concluded that the resultant coordinatively unsaturated 16-electron salt, $[Os(CO)_3(NCMe)Me]PF_6$, is unstable, however, and decomposes through an undetermined pathway to form a complex array of products (Fig. 2-33).

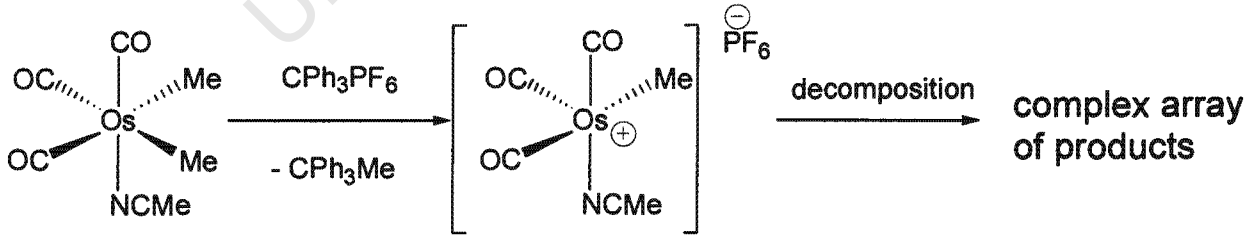

Fig. 2-33: Reaction of $Os(CO)_3(NCMe)Me_2$ with CPh_3PF_6

The reaction of $Os(CO)_3(PPh_3)Me_2$ with CPh_3PF_6 also gives a complicated mixture of products. In particular it was observed by monitoring the reaction with IR that more than one equivalent of trityl reagent was required to abstract a methyl from the osmium centre. Upon reflection, it became apparent that the trityl reagent reacts with the coordinated PPh_3 as well as with the osmium-methyl functionality. In a

separate test reaction, CPh_3PF_6 was found to react with free PPh_3. Further efforts were not made to isolate any identifiable products from the reaction of $Os(CO)_3(PPh_3)Me_2$ with CPh_3PF_6.

2.4.3 Reaction between $Os(CO)_3(NCMe)Me_2$ and CPh_3PF_6 in the presence of a trapping reagent

Following the failure to isolate $[Os(CO)_3(NCMe)Me]PF_6$ due to decomposition of this coordinatively unsaturated species, it was decided to 'trap' this species *in situ*. In this approach, $[Os(CO)_3(NCMe)Me]PF_6$, formed by abstraction of a methyl from $Os(CO)_3(NCMe)Me_2$, is immediately trapped by a coordinating ligand (L) to form $[Os(CO)_3(NCMe)(L)Me]PF_6$ (Fig. 2-34). This 18-electron coordinatively saturated species would then be stable and isolable, and would provide further proof for the initial formation of the desired cationic species, $[Os(CO)_3(NCMe)Me]PF_6$.

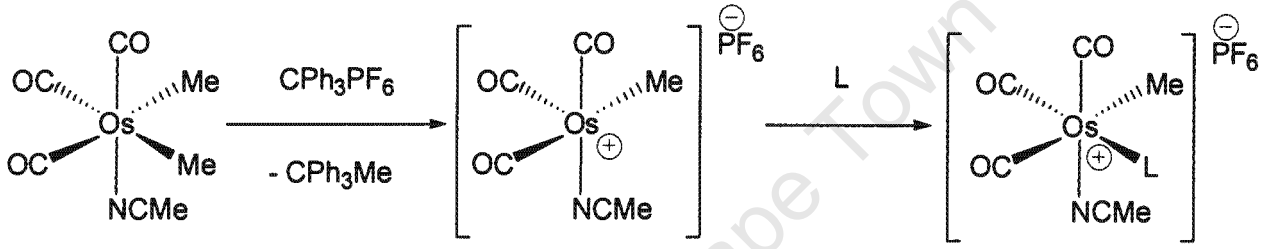

Fig. 2-34: Trapping of the unstable product $[Os(CO)_3(NCMe)Me]PF_6$ by a monodentate coordination ligand (L) to give a stable 18-electron species

In a very small scale reaction, $Os(CO)_3(NCMe)Me_2$ was treated with one equivalent of CPh_3PF_6 under an atmosphere of CO (Fig. 2-35). The reaction was monitored by IR spectroscopy. New bands developed at 2113, 2039, 2012 and 1963cm^{-1}. The pattern was characteristic of a *cis*-tetracarbonyl, and the shift to higher wavenumber (*c.f.* $Os(CO)_3(NCMe)Me_2$ 2072, 1980cm^{-1}) was consistent with a cationic species. Upon isolation of the complex, ^{1}H NMR spectroscopy confirmed the formation of the expected product *cis*-$[Os(CO)_4(NCMe)Me]PF_6$ (**12**) (singlets of equal integration at 2.59 and 0.62ppm for Os-NC*Me* and Os-*Me* respectively). However, significant other impurities were also apparent, and it appears that the limited solubility of CO in the reaction mixture prevents quantitative trapping before decomposition can occur.

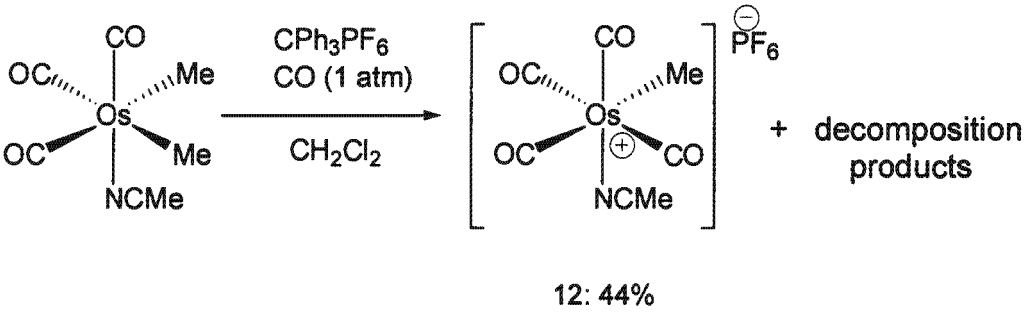

*Fig. 2-35: Reaction of $Os(CO)_3(NCMe)Me_2$ with CPh_3PF_6 under an atmosphere of CO to give **12***

However, when the reaction between $Os(CO)_3(NCMe)Me_2$ and CPh_3PF_6 was carried out in acetonitrile, the acetonitrile acted both as solvent and as a trapping reagent to give the isolable and air-stable ionic compound *fac*-$[Os(CO)_3(NCMe)_2Me]PF_6$ (**13**) as the exclusive organometallic reaction product (Fig. 2-36).

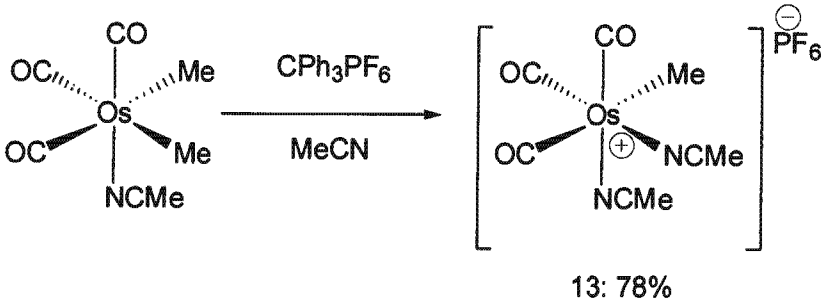

13: 78%

Fig. 2-36: The synthesis of $[Os(CO)_3(NCMe)_2Me]PF_6$ (13)

$[Os(CO)_3(NCMe)_2Me]PF_6$ was characterised by elemental analysis, NMR and IR spectroscopy and mass spectrometry. The ^1H NMR spectrum of $[Os(CO)_3(NCMe)_2Me]PF_6$ is shown in Fig. 2-37 together with the $Os(CO)_3(NCMe)Me_2$ starting material. A downfield shift is apparent in both the Os-NC*Me* (2.46 to 2.59ppm) and Os-*Me* (0.06 to 0.52ppm) singlets due to the cationic nature of the metal centre. The equivalence of the two MeCN ligands confirms the anticipated stereochemistry of the trapped complex, in which the second MeCN coordinates in the coordination site vacated by the abstracted methyl.

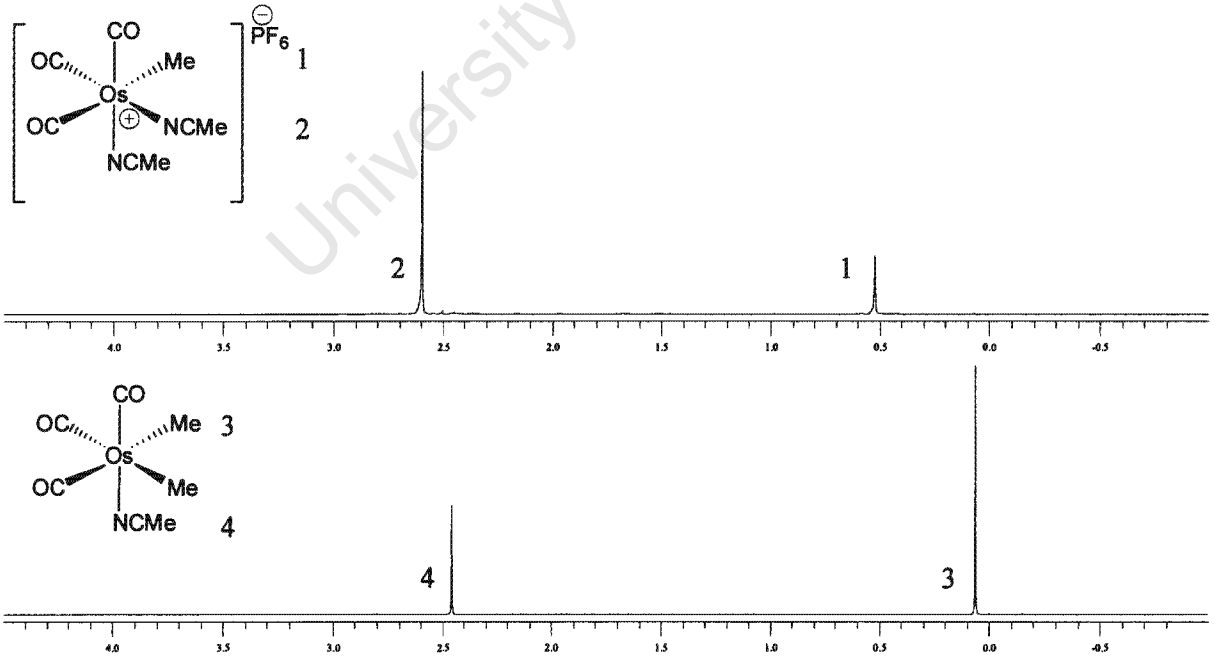

Fig. 2-37: ^1H NMR spectra of $[Os(CO)_3(NCMe)_2Me]PF_6$ (top) and $Os(CO)_3(NCMe)Me_2$ (bottom)

$[Os(CO)_3(NCMe)_2Me]PF_6$ is particularly amenable to mass spectrometry, as this compound is already ionic. The parent cation $[Os(CO)_3(NCMe)_2Me]^+$ at 373 a.m.u. is observed as the most abundant species in the spectrum, and the isotopic distribution corresponds with the theoretical pattern.

2.4.4 The attempted synthesis of $[Os(CO)_3(NCMe)(CH_2=CH_2)Me]PF_6$

It was hoped that ethene could be used as a trapping reagent to give the complex $[Os(CO)_3(NCMe)(CH_2=CH_2)Me]PF_6$ (Fig. 2-38) Cationic osmium complexes of ethene with PF_6^- counterion, for example $[C_6H_6Os(PMe_3)H(C_2H_4)]PF_6$, have been reported in the literature, although here the ethene molecule is formed by the coupling of two methyl groups after the abstraction of a hydride from one of them.[111,120,121]

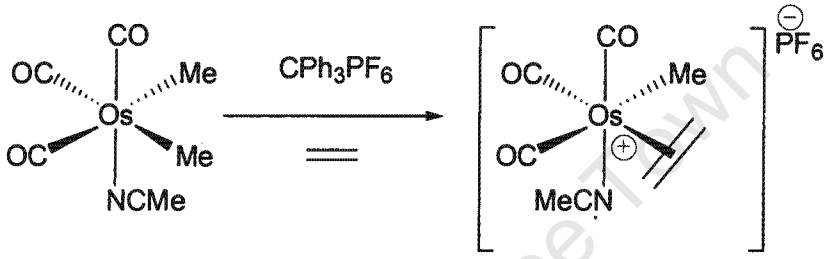

Fig. 2-38: The desired methyl abstraction from $Os(CO)_3(NCMe)Me_2$ with trapping by ethene

$[Os(CO)_3(NCMe)(CH_2=CH_2)Me]PF_6$ would be a good organometallic model for a proposed catalytic species in the oligomerisation of 1-alkenes, in which the alkene coordinates to the vacant coordination site of a cationic alkyl functionalised metal centre (see section 2.1). If this compound could be prepared, then interesting further reactions aimed at inserting the coordinated ethene into the Os-Me bond could be attempted. In the reactions of $Os(CO)_3(NCMe)Me_2$ with bidentate ligands, insertions (in this case of a CO, described as a methyl migration) into the Os-Me bond have already been demonstrated. Some speculative reactions of $[Os(CO)_3(NCMe)(CH_2=CH_2)Me]PF_6$ with monodentate and bidentate ligands involving ethene insertion into Os-Me are shown in Fig. 2-39. Of course, many other possible reactions involving, for example, displacement of ethene, are also possible.

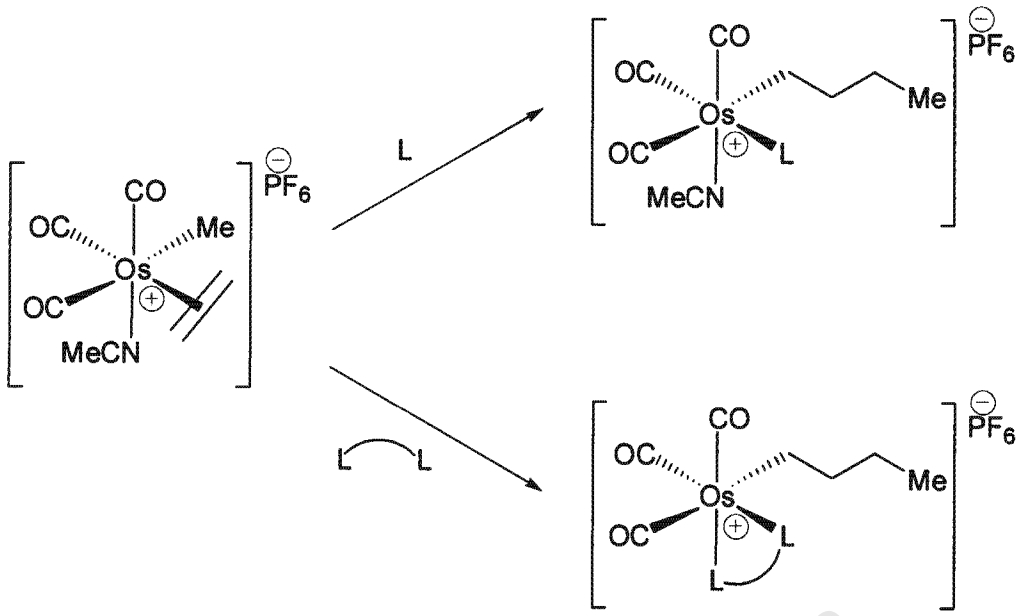

Fig. 2-39: Possible ethene insertion reactions of the complex [Os(CO)$_3$(NCMe)(CH$_2$=CH$_2$)Me]PF$_6$

Unfortunately, such speculation proved to be premature, as the complex [Os(CO)$_3$(NCMe)(CH$_2$=CH$_2$)Me]PF$_6$ could not be isolated in a preparative experiment or unambiguously observed in an NMR tube reaction. Treatment of Os(CO)$_3$(NCMe)Me$_2$ with CPh$_3$PF$_6$ under an atmosphere of ethene led to a complex array of products. In an NMR tube experiment, one equivalent of CPh$_3$PF$_6$ in CD_2Cl_2 was added against a flow of ethene into a Teflon-valved NMR tube containing Os(CO)$_3$(NCMe)Me$_2$ at -78°C. The tube was then sealed and warmed to room temperature, and an ^{1}H NMR spectrum was obtained (Fig. 2-40) A singlet at 5.40 ppm confirms the presence in solution of free ethene, and the singlet at 2.17 corresponds to CPh$_3$Me, indicating that methyl abstraction has taken place. The set of two complex multiplets between 4.32 and 4.51 (shown as an expansion) is assigned to a coordinated ethene molecule, although this ethene-complexed species cannot be identified. The two =C*H*$_2$ units are chemically non-equivalent, resulting in their coupling to each other. Second order distortions as a result of the large coupling relative to the difference in chemical shifts account for the non-symmetrical shape of the multiplets. The complex array of other peaks indicates that further reactions of the methyl abstracted species have taken place, and that the intended product [Os(CO)$_3$(NCMe)(CH$_2$=CH$_2$)Me]PF$_6$ has not been selectively formed. Ethene appears to be too poor a ligand to trap the methyl abstracted species before the decomposition observed in section 2.4.2 takes place.

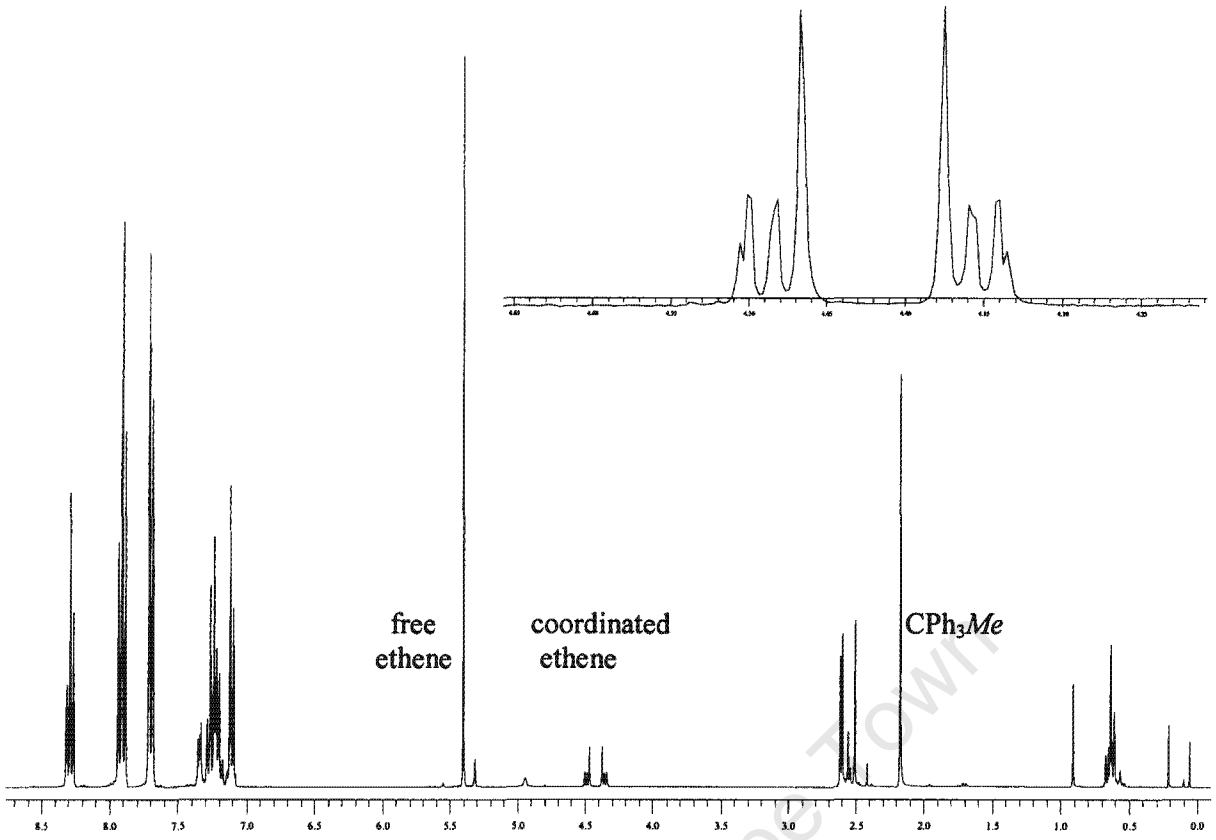

Fig. 2-40: ^1H NMR spectrum of the products formed by reaction of $Os(CO)_3(NCMe)Me_2$ with CPh_3PF_6 under an atmosphere of ethene. The expansion shows the multiplets assigned to a coordinated ethene molecule

2.5 Conclusions and future work

The chemistry of osmium complexes derived from $Os(CO)_4Me_2$ was thoroughly investigated, and in particular the new compound *fac*-$Os(CO)_3(NCMe)Me_2$ and its reactivity was studied. The reactions of this compound with both monodentate (section 2.2) and bidentate (section 2.3) ligands were investigated, and in the latter case a novel reaction involving MeCN displacement and subsequent methyl migration onto carbonyl accompanied by chelation was discovered. The unique reactivity and stereochemistry of this reaction was confirmed by solving the crystal structure of $Os(CO)_2(dppm)(COMe)Me$. Treatment of $Os(CO)_3(NCMe)Me_2$ with trityl salt resulted in methyl, and not hydride, abstraction (section 2.4) The resultant complex, $[Os(CO)_3(NCMe)Me]PF_6$ was unstable and could not be isolated; however, by trapping this intermediate with MeCN, the stable cationic complex $[Os(CO)_3(NCMe)_2Me]PF_6$ was isolated. Attempts to trap with ethene to give the complex $[Os(CO)_3(NCMe)(CH_2{=}CH_2)]Me]PF_6$ were not successful.

There are numerous avenues available for further exploration of this rich area of organometallic chemistry. Reaction of $Os(CO)_3(NCMe)Me_2$ with bidentate ligands (L^L) gave the product $Os(CO)_2(L\hat{}L)(COMe)Me$. It would be interesting to attempt the reaction with a tridentate ligand such as $MeC(CH_2PPh_2)_3$ to see if the

complex $Os(CO)(Me(CH_2PPh_2)_3)(COMe)_2$ would be formed by displacement of MeCN and two carbonyl insertions (Fig. 2-41).

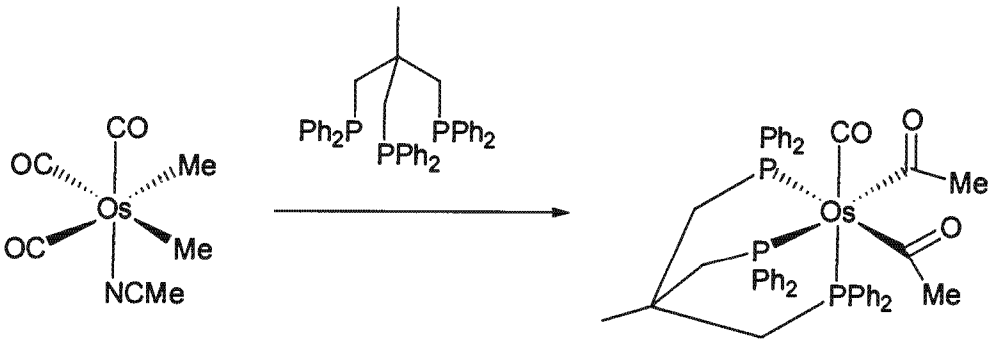

Fig. 2-41: Possible reaction of $Os(CO)_3(NCMe)Me_2$ with a tridentate ligand

When dppp was reacted with $Os(CO)_3(NCMe)Me_2$, the rate of MeCN displacement was substantially faster than the subsequent chelation/methyl migration, and the pendant complex $Os(CO)_3(dppp)Me_2$ was observed in solution. This compound could open up a new route to heterobimetallic compounds, as shown in Fig. 2-42.

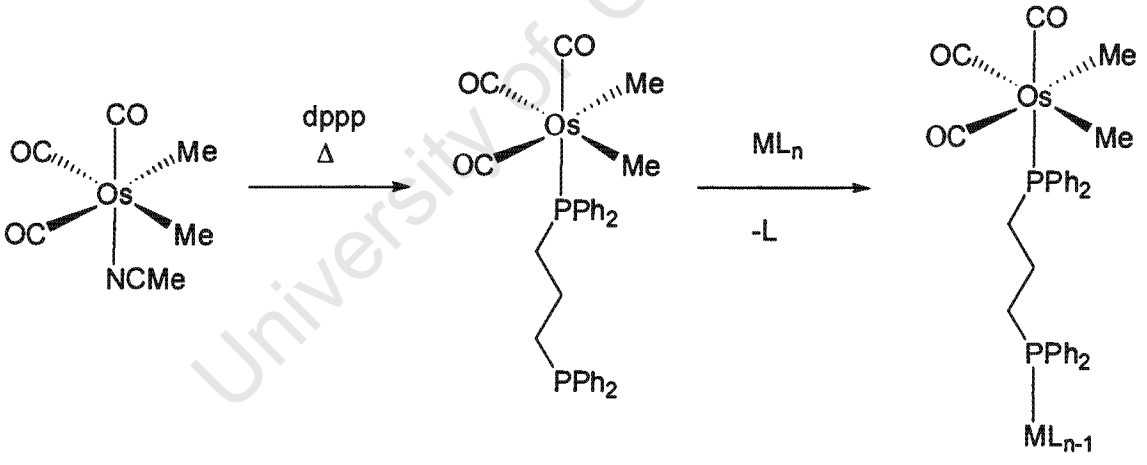

Fig. 2-43: Potential synthesis of heterobimetallic compounds utilising the spectroscopically observed pendant phosphine compound $Os(CO)_3(dppp)Me_2$

The stability of the methyl-abstracted complex $[Os(CO)_3(NCMe)Me]X$ could potentially be improved by choice of a less reactive counterion such as BPh_4^- or $B(C_6F_5)_4^-$. Attempts were made to prepare the literature compound $CPh_3B(C_6F_5)_4$; however due to a combination of the sensitivity of this compound and time constraints, this was not accomplished. In addition, low temperature NMR studies could be undertaken, in the hope of observing complexes such as $[Os(CO)_3(NCMe)Me]X$ and $[Os(CO)_3(NCMe)(ethene)Me]X$ before decomposition takes place.

Chapter 3:

Synthesis, characterisation and reactivity of new carbosilane dendritic wedges and dendrimers

3.1 Introduction

3.1.1 The nature and construction of dendritic molecules

Dendrimers form a fascinating class of macromolecules which has been the subject of a great deal of academic attention since the earliest reports.[122-124] They are characterised by a fractal like geometry, in which repeated steps of symmetrical branching (B) from a 'core' or focal point (C) create a large, globular molecule with numerous 'terminal groups' (T) on the 'periphery' (Fig. 3-1).

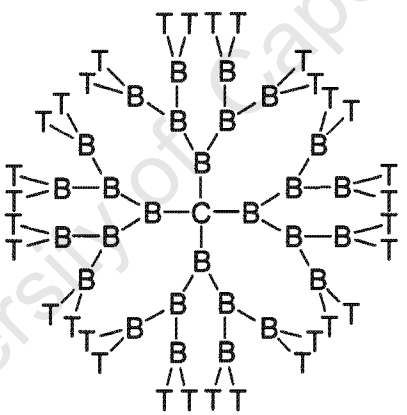

Fig. 3-1: Schematic representation of a dendrimer, showing core (C), branching (B) and terminal (T) units

The novel stepwise synthesis of dendrimers means that they are essentially monodisperse and have a highly controlled molecular architecture.[125] Dendrimers may be prepared by a divergent or convergent approach. In the divergent approach[122,123], synthesis starts at the core (C), and successive addition of branching units (B) to multiple reactive sites, followed by reactivation, gives successive generations of dendrimer (Fig. 3-2). Terminal functionality (T) may then be added to the peripheral groups.

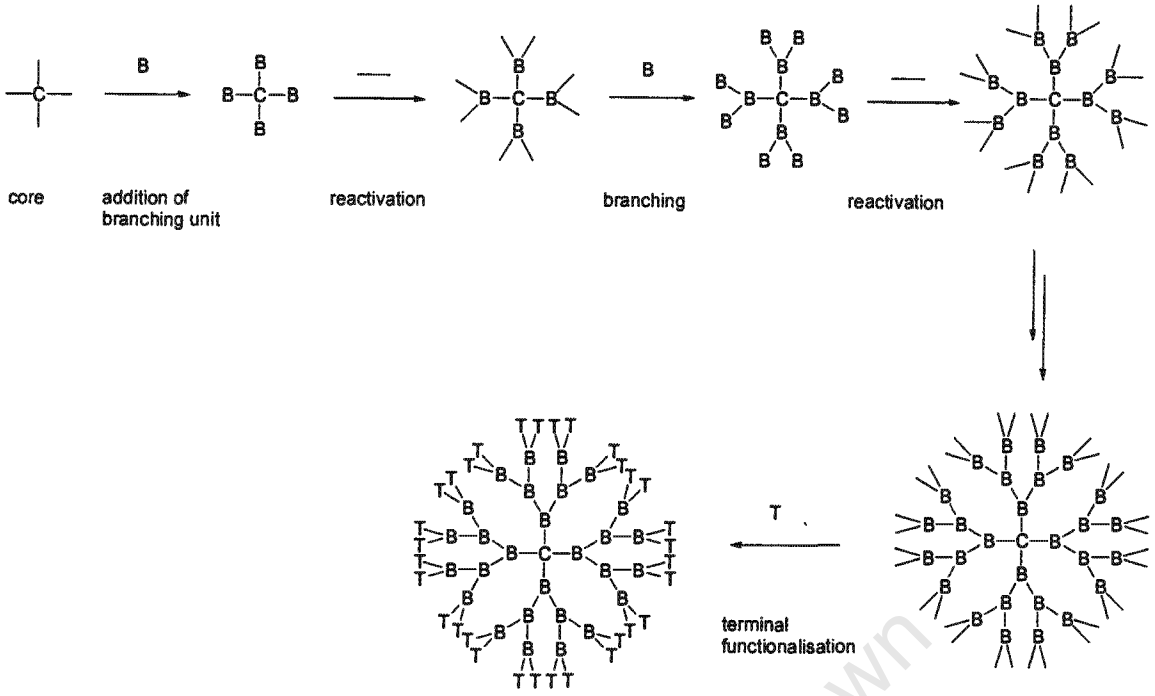

Fig. 3-2: Schematic representation of the divergent synthesis of dendrimers

In the convergent approach,[126,127] synthesis begins at what will become the periphery of the dendrimer (T). Successive generation n (n = 1,2,3…) 'dendritic wedges' with reactive core functionality are constructed by reaction of the generation n-1 wedge with a branching unit (B) , followed by reactivation (Fig. 3-3). The wedge may then be attached to a core unit (C).

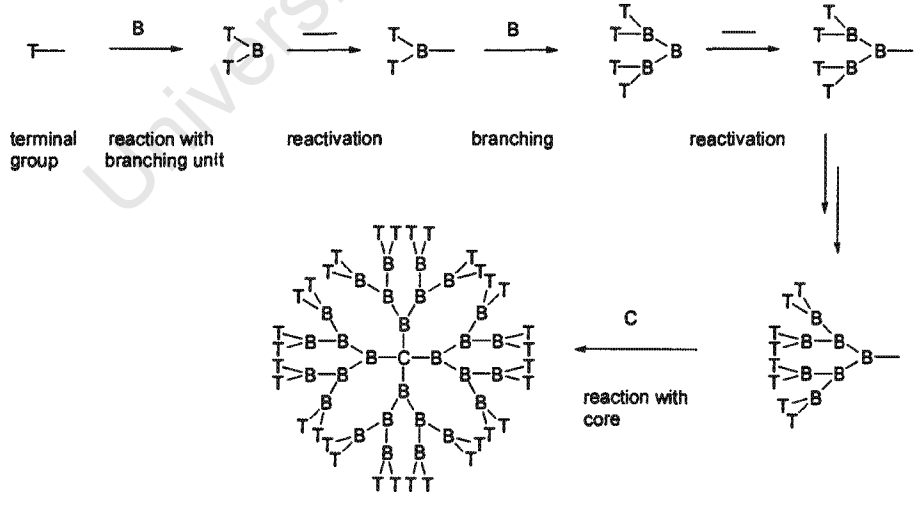

Fig. 3-3: Schematic representation of the convergent synthesis of dendrimers

A wide variety of different classes of dendrimers have been reported, including polyether[127,128], polyamide[129], polyol[130], polyphenylene[131], polyamidoamine[122], polyamine[124] and carbosilane[132,133] dendrimers.

3.1.2 Carbosilane dendrimers

Carbosilane dendrimers are of particular interest as their non-polar and relatively inert structure makes them ideal candidates for dendritic multisite catalysts. Many recent reports of dendritic homogeneous catalysts make use of carbosilane dendrimer frameworks.[Seyferth, 1994 #281; Zhou, 1992 #685; Van der Made, 1992 #278; Ropartz, 2002 #269; Ropartz, 2002 #581; Eric Oosterom, 1999 #85; Oosterom, 2001 #268; Hovestad, 2000 #173; Kleij, 2000 #513; de Groot, 1999 #7; Sato, 2002 #170]

Carbosilane dendrimers are prepared by a divergent synthesis as originally reported by van der Made, Roovers and Seyferth (Fig. 3-4).[132-134] Starting with tetraallylsilane (or tetravinylsilane), terminal alkene double bonds are activated by catalytic hydrosilylation with trichlorosilane or methyldichlorosilane. Platinum catalysts such as Speir's catalyst[135,136] (H_2PtCl_6 in n-BuOH) or Karstedt catalyst[137-139] (uncharacterised Pt(0) adducts of dimethyltetravinyldisiloxane) are typically used. The hydrosilylation is a completely regioselective reaction with quantitative conversions to the β-addition (anti-Markovnikov addition) product. The alkene terminal functionality is restored by reaction of all Si-Cl bonds with the appropriate alkenyl Grignard reagent. By iteration of this procedure, successively higher generations of dendrimers may be prepared (Fig. 3-4).

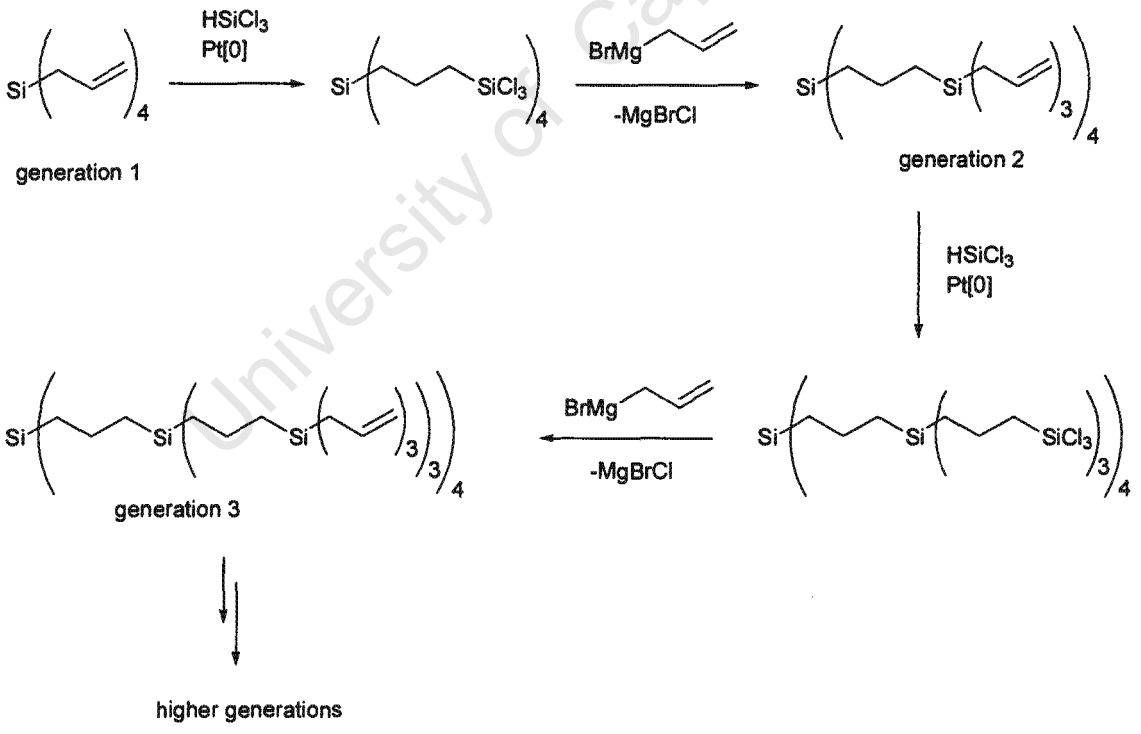

Fig. 3-4: Synthesis of carbosilane dendrimers[133]

Once an allyl dendrimer of the desired generation has been prepared, the terminal functionality may be modified. Typically this is done by a hydrosilylation reaction. Carbosilane dendrimers with -$SiMe_2Cl$ (hydrosilylation with $HSiMe_2Cl$) and -$SiMe_2CH_2Cl$ (hydrosilylation with $HSiMe_2CH_2Cl$) terminal

functionality have been prepared, both in our laboratory[140] and elsewhere. The -$SiMe_2Cl$ dendrimers in particular have been used as the precursors for a wide range of different terminal functionalities, including dendrimers with perfluoroaryl boranes[141], phosphines[142-145], silanols[146], chiral ligands for catalysis[147,148] and a wide variety of organometallic clusters[142,149], mononuclear organometallic species[142,143,150,151] and catalytically active organometallic species[144,152,153]. The synthesis of these molecules makes use of the high reactivity of the terminal Si-Cl bonds, which allow for quantitative reactions.

Far fewer reports of the -$SiMe_2CH_2Cl$ terminated dendrimers have been published.[154-156] In our own group, we have investigated the reaction of these dendrimers with organometallic nucleophiles $[CpFe(CO)_2]^-$ (Fp^-) and $[CpRu(CO)_2]^-$ (Rp^-).[157] Quantitative conversion to the metalloalkyl dendrimers (Fig. 3-5) proved problematic at the second generation level, particularly with the ruthenium nucleophile.

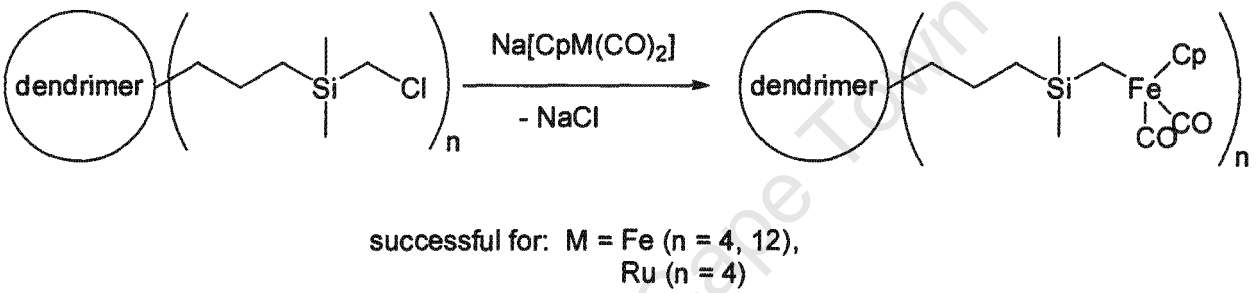

Fig. 3-5: Reactions of -$SiMe_2CH_2Cl$ terminated dendrimers with organometallic nucleophiles

3.1.3 Carbosilane dendritic wedges

Most research into carbosilane dendrimers has focused on periphery functionalisation. This is due to the current interest in multisite macromolecule catalysts, and to the divergent nature of the synthesis. More recently, however, several reports on core functionalised carbosilane dendritic wedges have been published.[Eric Oosterom, 1999 #85; Van Heerbeek, 1999 #577] In one example, a carbosilane wedge with core alkyl bromide functionality was prepared.[158] Starting with allyl bromide, successive hydrosilylation with trichlorosilane and alkenylation with allylmagnesium bromide is used to construct dendritic wedges up to the fifth generation (Fig. 3-6). The methodology is thus analogous to that used to prepare the original carbosilane dendrimers (Fig. 3-4).[133]

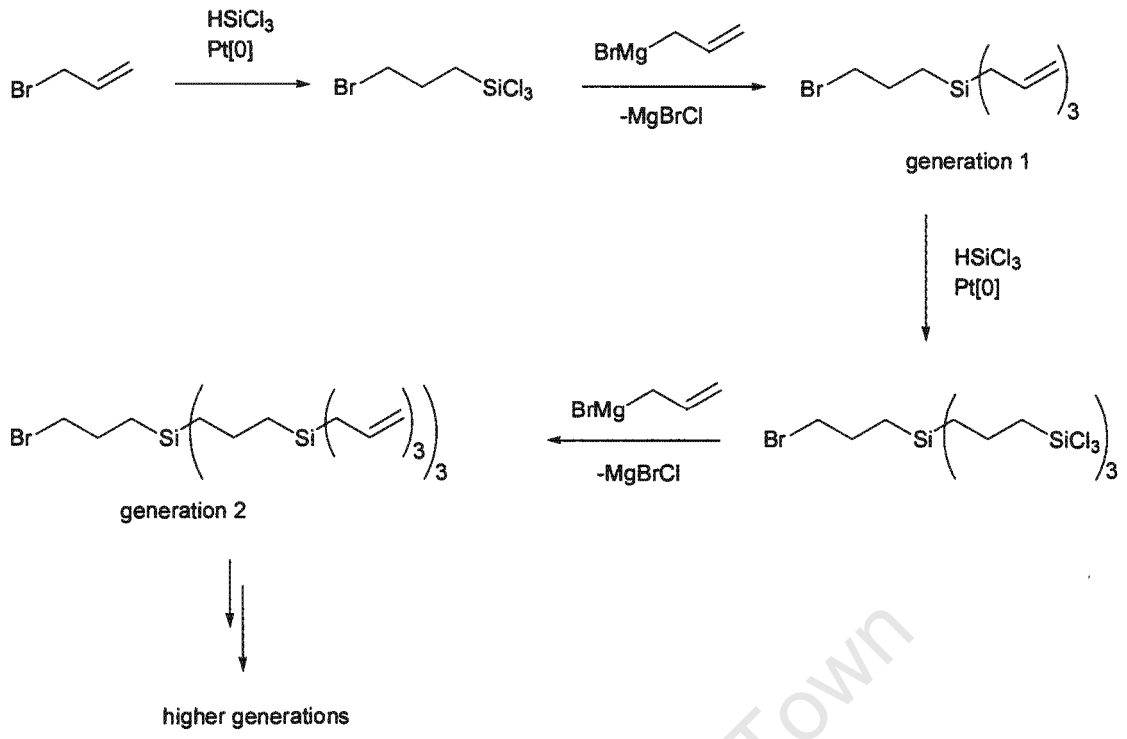

Fig. 3-6: Synthesis of carbosilane dendritic wedges[158]

Our interest in carbosilane dendritic wedges is in their use as components of ligands for catalysis (see chapters 4 and 6). The dendritic wedges thus are not used to create a large multisite catalytic 'ball', as with the more frequently reported approach.[159] Instead, a single catalytic centre is surrounded by one or more dendritic wedges, which modify the steric and/or electronic environment of the catalyst. This approach may be thought of as catalysis at the core of a dendrimer.[159,160]. For a detailed discussion, please refer to section 4.1.

In this chapter, we report new carbosilane dendritic wedges, similar in construction to those reported by van Leewen[158], but differing in certain key areas, including the core and peripheral functionality. We also report details of an investigation into the reactivity of these molecules. The synthesis and reactivity of a series of new carbosilane dendrimers with a novel peripheral functionality is also described.

3.2 Synthesis and characterisation of new carbosilane dendritic wedges

3.2.1 Platinum-catalysed reactions between allyl bromide and trichlorosilane or dimethylphenylsilane

As discussed in section 3.1.3, carbosilane dendritic wedges based on a bromopropyl core have previously been reported[158], although no experimental details were provided. The authors report that the starting material, 3-bromopropyltrichlorosilane was obtained by a 'platinum catalysed hydrosilylation of allyl

bromide with trichlorosilane'. This reaction has also been reported as long ago as 1967.[161] In this report, allyl bromide and trichlorosilane were heated to reflux over catalytic H_2PtCl_6, and the hydrosilylation product was isolated in 60% yield, although significant quantities of propene, bromotrichlorosilane and propyltrichlorosilane were also observed. However, our attempts at repeating this reaction were unsuccessful. Under a variety of conditions, including forcing conditions (100°C in a sealed vessel), only a low yield (<10%) of this product was obtained from the reaction between allyl bromide and trichlorosilane in the presence of Karstedt catalyst.

For this reason, an experimental investigation of the reactivity of allyl bromide in hydrosilylation reactions was undertaken. Dimethylphenylsilane was chosen as a test silane, because of its relative stability in air, its low volatility and its methyl groups, which facilitate NMR diagnosis of reaction products.

In order to test the activity of the freshly prepared Karstedt catalyst,[137,138] a hydrosilylation reaction of allyltrimethylsilane and dimethylphenylsilane to give **14** was performed (Fig. 3-7). The reaction was extremely exothermic, and was complete within a few seconds, as indicated by the decomposition of the platinum catalyst. This reaction established the activity and selectivity of the Karstedt catalyst and the likely reactivity of dimethylphenylsilane with dendritic double bonds.

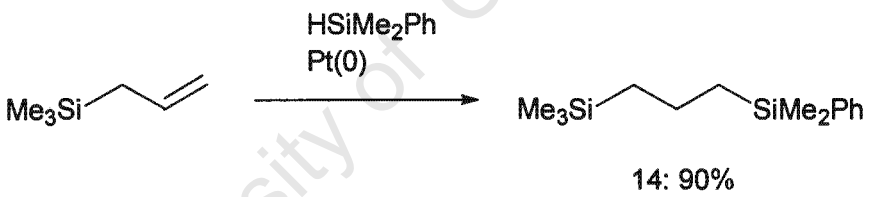

Fig. 3-7: Test platinum catalysed hydrosilylation reaction of allyltrimethylsilane with dimethylphenylsilane

A platinum catalysed reaction between allyl bromide and dimethylphenylsilane, performed at room temperature without solvent, followed by column chromatography, gave bis(dimethylphenylsilyl)ether (**15**), identified by NMR and mass spectrometry, in 65% yield (Fig. 3-8).

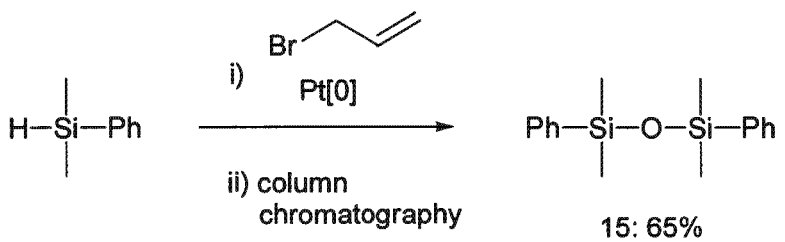

Fig.3-8: The platinum catalysed reaction of allyl bromide and dimethylphenylsilane

It was postulated that this result was due to the formation of bromodimethylphenylsilane in the reaction and subsequent hydrolysis on the column. A subsequent literature investigation revealed that the platinum catalysed reaction between allyl bromide and the series of silanes $HSi(^tBu)_n(O^iPr)_{3-n}$ (n = 0 – 3) or $HSiPh_3$ results exclusively in the formation of the corresponding bromosilanes and propene.[162] A full mechanism was not described, although it was suggested that allyl bromide is initially coordinated to the Pt(0) catalyst and oxidative addition of H-SiR_3 follows.[162] Presumably the ability of allyl halides to form η^3-allyl complexes with transition metals[163], explains the different reactivity that allyl bromide displays compared to other alkenes. It has been reported that Pt(0) complexes react by oxidative addition with allyl bromide to give η^1-allyl complexes[164], which however show dynamic behaviour and rearrange via an η^3-allyl complex to the η^1-allyl complex attached at the opposite end.[165] This proposed mechanism involving an η^3-allyl intermediate is further supported by the fact that 4-bromo-1-butene (which cannot form η^3-allyl complexes) undergoes standard hydrosilylation reactions.[166] Platinum catalysed reactions of allyl chloride with silanes give both hydrosilylation products and propene formation[167]; this is presumably because allyl chloride is less likely to form an η^3-allyl complex as chloride is a poorer leaving group than bromide. On the basis of the above assumption, it is possible to speculate a mechanism for the reaction (Fig. 3-9).

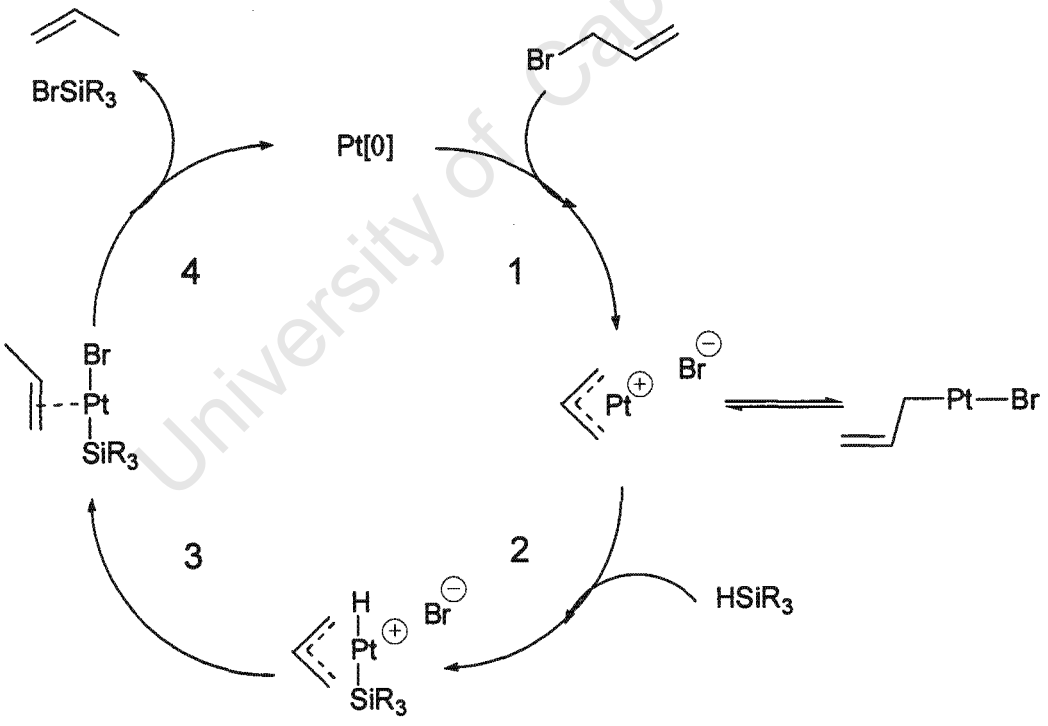

Fig. 3-9: Speculative mechanism for the platinum catalysed reaction of allyl bromide and silanes

Coordination of the allyl bromide results in the formation of a cationic η^3-allyl platinum complex (step 1). Oxidative addition of the Si-H bond (step 2) is followed by coupling of the allyl moiety and the hydrogen to form an η^2-alkene adduct (step 3). Reductive elimination of Br-SiR_3 and alkene dissociation completes

the cycle (step 4). Propene is volatile and is irreversibly removed from the reaction mixture, and this may be the driving force for the reaction.

As part of the initial attempts to understand the reactivity of allyl bromide with silanes, several other reactions were carried out which demonstrate the selectivity towards formation of bromosilanes. When the platinum catalysed reaction of allyl bromide and dimethylphenylsilane was carried out in THF, 4-bromobutyldimethylphenylsilylether (**16**), identified by elemental analysis, NMR and mass spectrometry, was obtained in 88% yield. This product is the result of a ring opening reaction of bromodimethylphenylsilane with THF (Fig. 3-10). Similar reactions of bromosilanes with cyclic ethers have been previously reported in the literature.[168, 169]

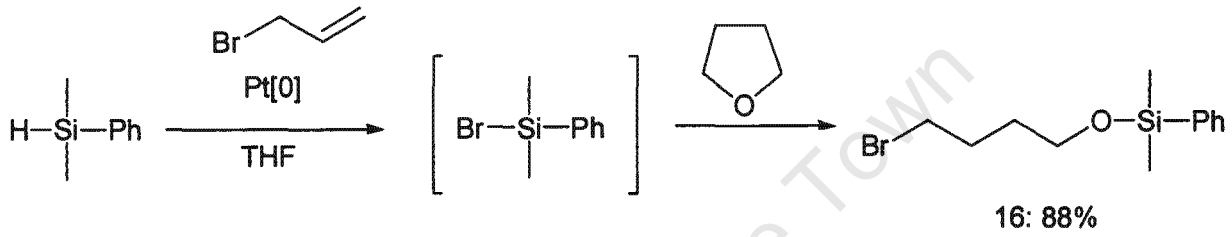

Fig. 3-10: Platinum-catalysed reaction of allyl bromide and dimethylphenylsilane in THF

The platinum-catalysed reaction between allyl bromide and dimethylphenylsilane was again carried out under rigorously moisture free conditions, this time in the inert solvent pentane, and the product was treated with a solution of *n*-butyl lithium (Fig. 3-11). The expected product, *n*-butyldimethylphenylsilane[170, 171] (**17**), was obtained after purification by column chromatography.

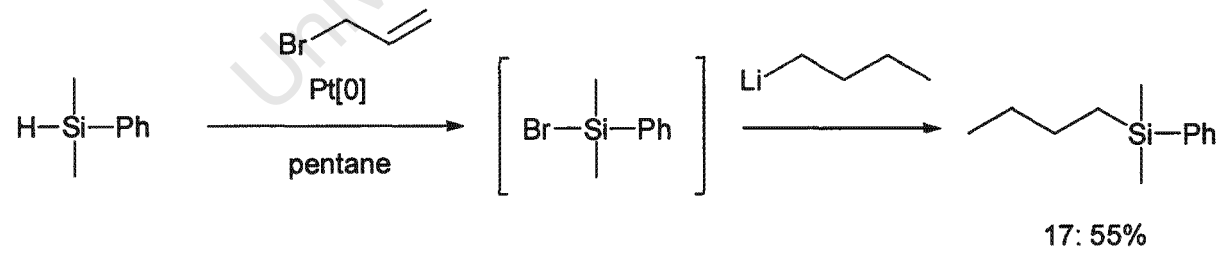

Fig. 3-11: Platinum-catalysed reaction of allyl bromide and dimethylphenylsilane, and subsequent reaction with n-butyl lithium

$BrSiMe_2Ph$, formed by the platinum catalysed reaction of allyl bromide and dimethylphenylsilane, was observed directly by ^1H NMR spectroscopy. The reaction was carried out in toluene, and after removal of the volatiles *in vacuo*, an NMR sample in C_6D_6 was prepared in a Teflon-valved NMR tube. The $BrSiMe_2Ph$ singlet was visible at 0.56ppm. This represents a significant downfield shift from other -$SiMe_2Ph$ shifts (e.g. *n*-$BuSiMe_2Ph$, 0.28ppm) due to the inductive effect of the electronegative bromine.

When D_2O was added to the NMR sample, the hydrolysis reaction to give bis(dimethylphenylsilyl)ether could be observed directly by ^1H NMR. Over a period of 45min, the singlet at 0.56ppm disappeared and was replaced by a singlet at 0.33ppm, corresponding to bis(dimethylphenylsilyl)ether. The reason for the slow reaction is presumably because of the poor miscibility of D_2O in the benzene-d_6 NMR solvent.

3.2.2 Synthesis and characterisation of dendritic wedges using 4-bromo-1-butene as a starting material

On the basis of the above investigation, it is not clear how the authors of the original report of carbosilane wedges obtained 3-bromopropyltrichlorosilane by means of a hydrosilylation reaction. No experimental details were provided.[158]

In order to overcome these difficulties, 4-bromo-1-butene was used instead as a substrate for the hydrosilylation reaction. This alkene cannot form an η^3-allyl complex with platinum, and will thus not be susceptible to the mechanism described in section 3.2.2. Hydrosilylation reactions of 4-bromo-1-butene are known.[166] The platinum catalysed reaction of 4-bromo-1-butene with dimethylphenylsilane gave the desired hydrosilylation product exclusively in 95% yield (Fig. 3-12). The reaction was carried out at room temperature using THF as a solvent. After the volatiles (including excess $HSiMe_2Ph$) were removed *in vacuo*, the decomposed catalyst was removed by taking up the product in hexane and filtering through silica. After removing the hexane *in vacuo*, 4-bromobutyldimethylphenylsilane (**18**) was obtained as a colourless oil.

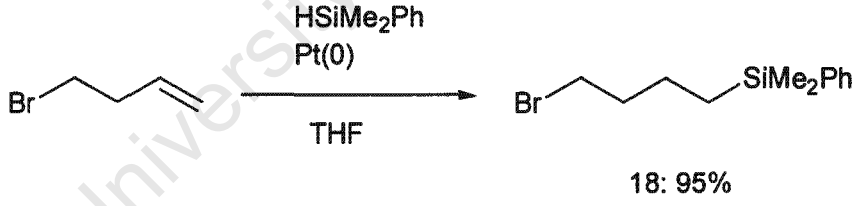

Fig. 3-12: Hydrosilylation reaction of 4-bromo-1-butene with dimethylphenylsilane

Although clearly 4-bromobutyldimethylphenylsilane is not dendritic, it may be thought of as a 'generation zero' dendritic wedge by analogy to higher generation wedges, and it serves both as a useful model for the core chemistry of higher generation wedges and as the first component of a series of different generation wedges.

In the previous report on the use of bromoalkyl core functionalised carbosilane wedges, the wedges were used in subsequent applications with unmodified allyl terminal functionality.[158] However, for our purposes (see chapters 4 and 6), this is undesirable, particularly because of the potential reactivity of dendritic double bonds in catalytic reactions. The use of the dimethylphenylsilyl terminal functionality was thus

made in the dendritic wedges described in this thesis. This terminal functionality is relatively inert, and adds steric bulk to the wedges. Greater bulk is desired to maximise potential dendritic effects and recovery in catalytic applications. In addition, the methyl singlets in the ^{1}H and ^{13}C NMR spectra provide a useful observational 'handle' for diagnosis of percentage conversion and purity, and the relevant starting silane, $HSiMe_2Ph$, is both sufficiently involatile for convenient use (unlike, for example $HSiMe_3$), and sufficiently volatile for any excess to be removed *in vacuo* from reaction mixtures.

A first generation carbosilane wedge (**21**) was prepared by standard carbosilane methodology using 4-bromo-1-butene as a starting material (Fig. 3-13).

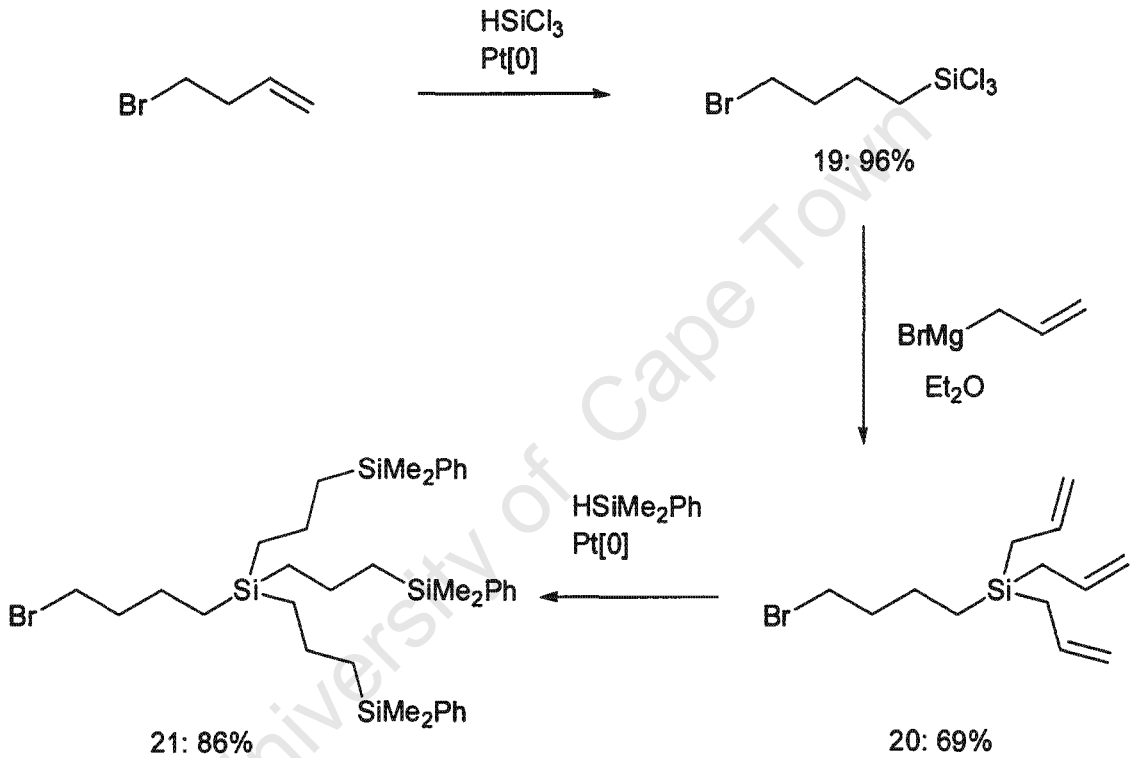

Fig. 3-13: Synthesis of first generation carbosilane dendritic wedge

The hydrosilylation reaction between 4-bromo-1-butene and trichlorosilane was performed in a thick-walled glass pressure tube at 70°C without the use of a solvent. After removal of excess trichlorosilane *in vacuo*, the highly air-sensitive intermediate, 4-bromobutyltrichlorosilane (**19**), was obtained and identified by ^{1}H and ^{13}C NMR spectroscopy. After reaction of **19** with excess allylmagnesium bromide and an aqueous work-up, the first generation allyl functionalised dendritic wedge (**20**) was obtained as a clear oil. The allyl Grignard reagent reacted selectively with the Si-Cl bonds, and no evidence of reaction with the bromobutyl core functionality was observed. **20** was characterised by ^{1}H, ^{13}C and ^{29}Si NMR, mass spectrometry and IR. The synthesis of **21** was completed by quantitative hydrosilylation of **20** with $HSiMe_2Ph$ to give the desired tris(dimethylphenylsilyl) functionalised wedge. After completion of the reaction, the excess silane was removed *in vacuo* and the crude product was filtered through silica as a

hexane solution to remove decomposed platinum catalyst. Upon removal of the hexane, the first generation dendritic wedge was obtained as a viscous clear oil and characterised by ^{1}H, ^{13}C and ^{29}Si NMR, mass spectrometry, elemental analysis and IR spectroscopy. The ^{1}H NMR spectrum of **21** is shown in Fig. 3-14.

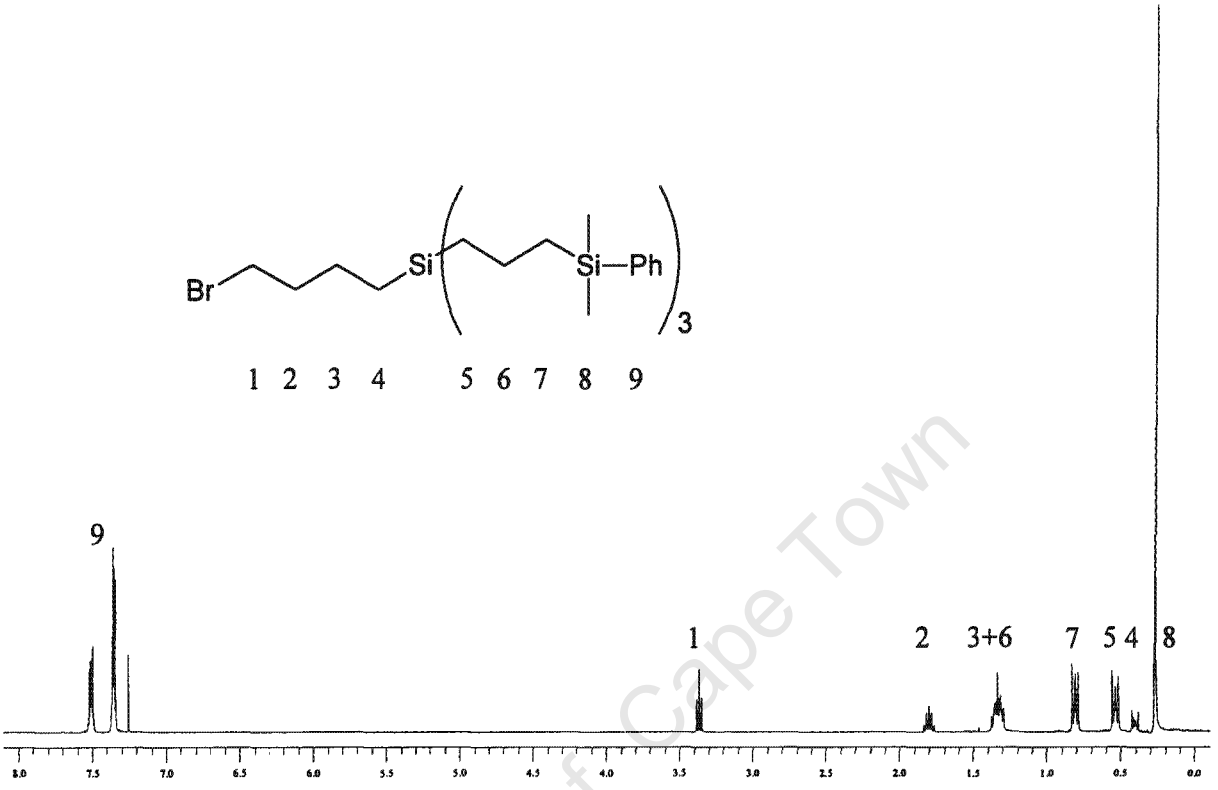

Fig. 3-14: ^{1}H NMR spectrum of 21

The second generation allyl wedge (**22**) was also prepared (Fig. 3-15), although no reactions were attempted on this compound. It remains a topic for further study to prepare the dimethylphenylsilyl derivative. This compound was not required for catalytic purposes (chapters 4 and 6) and therefore it was not prepared in this work. However, a simple hydrosilylation of **22** with $HSiMe_2Ph$ should yield the second generation wedge if this is required.

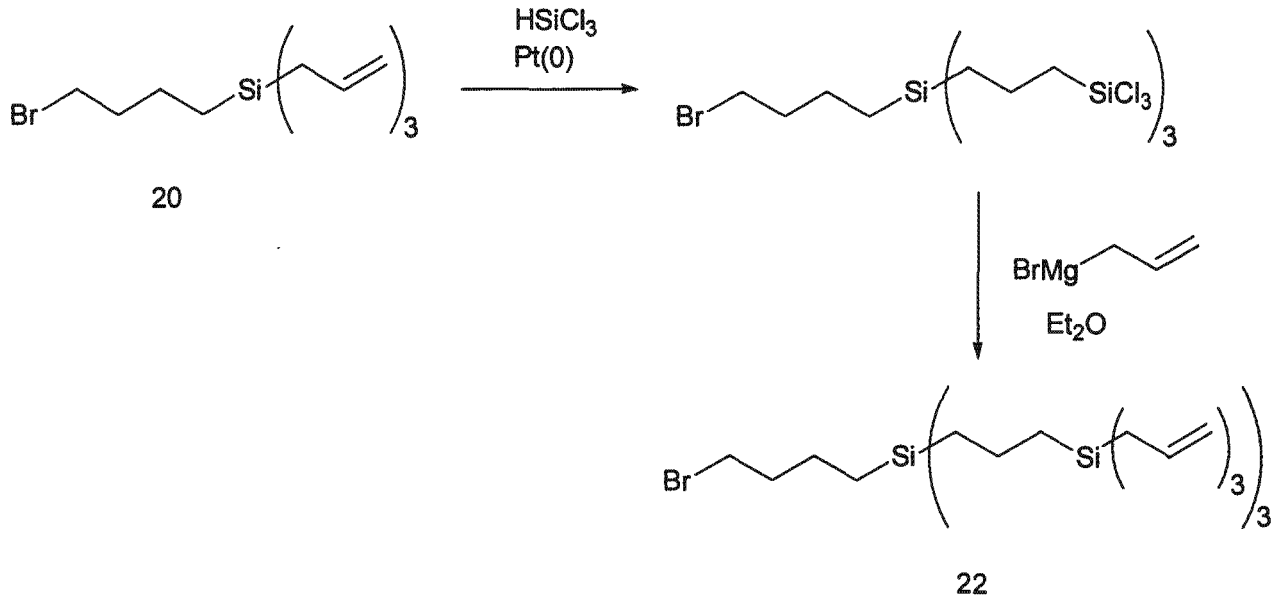

Fig. 3-15: Preparation of second generation allyl carbosilane wedge (22)

3.3 Reactivity of dendritic wedges

3.3.1 Halogen exchange reaction

Halogen exchange of alkyl halides ($RX + X'^{-} \leftrightarrow RX' + X^{-}$) is an equilibrium process.[172] However alkyl iodides can be selectively formed from alkyl chlorides and bromides by refluxing in acetone with NaI or KI. NaI is soluble in acetone, whereas NaBr or NaCl precipitate out, and this shifts the equilibrium to favour formation of alkyl iodide.[172] The bromobutyl carbosilane dendritic wedges (**18** and **21**) were converted to their iodobutyl analogues (**23** and **24**) by this methodology (Fig. 3-16). These compounds may be useful as iodide is a better leaving group than bromide, and hence alkyl iodides are more reactive with a variety of nucleophiles.

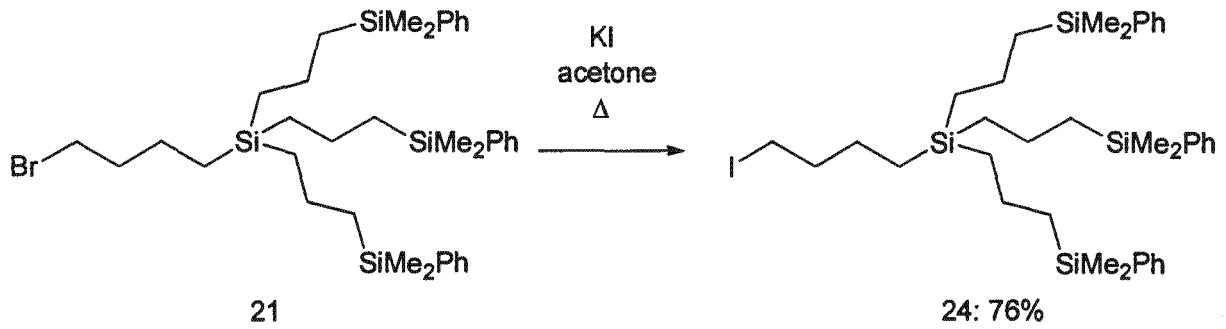

Fig. 3-16: Conversion of bromobutyl wedge (21) to the iodobutyl analogue (24)

A large excess of KI is used in the preparations. Although precipitation of KBr should favour selective formation of the iodide, in practice it was found that a large excess of KI is necessary to obtain quantitative conversion.

The iodobutyl wedges **23** and **24** were characterised by NMR and IR spectroscopy. The shifts of the -CH_2X signal in the ^{1}H NMR (X = Br : ~3.39ppm; X = I : ~3.18ppm) and of the -CH_2X signal of the ^{13}C NMR (X = Br : ~35ppm; X = I : ~7ppm) confirm the quantitative conversion to the iodide. The iodobutyl wedges are colourless oils upon isolation after an aqueous work-up; however after standing for a few hours, a yellow colour forms due to the liberation of iodine. This is characteristic of many alkyl iodides. For this reason, elemental analysis did not give good results.

3.3.2 Reaction with hydroxyaryl compounds

The reaction of alkyl halides with hydroxyaryl compounds is a well established reaction in organic chemistry[172], and this reaction has been used in the synthesis of poly(benzylphenylether) dendrimers.[127] The reaction of the new bromobutyl dendritic wedges with hydroxyaryl core compounds is discussed in detail in chapter 4, where the reaction is employed to functionalise bisiminopyridyl-type ligands with dendritic wedges. No details are given here, but the work in chapter 4 establishes that the bromobutyl dendritic wedges do react with hydroxyaryl compounds in the presence of a base to give the arylalkylether (Fig. 3-17) in good yield.

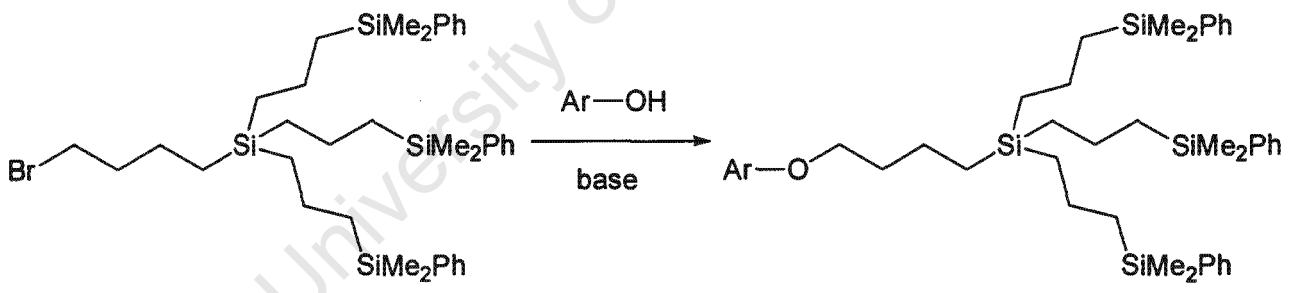

Fig. 3-17: Reaction of bromobutyl wedges (first generation shown) with hydroxyaryl cores

3.3.3 Attempted lithium-halogen exchange reaction

Recently, other workers in our group have synthesised a novel series of polylithiated dendrimers (see section 3.5.3 for a more detailed discussion).[173] To complement this work, attempts were made to prepare core-lithiated dendritic wedges by means of a lithium-halogen exchange reaction. These reagents would potentially open new synthetic pathways to compounds functionalised by carbosilane dendritic wedges. It is well known that treatment of a primary alkyl halide with a tertiary alkyl lithium reagent (such as *t*-butyl lithium) facilitates lithium-halogen exchange, particularly with alkyl bromides and iodides (Fig. 3-18).[174] If two equivalents of *t*-BuLi are used, the second equivalent reacts with the *t*-butyl halide by-product to give

2,2,3,3-tetramethylbutane ('ditert'), which prevents coupling of the *t*-butyl halide with the desired lithiated product.[174,175]

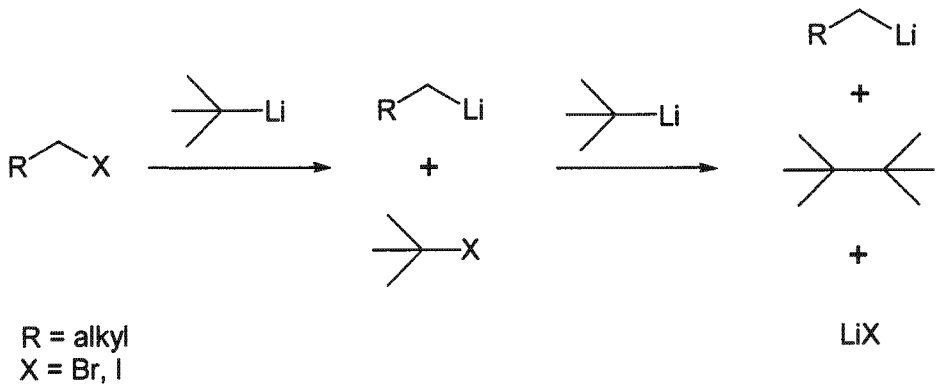

Fig. 3-18: Lithium-halogen exchange reaction with t-butyl lithium

The model 'zero generation' wedge **18** was treated with a three-fold excess of *t*-BuLi in ether at -78°C (Fig. 3-19). After 20 minutes, the reaction was quenched by the addition of $ClSiMe_3$ so as to obtain a stable product which would indicate if the lithium-halogen exchange had been successful. After workup, a colourless liquid was recovered with a mass greater than quantitative yield of the intended reaction, and NMR spectroscopy indicated a complex array of products. It was apparent that reactions at the $SiMe_2Ph$ moiety were competitive with the desired reaction at the alkyl-halide functionality. Although no attempts were made to identify these products, it is known that silyl-substituted phenyl rings are deprotonated by *n*-BuLi / KO^{t}Bu ('superbase') at both the *meta* and *para* positions, and that the silyl substituent enhances the rates of these reactions.[176] It is possible that a similar deprotonation at the phenyl ring of -$SiMe_2Ph$ occurs when *t*-BuLi is used as a base.

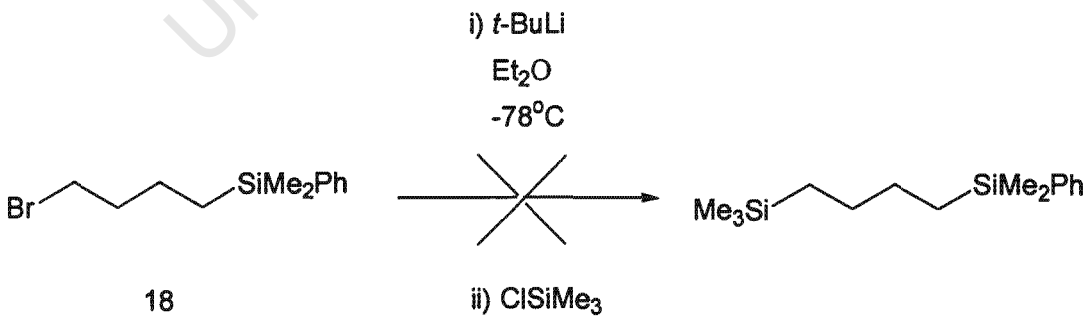

Fig. 3-19: The unsuccessful attempted lithium-halogen exchange reaction of the 'generation zero' carbosilane wedge

It is conceivable that the undesired side reactions could be eliminated by controlling the stoichiometry more closely (by adding, for example, exactly one equivalent of *t*-BuLi). Coupling of the lithiated wedge

and the *t*-butyl bromide by-product then presents a possible problem (see section 3.5.3). Alternatively, the use of terminal silyl functionality without Si-Ph (for example -$SiMe_3$ instead of -$SiMe_2Ph$) could provide an alternative route to the synthesis of core-lithiated dendritic wedges. These possibilities were not investigated further in this work.

3.4 Synthesis and characterisation of new bromobutyl functionalised carbosilane dendrimers

3.4.1 Rationale

As discussed in section 3.1.2, carbosilane dendrimers with terminal alkyl halide (-$SiMe_2CH_2Cl$) functionality have been reported.[154-156] However, our attempts at reacting these dendrimers with metal nucleophiles were hindered due to a lack of reactivity of the terminal -$SiMe_2CH_2Cl$.[Overett, 1998 #663]

The silicon atom has a profound and complex effect on the reactivity of adjacent carbons. It is well established that silicon stabilises an α-carbanion.[177] It is believed that this is due to polarisation and hyperconjugation effects[178,179] and not due to (p-d)π overlap (back-bonding) as originally thought.[180] The electrophilic character adjacent to silicon is reduced and no S_N1 processes α to silicon are known[67] Nucleophilic processes that do occur are believed to occur via an S_N2 mechanism, and it is believed that initial nucleophilic attack takes place at silicon with subsequent 1,2-migration to the α-carbon.[67] For example, Me_3SiCH_2Cl is less reactive than CH_3CH_2Cl towards ethoxide[181] and in solvolysis reactions[180], and does not react at all with $AgNO_3$ under conditions where *n*-alkyl halides do react.[180] However, other studies have shown a faster reaction of Me_3SiCH_2Cl with NaI than *n*-alkyl chlorides.[182] The effect of the silicon on the reactivity of α-alkyl halides is thus complex; however in general it appears to have a deactivating effect for reactions dependent on the electrophilicity of the α-carbon.

For this reason, it would be highly desirable to form a dendrimer with alkyl halide terminal functionality that avoids the complex reactivity of –$SiMe_2CH_2X$. If the carbon chain between the silicon and the halide could be lengthened ($Si[CH_2]_nX$; n>1), then the reactivity of the dendrimer terminal groups would more closely resemble that of general *n*-alkyl halides. The higher reactivity would facilitate a wider range of successful dendritic reactions, utilising the well-developed chemistry of *n*-alkyl halides, in particular their reactions with organometallic nucleophiles.[67] Higher generations of functionalised dendrimers would be potentially accessible, as problems with non-quantitative conversions may be overcome.

Following the successful synthesis of low generation carbosilane wedges (**18**, **21** and **22**) with *n*-bromobutyl core, a possible synthesis of *n*-bromobutyl terminated dendrimers was identified (Fig. 3-20). 4-Bromobutyldimethylsilane may be prepared by a hydrosilylation reaction between 4-bromo-1-butene and

chlorodimethylsilane, followed by reduction with $LiAlH_4$.[166] The dendrimers may then be synthesised by quantitative hydrosilylation of allyl-terminated dendrimer[133] with 4-bromobutyldimethylsilane (Fig. 3-20).

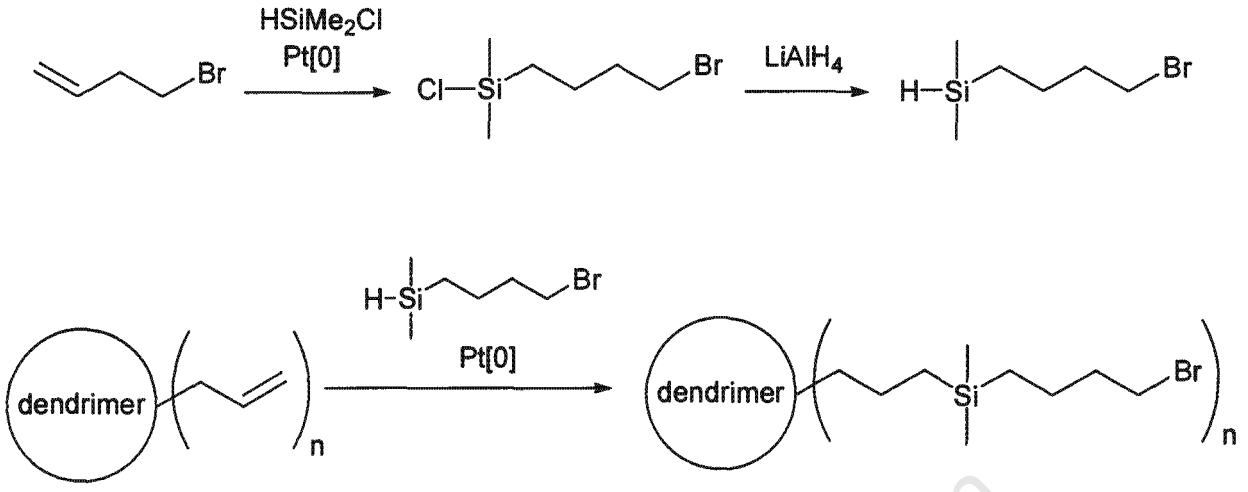

Fig. 3-20: Envisioned synthesis of n-bromobutyl terminated dendrimers

The choice of a four carbon spacer between silicon and halide is largely dictated by the available chemistry. The two carbon spacer silane, $HSiMe_2CH_2CH_2X$ (X = Cl, Br, I), has not been reported in the literature, although its possible precursor $ClSiMe_2CH_2CH_2X$ (X = Cl, Br) is known.[183] The three carbon analogue, $HSiMe_2CH_2CH_2CH_2X$ (X = Cl, Br, I) is also unknown, and will not be readily accessible via a hydosilylation reaction of allyl halide, for the reasons discussed in section 3.2.2.

It is worth noting the connection between the carbosilane wedges discussed in sections 3.2 and 3.3 and the envisioned dendrimers discussed above. The wedge core functionality and the dendrimer peripheral functionality are both bromobutyl groups, derived from 4-bromo-1-butene. Thus the core chemistry of the wedges and the peripheral chemistry of the dendrimers may be expected to be similar.

3.4.2 Synthesis of 4-bromobutyldimethylsilane (26)

4-Bromobutyldimethylchlorosilane (**25**) was readily synthesised by a platinum catalysed hydrosilylation reaction between 4-bromo-1-butene and chlorodimethylsilane according to a modified literature procedure.[166] The reaction was carried out in a thick-walled glass pressure tube at 85°C, and after removal of the excess $HSiMe_2Cl$, the air-sensitive product was obtained as a clear liquid and characterised by ^1H and ^{13}C NMR spectroscopy.

Several attempts were made to prepare 4-bromobutyldimethylsilane (**26**) according to the literature procedure. According to this procedure, **25** was reduced with $LiAlH_4$ in refluxing ether, and then, following an acid workup and distillation, **26** was obtained in 81% yield.[166] However in all attempts to repeat this result, yields of the desired product were extremely low (<20%) and the major product recovered was the

hydrolysis product bis(4-bromobutyldimethylsilyl)ether. This hydrolysis evidently occurs during the acidic work-up procedure. Si-H bonds are susceptible to hydrolysis by Bronsted bases. Although the acidic work-up is designed to neutralise basicity caused by the hydrolysed excess $LiAlH_4$, it is apparent that **26** was nevertheless hydrolysed despite the use of concentrated HCl to quench the reaction. It became clear later that **26** is in fact moderately air-sensitive, and hydrolysis of the pure compound took place slowly over a few days if left exposed to air.

A modification to the experimental procedure was therefore made. After the reduction in ether was complete, the volatiles, including **26** (boiling point: 70-71^{0}C at 18mm[166]), were separated from the lithium salts by trap to trap vacuum distillation, heating the reaction residues to 100°C to volatilise all the product. The ether was then removed *in vacuo* at 0°C. At this temperature, minimal loss of **26** was observed, and the pure product was isolated as a clear liquid in 83% yield and stored under an inert atmosphere.

3.4.3 Synthesis and characterisation of new bromobutyl functionalised dendrimers

New carbosilane dendrimers with terminal 4-bromobutyldimethylsilyl functionality up to the third generation were successfully prepared (Fig. 3-20). Second and third generation allyl-functionalised dendrimers were prepared by literature methodology (Fig. 3-4).[133,134] The platinum catalysed hydrosilylation reactions of these compounds with 4-bromobutyldimethylsilane were extremely exothermic, and conversion is quantitative, such that no allyl signals were apparent in the NMR and IR spectra of the products. The hydrosilylations appear to be completely regioselective to the β-addition product (anti-Markovnikov addition); no evidence of the α-addition (Markovnikov addition) product was observed. α-Addition products have a characteristic doublet at δ_H ~1.0ppm in the ^{1}H NMR spectra[154]; this was not seen. The reactions were carried out in the absence of solvent, and it was in fact observed that the use of THF as a solvent inhibits quantitative hydrosilylation. Elevated reaction temperatures (>100°C) were used in order to make sure that the reactions proceeded to completion. The first (**27**), second (**28**) and third (**29**) generation dendrimers have 4, 12 and 36 terminal bromobutyl groups and molecular masses of 973, 3144 and 9650 respectively.

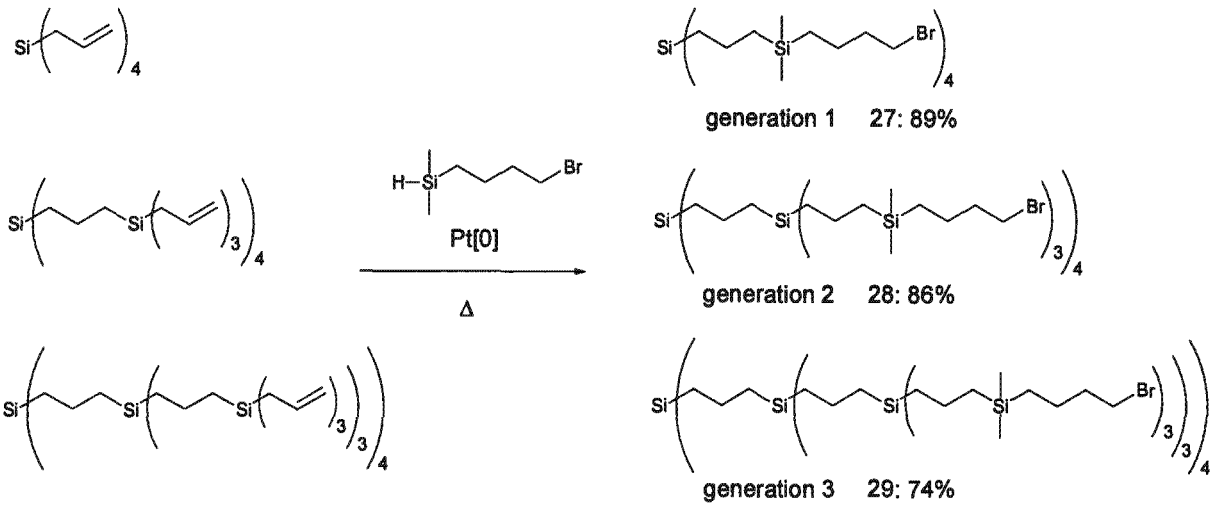

Fig. 3-20: Synthesis of generation 1 – 3 bromobutyl functionalised carbosilane dendrimers (27, 28, 29)

The new bromobutyl dendrimers were characterised by ^{1}H, ^{13}C and ^{29}Si NMR spectroscopy and IR spectroscopy. Elemental analyses were unfortunately outside of the acceptable limits, particularly for carbon, where typically the analysis was about 1% out. The dendrimers are oils which cannot be recrystallised, and due to the low polarity, column chromatography is of limited effectiveness in purification. Acceptable analyses were, however, obtained for derivatives of the dendrimers; see section 3.5.2 for details. Characterisation by mass spectrometry was also found to be problematic. Under electron ionisation (EI) or fast atom bombardment (FAB) conditions, the dendrimers fragmented completely, and neither the molecular ion nor recognisable fragments were observed. This has been found previously.[140] Nevertheless, NMR spectroscopy is a powerful tool for the characterisation of dendrimers. The ^{1}H NMR spectra of **27**, **28** and **29** are shown in Fig. 4-21. Although the molecules are large, their inherent symmetry means that their NMR spectra are relatively simple. Defects in the dendrimers will be seen. In the ^{1}H NMR spectra, the most characteristic signals are the terminal -CH_2Br (~3.41ppm, t, ^{3}J(HH) 7Hz), -CH_2CH_2Br (~1.87ppm, qn, ^{3}J(HH) 7Hz) and -SiMe_2- (~0.02ppm, s) signals (Fig. 3-21). The arrays of internal -$CH_2CH_2CH_2$- and -SiCH_2CH_2- signals tend to coalesce, but the integration of the combined signals is correct.

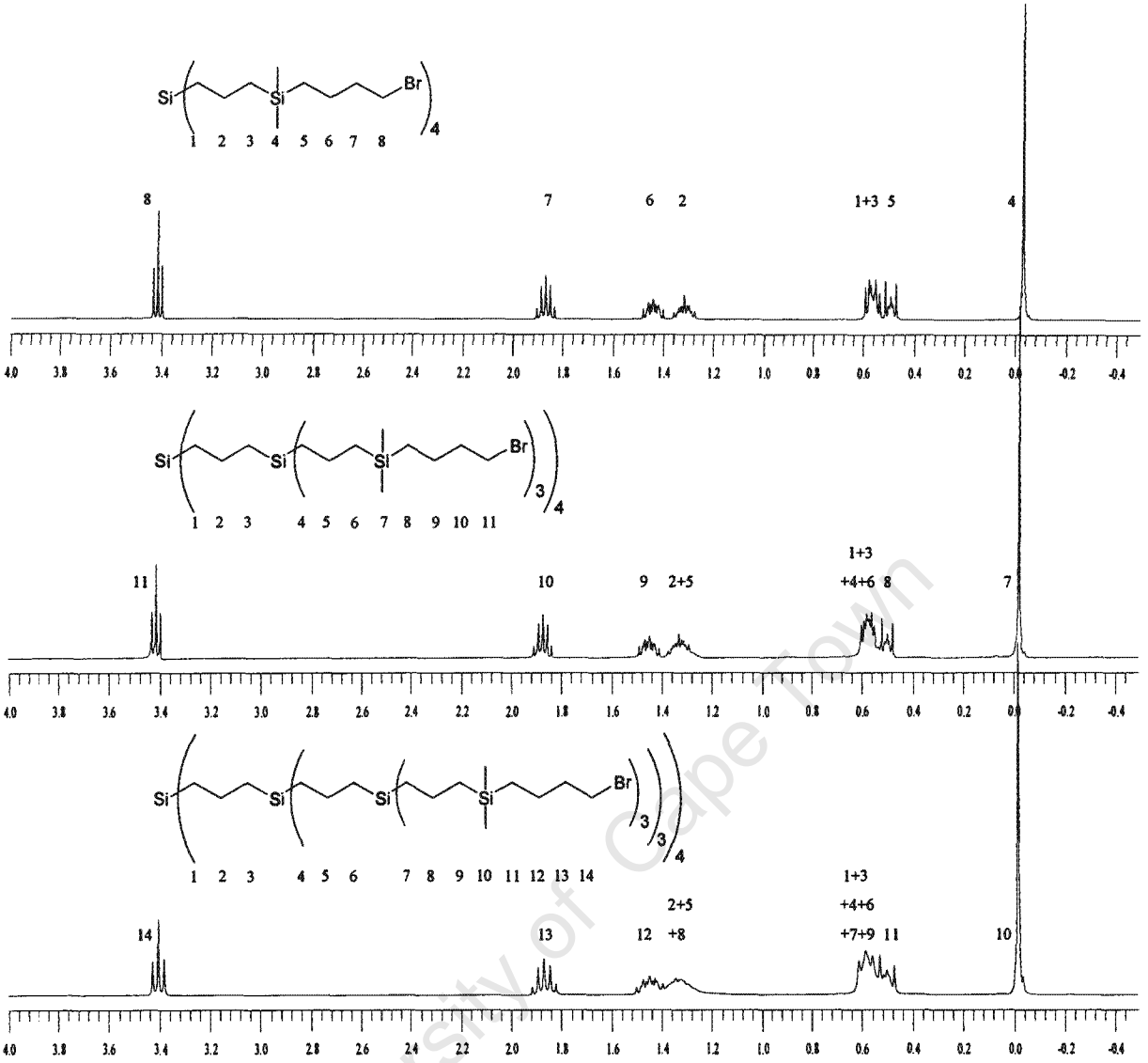

Fig. 3-21: ^{1}H NMR spectra of generation 1 – 3 bromobutyl functionalised dendrimers (27,28,29)

The ^{29}Si NMR spectra show two peaks at 2.3ppm (-SiMe$_2$(CH$_2$)$_4$Br) and 0.7ppm (internal silicons atoms). At the available resolution, all internal silicon atoms appear as a single peak.

3.5 Reactivity of bromobutyl functionalised carbosilane dendrimers

3.5.1 Halogen exchange reactions

The bromobutyl dendrimers may be converted to the iodobutyl analogues by means of a halogen exchange reaction (Fig. 3-22). First (**30**) and second (**31**) generation iodobutyl terminated dendrimers were prepared in this way; the third generation analogue was not attempted. These dendrimers may be synthetically useful in further dendritic functionalisations because iodide is a better leaving group than bromide. After refluxing

28 and **29** over a large excess of KI or NaI in acetone (see section 3.3.1), **31** and **32** are obtained as colourless oils after an aqueous work-up.

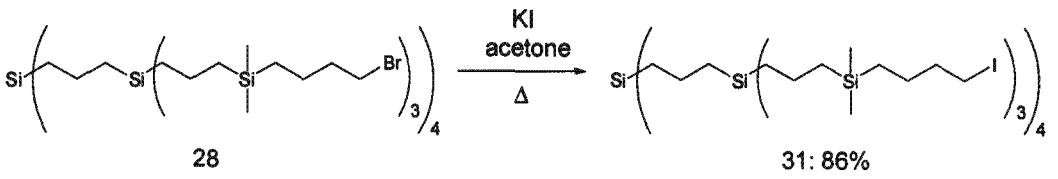

28 31: 86%

*Fig. 3-22: Synthesis of iodobutyl dendrimers (generation 2, **31**, shown) by halogen exchange reaction*

The iodobutyl dendrimers were characterised by NMR and IR spectroscopy. The shifts of the -CH_2X signal (X = Br, ~3.41ppm; X = I, ~3.19ppm) in the ^{1}H NMR spectra and the -CH_2X signal (X = Br, ~33.6ppm; X = I, ~6.9ppm) in the ^{13}C NMR spectra indicate quantitative conversion. As discussed in section 3.3.1, the use of large excesses of KI is necessary to prevent significant residual alkyl bromide due to equilibrium effects caused by the KBr reaction by-product.

3.5.2 Reaction with *p*-cresol

The reaction of alkyl halides with hydroxyaryl compounds is a well-known reaction in dendritic chemistry, as it is the basis for the synthesis of poly(benzylphenylether) dendrimers[127] and has been used previously in our group in the synthesis of periphery functionalised metal containing dendrimers.[184-186] As part of the investigation into the reactivity of the new bromobutyl dendrimers, the reaction of these dendrimers with a hydroxyaryl compound was attempted. This methodology may open a simple synthetic pathway to the functionalisation of the new dendrimers with useful peripheral groups such as catalytic organometallic fragments (see section 4.7). The hydroxyaryl compound chosen was *p*-cresol (4-methylphenol) rather than phenol. The additional methyl group is a diagnostic 'handle' in the NMR spectra on the basis of which purity, percentage conversion and the presence of unreacted *p*-cresol may be evaluated.

The conditions utilised were similar to those reported by Frechet and Hawker for the synthesis of poly(benzylphenylether) dendrimers.[127] The reactions were carried out in refluxing acetone using K_2CO_3 as the base and a small amount of 18-crown-6 to solubilise the base in the solvent (Fig. 3-23). After column chromatography, the expected aryl alkyl ether functionalised dendrimers (first generation, **32** and second generation, **33**) were obtained. The reaction was not attempted for the third generation dendrimer. Apart from the potential synthetic value of this reaction, the greater polarity of the new dendrimers meant that column chromatography was effective in obtaining analytically pure samples. Acceptable elemental analyses were thus obtained on these dendrimers.

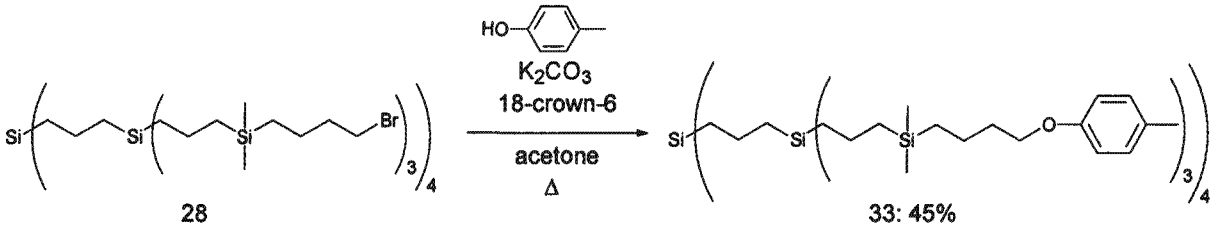

Fig. 3-23: Reaction of bromobutyl dendrimers with p-cresol (preparation of second generation aryl alkyl ether dendrimer, 33, shown)

Once again, NMR spectroscopy is particularly useful for purposes of characterisation. In the ^{1}H NMR spectra (Fig. 3-24), the shift in the -CH_2X signal (X = Br, ~3.41ppm; X = OAr, ~3.92ppm) indicates quantitative conversion. In addition, the characteristic Ar-*Me* singlet is apparent at ~2.29ppm, and the aryl protons are seen as two doublets at ~7.07 and ~6.80ppm.

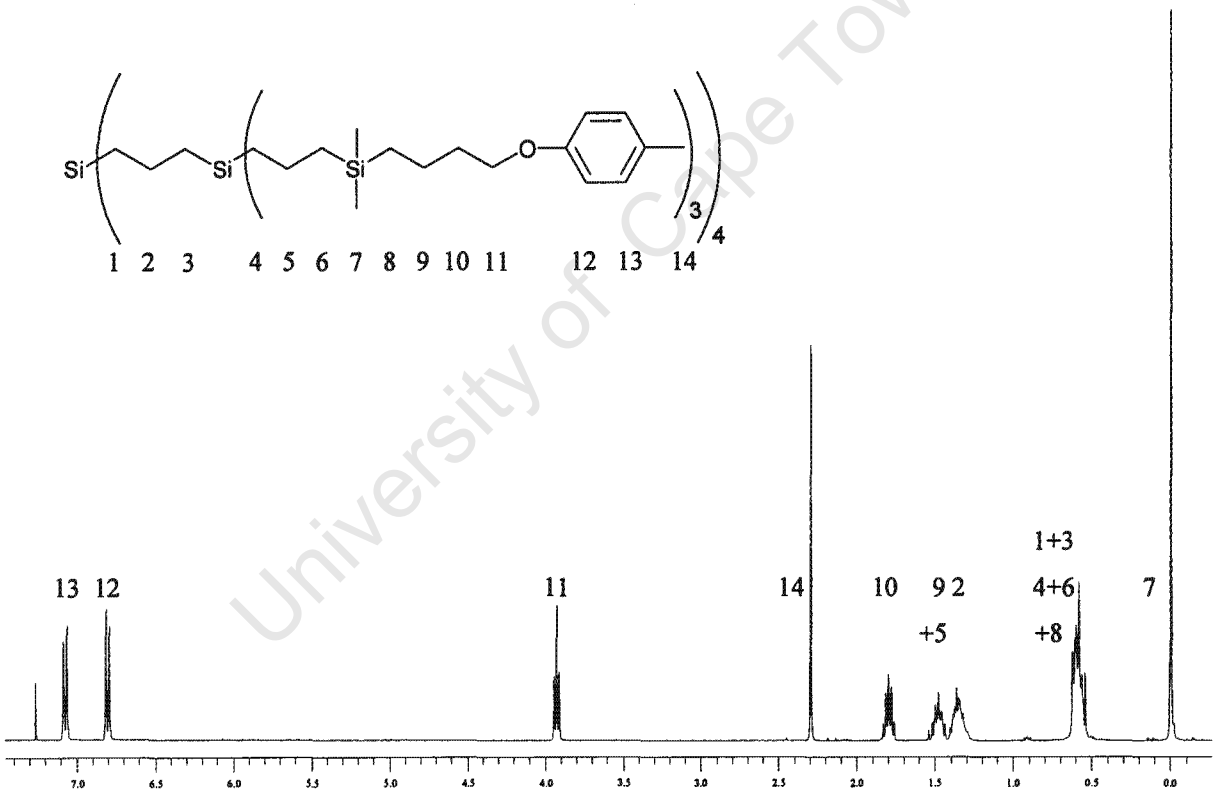

Fig. 3-24: ^{1}H NMR spectrum of second generation arylether functionalised dendrimer (33)

3.5.3 Lithium-halogen exchange reaction

Recently other workers in our group have synthesised a novel series of polylithiated carbosilane dendrimers, with -$SiMe_2CH_2Li$ end groups.[173] The preparation of these highly air-sensitive compounds requires a synthetically challenging cleavage of the CH_2-S bond of -$SiMe_2CH_2SPh$ functionalised dendrimers by lithium naphthalide, and separation of the by-products from the lithiated dendrimer proved

problematic. Complete lithiation of -$SiMe_2CH_2Cl$ functionalised dendrimers with metallic lithium proved impossible. It appeared possible that the new carbosilane dendrimers with *n*-bromobutyl end groups may be amenable to lithium-halogen exchange (Fig. 3-25), which is a facile process for general *n*-alkyl halides.[187] The anticipated *n*-butyl lithium functionalised dendrimers would potentially open new synthetic routes to a wide variety of functionalised dendrimers.

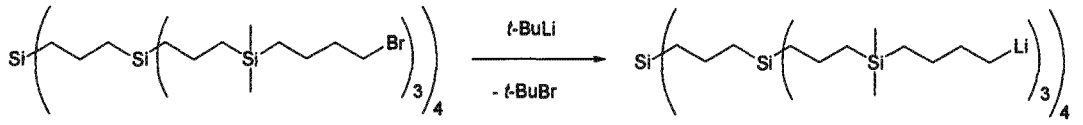

Fig. 3-25: Desired lithium halogen exchange reaction of bromobutyl dendrimers (second generation shown)

First generation bromobutyl functionalised dendrimer **28** was treated with a large excess of *t*-butyl lithium at -78°C in diethyl ether. An excess of the lithium reagent is used so that the *t*-BuBr by-product, which could potentially couple with a lithiated dendritic end group, reacts with a further equivalent of *t*-BuLi to give 'ditert' and LiBr.[175] The reaction is performed at low temperature to minimise potential side reactions, such as a direct coupling of the bromobutyl dendritic arm and the *t*-butyl lithium. After a few minutes, the reaction was quenched with $ClSiMe_3$, to give a stable product for analysis. Unfortunately, it was found that the lithium-halogen exchange and the coupling of the bromobutyl unit with the *t*-butyl lithium reagent were competitive. From the integrations in the ^1H NMR spectrum, it was estimated that approximately 70% of the terminal groups were the desired -$SiMe_3$ units, and 30% were -CMe_3 units from the unwanted coupling reaction (Fig. 3-26). Various attempts at altering solvents and reaction conditions did not eliminate this problem, and as non-quantitative or non-selective reactions are unsuited to dendritic chemistry, it was concluded that lithiated dendrimers could not be prepared by this route.

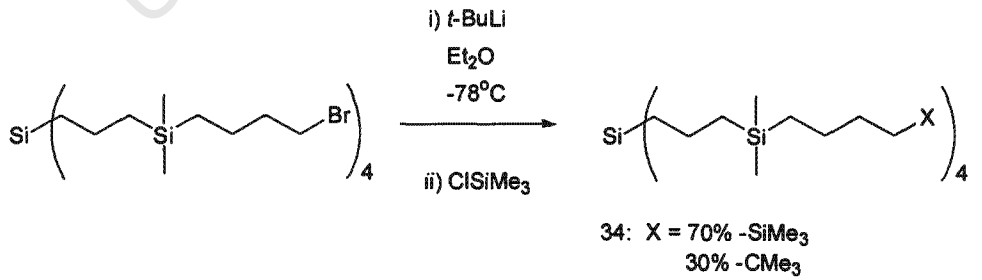

*Fig. 3-26: The reaction of **28** with t-BuLi and subsequent quenching with $ClSiMe_3$*

3.6 Conclusions and future work

New carbosilane dendritic wedges (generation 0-2) with core *n*-bromobutyl functionality and new carbosilane dendrimers (generation 1-3) with terminal *n*-bromobutyl functionality were successfully prepared, and the reactivity of these new dendritic molecules was investigated.

It was originally intended that metalloalkyl functionalised dendrimers would be prepared by reaction of the new dendrimers and dendritic wedges with organometallic nucleophiles (Fig. 3-27). In order to minimise potential β-hydride decomposition pathways to which iron alkyls are particularly susceptible[188], the reactions with $[CpRu(CO)_2]^-$ rather then $[CpFe(CO)_2]^-$ were to be investigated. However, due to time constraints and unavailability of the starting material $Ru_3(CO)_{12}$, these reactions were not attempted. The reactions of the new dendrimers with organometallic nucleophiles are thus an important aspect of future work on these dendritic systems.

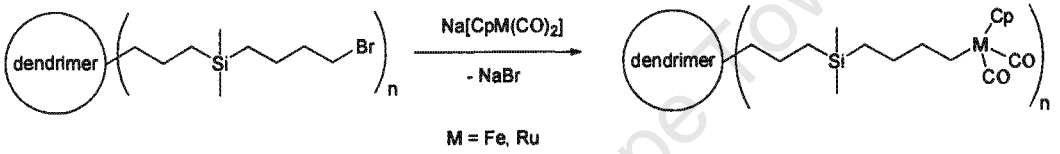

Fig. 3-27: Possible reactions of bromobutyl dendrimers with organometallic nucleophiles

Chapter 4:

Preparation and characterisation of new dendritically substituted Fe(II) bisiminopyridyl complexes

4.1 Introduction

4.1.1 Cationic late transition metal catalysts for oligomerisation and polymerisation of 1-alkenes

Since the independent reports by Gibson and Brookhart of iron and cobalt bisiminopyridyl catalysts and nickel and palladium α-diimine catalysts for the polymerisation and oligomerisation of 1-alkenes[10,11,13,15-18], much attention has been focused on these late transition metal catalysts as alternatives to established technologies. A full review of recent developments in this field is presented in chapter 1.

It is known that the position and steric bulk of the substituents of the aryl rings on the bisiminopyridyl and α-diimine catalysts play a crucial role in determining the selectivity of the catalyst (Fig. 4-1).

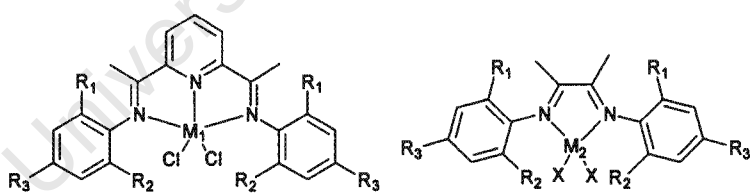

Fig. 4-1: Late transition metal precatalysts for the oligomerisation and polymerisation of 1-alkenes

In particular, it is the *ortho* substituents (R_1 and R_2) that have been identified as important. If both R_1 and R_2 are non-hydrogen substituents, and preferably bulky substituents such as isopropyl groups, then the catalysts are selective for the production of high molecular weight polymers from ethene. If R_1 = H and R_2 = Me, Et, ^{i}Pr or other alkyl substituent, the catalyst is selective for the oligomerisation of ethene to linear 1-alkenes with a Schultz-Flory chain length distribution, and for the dimerisation of longer chain olefins (such as 1-hexene). The *ortho* substituents are thought to be important because they directly impact on the

steric environment around the iron reaction site, enhancing the rate of propagation and inhibiting the chain termination reaction (β-hydride elimination).

The effect of substituents in the *para* position (R_3) has been less studied because this position is further removed from the complexed metal, and typical alkyl substituents thus do not directly affect the steric environment around the catalytic centre.

4.1.2 Catalysis at the core of a dendrimer

Much attention has been focused on the use of dendrimers in transition metal catalysis.[159] Homogeneous catalysts are typically more active and more selective than heterogeneous catalysts, require lower metal loading and milder reaction conditions and may be tuned by modification of the ligands. However, recovery of homogeneous catalysts from the reaction mixture is often impossible, and where expensive metals or ligands are required, this can render a process economically unviable.[160] Heterogeneous catalysts may simply be recovered from reaction mixtures by filtration. Thus despite the many advantages of homogeneous catalysts, heterogeneous catalysis remains the method of choice for most industrial processes. It has been hoped that dendritic catalysts may combine the advantages of both homogeneous and heterogeneous catalysts by retaining the high selectivity and activity of homogeneous systems while enabling the recovery of the catalysts by membrane or nanofiltration techniques which make use of the large size of the dendritic molecules.[159]

The most common approach in this field is to functionalise a dendrimer with multiple catalytically active fragments at the dendritic periphery.[159] This has the advantage of having a high concentration of catalytic centres relative to the dendrimer framework, and in principle the catalytic sites are located on the outside of the globular dendritic structure and are thus easily accessible to the substrates. Many examples of such dendritic multisite catalysts have been reported. Reactions such as polymerisations, Karasch additions, hydrolysis, Heck couplings, decarboxylation, hydroformylation, allylic alkylation, oxidation of bromides and thiophenes, Michael additions and many others have been performed using periphery-functionalised dendritic catalysts.[159,160]

Less attention has been given to the use of dendritic catalysts where a single catalytic site is located at the core of a dendrimer. The advantage of this approach is that the microenvironment around the catalytic centre may be controlled to allow the modification of catalytic selectivity.[159,160] This was demonstrated first for the anionic ring opening polymerisation of caprolactams.[189] Poly(benzylphenylether) dendrimers with an alkoxide core were found to be effective initiators for producing high molecular weight polymers with narrow polydispersities. The large bulk of the dendrimer surrounding the core improves the solubility of the growing polymer and prevents chain termination by 'back-biting' reactions in which the reactive chain end reacts intramolecularly with the growing chain. These side reactions cause conventional metal alkoxide initiators to produce low molecular weigh products with broad polydispersities.

The allylic alkylation reaction of 3-phenylallyl acetate with sodium diethyl methylmalonate using palladium catalysts at the core of carbosilane dendrimers has also been reported.[190] The activity of the catalysts decreased with increasing generation of the dendrimer due to mass transport limitations, but the selectivity for branched relative to linear *trans* products was increased. This was ascribed to the increased steric demand of the dendritic ligands or to the apolar environment within the carbosilane dendritic framework.

4.1.3 Dendritic functionalisation

Our interest in dendritic molecules and their applications in catalysis and as new materials led us to consider the possibility of functionalising late transition metal oligomerisation catalysts with dendritic components. This could take the form of attaching dendritic wedges to the catalysts, thus creating a catalyst at the core of a dendrimer as described in section 4.1.2. There are several potential advantages to this:

- **Potential effects on the selectivity of the catalysts**

  Large dendritic components may affect the steric and electronic environment around the catalytic centre, thereby modifying the selectivity towards higher (or lower) molecular weight products. The product distributions of ethene oligomerisation reactions are typically Schultz-Flory. This means that the probability of propagation (alkene insertion into the growing chain) relative to chain transfer (β-hydride elimination) is independent of the length of the growing chain, and thus a wide range of products is obtained, with a distribution such that $C_n > C_{n+2} > C_{n+4} > C_{n+6}$ etc. It is possible that a sufficiently bulky dendritic moiety may interfere with the growing chain in such a way that the Schultz-Flory statistics are broken, resulting in more selective product formation. Interactions between the dendritic framework and the active site may also have an effect on selectivity.

- **Potential effects on the catalyst lifetime**

  Although late transition metals are substantially less oxophilic than early transition metals (group 4 metallocene catalysts are exceptionally sensitive to poisoning by polar functionalities), the late transition metal catalytically active species are still likely to be vulnerable to deactivation by polar heteroatom-containing poisons. By surrounding the active centre with a large non-polar dendritic 'screen' (for example, carbosilane dendritic wedges), the active centre is placed in an apolar environment and may thus may be protected against poisoning. The monomer (ethene) will have access to the catalytic centre due to its non-polarity and small size, but larger and very polar molecules may be excluded.

- **Potential catalyst retention in continuous flow processes**

  One of the main potential uses of dendrimers in catalysis is as soluble catalytic supports which can be separated from the reaction products by nanofiltration or membrane techniques.

4.2 Synthetic strategies

Utilising the iron bisiminopyridyl catalyst system, different potential sites for dendritic functionalisation were identified (Fig. 4-2).

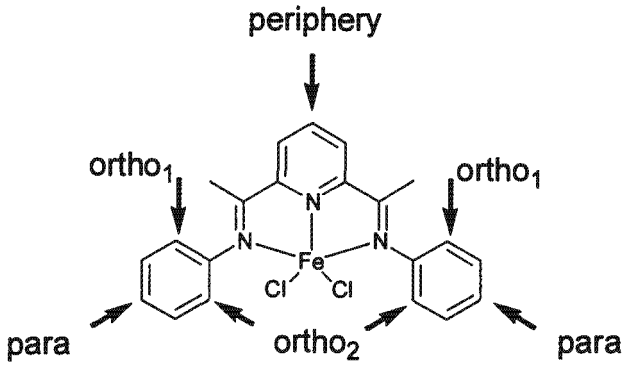

Fig. 4-2: Possible sites for dendritic functionalisation

In order to functionalise a dendrimer at the periphery with multiple bisiminopyridyl ligands, a single attachment point on the bisiminopyridyl framework is required. The attachment functionality should be unique on the molecule, otherwise crosslinking reactions between dendrimers will occur. The logical site for connection would be the *para* position on the pyridyl ring (marked 'periphery' in Fig. 4-2). However, functionalisation of the pyridyl ring is not easily synthetically accessible. Other attachment sites on the molecule would require a synthetic approach which breaks the C_2 symmetry. Although unsymmetrical bisiminopyridyls (two different aryl rings) have been reported[59] (see section 1.12 for more details), it was observed that mixtures of the desired unsymmetrical compounds and symmetrically substituted bisiminopyridyls were sometimes obtained. Thus preparing a sufficiently pure unsymmetrical bisiminopyridyl with a single functionality suitable for attachment to a dendrimer is unlikely to be feasible.

Functionalising a bisiminopyridyl ligand with dendritic wedges to create a catalytic ligand at the core of a dendrimer is likely to be more synthetically achievable. The potential advantages of this have been discussed in section 4.1.3. The aryl components of the ligand are particularly amenable to dendritic functionalisation, as a wide range of anilines with different functionality for substitution are commercially available. These may be reacted in standard Schiff-base type reactions with 2,6-diacetylpyridine to form the bisiminopyridyl framework with aryl rings suitable for attachment of dendritic wedges. *Ortho* and *para* dendritic substitution (Fig. 4-2) will have substantially different effects on the metal centre. *Ortho* functionalisation would have a major direct steric effect on the catalytic centre and any heteroatomic attachment functionality may interact with the metal centre. Dendritic functionalisation at the *para* position is likely to have less direct steric effect, while retaining a general steric demand around the entire catalyst. The direct steric control around the catalytic centre may still be controlled by appropriate *ortho* substitution (e.g. a methyl) and heteroatomic attachment functionality is removed from the active catalytic centre.

Bisiminopyridyl 'core' ligands with hydroxy-functionalised aryl rings will provide an 'attachment point' for dendritic substituents (Fig. 4-3). These core ligands may be prepared using Schiff-base condensation reactions between 2,6-diacetylpyridine and two equivalents of the appropriate hydroxyaniline.

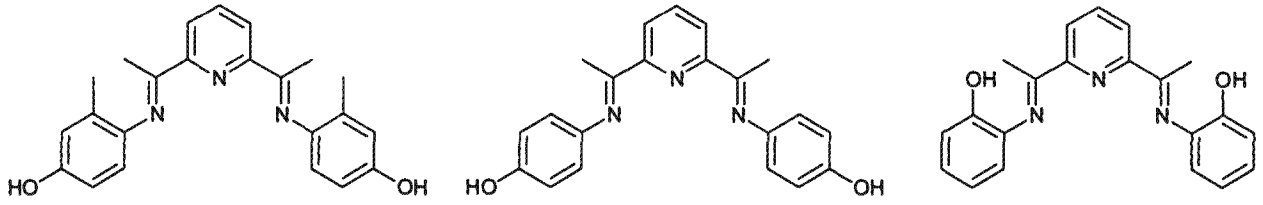

para-hydroxy, *ortho*- methyl *para*-hydroxy *ortho*-hydroxy

Fig. 4-3: Possible hydroxyaryl bisiminopyridyl 'cores'

Hydroxyaryl compounds may be reacted in quantitative yield with alkyl halide core-functionalised dendritic wedges, and this reaction forms the basis for the synthesis of Fréchet's poly(benzylphenylether) dendrimers.[127] It may thus be envisioned that the hydroxyaryl bisiminopyridyl cores in Fig. 4-3 could be functionalised with dendritic wedges of various generations as desired (Fig. 4-4).

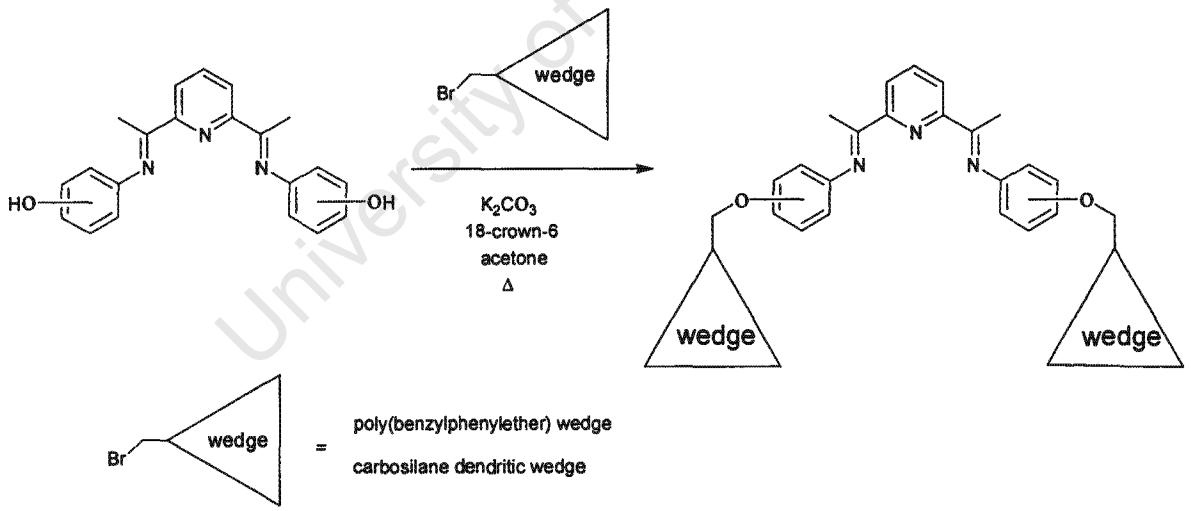

Fig. 4-4: Schematic representation of the synthesis of dendritically substituted bisiminopyridyl ligands

The choice of dendritic wedge to be used is likely to be important. Fréchet's poly(benzylphenylether) dendritic wedges (Fig. 4-5) are easily prepared and react readily with hydroxyaryls. They have also been used previously as dendritic catalysts for anionic ring opening polymerisation reactions.[189] Possible interactions between the oxygen heteroatoms in the dendritic framework and the active site during the

catalytic reaction cannot be discounted, and may have an effect on the activity and selectivity of the catalysts.

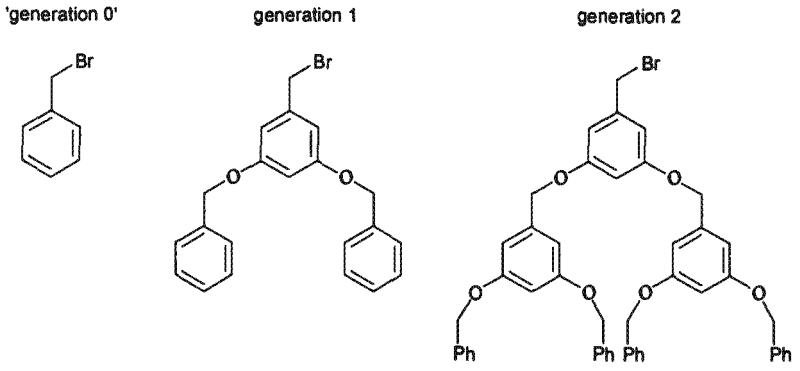

Fig. 4-5: Fréchet's poly(benzylphenylether) dendritic wedges[127]

Carbosilane dendritic wedges with a bromoalkyl focal point have been previously reported[158] and similar compounds have been prepared in this work (chapter 2). These wedges have the advantage of being inert and non-polar, so the possibility of interactions between dendritic substituents and the catalytic centre is minimised. The apolar character of carbosilanes may potentially shield the active catalyst against poisoning by polar molecules if sufficiently high generation wedges are used.

4.3 Synthesis of bisiminopyridyl, α-diimine and monoiminopyridyl core ligands

For the purposes of comparison, literature bisiminopyridyls **35**[17] and **36**[13] were prepared. $FeCl_2$ complexes of these ligands are active for the oligomerisation and polymerisation of ethene respectively.[13,17] The ligands are prepared by refluxing 2,6-diacetylpyridine with a slight excess of the appropriate aniline in dichloromethane (Fig. 4-6). The reaction is carried out over anhydrous sodium sulphate to irreversibly remove the water by-product, and a few drops of formic acid are added to catalyse the condensation.

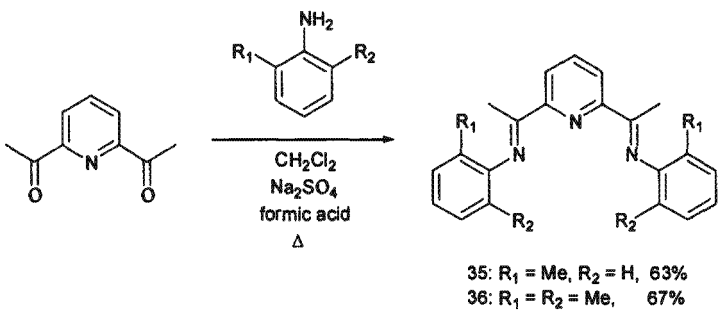

Fig. 4-6: Synthesis of 35 and 36

A different synthesis for the new hydroxylaryl bisiminopyridyls is necessary, as the hydroxyaniline precursors are not soluble in dichloromethane. Compound **37** was prepared by treatment of 2,6-diacetylpyridine with 4-hydroxy-2-methylaniline (4-amino-*m*-cresol) in methanol at 60°C with a few drops of formic acid (Fig. 4-7). The yields were generally low. This is because Schiff-base condensation reactions are equilibria between the ketone starting material and the imine product, and with the desired product being a bis(imine), some means of shifting the equilibrium towards the products is necessary to achieve good yields. Irreversible removal of water from the reaction mixture is difficult with methanol as solvent. Nevertheless, by using a large excess of the aniline and rigorously dried methanol, a yield of 81% for **37** was obtained on one occasion.

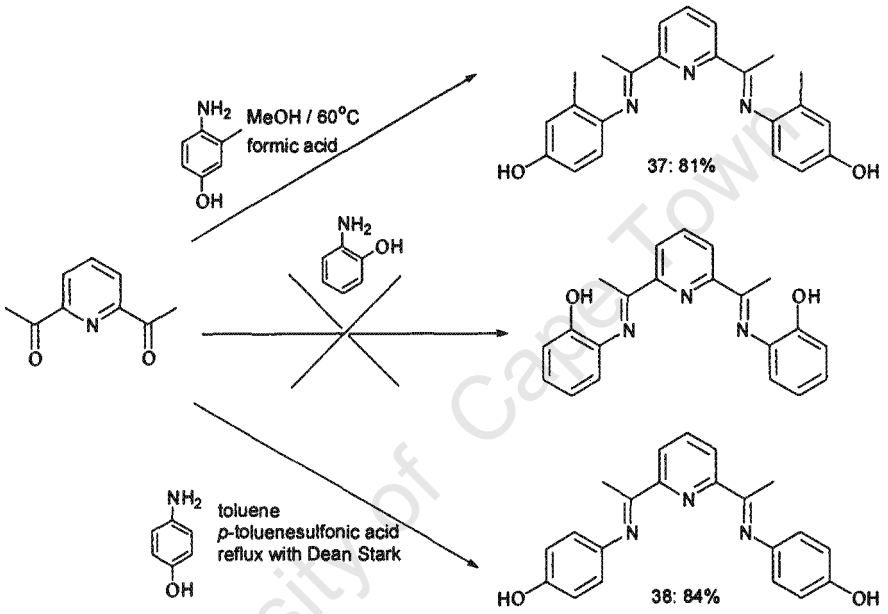

Fig. 4-7: Synthesis of hydroxyaryl bisiminopyridyl cores

Several attempts to prepare **38** using similar conditions failed. In every case, a dark yellow-brown reaction mixture resulted, and upon concentration and cooling, an impure brown material was recovered. However it was discovered that **38** may be prepared in high yield by refluxing 2,6-diacetylpyridine and 4-hydroxyaniline in toluene with a few crystals of *p*-toluenesulfonic acid (Fig. 4-7). The water by-product is removed by azeotropic distillation using a Dean-Stark condenser. Although the 4-hydroxyaniline is practically insoluble in cold toluene, at the reflux temperature of toluene (110°C) it is sufficiently soluble to allow the reaction to proceed, and the reaction is driven to completion by the removal of the water. No excess of aniline is thus required, and the product precipitates out of solution as a pale yellow powder in excellent yield.

All attempts to prepare 2,6-bis[1-(2-hydroxyphenylimino)ethyl]pyridine by reaction of 2,6-diacetylpyridine with 2-hydroxyaniline failed (Fig. 4-7). The reaction in anhydrous methanol again resulted in the recovery of an impure brown material, and refluxing in toluene or benzene resulted in decomposition or complex

mixtures of products. This may be due to the greater polarity of the starting aniline preventing adequate solubility in the reaction mixture.

Although the main focus of interest was the iron bisiminopyridyl systems, hydroxyaryl α-diimine (**39**) and monoiminopyridyl (**40**, **41**) cores were also prepared (Fig. 4-8). α-Diimine compound **39** was prepared by treatment of 2,3-butadione with 4-hydroxy-2-methylaniline in methanol, while the monoiminopyridyl compounds **40** and **41** were prepared by azeotropic reflux in toluene with a Dean-Stark condenser.

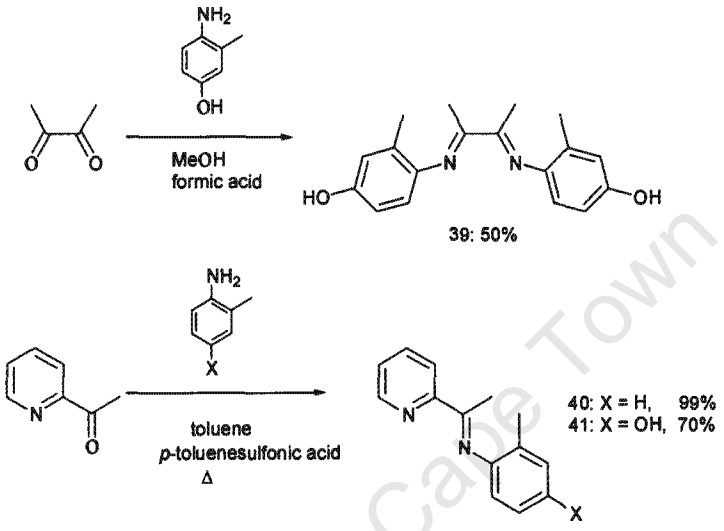

*Fig. 4-8: Synthesis of α-diimine compound **39** and monoiminopyridyl compounds **40** and **41***

All of the new compounds above were fully characterised by NMR and IR spectroscopy, satisfactory elemental analysis and mass spectrometry.

4.4 Preparation of poly(benzylphenylether) dendritic wedges

First and second generation poly(benzylphenylether) dendritic wedges (**pbpeG1** and **pbpeG2**) were prepared according to the method of Hawker and Fréchet (Fig. 4-9).[127] One minor modification was made: in order to obtain analytically pure samples, it was found to be helpful to subject the bromide core wedges to column chromatography before recrystallisation.

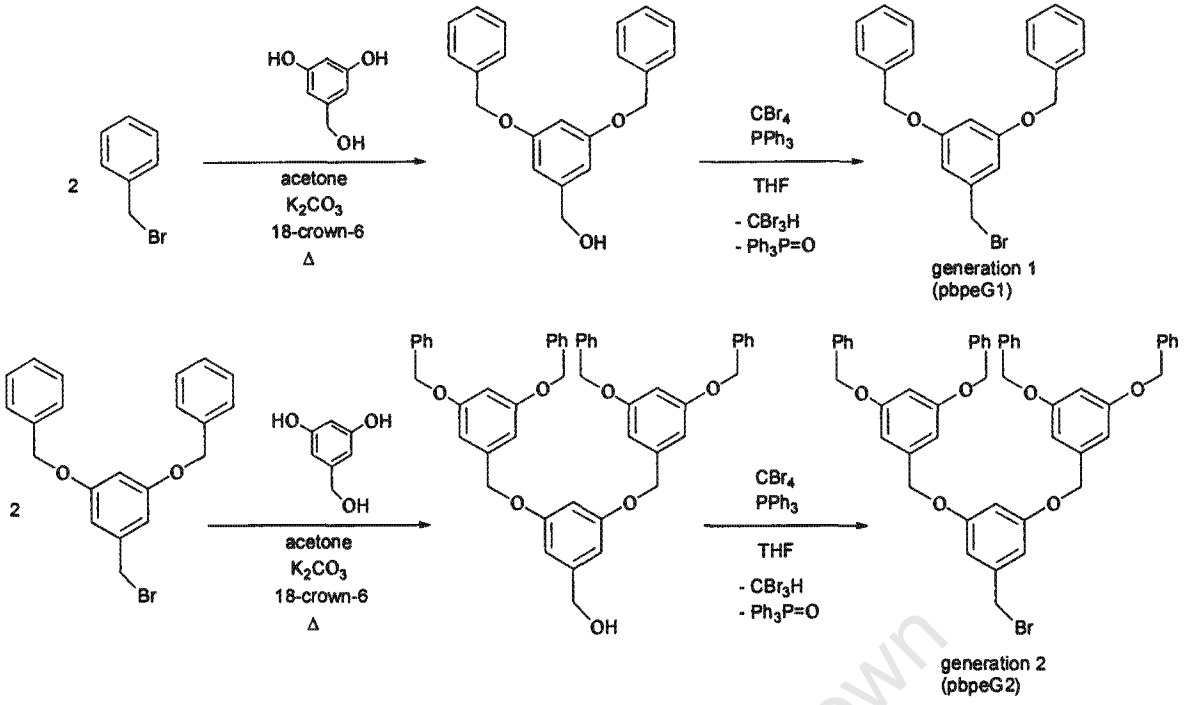

*Fig. 4-9: Preparation of first and second generation poly(benzylphenylether) dendritic wedges (**pbpeG1** and **pbpeG2**)* [127]

4.5 Synthesis of dendritically substituted ligands

The substitution of the hydroxyaryl bisiminopyridyl, α-diimine and monoiminopyridyl ligands with dendritic wedges was accomplished by the same reaction in each case. Both poly(benzylphenylether) (generation 0, 1 and 2) and carbosilane dendritic wedges (generation 0 and 1) were used. The zero generation wedges (benzyl bromide and **18** respectively) are non-dendritic but form a natural first component of a series of wedges. The same reaction conditions were used as was reported by Hawker and Fréchet for the synthesis of the poly(benzylphenylether) dendritic wedges.[127] One equivalent of the appropriate bromoalkyl wedge for each aryl hydroxyl group was utilised, and the reaction was done in refluxing acetone using K_2CO_3 as the base and a substoichiometric amount of 18-crown-6 to solubilise the base in the acetone. The reactions typically were allowed to proceed for 48 or 72 hours, and an aqueous work-up was then employed. The water and brine used were rendered slightly alkaline by the addition of a few drops of 0.1M NaOH; this is necessary to prevent the acid-catalysed hydrolysis of the imine functionality. Analytically pure samples were obtained by recrystallisation from an appropriate solvent or solvents. Some of the ligands were amorphous solids or oils, but purification was still accomplished by a 'recrystallisation' in which the compounds were selectively oiled out. The full range of ligands prepared is shown in Fig. 4-10.

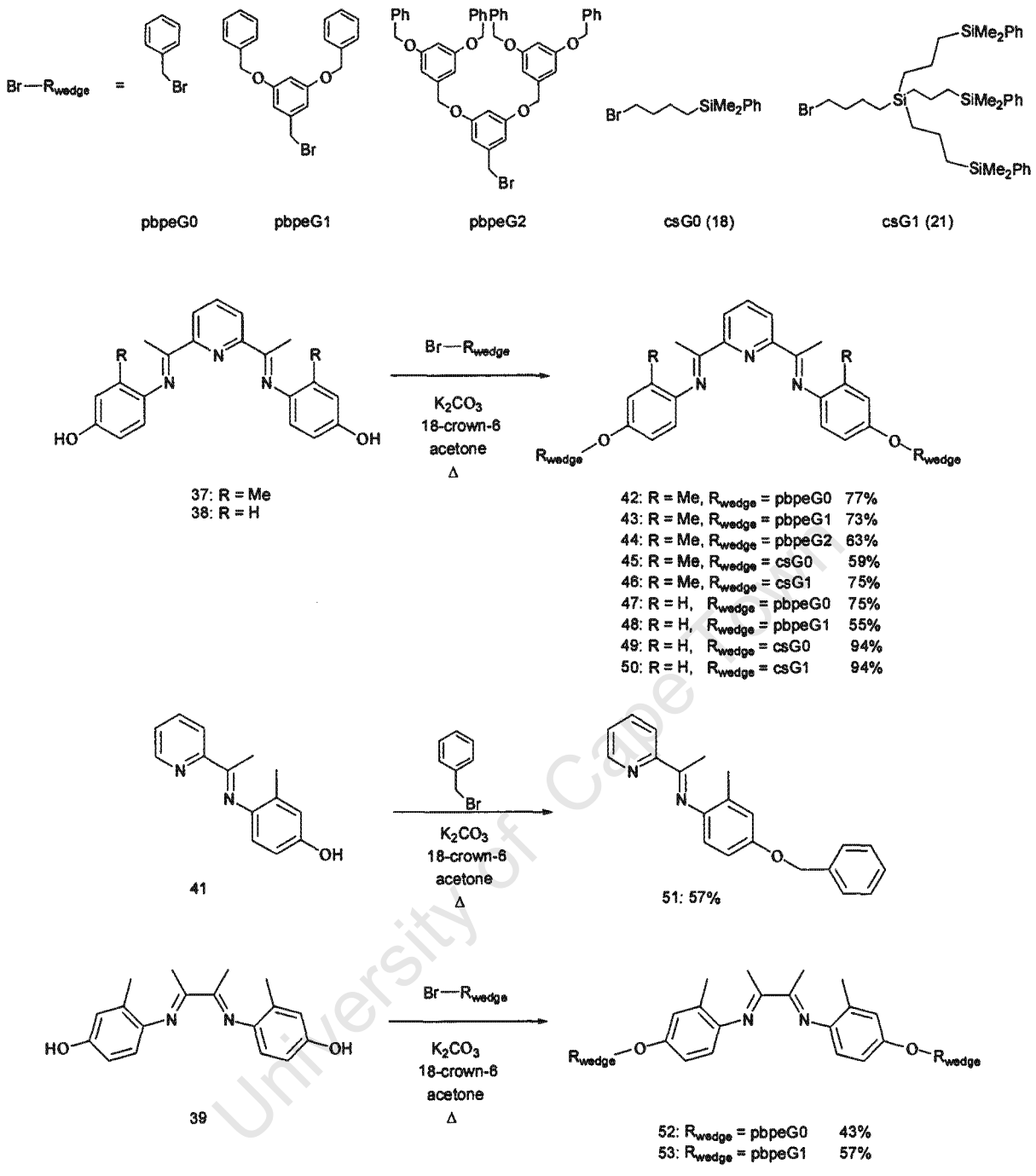

Fig. 4-10: Synthesis of dendritically substituted bisiminopyridyl, α-diimine and monoiminopyridyl ligands

All the ligands were characterised by ^{1}H, ^{13}C and where appropriate ^{29}Si NMR spectroscopy, IR spectroscopy and satisfactory elemental analysis. For all of the ligands except **44**, **52** and **53**, mass spectra were obtained and the molecular ion was observed. Two representative ^{1}H NMR spectra (of **43** and **46**) are shown in Fig. 4-11.

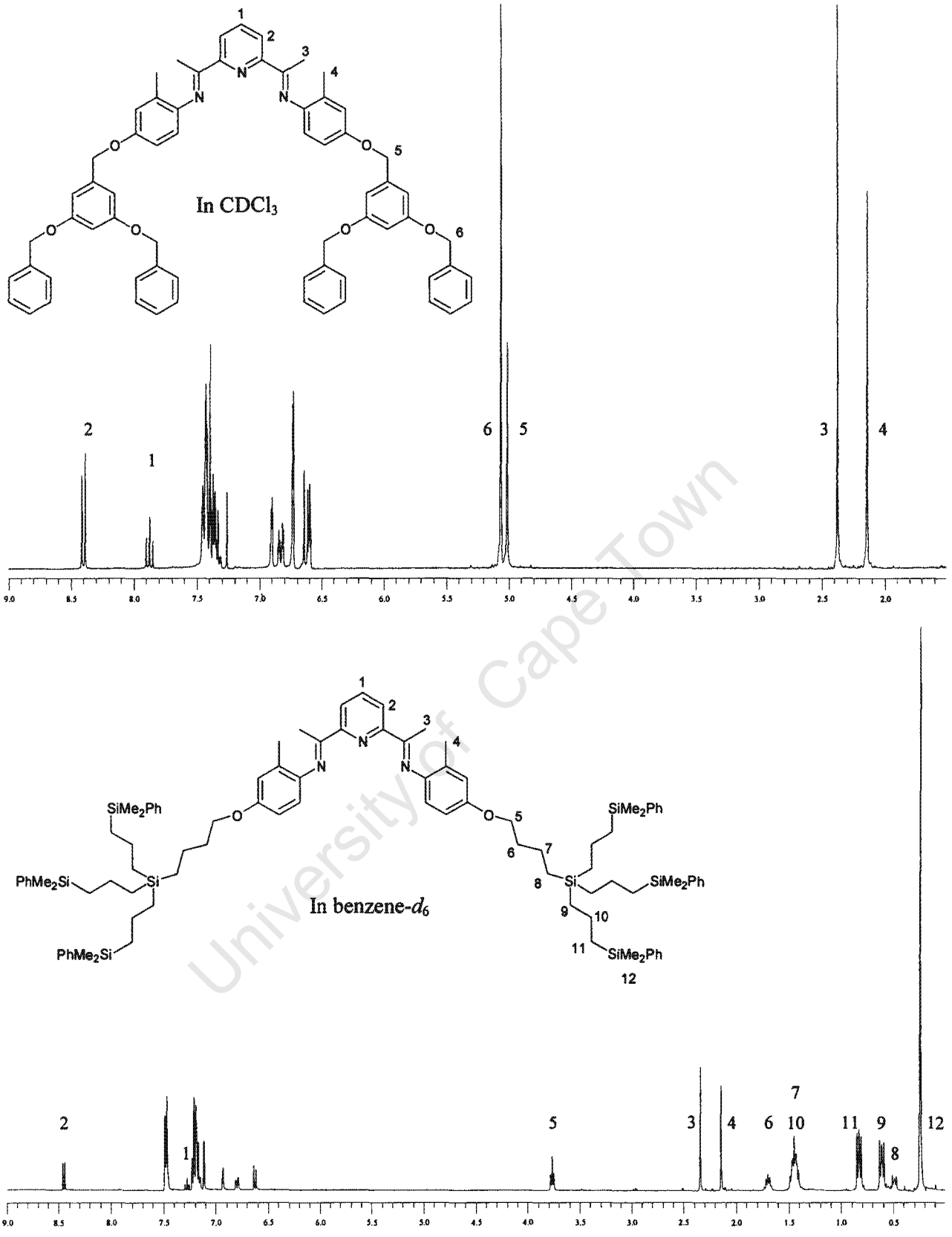

*Fig. 4-11: ^{1}H NMR spectra of **43** and **46** (note the shifts in pyridyl protons due to different NMR solvents)*

4.6 Preparation of the metal complexes

The iron precatalyst complexes were prepared by stirring a slight excess of the bisiminopyridyl ligands with $FeCl_2.4H_2O$ in THF (Fig. 4-12), as reported in the literature.[13] The literature precatalysts **54**[17] and **55**[13] and eight new iron complexes with dendritic substituents (**56** to **63**) were prepared (Fig. 4-12). After completion of the reaction (judged by the absence of solid particles of $FeCl_2$), the intensely coloured complexes were precipitated out of solution by the addition of diethyl ether (in some cases, the complexes partially precipitated out during the course of the reaction). After washing the precipitates with diethyl ether or THF/diethyl ether mixtures to remove excess ligand (this was done under argon using centrifuge techniques), the complexes were obtained as dark green, dark blue or purple powders in near quantitative yields.

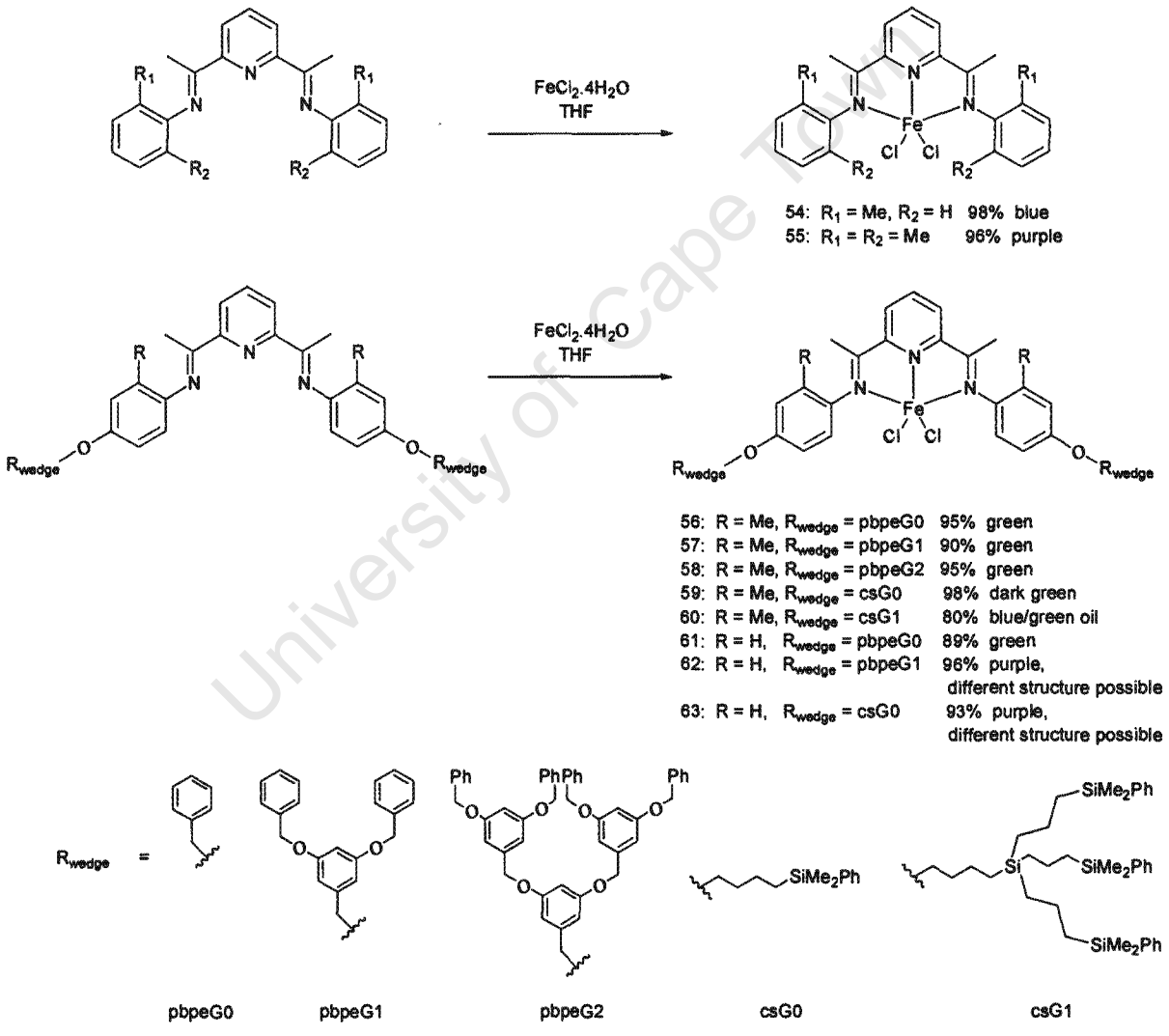

Fig. 4-12: Synthesis of iron bisiminopyridyl complexes

Compound **60** was an oil which was fully soluble in a wide range of solvents; this complex was prepared by using an excess of the poorly soluble $FeCl_2.4H_2O$ relative to the ligand, and the complex was isolated by

syringing off the THF solution of the compound from the excess $FeCl_2$ and removing the THF. This compound is also air-sensitive, and decomposes in solution upon exposure to air or upon treatment with methanol to give a brown mixture. The reason for this is not clear, as the coordinated water molecules of the $FeCl_2$ starting material did not appear to have a detrimental effect on the compound. Compounds **62** and **63** were bright purple in colour, and it is possible that they have a different structure to the other complexes (see section 6.4.7, in which it was found that these two complexes were completely unreactive towards MAO, unlike all the other complexes). It is unclear what this structure might be, and attempts to grow single crystals suitable for X-ray structure determination were unsuccessful.

Full characterisation of the complexes is difficult. High spin d^6 iron complexes are paramagnetic, and while in some instances ^1H NMR data have been reported[12], in our experience obtaining interpretable spectra proved impossible. Many of the complexes are not soluble in readily available NMR solvents ($CDCl_3$, benzene-d_6), and the line broadening and unpredictable shifts of the peaks meant that assignment was speculative at best. IR spectroscopy is of limited value as a diagnostic technique for these compounds. Thus useful characterisation techniques were limited to elemental analysis and mass spectrometry. Obtaining good analyses is also challenging. The complexes are obtained as precipitates, some of which are poorly soluble in inert solvents, making recrystallisation difficult. Recrystallisations were not used to purify bisiminopyridyl iron complexes in other published reports.[12,13,17] The larger dendritic complexes are amorphous solids or oils, and may retain some solvent even after long periods of evacuation. Finally, the carbosilane substituted complexes appear to be moderately air-sensitive, and were thus stored in inert conditions before use in catalytic reactions. Reasonable elemental analyses were generally obtained for the poly(benzylphenylether) substituted complexes. For the carbosilane substituted complexes, some of the analyses were outside an acceptable range for analytically pure compounds; nevertheless they are close enough to the calculated values to suggest the formation of the correct complexes, possibly with some decomposition taking place before the analysis was done.

The FAB mass spectra were more instructive, and in all cases the parent ion and fragments involving loss of chlorine were observed. For some of the larger complexes, the observed molecular ion was fairly low in intensity, but the isotopic patterns corresponded with the theoretical patterns for the calculated empirical formula.

Palladium complexes of the α-diimine and monoiminopyriyl ligands **40**, **41**, **52** and **53** were prepared by treating a slight excess of the ligand with $(COD)PdCl_2$ in dichloromethane (Fig. 4-13). The resulting yellow complexes (**64** to **67**) were fully characterised by NMR and IR spectroscopy and elemental analysis.

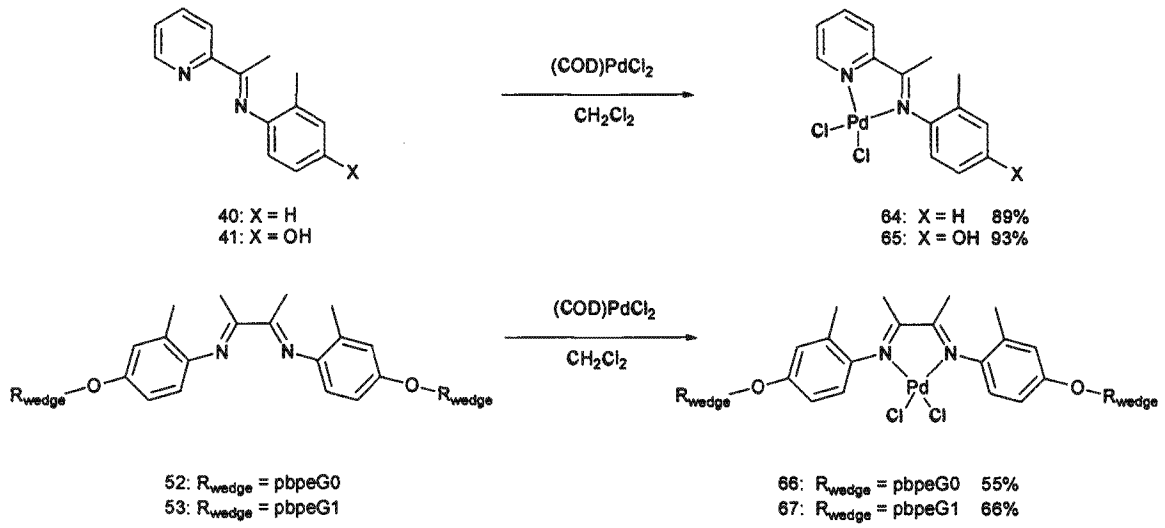

Fig. 4-13: Synthesis of α-diimine and monoiminopyridyl palladium complexes

Preliminary attempts to prepare the analogous nickel complexes failed. Treatment of the substituted α-diimine and monoiminopyridyl ligands with $(DME)NiBr_2$ in dichloromethane[10] lead to the formation of highly insoluble brown-yellow precipitates, the elemental analyses of which were far removed from expected values. The paramagnetic nature of the precipitates prevented the use of NMR in identifying possible reaction products. The reactions were not pursued further, and it is not clear why the expected complexes were not obtained.

4.7 Attempted synthesis of periphery functionalised dendritic bis- or monoiminopyridyl ligands

In section 3.4, the synthesis of carbosilane dendrimers with terminal bromobutyl functionality has been described. Following publication of the report on unsymmetrically substituted bisiminopyridyl ligands[59], it was hoped that an unsymmetrical bisiminopyridyl ligand with only one hydroxyaryl group might be prepared as shown in Fig. 4-14, and that this might allow the synthesis of a multisite bisiminopyridyl dendrimer by reaction of this compound with the multiple terminal bromobutyl groups of the carbosilane dendrimers.

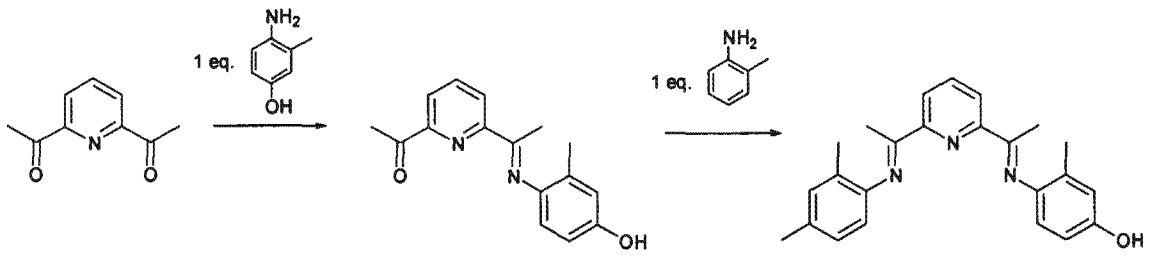

Fig. 4-14: Envisioned synthesis of an unsymmetric bisiminopyridyl with a single hydroxyaryl functionality

However when 2,6-diacetylpyridine was treated with one equivalent of 4-hydroxy-2-methylaniline under a variety of conditions, the resulting product was found by ^{1}H NMR spectroscopy to be a mixture of 2,6-diacetylpyridine, mono- and bisiminopyridines. It is evident that in our attempts, 2,6-diacetylpyridine did not selectively react with a single aniline to obtain the exclusively monosubstituted product; rather a statistical distribution of the three possible products (0, 1 and 2 imines groups) was formed.

Following this perhaps unsurprising result, a reaction of the monoiminopyridyl compound **41** with the first generation carbosilane dendrimer **27** was attempted (Fig. 4-15). **41** is intrinsically unsymmetrical and has a single hydroxyaryl group, so this compound is better suited to multiple functionalisation of the periphery of a dendrimer. The reaction was carried out with the same conditions as for the reactions with the dendritic wedges, and after aqueous work-up, a dark yellow oil was obtained. Unfortunately it was not possible to purify the crude product, as it was soluble in a wide range of organic solvents and the imine functionality is susceptible to hydrolysis during column chromatography. NMR analysis indicated that all the terminal bromobutyl groups had reacted (absence of the characteristic $-CH_2Br$ triplet at 3.41ppm). However, a proportion of the imine functionality had hydrolysed, and the resulting dendrimer had a mixture of terminal iminopyridyl and methylaniline groups. Since in dendritic chemistry extremely high conversions and extremely selective reactions are required to obtain pure products, no further attempts were made to prepare dendritic ligands in this way. An attempt was made to prepare a dendrimer with palladium complexes at the periphery by reacting the first generation bromobutyl dendrimer with the palladium monoiminopyridyl complex **65** under the same conditions (acetone, K_2CO_3, 18-crown-6). However, under these conditions the palladium complex decomposed and an intractable black tar resulted.

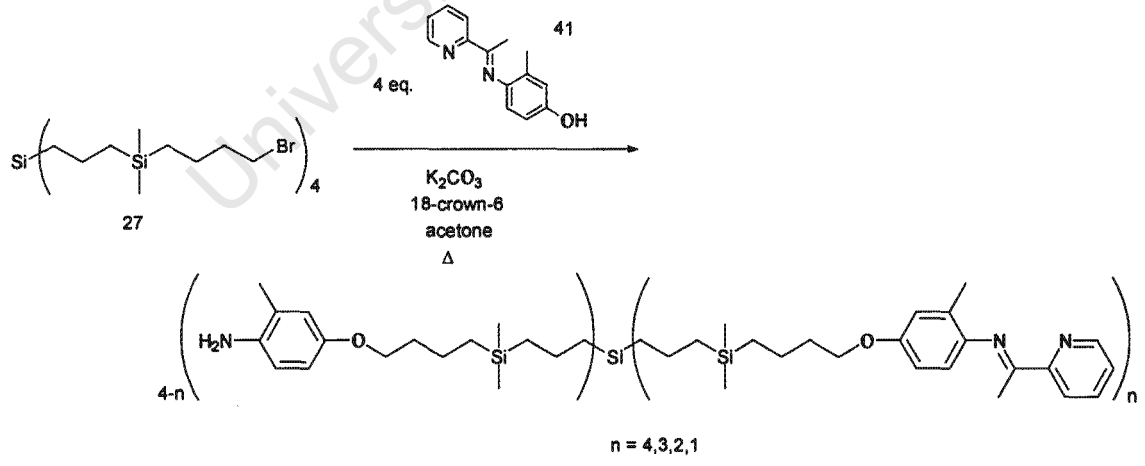

*Fig. 4-15: Reaction of monoiminopyridyl compound **41** with first generation carbosilane dendrimer **28***

Chapter 5:

Preparation and characterisation of new bisiminopyridyl Fe(II) complexes with electron donating and -withdrawing groups

5.1 Introduction

Steric effects around the catalytic centre in the new iron- and cobalt bisiminopyridyl systems have been studied in detail (see chapter 1), and have been found to play a crucial role in determining the catalytic activity and selectivity. Few studies of electronic effects have been reported, and those that have been are described in section 1.9. Generally it has been suggested that electron deficient ligands should increase the electrophilicity of the metal catalytic centre, increasing the rate of alkene insertion (the rate determining step) and thereby the catalytic activity.[15]

The synthesis of the dendritically substituted bisiminopyridyl complexes **56** to **63** described in chapter 4 involves the attachment of the dendritic wedges to the aryl rings of the ligand by means of an ether linkage (see Fig. 4-10 and Fig. 4-12). Thus any differences in catalytic activity of these complexes relative to the well-known literature compound **54** may be due to two competitive effects:

- a 'dendritic effect', in which the large dendritic component modifies the activity / selectivity / lifetime of the catalyst by steric effects, by through-space polarity / electronic effects or by interactions of the dendritic framework with the catalytic centre
- an 'electronic effect', in which the aryl *para*-ether attachment functionality modifies the catalytic properties by a through-bond electronic effect. The ether oxygen will have an electron donating resonance effect to the aryl ring, and because of the conjugation implicit in the ligand design, this may increase electron density on the catalytic centre.

In an effort to quantify the contribution of the second effect to the catalytic performance of the dendritically substituted complexes, a range of different ligands with different electronic properties but similar steric catalytic environments has been prepared. Apart from a better understanding of the dendritic catalysts, ligands with other non-ether electron donating or withdrawing groups may have interesting effects on catalytic performance.[15] The synthesis of these new ligands and their $FeCl_2$ complexes is described in this chapter.

5.2 Synthesis of ligands

The method for preparation of the ligands is shown in Fig. 5-1. Compounds **68**, **69** and **70** are new compounds, while **71** has been reported in the literature.[18] Compound **68** with an ethoxy substituent rather than a methoxy group was prepared as this is a closer electronic model for the dendritically substituted ligands and because it may be prepared from **37** under the same conditions. An attempt to prepare the *para*-methoxy substituted ligand by treatment of **37** with MeI under similar conditions failed. Compounds **69**, **70** and **71** were all prepared by azeotropic reflux in toluene, collecting the water by-product in a Dean-Stark condenser.

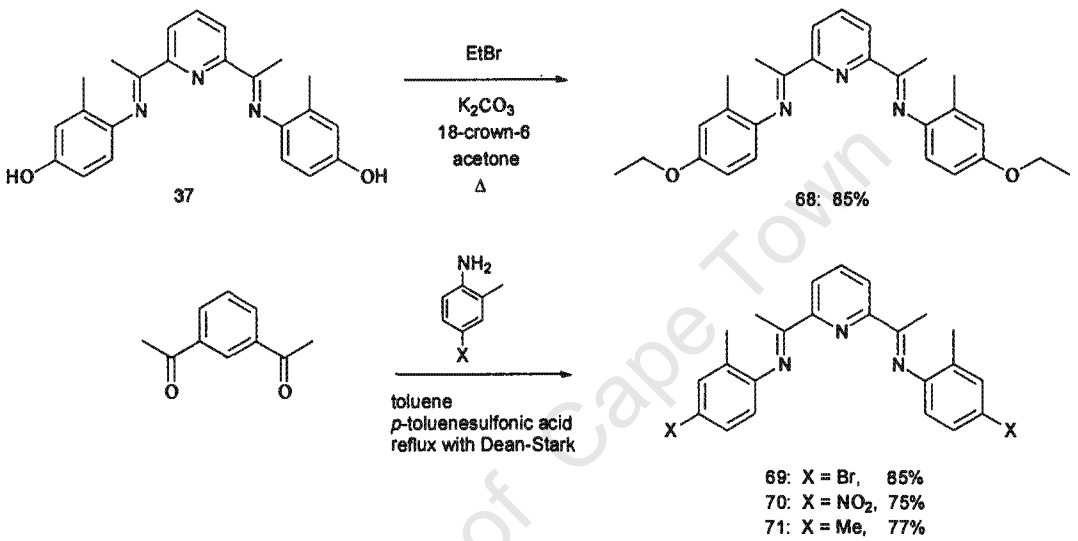

Fig. 5-1: Synthesis of ligands with para groups of differing electron-withdrawing and donating properties

All of the ligands were characterised by NMR and IR spectroscopy, satisfactory elemental analysis and mass spectrometry.

5.3 Empirical analysis of the electronic properties of the ligands

Together with **37** and **54** described in chapter 4, a range of six bisiminopyridyl ligands with the same immediate steric environment around the iron centre (one *ortho* methyl) but different electronic properties (*para* substitution) has been prepared. An empirical way of attaching numerical values to the effects of different *para* and *meta* substitution on aryl rings is by using the Hammett equation.[172] This applies to reactions or equilibria of aryl XC_6H_4Y systems, where Y is the reacting or equilibrated group and X is the variable *para* or *meta* substituent.

$$\log\frac{k}{k_0} = \sigma\rho \quad \ldots\ldots\ldots\ldots \quad \text{the Hammett equation}$$

In this equation, k is the rate or equilibrium constant for the substituted species while k_0 is the rate or equilibrium constant for the unsubstituted reference (X = H). The variable ρ is specific to the reaction or equilibrium in question, and σ is thus the parameter which quantifies the electronic (both inductive and resonance) effect of the X substituent, and is dependent both on the nature of the substituent and its position (*para* or *meta*). Standard σ values are determined by utilising the acidic dissociation constant of XC_6H_4COOH. The value of ρ for this equilibrium is defined as 1, and thus a list of standard σ parameters ($-1<\sigma<1$) for *para*- (σ_p) and *meta* (σ_m) substitution has been determined.[191] These may be used as an approximate indication of the electronic effects of various substituents in other reactions or processes. Negative σ values denote an electron donating substituent and positive values an electron withdrawing substituent.

Table 5-1 indicates the full range of *para* substituted bisiminopyridyls, and the Hammett σ_p parameters associated with these substituents. The experimental values of the ^{13}C NMR δ value for the 1-C_{aryl} carbon (marked *) and the $\upsilon_{C=N}$ infrared stretching frequency are also included, and the trend towards higher δ value and $\upsilon_{C=N}$ wavenumber with increased electron withdrawal at the *para* aryl position can clearly be observed. These two parameters indicate that the electronic effects of the *para* substituents are transferred to the imine nitrogens which, upon complexation, chelate the iron catalytic centre. By inference it is likely that these electronic effects will thus be experienced by the metal itself.

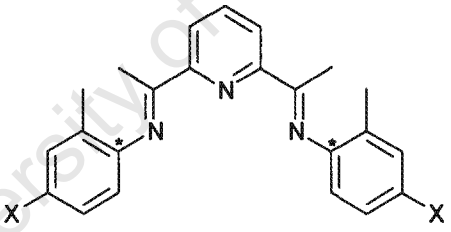

Compound	X	σ_p	δ_C for 1-C_{aryl} (marked *)	$\upsilon_{N=C}$ (cm^{-1})
37	OH (O^-)	-0.37 (-0.52)	142.4	1635
68	OEt	-0.24	143.1	1636
71	Me	-0.17	147.6	1640
35	H	0	152.8	1644
69	Br	0.23	149.3	1644
70	NO_2	0.78	154.5	1652

Table 5-1: A table showing the Hammett parameters[191] and selected ^{13}C NMR and IR spectroscopy data for bisiminopyridyl ligands with different para substitution

5.4 Preparation of the metal complexes

The Fe(II) complexes **72**, **73**, **74** and **75** of ligands **68**, **69**, **70** and **71** were prepared as described in section 4.6 and were obtained as dark green or blue/purple paramagnetic powders (Fig. 5-2).

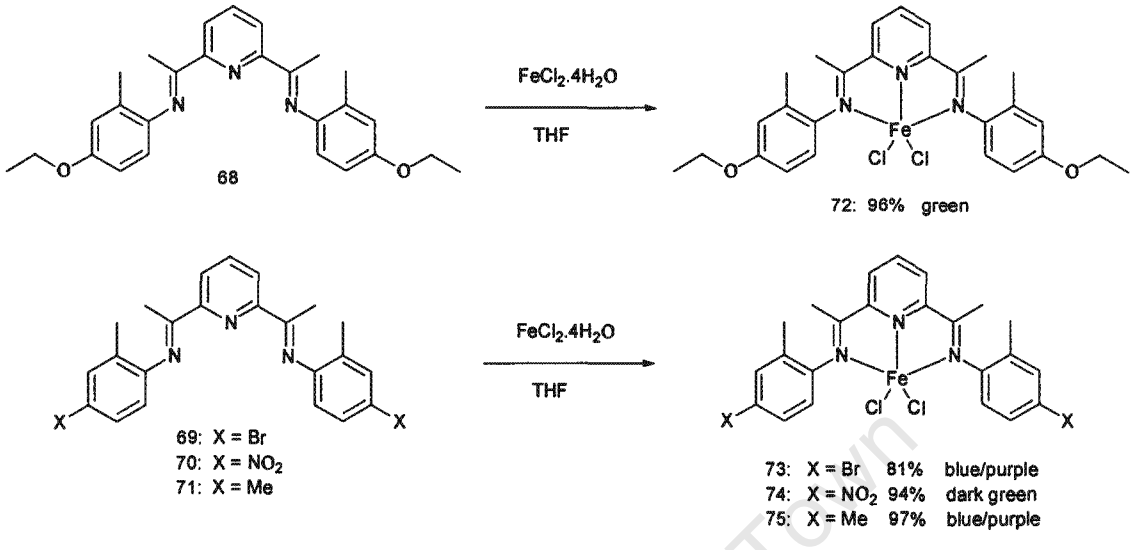

Fig. 5-2: Synthesis of iron bisiminopyridyl complexes with different para-substitution

The complexes were characterised by elemental analysis and mass spectrometry. The elemental analyses were generally satisfactory considering that the compounds were not recrystallised, although for reasons which are not clear, in some cases (compounds **74** and **72**) the nitrogen analysis was quite far out (>1%) while the carbon and hydrogen analyses were close to the calculated values. In all cases the molecular ion and fragments involving loss of chlorine were observed with the correct isotopic distribution in the mass spectra.

An attempt was made to prepare the iron complex of ligand **37** (*para*-hydroxy substitution). A bright green colour formed in the THF solution, indicative of complex formation. However upon precipitation with diethyl ether and the process of washing with THF/ether mixtures, centrifuging and removing the supernatant liquid (this was done so as to achieve a 'filtration' under inert conditions), significant decomposition was observed, as indicated by the formation of a black precipitate. A portion of the dark green precipitate suspended in THF / ether was transferred to an open flask, and within a few minutes, the precipitate had turned completely black. A mass spectrum of the dark green precipitate showed the presence of the expected molecular ion at 399 and M^+ - Cl and M^+ - 2Cl at 464 and 429 respectively. However the elemental analysis was very poor. It was concluded that, while the complex had been formed, it was thermally unstable in the solid state and decomposed substantially during work-up and before the elemental analysis.

Chapter 6:

Ethene oligomerisation reactions with new *para*-substituted Fe(II) bisiminopyridyl catalysts

6.1 Introduction

In this chapter, the results of the catalytic ethene oligomerisation experiments using new *para*-substituted Fe(II) bisiminopyridyl and Pd(II) α-diimine complexes are discussed. The syntheses of these complexes are described in chapters 4 and 5. Most of the complexes were found to be active catalysts for the formation of predominantly linear 1-alkenes from ethene, and the catalytic results are discussed with respect to α-values (propagation constant) and activity.

6.2 Catalytic conditions

All of the catalytic runs were carried out at 1 atmosphere ethene pressure under Schlenk-line conditions. For accurate comparison of different catalysts, conditions such as catalyst loading (20μmol), co-catalyst concentration (Al:Fe = 400:1), temperature (30°C), solvent (toluene), total volume (30 ml) and stirring rate were kept constant to within experimental error for all the catalytic experiments.

Controlling the exact Al:Fe ratio is difficult. MAO is a poorly defined substance, the composition of which may vary from batch to batch. MAO also may contain a significant amount of unhydrolysed $AlMe_3$ and has an uncertain shelf-life, even when stored under inert conditions. Nevertheless, by using MAO from one source (Aldrich) it is hoped that the ratio is constant throughout the catalytic runs. The volume of MAO required to achieve a theoretical Al:Fe ratio of 400:1 (8.0 mmol Al for 20μmol Fe) is calculated as follows. Assuming a formulation of $(\text{-AlMeO-})_n$, a concentration of 10% in toluene and a density of 0.875 $g.cm^{-3}$ as reported by the supplier, then

8.0 mmol Al	≡	464 mg $(\text{-AlMeO-})_n$
	≡	4.64 g MAO solution (10% by weight)
	≡	5.3 cm^3 (density 0.875 $g.cm^{-3}$)

The temperature of the run (30°C) is only an approximate initial reaction temperature. The catalytic reactions are very exothermic, resulting in a temperature rise of the reaction mixture. This was controlled to some degree by utilising a large oil bath (1.5 litre) to dissipate the heat given off as much as possible, although the delay in reaching equilibrium means that the temperature of the reaction mixture probably

rises substantially above that of the surrounding oil bath during the reaction. The temperature of the oil bath was observed to increase by up to 4°C during the reaction.

6.3 Work-up and analysis of oligomers

The reactions were quenched by addition of isopropanol (5.0ml) and then addition of 1M HCl. An aqueous work-up was used to remove aluminium salts, and the organic phase was dried over Na_2SO_4 and filtered. In some cases small amounts of insoluble low molecular weight polymers (waxes) formed as well; these were recovered by decanting the toluene solution with the suspended waxes into the filter paper, leaving the Na_2SO_4 behind. An internal standard of undecene (C11 1-alkene) was then added to the filtered solution (100mg in 5.0ml toluene) in order to determine the absolute amounts of each 1-alkene formed (only even 1-alkenes, C4, C6, C8, C10, C12 etc are formed in the oligomerisation of ethene). C11 is a good choice of standard, as its GC response factor is likely to be the same as the 1-alkene reaction products. The reaction products in toluene were then made up to 250ml total volume by addition of extra toluene, and analysis was carried out by gas chromatography (trace 1). The volatiles were then removed *in vacuo*, leaving behind the involatile oligomers (some C10, most C12, all C14+) along with a certain amount of residual toluene. After determining the mass (isolated yield), the involatile oligomers were taken up in hexane, and GC analysis (trace 2) was used to determine the contribution to the mass of the residual toluene and the amounts of C10 and C12 still present. From the GC results (trace 1 and trace 2), the propagation constant, α, and the total yield of oligomers was calculated using a simple TRUE BASIC computer program, which determines by extrapolation the mass of volatile oligomers lost and the mass of residual toluene still in the sample (see Appendix C).

6.4 Catalytic results

6.4.1. Table of catalytic results

The catalytic results are presented in Table 6-1 below. For most of the runs, the oligomerisation products were analysed by GC; however for some, notably the 20 minute runs, GC analysis was not carried out. The calculated yield and α-values are therefore not reported; however, comparison of the isolated yields is a qualitative indication of the activity of these runs. The reported α-value is calculated over the product range C10 to C20, i.e.

$$\alpha = \sqrt[5]{\alpha_{C10-C12} \times \alpha_{C12-C14} \times \alpha_{C14-C16} \times \alpha_{C16-C18} \times \alpha_{C18-C20}} = \sqrt[5]{\frac{n_{C20}}{n_{C10}}}$$

where $\alpha_{Cn-Cn+2} = \frac{n_{Cn+2}}{n_{Cn}}$ and n_{Cn} = *number of moles of the Cn 1-alkene*

From the calculated yield, the turnover number (TON), defined as the number of moles of ethene reacted per mole of catalyst per hour, was calculated.

Table 6-1: Results for the oligomerisation of ethene (1atm) using precatalysts of the form

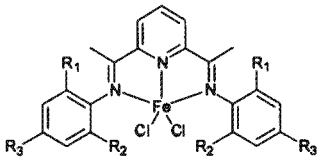

Run	Catalyst	R_1	R_2	R_3	Time (min)	Comments/ Observations	Isolated yield (g)	Calc. yield (g)	% 1-alkene	α	T.O.N. ($x10^3$/h)
1	54	Me	H	H	60	Blue → orange	2.75	2.98	85	0.71	5.32
2	54	Me	H	H	60	Blue → orange	3.03	3.48	85	0.68	6.21
3	54	Me	H	H	60	Blue → orange	3.31	–	–	–	–
4	54	Me	H	H	20	Blue → orange	2.31	–	–	–	–
5	56	Me	H	OpbpeG0	60	green → orange	4.71	4.56	82	0.77	8.13
6	57	Me	H	OpbpeG1	60	green → orange	5.90	5.85	80	0.77	10.45
7	57	Me	H	OpbpeG1	60	green → orange	4.21	4.63	85	0.72	8.27
8	57	Me	H	OpbpeG1	20	green → orange	2.68	–	–	–	–
9	58	Me	H	OpbpeG2	60	green → orange	4.89	4.83	83	0.76	8.62
10	59	Me	H	OcsG0	60	green → orange	3.37	3.82	91	0.72	6.82
11	60	Me	H	OcsG1	60	Blue/green → orange	5.83	6.29	90	0.75	11.23
12	61	H	H	OpbpeG0	60	green → orange	4.33	4.47	89	0.75	7.98
13	62	H	H	OpbpeG1	60	Inactive, no colour change from purple	0	–	–	–	0
14	63	H	H	OcsG0	60	Inactive, no colour change from purple	0	–	–	–	0
15	55	Me	Me	H	30	Polymer (m.p. 120 - 124°C) formed	6.08	–	–	–	21.72
16	72	Me	H	OEt	60	green → orange	4.22	4.39	87	0.76	7.84
17	72	Me	H	OEt	20	green → orange	3.03	–	–	–	–
18	75	Me	H	Me	60	purple → orange	3.06	3.23	86	0.71	5.77
19	73	Me	H	Br	60	purple → orange	3.64	3.86	86	0.69	6.89
20	73	Me	H	Br	20	purple → orange	2.73	–	–	–	–
21	74	Me	H	NO_2	60	Dark green → orange	4.39	4.69	86	0.71	8.37
22	74	Me	H	NO_2	60	Dark green → orange	4.16	4.88	85	0.71	8.71
23	74	Me	H	NO_2	20	Dark green → orange	2.88	–	–	–	–
24	54	Me	H	H	60	2 equiv. pbpeG1 added	5.66	6.62	88	0.68	11.82
25	54	Me	H	H	60	2 equiv. pbpeG1 added	5.44	6.50	86	0.71	11.61
26	57	Me	H	OpbpeG1	60	2 equiv. pbpeG1 added	5.25	5.88	82	0.73	10.50
27	55	Me	Me	H	30	2 equiv. pbpeG1 added, polymer (m.p. 119 – 123°C) formed	6.49	–	–	–	23.18

6.4.2. Catalytic results with literature catalyst 54

In order for useful comparisons to be made, the catalytic activity of the new precatalysts were compared against the standard literature oligomerisation catalyst **54**.[17,18] Four runs were done using this catalyst. The reaction time was 60 minutes for three of the runs (runs 1, 2 and 3), and in the other run (run 4) it was 20 minutes. For runs 1 and 2, for which GC analyses were obtained, α-values of 0.71 and 0.68 and TON's of $5.32 \times 10^3 h^{-1}$ and $6.21 \times 10^3 h^{-1}$ were determined.

These activities are an order of magnitude lower than reported in the literature for oligomerisation of ethene with **54** at 1 atmosphere, where a TON of $47 \times 10^3 h^{-1}$ was observed[17], but slightly higher than the activity reported in another study for the very similar catalyst **75** (additional methyl in the *para* position), for which a TON of $4.2 \times 10^3 h^{-1}$ was obtained.[11] Catalytic results in different reports are, however, difficult to compare, as substantially different reaction conditions are typically used. For example, in the literature report of oligomerisation of 1 atmosphere ethene with **54**/MAO, the catalyst concentration was lower (5.7μmol in more than 50ml toluene) and the Al:Fe ratio was higher (between 600 and 800). Most of the literature catalytic experiments have been carried out at elevated pressures, with consequently much higher activities. Thus the main value of the catalytic results with **54** is not for comparison with other literature results, but rather for comparison of the catalytic properties of the new catalysts against an established literature catalyst.

The isolated yield for the 20 minute run (run 4) was 2.31g, compared to isolated yields of between 2.75g and 3.31g for the 60 minute runs (runs 1 - 3). Comparison of runs 4 and 2, which were done with the same batch of MAO in immediate succession, suggests that 76% of the product formation occurs in the first 20 minutes of the reaction. This confirms the previously reported observation that substantial deactivation of the catalyst occurs during the oligomerisation experiments.[18]

6.4.3. Reproducibility of catalytic results

Some idea of the reproducibility of the experiments may be obtained from runs 1, 2 and 3. The isolated yields were 2.75g, 3.03g and 3.31g respectively. For runs 1 and 2, for which GC analysis was obtained, α-values of 0.71 and 0.68 and TON's of $5.32 \times 10^3 h^{-1}$ and $6.21 \times 10^3 h^{-1}$ were determined. These results suggest that the catalytic results are reasonably reproducible. The experiments were carried out at different times and using different batches of MAO. Other repeated experiments with different catalysts (runs 21 and 22, runs 24 and 25) further demonstrate the reproducibility of the catalytic results. In runs 6 and 7, significantly different results were obtained, particularly with respect to the α-values. The reason for this is not clear; although differences in the MAO composition used for run 7 may be one possible reason. Although for the most part the catalytic results have been shown to be reproducible, where direct comparison between runs was desirable, for example with a series of catalysts with different generation wedges attached, the same batch of MAO was used, and the runs were carried out one after the other over a

short space of time. In this regard, runs 1, 5, 6, 9, 10 and 12 were carried out together, as were runs 15 and 27, runs 7, 8 and 26, runs 2, 16, 18, 19 and 21 and runs 2, 24 and 25.

6.4.4. Selectivity of the catalysts to 1-alkenes and other products

As expected, in all cases a Schultz-Flory chain length distribution for the oligomer products was observed. In previous reports of ethene oligomerisation with **54** and other bisiminopyridyl iron oligomerisation catalysts, selectivities of greater than 99% for linear 1-alkene oligomers have been reported, particularly at elevated ethene pressure.[17,18] However, at 1 atmosphere ethene, a lower selectivity (>95%) was in one case reported.[17] In all the catalytic oligomerisation experiments carried out in this study, lower selectivities to linear 1-alkenes were observed. In the GC traces, each peak due to 1-alkene is accompanied by a minor peak at slightly longer retention time. Analysis by GC-MS indicates that these products are the corresponding *n*-alkanes. The catalytic selectivity for the alkane and alkene products may be estimated from the ratios of their GC integrals. The selectivity to linear 1-alkenes was found to range between 80% and 91%.

The *n*-alkane oligomers are formed by a different chain transfer mechanism to the 1-alkene products. In studies of ethene polymerisation using iron bisiminopyridyl catalysts, chain transfer to aluminium co-catalyst has been identified as the mechanism responsible for saturated polyethene end groups (see section 1.5).[12] This transfer mechanism is particularly favoured at low ethene pressures. At low pressure, the rate of the β-hydrogen transfer process is reduced, and thus chain transfer to co-catalyst is more competitive.[18] It is thus likely that higher selectivities to 1-alkenes could be achieved with all the catalysts in this work at elevated ethene pressure.

6.4.5. Effects of dendritic wedges in the aryl *para* position

The effects of the poly(benzylphenylether) dendritic wedges attached at the aryl *para* position may be deduced from runs 1 (literature catalyst **54**), 5 (**56**, generation 0), 6 (**57**, generation 1) and 9 (**58**, generation 2). The effect on the α-value is significant, with the dendritically substituted catalysts having higher values for α (0.77, 0.77 and 0.76 for **56**, **57** and **58**) compared with the literature catalyst (0.71 for **54**). However, α does not appear to depend on the size of the dendritic wedge. This suggests that the increased rate of propagation relative to chain transfer is caused either by the immediate bulk of the benzyloxy functionality attached directly to the aryl ring, or more likely as an electronic effect caused by the electron donating ether linkage. The second hypothesis is further supported by the observed α-value of 0.76 for run 16, where the catalyst with non-dendritic ethoxy functionality in the *para* position (**72**) was used.

The effect of the dendritic substituents on the activity of the catalysts is unexpected. The results are shown in Fig. 6-1, in which a graph of TON's for the catalysts with poly(benzylphenylether) wedges attached is displayed. The TON's resulting from these complexes are compared against those from literature catalyst **54** and ethoxy substituted catalyst **72**.

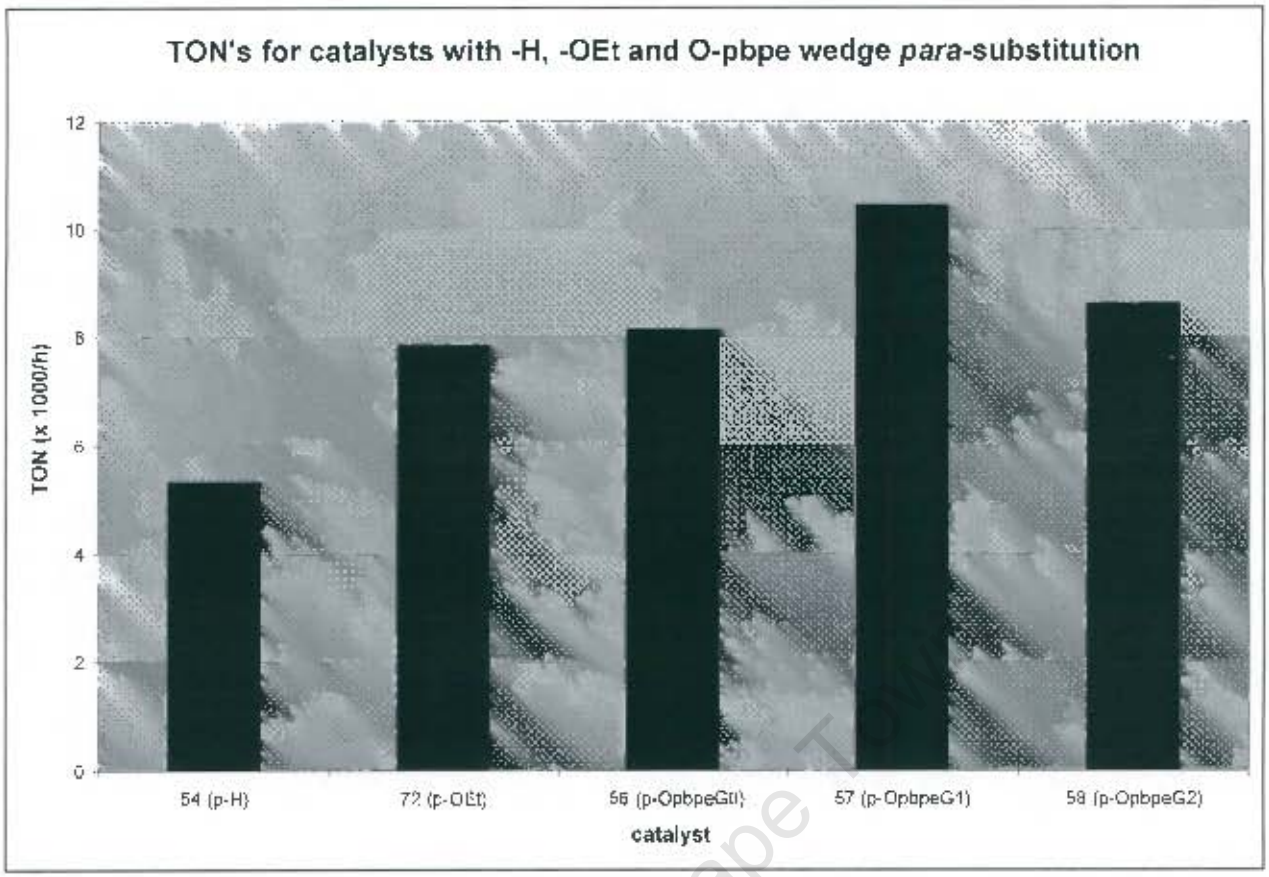

*Fig 6-1: TON's of catalysts with substitution by different generation poly(benzylphenylether) wedges (catalysts **56-58**), and comparisons with literature catalyst **54** and ethoxy substituted catalyst **72***

The calculated TON's for **56**, **57** and **58** are 8.13 x 10^3 h^{-1}, 10.45 x 10^3 h^{-1} and 8.62 x 10^3 h^{-1} respectively, which are significantly higher than for **54** (5.32 x 10^3 h^{-1}). Again this appears to be partly due to the ether linkage on the aryl ring, as can be deduced from the TON of 7.84 x 10^3 h^{-1} obtained using the non-dendritic catalyst **72**. However, there does appear to be some connection between the size of the dendritic wedge and the observed activity. This may be seen by the increase in activity from ethoxy (7.84 x 10^3 h^{-1}) to generation 0 wedge (8.13 x 10^3 h^{-1}) to generation 1 wedge (10.45 x 10^3 h^{-1}) *para* substitution. Substitution by a generation 2 wedge caused an apparent drop in activity (8.62 x 10^3 h^{-1}). This breaks the trend towards higher activity for larger wedges. The drop in activity may be due to hindered access for ethene to the catalytic centre caused by the two very bulky second generation wedges. The improved activity of the dendritically functionalised catalysts remains something of a mystery. Results presented in section 6.4.6 suggest that interactions of the dendritic ether functionality with either the MAO co-catalyst or the catalytic centre may be partially responsible. It has been previously suggested in work on nickel α-diimine oligomerisation catalysts that Lewis acid-base interactions of MAO with a methoxy group in the *para* position may explain an unexpectedly high catalytic activity.[15] The increased activity for catalysts with larger wedge substituents may thus be due to the increase in the number of ether functionalities present.

One experiment was carried out to investigate the effect of the dendritic wedges on catalyst lifetime. In runs 7 and 8, catalytic experiments over 60 and 20 minutes were carried out using **57**. GC analysis was not carried out for run 8; however the isolated yields give an approximate indication of the true reaction yields for the two runs. In 20 minute run 8, the isolated yield was 2.68g while in 60 minute run 7, the isolated yield was 4.21g. This suggests that approximately 64% of product formation occurs during the first 20 minutes of the run. It is thus apparent that there is still substantial deactivation of the catalyst over time during the run. However, this should be compared against a similar study of catalyst deactivation with **54** (runs 2 and 4). With **54**, the isolated yield for the 20 minute run 4 was 76% of the 60 minute run 2. Although these results are not quantitative and have not been repeated, they suggest that the dendritically substituted catalyst **57** could be more robust than the literature catalyst **54**. This may partially explain the higher TON's observed for the dendritically substituted catalysts. The increase in TON's may be caused, not by an intrinsic increase in activity, but by a lower susceptibility to deactivation during the run. Indeed, the isolated yields recovered after 20 minutes for catalysts **54** and **57** are similar (2.31g and 2.68g respectively in runs 4 and 8).

The effects of substitution by carbosilane dendritic wedges was investigated in runs 10 (**59**, generation 0) and 11 (**60**, generation 1). There appears to be a substantial increase in activity for the bulkier catalyst **60** ($11.23 \times 10^3\ h^{-1}$ compared with $6.82 \times 10^3\ h^{-1}$ for **59**.) Unfortunately this result could not be repeated due to decomposition of the sample of catalyst **60** before a second run could be attempted (see section 4.6). The selectivity towards 1-alkenes appeared to be higher for the carbosilane substituted catalysts (90-91%) than for the poly(benzylphenylether) substituted analogues (80-85%). More work needs to be done to fully understand the effects of the carbosilane dendritic substituents on catalytic activity and α-values. In particular, the preparation of a catalyst with a second generation carbosilane dendritic wedge will extend the series, and experiments to establish the reproducibility of the results found above need to be carried out.

6.4.6. The use of a first generation poly(benzylphenylether) wedge as a co-catalyst

The catalytic results using precatalysts functionalised with poly(benzylphenylether) dendritic wedges suggest that the wedges increase catalytic activity by means of some interaction between the wedge framework and the catalytic centre. In order to establish whether this is dependent on the attachment of the wedges to the catalytic ligand, experiments were carried out in which two equivalents of the first generation poly(benzylphenylether) wedge (**pbpeG1**, see Fig. 4.9) was added as a co-catalyst. This wedge contains two benzylphenylether functionalities and one benzyl bromide functionality. Thus the use of two equivalents of **pbpeG1** gives an equivalent stoichiometric presence of benzylphenylether functionalities in the catalytic reaction to the dendritically substituted catalyst **57**. Remarkable catalytic results using literature catalyst **54** with two equivalents of **pbpeG1** as co-catalyst were obtained in runs 24 and 25. The α-values for these experiments (0.68 and 0.71) are unchanged compared to the runs without addition of

pbpeG1 (0.71 and 0.68 for runs 1 and 2). This supports the hypothesis that the increased α-values for catalysts **56**, **57** and **58** is due to the through-bond electronic effect of the aryl ether linkage on the metal centre and not to through space electronic interactions of the wedges with the metal centre.

The effect of the **pbpeG1** co-catalyst on catalytic activity is dramatic and unexpected. TON's of 11.82 x 10^3 h^{-1} and 11.61 x 10^3 h^{-1} were calculated for runs 24 and 25; this represents an increase in catalytic activity of almost 100% compared with the results for **54** without **pbpeG1** co-catalyst, where a TON of 6.21 x 10^3 h^{-1} was found in run 2 under otherwise identical reaction conditions. The similar results obtained in runs 24 and 25 confirm that the increase in activity is reproducible, and not an anomalous result. Similar effects on activity were noted when catalyst **57** was used (compare runs 26 and 7, which were carried out consecutively with the same batch of MAO). The α-values are not significantly changed, but there is an increase in activity from 8.27 x 10^3 h^{-1} for run 7 to 10.50 x 10^3 h^{-1} for run 26, in which two equivalents of **pbpeG1** were added. The increase in activity is presumably less dramatic due to the fact that **57** already contains benzylphenylether functionalities in the attached dendritic wedges.

An investigation was then carried out to determine if using **pbpeG1** as a co-catalyst in a polymerisation reaction with catalyst **55** would similarly increase the activity. Under identical catalytic conditions to the oligomerisation experiments except for the reaction time (30 minutes), catalyst **55** gave 6.08g of polyethene with a TON of 21.72 x 10^3 h^{-1}. When 2 equivalents of **pbpeG1** were added, 6.49g of polymer were recovered with a TON of 23.18 x 10^3 h^{-1}. The TON's found are in the same order of magnitude as reported literature TON's using similar catalytic conditions (in separate studies, TON's of 20 x 10^3 h^{-1} and 33 x 10^3 h^{-1} with **55**/MAO at 1 bar ethene have been reported[11,44]). While a slight increase in activity is thus observed for the run with added **pbpeG1**, it is questionable as to whether this increase is significant or simply due to random experimental variation. Certainly a dramatic increase in activity as with catalyst **54** is not apparent. There also appeared to be no significant difference in the melting points of the polymers formed in runs 15 and 27. Both samples of polyethene melted in the range 119 – 124°C. This is close to literature values of melting points for the same catalyst. For example, a reported polymerisation with **55** carried out at 20°C at 1 bar ethene and with Al:Fe of 400 gave polyethene with a melting point of 126°C (determined by DSC).[44] The slightly higher melting point is most likely due to the lower reaction temperature.

The results discussed above are very significant as they suggest that the increase in catalytic activity due to the functionalisation of the bisiminopyridyl catalysts with poly(benzylphenylether) wedges may be unrelated to the fact that the wedges are attached to the catalytic ligands. The higher activity for larger wedges may simply be due to the greater concentration of benzylphenylether moieties in the reaction mixture. It is apparent that the closer proximity to the catalytic centre of the wedges when attached to the ligand does not result in higher activity than when the same concentration of free wedges is present in solution. This suggests that for the dendritically substituted catalysts, the proposed interactions between the

wedges and the metal centre are primarily intermolecular in nature. This is supported by a qualitative examination of the structure of the substituted catalysts. For geometric reasons, it appears impossible for catalysts **56** and **57** and improbable for catalyst **58** that there could be interactions between the ether moieties in the wedges and the metal catalytic centre of the same complex.

There are a number of unanswered questions relating to the unexpected increase in activity caused by the use of **pbpeG1** as a co-catalyst. An investigation of the effect of changing the **pbpeG1** co-catalyst concentration on catalytic activity would be extremely useful, and would potentially provide evidence to support the hypothesis that the increased activity of catalysts with larger wedges attached is due to the increased concentration of benzylphenylether moieties present in the catalytic reaction. In addition, it seems unlikely that a co-operative effect between the two ether functionalities in **pbpeG1** is responsible for the increased catalytic activity. It would thus be useful to investigate whether a much simpler compound such as benzyl phenyl ether ($PhOCH_2Ph$) would similarly improve catalytic performance.

The reason for the effect described above is unclear and will require further study. In particular it is necessary to establish whether the higher TON's are due to an intrinsic increase in activity or to a reduction in catalyst deactivation. This could be investigated by varying the length of the catalytic runs and determining if in a shorter experiment the proportional increase in activity caused by added **pbpeG1** is similar to the increase in longer experiments. In either event, further investigations are necessary to determine the nature of the interactions between the **pbpeG1** co-catalyst and the iron catalyst responsible for the interesting and potentially useful increase in activity that is observed.

6.4.7. Catalytic results using bisiminopyridyl complexes with no *ortho* methyl substitution (61, 62, 63)

In runs 12, 13 and 14, the catalytic results using complexes **61**, **62** and **63** were investigated. These complexes are analogous to complexes **56**, **57** and **59**, except that there is no methyl substitution in the *ortho* positions of the aryl rings. For **61** (run 12), the observed α-value of 0.75 is surprisingly high when compared with the value of 0.77 for catalyst **56**, which has an *ortho* methyl substituent. It would be expected that a reduction in steric bulk around the catalytic centre would result in a shift to lower molecular weight products.[17] The activity of **61** appears to be similar to that of **56** to within experimental error (TON's of 7.98 x 10^3 h^{-1} and 8.13 x 10^3 h^{-1} respectively). Unfortunately, the reference catalyst with completely unsubstituted aryl groups, {2,6-bis-[1-(phenylimino)ethyl]pyridine}iron dichloride, was not prepared. It would be useful to compare the activity and α-values for **61** with this catalyst.

Complexes **62** and **63** were found to be completely inactive. It is apparent from observations during the experiment that these complexes are not activated by MAO. In all the active catalytic runs, there is an immediate colour change of the catalytic complexes to orange upon addition to MAO. The toluene

insoluble complexes also immediately go into solution upon activation. However, upon addition of **62** and **63** to MAO, the purple colour of the complex remains unchanged, and the complexes remain as suspensions in the reaction mixture. No exotherm is detected during the run as with all the other complexes, and no oligomeric products were formed. It is notable that **62** and **63** are purple complexes while all the catalytically active complexes with 4-alkoxy aryl substitution (**56**, **57**, **58**, **59**, **60**, **61** and **72**) are green or blue/green. The elemental analyses of **62** and **63** and the mass spectrum of **62** indicate that the complexes are 1:1 ligand to metal complexes like all the other complexes, and probably exist as monomers. However, the different colour and the complete lack of reactivity towards MAO suggest that the complexes have a different coordination structure. Attempts to grow single crystals for X-ray structure determination were unsuccessful, and the structures of these complexes have thus not been determined.

6.4.8. Effects of electron withdrawing and donating groups in the *para*-position

It appears that the difference in selectivity and activity between the dendritically substituted bisiminopyridyl catalysts and the literature catalyst **54** may at least partly be due to the ether linkage in the aryl *para* position. With this in mind, the series of bisiminopyridyl iron complexes with different electron withdrawing and donating *para* substituents described in chapter 5 was prepared. The relative catalytic performance of these complexes was then investigated (runs 2, 16, 18, 19 and 21). As discussed in section 6.4.5, catalyst **72** with *para* ethoxy substitution gave an oligomer distribution with an α-value of 0.76 (run 16). This is significantly higher than for literature catalyst **54**, which has no *para* substitution (run 2), and comparable to the α-values obtained with the dendritically substituted catalysts, which have the same *para* ether linkage (runs 5, 6 and 9). This could be due to increased electron density on the catalytic centre caused by the electron donating aryl ether functionality. Alternatively, Lewis acid-base interactions of the ether moiety with the aluminium co-catalyst may be responsible for the modified catalytic selectivity.[15] Ethene oligomerisation using an α-diimine nickel oligomerisation catalyst with *para* methoxy substitution has been reported.[15] An increase in α-value was observed relative to the unsubstituted analogue (from 0.70 to 0.74), although the authors regarded this as insignificant.

There do not appear to be significant differences in α caused by other *para* substitution. The α-values for catalysts **75** (*p*-Me; run 18), **54** (*p*-H; run 2), **73** (*p*-Br; run 19) and **74** (*p*-NO_2; run 21) were found to be 0.71, 0.68, 0.69 and 0.71 respectively.

The effect of different *para*-substitution on catalytic activity does appear to be significant. There appears to be a trend towards increased activity with greater electron withdrawal at the *para* position. This may be seen in Fig. 6-2, where the TON's are plotted against the σ_p Hammett parameter for the *para* substituent (see section 5.3 for a discussion of the Hammett equation).

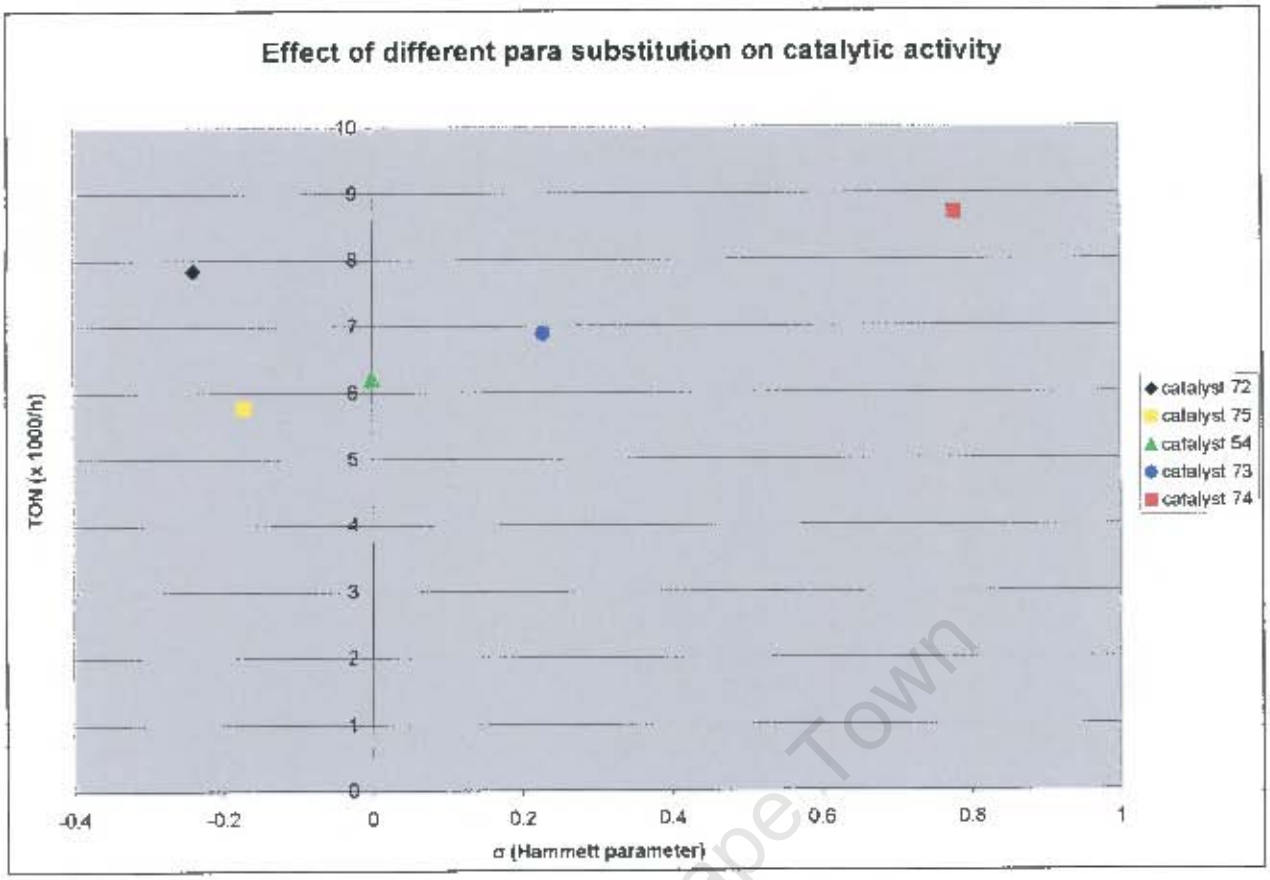

Fig. 6-2: A scatter plot representing the effect of increased σ_p (electron withdrawal by para substitution) on catalytic activity

For catalysts **75**, **54**, **73** and **74**, the relationship between TON and σ_p appears to be approximately linear. Greater electron withdrawal by the *para*-substituent (larger σ_p) will reduce electron density on the metal centre. The resulting higher electrophilicity should increase the rate of ethene insertion into the metal alkyl bond, which is the rate determining step in the catalytic cycle.[15] The exception to the trend is catalyst **72**, where the activity is higher than expected. Similar results have been noted before with *para*-substituted α-diimine nickel catalysts.[15] An electron withdrawing trifluoromethyl substituent increased the catalytic activity of the catalyst relative to an unsubstituted catalyst. However, an electron donating *para*-methoxy substituent did not conversely reduce the activity. This was ascribed to formation of Lewis acid-base complexes of the methoxy group with excess aluminium co-catalyst. These interactions will reduce the electron donating ability of the alkoxy substituent, and thus the activity of the catalyst is not diminished by an increase in electron density on the metal centre. Other studies have demonstrated an increase in polymerisation activity caused by halogen substitution on the aryl rings of late transition metal catalysts.[43,44]

The catalytic results of **74** are particularly impressive. The strongly electron withdrawing NO_2 substituents result in TON's of $8.37 \times 10^3\ h^{-1}$ and $8.71 \times 10^3\ h^{-1}$ (runs 21 and 22) compared with TON's of $5.32 \times 10^3\ h^{-1}$

and 6.21 x 10^3 h^{-1} obtained with literature catalyst **54** (runs 1 and 2). This represents an increase in activity of approximately 50%.

A 20 minute experiment using **74** (run 23) gave an isolated yield of 2.88g, representing 69% of the isolated yield of 60 minute run 22 (runs 22 and 23 were carried out consecutively). Catalyst deactivation of **74**, while possibly slightly reduced compared with **54**, is thus still substantial during the oligomerisation experiments. For catalysts **73** and **72**, the proportion of product formed in the first 20 minutes was approximated at 75% and 72% respectively.

6.4.9. Catalytic results with palladium complexes

Palladium complexes of α-diimine ligands with poly(benzylphenylether) substitution were prepared (see section 4.6). The preparation of the analogous nickel complexes was unsuccessful. Some catalytic experiments were carried out using the palladium complexes **66** and **67**. The complexes appeared to be activated by MAO; however only trace amounts of oligomer products were obtained, and no attempts were made to quantify these results. It is known from other work on α-diimine catalysts that the palladium complexes show significantly lower activity than the nickel analogues.[10]

6.5 Summary of key results

- Most of the new bisiminopyridyl iron complexes were found to be active ethene oligomerisation catalysts when activated with MAO

- The ethene oligomers were found to be mainly linear 1-alkenes with a Schultz-Flory chain length distribution. The selectivities for linear 1-alkenes were in the range of 80% to 91%. The remainder of the products was found to be the corresponding *n*-alkanes, which are formed by chain transfer from the iron catalytic centre to excess aluminium co-catalyst.

- Bearing in mind the differences in catalytic conditions used in previously reported studies, the observed catalytic activities are comparable with literature results.

- The observed catalytic activities and α-values with the same catalyst under the same conditions were found to be reproducible, thus allowing for meaningful comparison of results using different catalysts.

- Functionalisation of bisiminopyridyl catalysts with dendritic wedges in the aryl *para*-position has a significant effect on α, the propagation constant for chain growth. The α-value increased from c.a. 0.68 – 0.71 to c.a. 0.66 – 0.77 upon functionalisation with poly(benzylphenylether) wedges. The value of α does not appear to depend on the size of the attached wedge, and it is thus believed that the increase in α is due to the influence of the ether linkage between the aryl ring and the attached wedge.

- Functionalisation of the bisiminopyridyl iron catalysts with dendritic wedges results in a surprising increase in catalytic activity. Although the aryl ether linkage plays a role in this improved activity, the increase in activity also appears to be related to the size of the attached wedge, with larger wedges resulting in high activity. However, attachment of a very large second generation wedge caused a drop in activity compared with the first generation analogue. This may be due to hindered access to the catalytic centre caused by the steric bulk of the wedges. The highest activities for the *para*-substituted catalysts were obtained with the first generation poly(benzylphenylether) and first generation carbosilane substituted complexes (**57** and **60**), for which TON's of 10.45 x 10^3 h^{-1} and 11.23 x 10^3 h^{-1} were obtained. These activities compare favourably with the observed TON for literature catalyst **54** of 5.32 x 10^3 h^{-1}.

- It was discovered that the use of 2 equivalents of an unattached first generation poly(benzylphenylether) dendritic wedge (**pbpeG1**) as a co-catalyst increases the catalytic activity without affecting α. This reproducible effect is particularly dramatic with literature catalyst **54**, where the activity was almost doubled. Lesser increases in activity were also observed with catalysts **57** and polymerisation catalyst **55**. It is believed that this effect is due to interactions between the ether functionality of the wedge and either the catalyst or the aluminium co-catalyst, although the nature of these interactions has not been determined. This result suggests that, for the catalysts with attached poly(benzylphenylether) wedges, the increased activity is due to intermolecular interactions between the wedges and catalytic centres, and that the increased activity with larger wedges may be due to the greater concentration of benzylphenylether functionalities in the reaction mixture.

- Complexes **62** and **63**, which have no *ortho* methyl substitution, were found to be catalytically inactive. Their different colour and lack of reactivity with MAO suggest that they have a different coordination structure to the other complexes.

- The introduction of electron withdrawing groups at the *para*-position results in an increase in catalytic activity but has no significant effect on α. The relationship between TON and σ_p was found to be approximately linear. An exception is with **72**, where the electron donating ethoxy group has a higher activity than expected. This is attributed to Lewis acid-base interactions of the ethoxy group with the aluminium co-catalyst, which reduce the electron donating ability of the substituent. Complex **74**, with the very electron deficient NO_2 substituent, gave the highest activity. TON's of 8.37 x 10^3 h^{-1} and 8.71 x 10^3 h^{-1} were observed. This represents an increase in activity of c.a. 50% compared to the literature catalyst **54**.

- The palladium α-diimine catalysts, though reactive towards MAO, were found to be almost completely inactive as ethene oligomerisation catalysts.

6.6 Future work

There is enormous scope for further work on the catalytic systems here investigated. A few key points may be highlighted

- Oligomerisation studies at higher ethene pressure will probably result in a large increase in activity and increased selectivity to 1-alkenes. It would be interesting to investigate whether the same trends apparent in the 1 atmosphere experiments are observed at higher pressure.

- More experiments with the carbosilane functionalised catalysts are necessary. Reproducibility and deactivation studies and the attachment of higher generation wedges would provide more information about these systems.

- Further study is needed to understand the nature of the interactions between the poly(benzylphenylether) wedges and the catalytic centre or aluminium co-catalyst responsible for the increased catalytic activity. In particular, it is not clear whether the observed increase in TON's is due to an increase in intrinsic activity or to a reduction in catalyst deactivation during the experiments. Catalytic runs over shorter time periods may clarify this question. Experiments using benzyl phenyl ether as a co-catalyst will provide evidence as to whether the improvement in activity is due to the ether moieties in the wedges. Experiments with different ratios of **pbpeG1** or benzyl phenyl ether to iron catalyst will also be informative.

- To the best of our knowledge, the use of an NO_2 aryl substituent to promote catalytic activity has not been made before with late transition metal catalysts. The resultant increase in oligomerisation activity may potentially also be observed with an analogous polymerisation catalyst, and the synthesis and catalytic properties of such a nitro-functionalised bisiminopyridyl polymerisation catalyst would be worthy of investigation.

Chapter 7:

Attempts to synthesise a carbosilane dendrimer with bis(diphenylphosphino)methyl terminal functionalities

7.1 Introduction and rationale

Tertiary phosphines (PR_3) are extremely important ligands in a wide range of homogeneous catalytic reactions.[192] Bidentate diphosphine ligands in particular have found many applications due to the stability conferred by chelation. Diphosphine transition metal complexes have been used in, among others, hydroformylations, hydrogenations, hydrocyanations, hydrosilylations, and isomerisations.[192]

One of the main potential applications for dendrimers is as anchors for homogeneous catalysts.[159] These multisite catalysts may retain the benefits of homogeneous catalysts such as high activity and selectivity, but may be recovered from reaction mixtures by ultrafiltration techniques or retained in continous flow reactors by membrane technology.[159] This is particularly important for expensive platinum group metal catalysts, where losses of the catalyst can render a catalytic process uneconomical. In addition to the potential advantages of separation, 'dendritic effects' have been observed where beneficial effects on catalyst selectivity are observed relative to the single site model catalyst.[193] Most attention has been focused on periphery functionalised dendrimers[159], where the catalytic sites are located on the surface of the globular macromolecule and are therefore available for reaction, although there are examples of catalysis at the core of a dendrimer.[160]

Given the importance of diphosphine ligands in homogeneous catalysis, there has been much research into the periphery functionalisation of dendrimers with diphosphine units, and the coordination of these dendritic diphosphines to transition metal species. Diphosphine functionalisation has been reported on poly(propyleneimine) (DAB)[194], poly(amido amine)(PAMAM)[195] and carbosilane dendrimers. Transition metal complexes of these dendrimers have been used in homogeneous Heck reactions, hydrogenations and hydroformylations.[159]

Carbosilane dendrimers with $-SiMe(CH_2PPh_2)_2$ functionalisation (Fig. 7-1)[de Groot, 2000 #83; Benito, 1999 #185; de Groot, 1999 #7] and their complexes with organometallic clusters[Benito, 1999 #185; Benito, 2001 #6] and Pd[144], Pt[Benito, 2002 #181] and Rh[145] species have been reported.

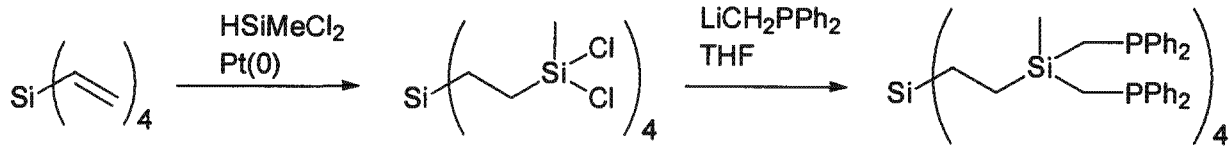

Fig. 7-1: Synthesis of a first generation carbosilane dendrimer with terminal -SiMe(CH_2PPh_2)$_2$

More recently, other elegantly synthesised carbosilane dendrimers with terminal -CMe(CH_2PPh_2)$_2$ groups have been reported (Fig. 7-2), and their complexes with $PdCl_2$ prepared.[196]

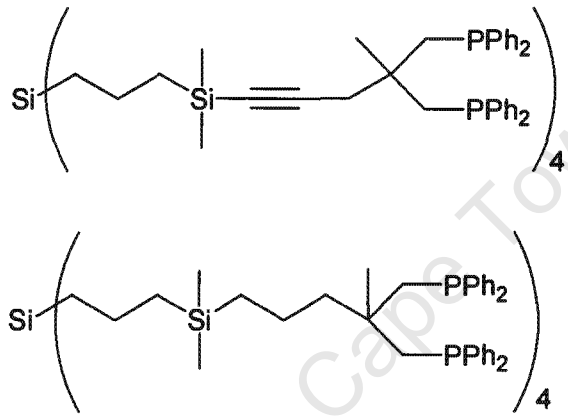

Fig. 7-2: Carbosilane dendrimers with terminal -CMe(CH_2PPh_2)$_2$

These dendritic diphosphines all have 3 atom spacers between the phosphines, thus making them equivalent to bis(diphenylphosphino)propane in their bite angle and coordination chemistry. Given our interest in the development of new dendrimers and dendritic wedges (chapter 3) and the use of dendritic molecules as anchors for catalytic species (chapter 4), the idea of developing a novel diphosphine dendrimer with a smaller bite angle, for example equivalent to that of bis(diphenylphosphino)methane (dppm), was appealing. In addition, we have also developed new chemistry of dppm with osmium carbonyl systems (sections 2.3.1 and 2.3.2), and we were interested in the possibility of extending this highly selective chemistry to dendritic diphosphines (Fig. 7-3).

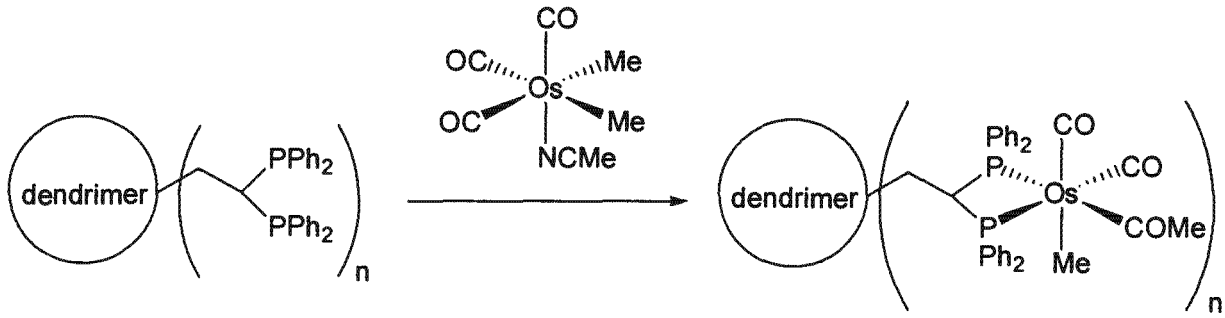

Fig. 7-3: Proposed reaction between dendritic dppm and $Os(CO)_3(NCMe)Me_2$

With these ideas in mind, the possibility of preparing a carbosilane dendrimer with terminal dppm functionality was investigated.

7.2 Synthetic approaches

The deprotonation of dppm by treatment with BuLi/TMEDA was first reported in the early 1970's.[197] The subsequent reactions of this metallated species with, for example, $ClSiMe_3$[198], MeI[199], CH_2Cl_2[Hietkamp, $ClPPh_2$[197], $ClAuPPh_3$[200], 1984 #273] and $HgCl_2$[201] have also been investigated.

Carbosilane dendrimers with terminal $-SiMe_2Cl$[150,202] and $-SiMe_2CH_2X$ (X = Cl, Br, I)[144] functionality have been reported in the literature and also prepared in our laboratory.[140] These dendrimers are prepared from the corresponding allyl terminated dendrimer by hydrosilylation with the appropriate silane (Fig. 7-4).

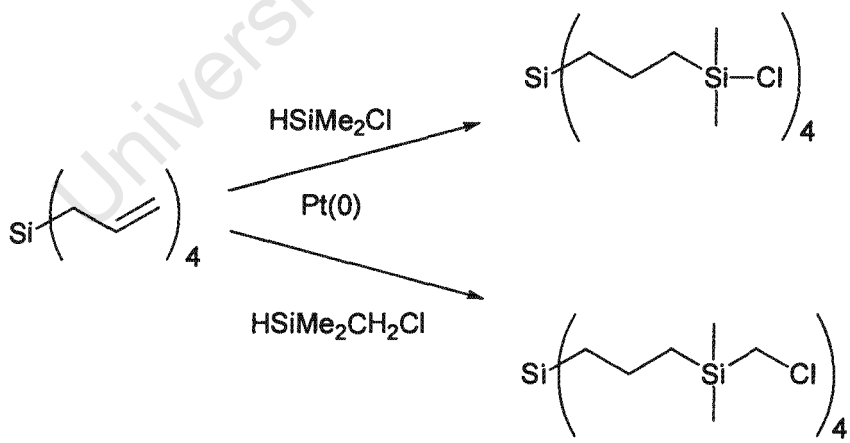

Fig. 7-4: Synthesis of first generation $-SiMe_2Cl$ and $-SiMe_2CH_2Cl$ functionalised dendrimers

Utilising these dendrimers or their allyl-terminated dendrimer precursors, several synthetic approaches to dppm dendrimers were envisioned (Fig. 7-5).

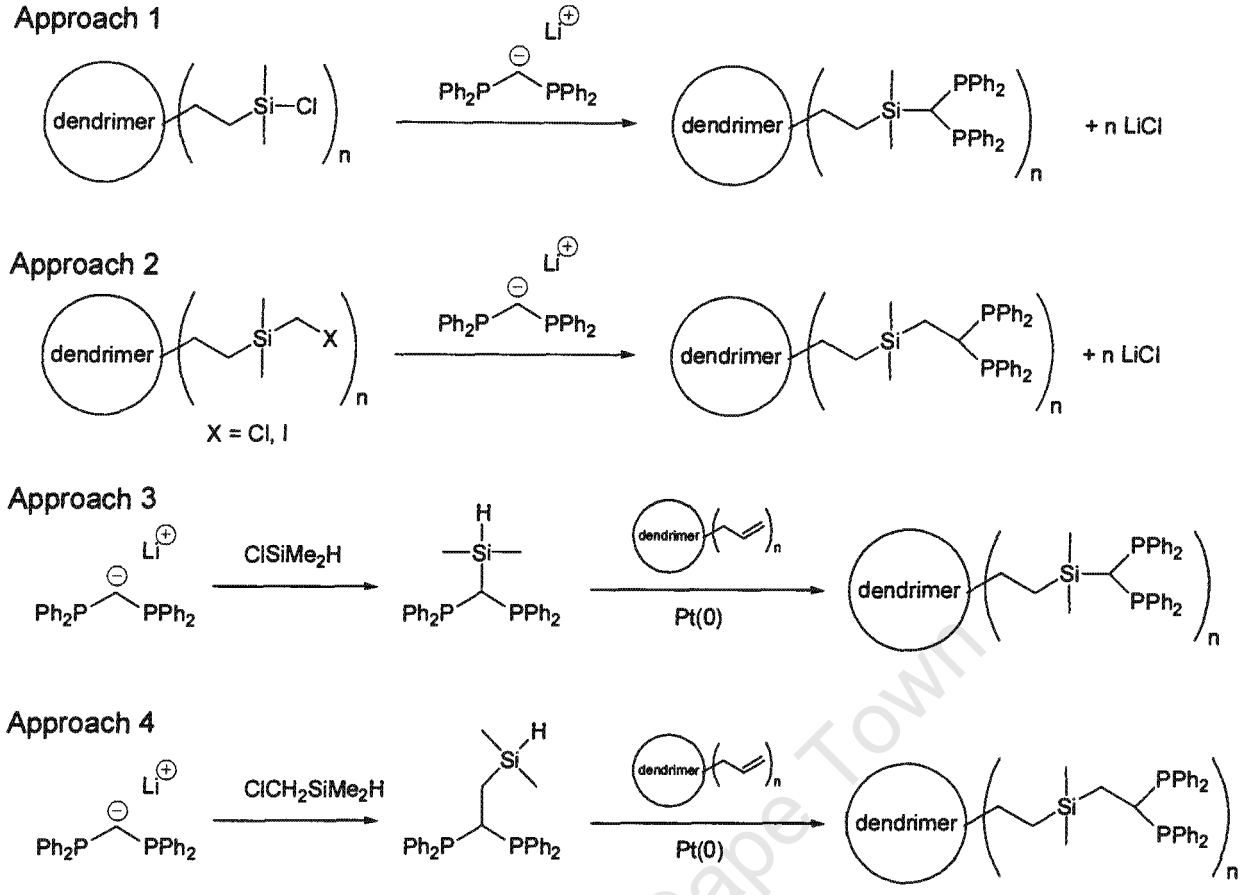

Fig. 7-5: Envisioned approaches for the synthesis of dppm-functionalised dendrimers

In approach 1, the reaction of deprotonated dppm with terminal $-SiMe_2Cl$ functionalised dendrimers would give terminal $-SiMe_2CH(PPh_2)_2$ functionality directly (Fig. 7-5). This dendritic reaction is analogous to the reaction between deprotonated dppm and $ClSiMe_3$ to give $Me_3SiCH(PPh_2)_2$.[198] This approach has the advantage of simplicity; however the stability of the final product is unknown. The bond between Si and the dppm moiety is likely to be fairly reactive because of the proximity to the strongly electron-donating phosphines. For example, $Me_3SiCH(PPh_2)_2$ is known to react with chlorinated compounds such as hexachloroethane.[198]. In addition, the issue of quantitative and completely selective conversion is key in all dendritic reactions: even marginally less than 100% conversion leads to intractable distributions of flawed dendrimers.

In approach 2, deprotonated dppm reacts with a dendrimer with terminal $-SiMe_2CH_2X$ (X = halogen) functionality (Fig. 7-5). The desired product would thus have terminal $-SiMe_2CH_2CH(PPh_2)_2$ functionality. This may be more stable, due to the methylene spacer between the silicon and the dppm moiety. However, $-SiCH_2X$ is a particularly unreactive alkyl halide because of reduction of the electrophilic character of the α-carbon and stabilisation of the C-X bond by interactions with the silicon *d* orbital and the Si-C σ^* orbital.[67,177] It is thus doubtful whether the necessary quantitative conversion in this reaction can be achieved. In addition it is known that treatment of deprotonated dppm with a large excess of MeI results in

alkylation of the methylene bridge and quaternisation of a phosphine (Fig. 7-6).[199] In approach 2, however, an excess of deprotonated dppm relative to -$SiCH_2X$ would be used and the α-silicon stabilisation will probably prevent this quaternisation. The model reaction between Me_3SiCH_2X and deprotonated dppm should first be investigated before dendritic reactions are attempted.

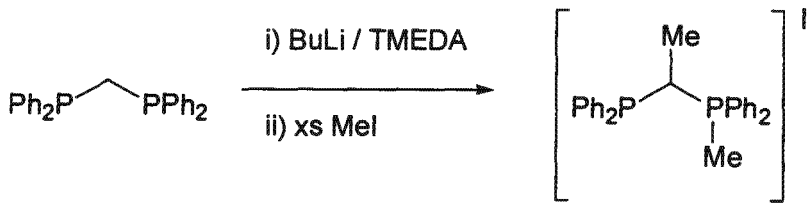

Fig. 7-6: Reaction of deprotonated with excess MeI[199]

In approaches 3 and 4, silanes $HSiMe_2CH(PPh_2)_2$ and $HSiMe_2CH_2CH(PPh_2)_2$ are first prepared (by treatment of deprotonated dppm with $HSiMe_2Cl$ and $HSiMe_2CH_2X$ respectively) and then these silanes are reacted via hydrosilylation to an allyl functionalised dendrimer to give products identical to those in approach 1 and 2 (Fig. 7-5). The hydrosilylation reaction is a proven reaction in dendritic chemistry because of its quantitative and selective conversion.[133,134] Again, model chemistry is useful before dendritic reactions are attempted. In this case, hydrosilylation reactions of $HSiMe_2CH(PPh_2)_2$ and $HSiMe_2CH_2CH(PPh_2)_2$ with a model compound such as allyltrimethylsilane should be attempted.

7.3 Model chemistry

7.3.1 Synthesis of $Me_3SiCH(PPh_2)_2$ (76) and $HSiMe_2CH(PPh_2)_2$ (77)

$Me_3SiCH(PPh_2)_2$ (76) was prepared in 66% yield according to a modified literature preparation (Fig. 7-7).[198] This reaction is a model reaction for the reaction of deprotonated dppm with a -$SiMe_2Cl$ functionalised dendrimer (approach 1 in Fig. 7-5). The low isolated yield is due to losses in the workup, and it is assumed that the actual conversion is quantitative due to the high reactivity of the Si-Cl bond. **76** is unstable in the presence of chlorinated solvents, in particular deuterated chloroform.

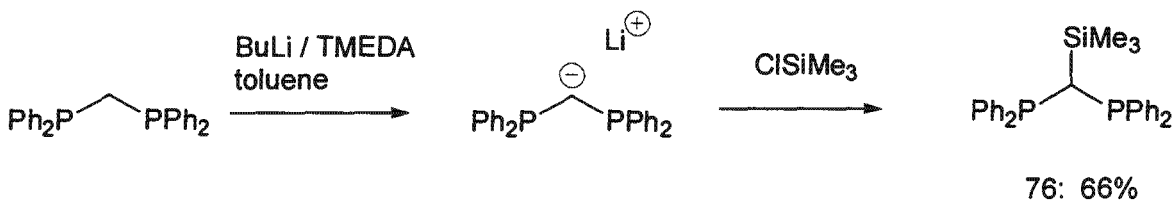

Fig. 7-7: Synthesis of $Me_3SiCH(PPh_2)_2$ (76)

$HSiMe_2CH(PPh_2)_2$ (77) was prepared by a similar route to $Me_3SiCH(PPh_2)_2$. Quantitative hydrosilylation of this compound with an allyl-functionalised dendrimer would be expected to give the desired dppm-functionalised dendrimer (approach 3, Fig. 7-5) Deprotonated dppm (prepared by a TMEDA-mediated metallation of dppm by BuLi) was treated with excess $HSiMe_2Cl$, and the product was obtained as an impure oil after separation from the LiCl by-product (Fig. 7-8). After recrystallisation from toluene / hexane, **77** was obtained as a white powder with free dppm as an impurity. Attempts at purification by recrystallisation from a variety of different solvent systems were frustrated due to the sensitivity to chlorinated solvents or polar solvents such as ethanol (from which **76** is recrystallised.) **77** was also found to be moderately moisture-sensitive, decomposing upon prolonged exposure to air.

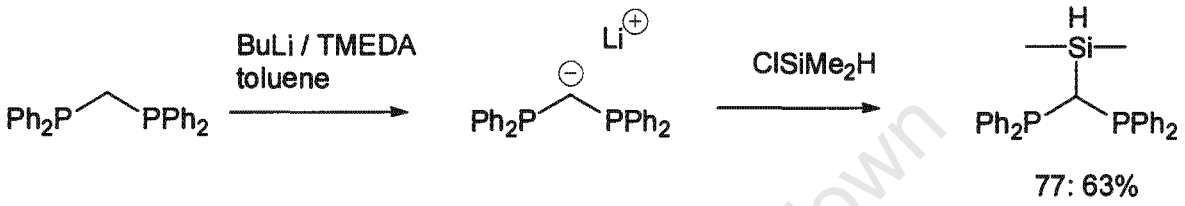

Fig. 7-8: Synthesis of $HSiMe_2CH(PPh_2)_2$ (77)

Despite the failure to obtain an analytically pure product, the characterisation by ^1H, ^{13}C and ^{31}P NMR suggested that **77** was sufficiently pure to attempt subsequent reactions in the hope that the products could be purified and more fully characterised.

7.3.2 Reactions of deprotonated dppm with Me_3SiCH_2X (X = Cl, I)

The reaction of deprotonated dppm with Me_3SiCH_2X (X = Cl, I) is a model for both the proposed reaction of deprotonated dppm with a -$SiMe_2CH_2X$ (X = Cl, I) functionalised dendrimer (approach 2 in Fig. 7-5) and the synthesis of $HSiMe_2CH_2CH(PPh_2)_2$ (an intermediate in approach 4 in Fig. 7-5).

Several attempts were made to prepare $Me_3SiCH_2CH(PPh_2)_2$ using BuLi / TMEDA as the deprotonation agent. It was found that the stabilising effect of the α-silicon rendered the alkyl halide insufficiently reactive towards the deprotonated dppm. Even when long reaction times, elevated reaction temperatures and the use of the iodide, Me_3SiCH_2I, was employed, no formation of the desired product could be detected, and after hydrolysis during work-up, free dppm was recovered.

In an effort to increase the nucleophilicity of the deprotonated dppm, the 'superbase' method for deprotonations was employed.[187] The superbase approach involves the introduction of potassium *tert*-butoxide as a co-reagent with an organolithium base. The resulting metallated product is not simply the potassium salt, but should be thought of as a mixed metal system. In many examples, the reactivity and

stability achieved through the superbase approach is superior to that from either the lithium or the potassium reagent.[203]

A stoichiometric mixture of dppm and KO^{t}Bu in toluene was treated with a slight excess of butyl lithium at –78°C (Fig. 7-9). Upon warming to room temperature, a thick yellow precipitate formed, which is believed to be the metallated dppm. The supernatant, containing unreacted dppm, LiO^{t}Bu, and excess BuLi, was removed by syringe after centrifuging the mixture, and then washed out with a further addition of toluene followed by centrifuging and removal of supernatant.

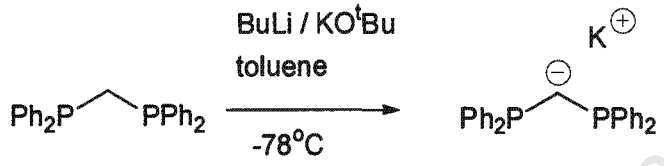

Fig. 7-9: Superbase method for the deprotonation of dppm

The precipitate was then suspended in toluene and treated with excess Me_3SiCH_2I. After heating to 50°C for 4 hours, the voluminous yellow precipitate had gone into solution, and a white precipitate had formed in its place. The mixture was centrifuged to remove this precipitate and the supernatant was syringed off. Removal of the solvents from the supernatant left a small amount of oily material. A ^{1}H NMR spectrum of this suggested that the desired product had been formed but in very low yield, although free dppm remained the predominant species.

On the basis of these results, it was concluded that the reaction between -$SiMe_2CH_2X$ and deprotonated dppm cannot be a viable route for the synthesis of dppm dendrimers, thus excluding approaches 2 and 4 (Fig. 7-5).

7.3.3 Hydrosilylation reactions with $HSiMe_2CH(PPh_2)_2$

A model platinum catalysed hydrosilylation reaction between allyltrimethylsilane and $HSiMe_2CH(PPh_2)_2$ (77) was attempted using Karstedt catalyst (Fig. 7-9). This reaction is a model for approach 2 to the synthesis of dppm dendrimers (Fig. 7-5). However, even after extended reaction times and elevated temperatures, no reaction was observed, and ^{1}H NMR spectrum indicated that the starting materials remained unchanged.

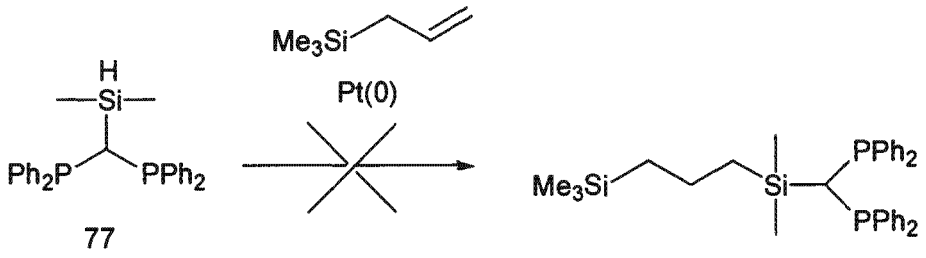

Fig. 7-9: Attempted platinum catalysed reaction between 77 and allyltrimethylsilane

It became apparent that the catalyst was immediately deactivated by **77**. On reflection, this is in fact not surprising, as the Karstedt catalyst used for hydrosilylations consists of Pt(0) species associated in an oligomeric structure with the vinyl bonds of the dimethyltetravinyldisiloxane ligand. In the presence of a strongly chelating ligand such as the dppm functionality in **77**, the Karstedt catalyst is immediately deactivated through irreversible coordination of platinum. Confirmation of this was obtained by adding a trace amount of dppm to the reaction mixture of a known hydrosilylation reaction. The platinum catalysed reaction between allyltrimethylsilane and (chloromethyl)dimethylsilane is extremely facile, achieving complete conversion to **78** within a few seconds of the addition of the Karstedt catalyst (0.1% Pt relative to allyltrimethylsilane) (Fig. 7-10). However, when approximately 1% dppm relative to allyltrimethylsilane was present in the reaction mixture, the reaction was completely inhibited (Fig. 7-10). A report published subsequent to this work also records the failure of a hydrosilylation with Karstedt catalyst of a diphosphine containing silane compound.[196]

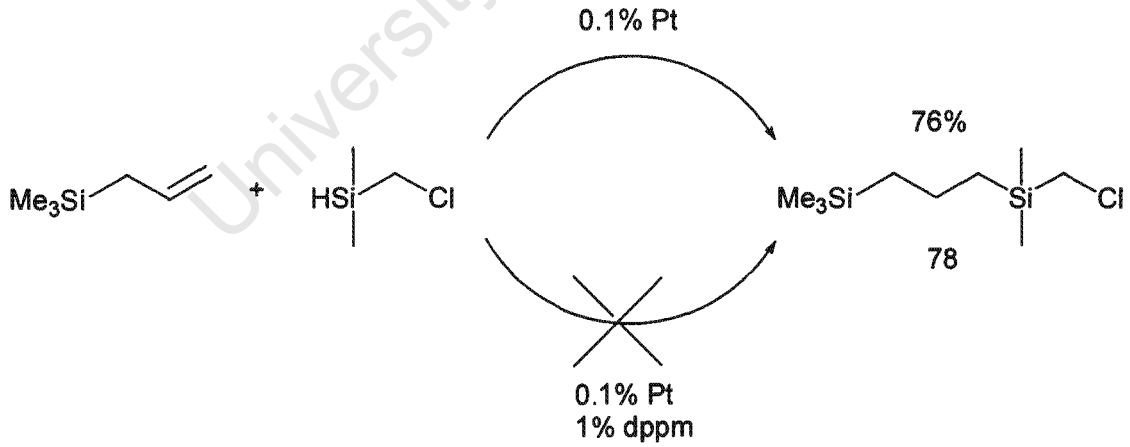

Fig. 7-10: Inhibition of a platinum-catalysed hydrosilylation reaction by dppm

This result establishes that approaches 3 and 4 (Fig. 7-5) are not viable, as both rely upon the hydrosilylation of a dppm functionalised silane to the alkene bonds of an allyl functionalised carbosilane dendrimer.

7.3.4 Synthesis of $Me_3Si(CH_2)_3SiMe_2CH(PPh_2)_2$ (80)

On the basis of the model chemistry discussed above, it is apparent that only approach 1 of the four proposed (Fig. 7-5) represents a viable strategy for the synthesis of dppm dendrimers. The successful preparation of **76** and **77** establishes the reactivity of the -$SiMe_2Cl$ moiety towards deprotonated dppm. However a more accurate model for the dendritic reactivity of $Si[CH_2CH_2CH_2SiMe_2Cl]_4$ is the reaction between $Me_3SiCH_2CH_2CH_2SiMe_2Cl$ (effectively a single 'arm' of the above dendrimer) and deprotonated dppm. $Me_3SiCH_2CH_2CH_2SiMe_2Cl$ (**79**) was prepared by a hydrosilylation of allyltrimethylsilane and chlorodimethylsilane (Fig. 7-11).

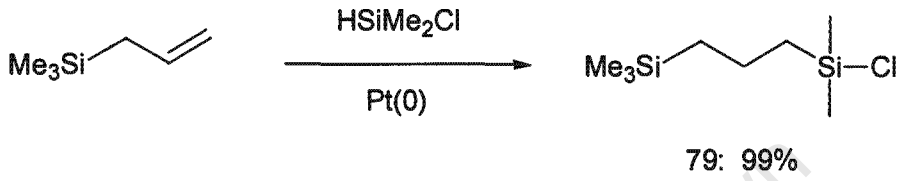

*Fig. 7-11: Synthesis of **79***

The reaction between deprotonated dppm and **79** gave the desired product $Me_3SiCH_2CH_2CH_2SiMe_2CH(PPh_2)_2$ (**80**) in high yield after recrystallisation from pentane (Fig. 7-12).

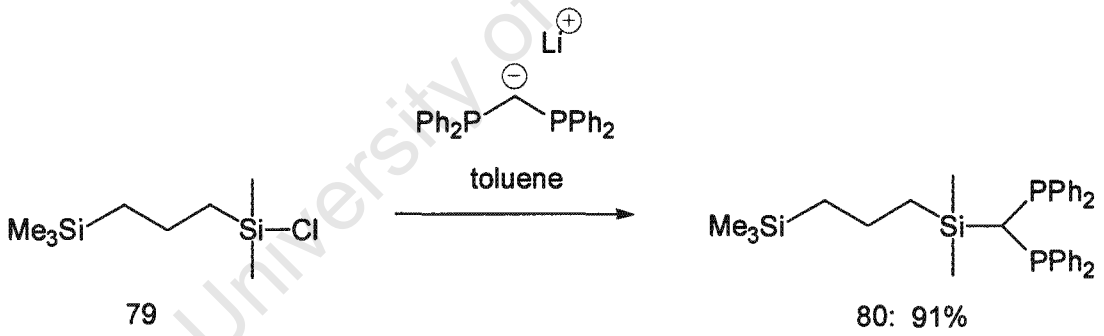

*Fig. 7-12: Synthesis of $Me_3SiCH_2CH_2CH_2SiMe_2CH(PPh_2)_2$ (**80**)*

New compound **80** was fully characterised, and its ^1H NMR spectrum is shown in Fig. 7-13.

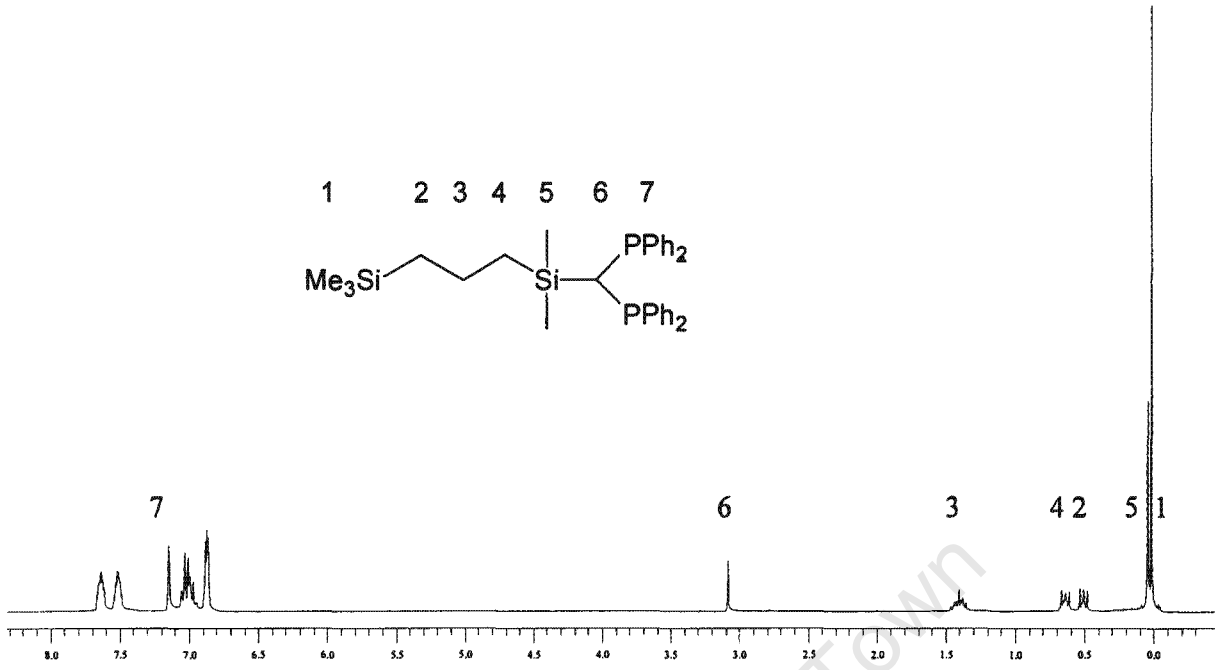

*Fig. 7-13: ^{1}H NMR spectrum of **80***

A notable feature of this spectrum is the absence of an observable ^{2}J(PH) coupling for the -$SiMe_2CH(PPh_2)_2$ signal at δ_H = 3.09ppm. The ^{1}H NMR spectrum of $Me_3SiCH(PPh_2)_2$ is not reported in the literature, but the ^{1}H NMR of a sample of this compound prepared by a literature procedure[198] similarly showed no observable coupling (δ_H = 3.00ppm). In the ^{1}H NMR spectrum of dppm, a very small ^{2}J(PH) coupling (1.9Hz) is observed for $CH_2(PPh_2)_2$ (δ_H = 2.79ppm).

7.4 Attempts towards the synthesis of $Si[CH_2CH_2CH_2SiMe_2CH(PPh_2)_2]_4$

7.4.1 Preparation of $Si[CH_2CH_2CH_2SiMe_2Cl]_4$ (81)

$Si[CH_2CH_2CH_2SiMe_2Cl]_4$ (**81**) was prepared by a modified literature procedure.[204,205] $HSiMe_2Cl$ is a relatively unreactive silane in the hydrosilylation reaction[140]. In order to obtain quantitative conversion it was found to be necessary to perform the reaction at elevated temperature in a thick-walled glass pressure tube (b.p. $HSiMe_2Cl$ = 34.7°C), using Karstedt catalyst (Fig. 7-14). After 48h reaction time at 100°C, complete hydrosilylation was achieved, as indicated by the absence of allyl signals in the ^{1}H and ^{13}C NMR.

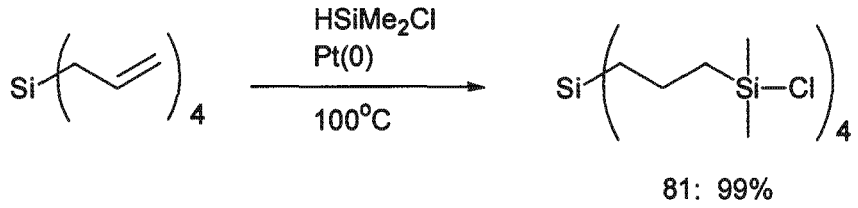

Fig. 7-14: Synthesis of $Si[CH_2CH_2CH_2SiMe_2Cl]_4$ (81)

7.4.2 Reaction of deprotonated dppm with $Si[CH_2CH_2CH_2SiMe_2Cl]_4$

The reaction between deprotonated dppm and **81** was attempted numerous times. Dppm was deprotonated with BuLi in the presence of TMEDA, and **81** was added as a solution in toluene (Fig. 7-15). Control of the stoichiometry was an essential consideration. Excess dppm had to be used relative to BuLi, as excess BuLi will react directly with the dendritic $-SiMe_2Cl$ functionality. In turn, a slight excess of deprotonated dppm relative to $-SiMe_2Cl$ is necessary to prevent the formation of incompletely substituted dendrimers. Considering the limits on stoichiometric control imposed by volumetric measurements of quantity and uncertainty in the BuLi concentration, significant excesses (5 – 10%) of dppm to BuLi, and BuLi to $-SiMe_2Cl$ were necessary.

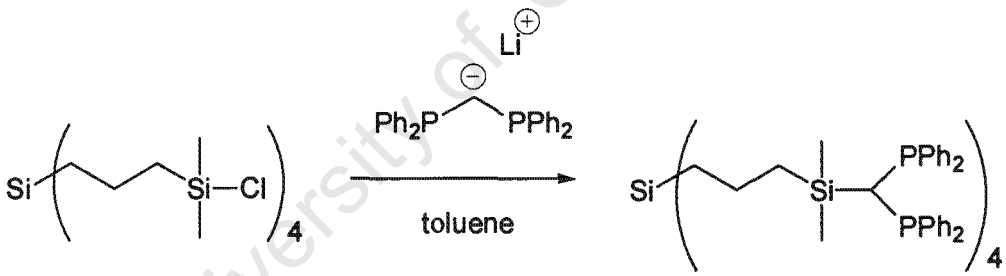

Fig. 7-15: Attempted synthesis of dendritic dppm

Upon the addition of **81** to the deprotonated dppm, a precipitate of LiCl formed, and after separation of the solution from the LiCl by centrifuging, a crude oil was obtained after removal of the volatiles. ^1H NMR analysis suggested the formation of the desired product, although significant impurities, in particular dppm, were also present. Various attempts were made to recrystallise the product, although the range of available solvent systems was limited due to the sensitivity of the Si-dppm linkage. In each case, oiling out occurred, and after removal of the supernatant solution, the product was found to be no purer, or less pure, than before the recrystallisation attempt. It was thus concluded that although the desired product may in principle be formed, isolation of the pure compound presents an insurmountable obstacle to its characterisation.

7.5 Complexation of dppm model- and dendritic derivatives to molybdenum tetracarbonyl

7.5.1 Rationale

Due to the inherent instability of the silyl-substituted dppm derivatives described above, and the problems with purifying the dppm dendrimer, efforts were made to attempt similar chemistry using a dppm species complexed to $Mo(CO)_4$. The synthesis of $M(CO)_4$(dppm) (M = Cr, Mo, W), either directly by thermal decarbonylation from $M(CO)_6$[206,207] or indirectly by displacement of a dialkene such as norbornadiene or 1,5-cylclooctadiene (COD) from $M(CO)_4$(dialkene)[208-210], is well established. The deprotonation of $M(CO)_4$(dppm) (M = Cr, Mo, W) and substitution with a variety of groups including -$SiMe_3$, alkyl and acyl groups is also described in the literature (Fig. 7-16).[211-213]

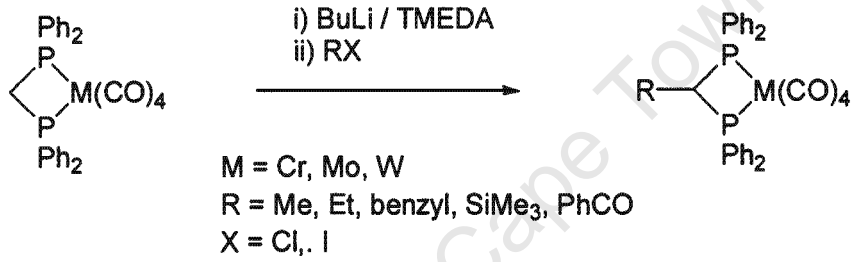

Fig.7-16: Deprotonation and substitution reactions of $M(CO)_4$(dppm) (M = Cr, Mo, W)

7.5.2 Preparation of $[HSiMe_2CH(PPh_2)_2]Mo(CO)_4$ and the attempted hydrosilylation of this compound with allyltrimethylsilane

$Mo(CO)_4$(dppm) was prepared by a literature synthesis[209] and a literature preparation of $Me_3SiCH(PPh_2)_2Mo(CO)_4$ by deprotonation of $Mo(CO)_4$(dppm) and treatment with $ClSiMe_3$ was successfully repeated.[212]

As discussed in section 7.3.3, the platinum catalysed hydrosilylation reaction of $HSiMe_2CH(PPh_2)_2$ (**77**) with alkenes is inhibited due to deactivation of the platinum catalyst by chelation of the platinum species by the dppm moiety. It was hoped that this problem could be overcome by attempting a hydrosilylation with the analogous Mo-complexed analogue, $[HSiMe_2CH(PPh_2)_2]Mo(CO)_4$, in which the dppm moiety is already complexed and will thus not complex to the platinum catalytic species.

$HSiMe_2CH(PPh_2)_2Mo(CO)_4$ (**82**) was prepared by treatment of deprotonated $Mo(CO)_4$(dppm) with $ClSiMe_2H$ (Fig. 7-17).

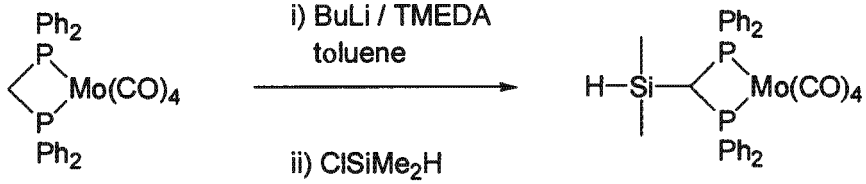

82: 79%

Fig. 7-17: Synthesis of ***82***

It is apparent from visual observation of the rates of reaction that deprotonated $Mo(CO)_4$(dppm) is less nucleophilic than deprotonated dppm. Whereas the reactions of deprotonated dppm with Si-Cl functionality proceeds instantaneously, as indicated by the immediate change in colour and formation of a precipitate of LiCl, the reactions of deprotonated $Mo(CO)_4$(dppm) with $ClSiMe_3$ or $ClSiMe_2H$ required stirring for several hours at 50°C. This is in agreement with similar literature preparations.[213]

The ^{1}H NMR spectrum of **82** is shown in Fig. 7-18. It is notable that the ^2J(PH) coupling for the $HSiMe_2CH(PPh_2)_2Mo(CO)_4$ signal at 4.81ppm is clearly seen (10Hz), whereas this coupling is either not observed or is very small in the case of uncomplexed dppm compounds (see section 7.3.4).

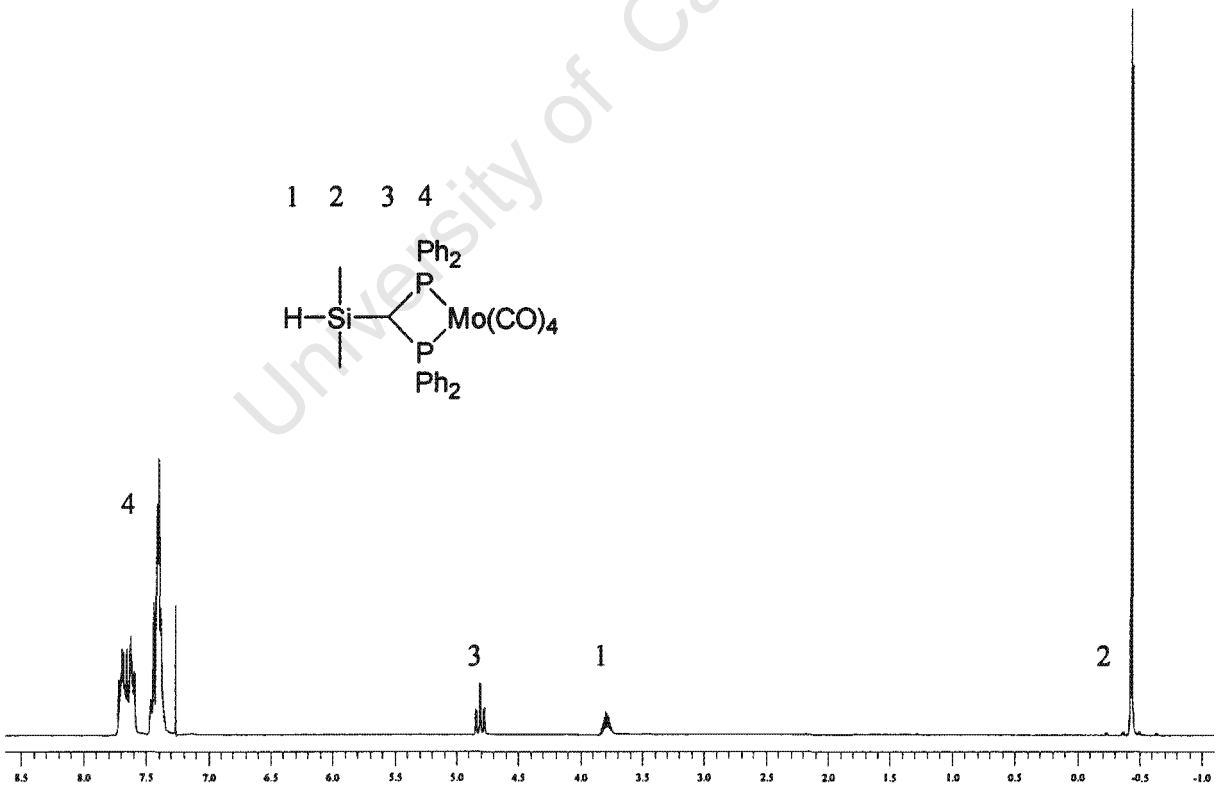

Fig. 7-18: ^{1}H NMR spectrum of ***82***

The platinum catalysed hydrosilylation reaction between **82** and allyltrimethylsilane was attempted (Fig. 7-19). Unfortunately the reaction is again completely inhibited and the starting materials are recovered.

This inhibition is a result of the presence of the Mo-complexed dppm moiety and not a fundamental lack of reactivity of the Si-H bond. This can be ascertained by observing the inhibition of a known hydrosilylation reaction in the presence of a trace amount of $Mo(CO)_4$(dppm) as was discussed in section 7.3.3. The reason for this deactivation of the platinum catalyst is not immediately clear. It is conceivable that trace amounts of uncomplexed dppm moieties were present in the **82** or that decomplexation of molybdenum and coordination to platinum takes place in solution.

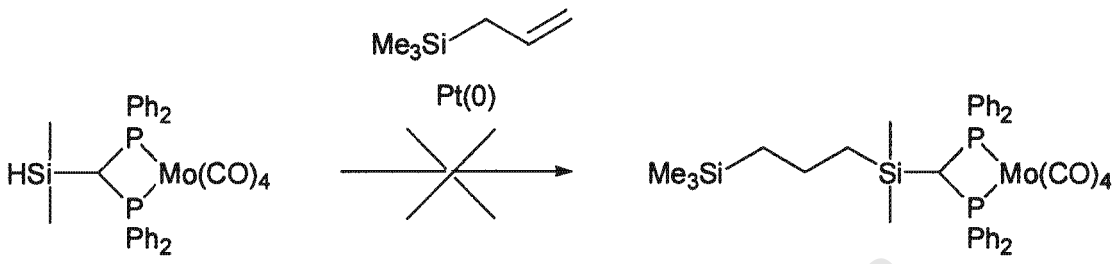

*Fig. 7-19: Attempted hydrosilylation reaction between **82** and allyltrimethylsilane*

7.5.3 Synthesis of $Me_3SiCH_2CH_2CH_2SiMe_2CH(PPh_2)_2Mo(CO)_4$ (83)

As discussed in section 7.4.2, some NMR evidence was obtained for the synthesis of a dppm dendrimer by reaction of deprotonated dppm with $Si[CH_2CH_2CH_2SiMe_2Cl]_4$ (**81**). However, the isolation of this dendrimer proved problematic due to the reactivity of the Si-dppm linkage, which excludes chromatography or recrystallisations from chlorinated or polar solvents. It was hoped that an analogous dendrimer prepared with Mo-complexed dppm (Fig. 7-20) might be more amenable to isolation and purification.

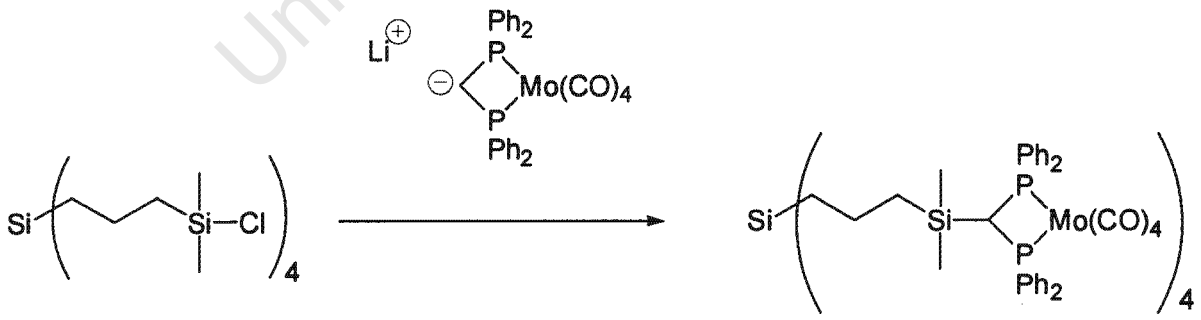

Fig. 7-20: Envisioned synthesis of a Mo-complexed dppm dendrimer

Although the reaction of deprotonated $Mo(CO)_4$(dppm) with $ClSiMe_3$ and $ClSiMe_2H$ has been described (section 7.5.2), the silanes are typically used in large excess. In the envisioned dendritic synthesis (Fig. 7-20), a small excess of deprotonated $Mo(CO)_4$(dppm) relative to Si-Cl is necessary, and it is essential that conversion of Si-Cl to Si-dppm(Mo) is quantitative. A model reaction of stoichiometric equivalents of

deprotonated $Mo(CO)_4$(dppm) and **79** was thus first attempted. After 16h reaction time at 50°C and an aqueous work-up, the crude product was found by ^1H NMR spectroscopy to contain the desired product $Me_3SiCH_2CH_2CH_2SiMe_2CH(PPh_2)_2Mo(CO)_4$ (**83**) and $Mo(CO)_4$(dppm) in a 35:65 ratio (Fig. 7-21). Since dendritic reactions require complete conversion, it was concluded that the proposed synthesis of a Mo-complexed dppm dendrimer (Fig. 7-20) is not viable.

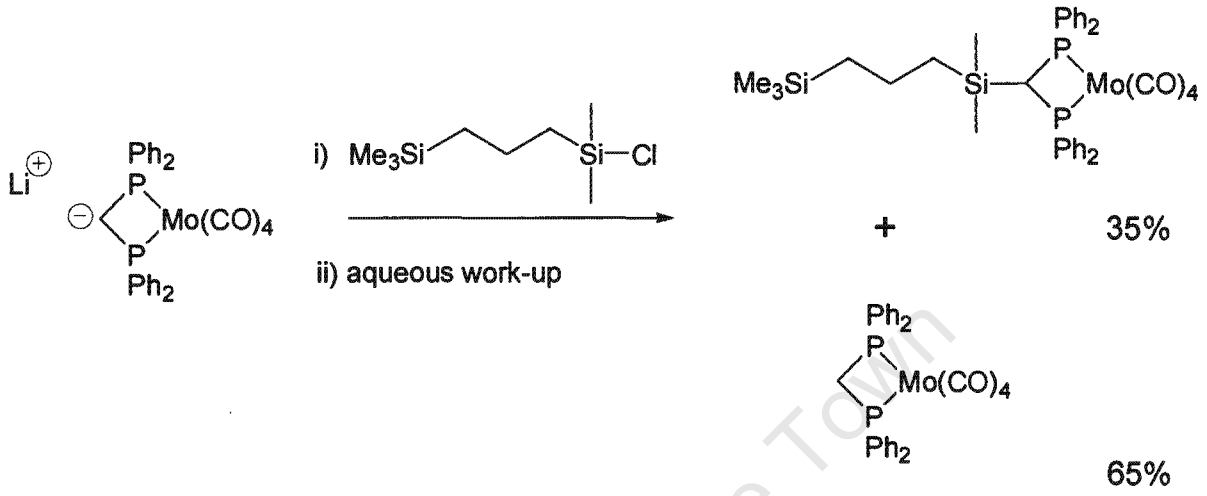

Fig. 7-21: Reaction between deprotonated $Mo(CO)_4$(dppm) and $Me_3SiCH_2CH_2CH_2SiMe_2Cl$

83 was successfully prepared in good yield by a different route: the reaction of **80** with $Mo(CO)_4$(COD) (Fig. 7-22). This uses similar conditions to the literature preparation of $Mo(CO)_4$(dppm).[209]

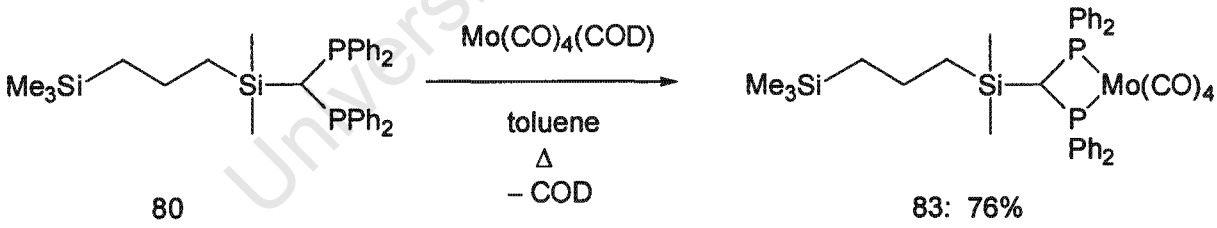

*Fig. 7-22: Synthesis of **82** from **79***

The ^1H NMR of **83** is shown in Fig. 7-23. The signal for $Me_3SiCH_2CH_2CH_2SiMe_2CH(PPh_2)_2Mo(CO)_4$ (δ_H = 4.94) is significantly shifted from the same signal in **80** (δ_H = 3.09ppm, see Fig. 7.13) as a result of the electron donation by the phosphines to the molybdenum centre. The ^2J(PH) coupling (10 Hz) for this signal is clearly observed, whereas it is not observed at all in the uncomplexed analogue **80**. This is consistent with observations from other free and complexed dppm compounds (see sections 7.3.4 and 7.5.2). The effect of the molybdenum coordination can also be seen in the ^{31}P NMR spectra, where a shift from -12.8 to 16.2ppm is observed upon complexation of the dppm moiety to the $Mo(CO)_4$ fragment.

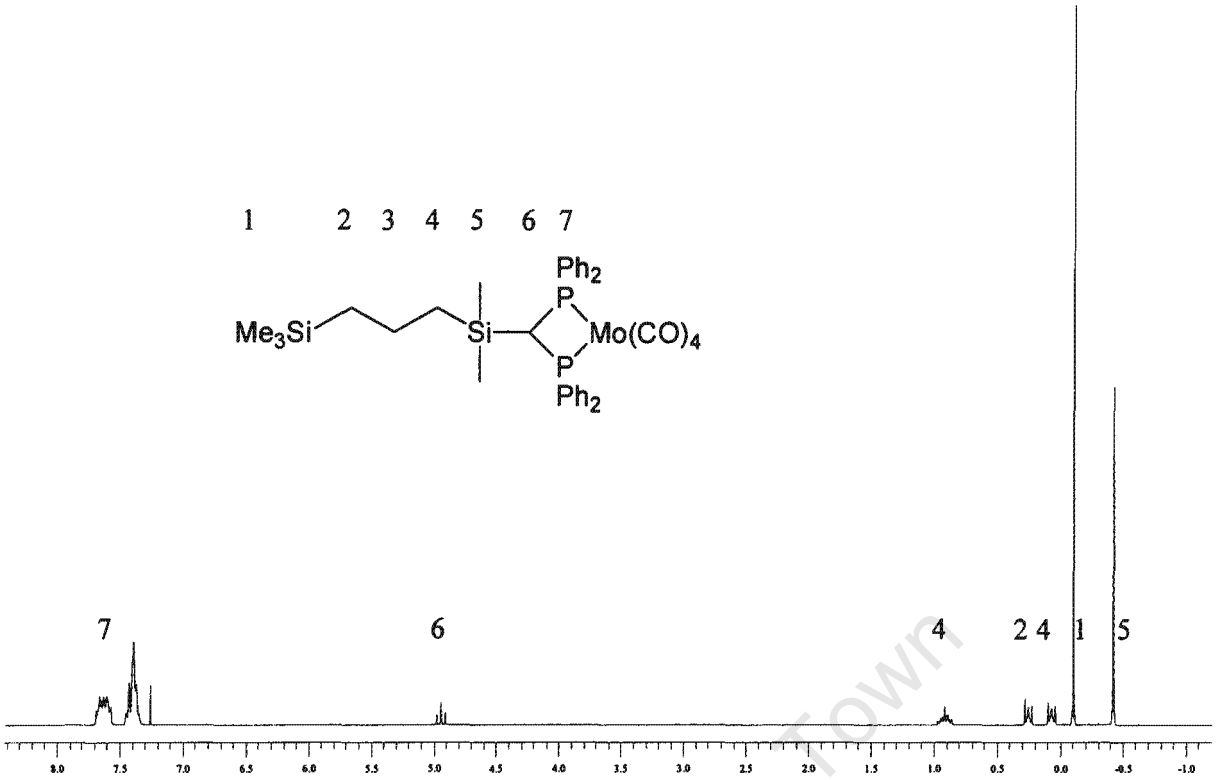

Fig. 7-23: ^1H NMR spectrum of 83

7.6 Conclusions and future work

Although the preparation of a dppm functionalised dendrimer was not achieved, interesting model chemistry was developed, both of free and complexed dppm derivatives. It was established that hydrosilylation in the presence of dppm containing compounds is unsuccessful, due to deactivation of the platinum catalyst by coordination to the phosphine. This occurs regardless of whether the dppm is complexed or not. Alkylation of deprotonated dppm with $-SiMe_2CH_2X$ (X = Cl, I) was also unsuccessful. This is ascribed to the effect of the silicon in the alpha position, which is known to reduce the reactivity of alkyl halides. Deprotonated dppm does react successfully with $-SiMe_2Cl$ functionality, and the model compound $Me_3SiCH_2CH_2CH_2SiMe_2CH(PPh_2)_2$, as well as its complex with $Mo(CO)_4$, were successfully prepared and characterised. The reaction of a $-SiMe_2Cl$ functionalised dendrimer with deprotonated dppm was attempted, and although analysis of the crude product suggests formation of the desired product, all attempts at purification failed due to the sensitivity of the Si-dppm linkage.

In view of the chemistry developed in chapter 3 (which was done after the work in this chapter), an intriguing new potential synthesis of a dppm functionalised dendrimer becomes apparent (Fig. 7-24). The synthesis of the starting material, 4,4-dibromo-1-butene, is described in the literature.[214,215] An analogous synthesis starting from 4-bromo-1-butene, described in section 3.4, results in the formation of a 4-bromobutyl functionalised dendrimer. The reaction of $LiPPh_2$ with alkyl halides is successful in the synthesis of other dendritic diphosphines[196] and in the synthesis of dppm derivatives such a

1,1-bis(diphenylphosphino)ethane.[199] The final dppm dendrimer does not have the disadvantage of a Si-dppm linkage, and the synthesis avoids the introduction of the sensitive phosphines until the final step.

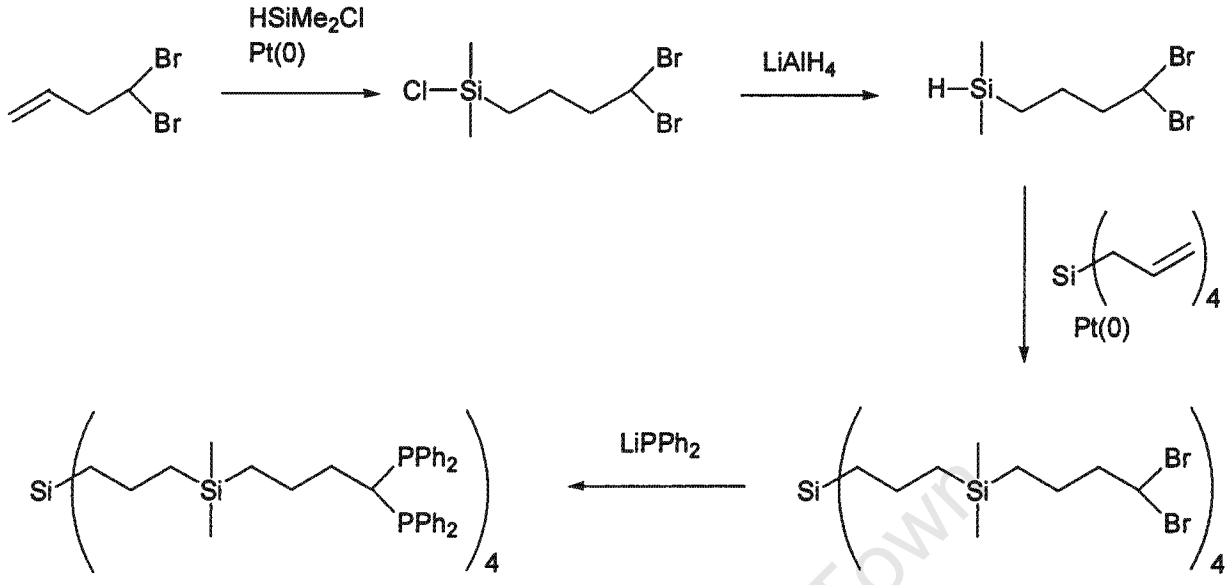

Fig. 7-24: Proposed synthesis of dppm functionalised carbosilane dendrimer

Chapter 8:

Conclusions

In approaching the broad goal of developing new catalysts for the oligomerisation of 1-alkenes, a wide range of chemistry has been investigated.

In chapter 2, a study of fundamental organometallic compounds and reactions of osmium carbonyls has been made. Osmium is the 5d congener of iron, and thus an investigation of the chemistry of osmium compounds may model individual steps in catalytic reactions involving iron, which are too fast to be observed directly. *cis*-$Os(CO)_4Me_2$ has been little studied, and new and interesting reactions of this system are worthy of study in their own right as well as being models for catalytic species of or derived from the general form ML_nR_2.

The reactive compound *fac*-$Os(CO)_3(NCMe)Me_2$ was prepared by chemical decarbonylation of *cis*-$Os(CO)_4Me_2$, and the reactions of this compound with monodentate and bidentate ligands were explored. Reaction with PPh_3 gives *fac*-$Os(CO)_3(PPh_3)Me_2$, which may be substituted further to give *cis,cis*-$Os(CO)_2(PPh_3)(NCMe)Me_2$. Treatment of this with PPh_3 gives *cis,trans*-$Os(CO)_2(PPh_3)_2Me_2$ by displacement of MeCN and subsequent isomerisation. The reactions of *fac*-$Os(CO)_3(NCMe)Me_2$ with bidentate ligands L^L (L^L = 2,2'-bipyridyl, bis(diphenylphosphino)methane and bis(diphenylphosphino)ethane) give the novel compounds $Os(CO)_2(L^L)(COMe)Me$ with high selectivity and yield. The X-ray crystal structure of $Os(CO)_2$(dppm)(COMe)Me (dppm = bis(diphenylphosphino)methane) has been determined. These compounds are formed by displacement of MeCN by one coordinating atom of the bidentate ligand and subsequent chelation with accompanying methyl migration onto CO. To the best of our knowledge, these compounds are the first isolated osmium compounds with both alkyl and acyl groups. If *fac*-$Os(CO)_3(NCMe)Me_2$ is treated with bis(diphenylphosphino)propane (dppp), the intermediate *fac*-$Os(CO)_3(dppm)Me_2$ with pendant phosphine may be spectroscopically observed. Chelation is less favoured than with dppm and dppe because of the greater spacer length between phosphines. Under the harsh conditions required to obtain chelation, thermal decarbonylation occurs, and $Os(CO)_2(dppp)Me_2$ was isolated. Reaction of *fac*-$Os(CO)_3(NCMe)Me_2$ with dppp in a 2:1 ratio gives the bridged diphosphine compound $CH_2[CH_2PPh_2Os(CO)_3Me_2]_2$.

Treatment of *fac*-$Os(CO)_3(NCMe)Me_2$ with CPh_3PF_6 results in the abstraction of a methyl to give $[Os(CO)_3(NCMe)Me]PF_6$. This 16-electron osmium species is unstable and decomposes rapidly. However, if the reaction is performed in acetonitrile, the acetonitrile acts as a trapping reagent to give the stable 18-

electron species $[Os(CO)_3(NCMe)_2Me]PF_6$. Attempts to prepare $[Os(CO)_3(NCMe)(CH_2{=}CH_2)Me]PF_6$ by a similar *in situ* trapping with ethene were unsuccessful.

The use of carbosilane dendrimers as supports for homogeneous catalysts is currently of great interest. In chapter 3, the preparation of a series of novel carbosilane dendritic wedges (generations 0, 1 and 2) with bromobutyl core functionality is described. A series of dendrimers (generations 1, 2 and 3) with 4, 12 and 36 terminal bromobutyl groups has also been prepared. These dendrimers may have useful applications, as the chemistry of the terminal groups is expected to resemble the chemistry of *n*-alkyl halides more closely than (chloromethyl)dimethylsilyl functionalised carbosilane dendrimers, in which the silicon deactivates the adjacent carbon for reactions with, for example, organometallic nucleophiles. The reactivity of the wedges and the dendrimers in halogen exchange and halogen-lithium exchange reactions and with hydroxyaryl complexes was also investigated.

A series of iron bisiminopyridyl complexes with dendritic wedges attached *via* an ether linkage at the *para* positions of the ligand aryl rings has been prepared (chapter 4). Both poly(benzylphenylether) and carbosilane dendritic wedges were used. The synthesis of the core ligands with *para*-hydroxy substitution, the reactions of these complexes with dendritic wedges and the complexation of the dendritic wedge substituted ligands with $FeCl_2$ is described. Some palladium complexes of similarly substituted α-diimine and monoiminopyridyl ligands were also prepared. In chapter 5, the preparation of a series of iron bisiminopyridyl complexes with *para* substitution by electron donating (OEt, Me) and electron withdrawing (Br, NO_2) ligands is reported.

Most of the new iron complexes were found to be active ethene oligomerisation catalysts when activated with MAO (chapter 6). Experiments were carried out at 1 atmophere ethene. The reaction products were found to be predominantly linear 1-alkenes (80-91%) with a Schultz-Flory chain length distribution. The most abundant other products were linear *n*-alkanes. *Para*-substitution by poly(benzylphenylether) dendritic wedges increases both the propagation constant, α, and the catalytic activity compared with an unsubstituted literature catalyst. The α-value does not depend on the the size of the attached wedge, and the increase in α is thus ascribed to the influence of the ether linkage between the aryl ring and the wedge. The α-value for the ethoxy substituted catalyst was found to be similar to the dendritically substituted catalysts. There does, however, appear to be a relationship between the size of the attached dendritic wedge and the resultant increase in activity. This is tentatively ascribed to intermolecular interactions between the attached wedges and either the catalytic centre or the aluminium co-catalyst. It is not clear whether the observed increase in TON is due to an intrinsic increase in activity or to a reduction in deactivation of the catalyst during the catalytic reaction.

The hypothesis that the increased activity is due to *intermolecular* interactions between the wedges and the catalytic centre or aluminium co-catalyst is supported by the unexpected observation that addition of two

equivalents of an unattached first generation poly(benzylphenylether) dendritic wedge as a co-catalyst with the literature iron catalyst results in an increase in activity of close to 100%. This result was found to be reproducibly. The α-value of the reaction is not affected by the addition of the co-catalyst. The reason for this remarkable increase in catalytic activity remains unexplained.

Substitution with more electron withdrawing groups in the *para* position results in an increase in catalytic activity but not α. The observed turnover numbers increase approximately linearly with increased σ_p, the Hammett parameter for the substituent. *Para* substitution by NO_2 increased the activity by almost 50% relative to the literature catalyst. The exception to this trend occurred with the ethoxy substituted complex, for which the activity was higher than expected and for which the α-value increased significantly. This is ascribed to Lewis acid-base interactions between the ethoxy group and the aluminium co-catalyst, which reduce the electron donating ability of the ethoxy substituent.

The work in this thesis has involved the synthesis of model compounds, dendritic molecules with potential applications in homogeneous catalysis and new catalysts for the oligomerisation of ethene. The catalytic activity of these catalysts has been investigated. It is hoped that this work has shed some light on an industrially important catalytic reaction and its mechanism.

Chapter 9:

Experimental details

9.1 General experimental details

General procedures

All reactions (unless otherwise specified) were carried out under nitrogen or argon using standard Schlenk-tube techniques. A Braun Unilab glovebox containing N_2 was used for some manipulations of moisture- and oxygen sensitive materials. Inert gases were purified by passage through columns of molecular sieves (5Å) and BASF catalyst. Syringes were stored at 60°C and other glassware was dried for a minimum of 2h at 210°C.

Materials

The solvents used in reactions were obtained as analytical grade and further purified by drying and distilling according to literature procedures[216] as indicated in Table 9-1. Solvents were typically stored under argon in Teflon-valved storage vessels

Table 9-1: Solvent purification and drying procedures

Solvent	Drying Agent	Distillation	Indicator / colour
Acetonitrile	CaH_2	Yes	none
Acetone	Drierite™	Yes	blue
Benzene-d_6	Na/K alloy	Vacuum transfer	none
Chloroform-*d*	CaH_2	Vacuum transfer	none
Dichloromethane	CaH_2	Yes	none
Diethylether	Na / tetraglyme	Yes	benzophenone / blue
Heptane	Na	Yes	none
Methanol	Mg turnings / I_2	Yes	none
Pentane	Na / tetraglyme	Yes	benzophenone / blue
Tetrahydrofuran (THF)	Na / tetraglyme	Yes	benzophenone / blue
Toluene	Na	Yes	none

With the exception of hexane and dichloromethane, the solvents used for work-up procedures and chromatography were of analytical grade and used without purification. Hexane and dichloromethane were obtained as chemically pure reagents and distilled in air prior to use.

Precious metals were obtained on loan from Johnson-Matthey. Other chemicals and reagents were obtained commercially (Aldrich, Merck etc) and used without purification, with the exceptions detailed in table 9-2. Air-sensitive chemicals and chemicals to be used in reactions with air-sensitive reagents were stored, after any necessary purification prodedure, in Teflon-valved storage vessels or the glovebox, as indicated in Table 9-2.

Table 9-2: Purification and storage of chemicals

Chemical / Reagent	Purification	Storage
n-BuLi (1.6M in hexanes)	None	Teflon-valved storage vessel
t-BuLi (1.7M in pentane)	None	Teflon-valved storage vessel
$HSiMe_2Ph$	None	Teflon-valved storage vessel
$HSiMe_2Cl$	vacuum transfer	Teflon-valved storage vessel
$HSiMeCl_2$	vacuum transfer	Teflon-valved storage vessel
$HSiCl_3$	vacuum transfer	Teflon-valved storage vessel
$ClSiMe_2CH_2Cl$	vacuum transfer	Teflon-valved storage vessel
Methylaluminoxane (MAO) (10% weight in toluene)	None	Teflon-valved storage vessel
Allyl bromide	distillation from CaH_2	Teflon-valved storage vessel
4-bromo-1-butene	distillation from CaH_2	Teflon-valved storage vessel
Tetramethylethylenediamine	Distillation from Na	Teflon-valved storage vessel
$Me_3NO.2H_2O$	stripped with dry THF, dried under high vacuum and sublimed at 60°C	Glovebox
CPh_3PF_6	None	Glovebox
$B(C_6F_5)_3$	None	Glovebox
PPh_3	recrystallised from hot hexane	dessicator
2,2'-bipyridyl	recrystallised from hot hexane	dessicator
p-cresol	recrystallised from hot hexane	dessicator

Instrumentation

Melting points were recorded on Kofler hotstage microscope (Reichert Thermovar) and are uncorrected. Microanalysis data were obtained from the University of Cape Town Microanalytical Laboratory. Infrared

spectra were recorded on a Perkin-Elmer 983 spectrometer in solution with NaCl windows, or as nujol mulls or neat thin films between NaCl plates. NMR spectra were recorded on a Varian Unity-400 spectrometer (^{1}H, ^{13}C, ^{29}Si) or a Varian Mercury-300 spectrometer (^{1}H, ^{13}C, ^{31}P), and some ^{1}H NMR spectra were recorded on a Varian VXR 200 spectrometer. ^{1}H spectra were referenced internally using the residual protio impurities in the deuterated solvent and reported relative to tetramethylsilane. ^{13}C spectra were refernced internally using the solvent signals and reported relative to tetramethylsilane. ^{29}Si spectra were reference externally against tetramethylsilane ($\delta = 0.0$). ^{31}P NMR spectra were referenced externally against H_3PO_4. Mass spectrometry was carried out using electron ionisation (EI) or fast atom bombardment (FAB) by Dr Phillip Boshoff of the Cape Technikon, and the reported *m/z* value corresponds to the most abundant isotopes for each element (^{1}H, ^{12}C, ^{14}N, ^{28}Si, ^{31}P, ^{35}Cl, ^{56}Fe, ^{58}Ni, ^{79}Br, ^{106}Pd, ^{127}I, ^{192}Os). In each case the observed isotopic distribution corresponds to the theoretical distribution. The X-ray diffraction data were collected at room temperature on a Nonius Kappa CCD with 1.5kW graphite-monochromated Mo radiation. The GC analysis of ethene oligomers was carried out on an HP 5890 Series II Gas Chromatograph fitted with a 50m PONA (Crosslinked Methyl Siloxane) column with a film thickness of 0.5 mm. Flame ionisation detection (FID) was used.

9.2 Experimental details pertaining to Chapter 2

Synthesis of *cis*-$Os(CO)_4Me_2$ (1)

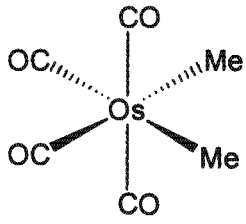

$Os(CO)_4Me_2$ was prepared by a modified literature procedure.[78] $Os_3(CO)_{12}$ (2.95g, 3.25mmol) was weighed out, and approximately three quarters was added to liquid ammonia (50ml). The mixture was stirred at –78°C. Sodium metal (c.a. 0.45g, 20mmol) was added in small pieces. After addition of each piece, the mixture was stirred until the blue colour disappeared, indicating consumption of the sodium. When a blue colour persisted, a further portion of $Os_3(CO)_{12}$ was added, and the process was repeated until all $Os_3(CO)_{12}$ was added. A small quantity of unreacted $Os_3(CO)_{12}$ remained. MeI (2.0ml, 32mmol) was added, and the mixture was stirred for 1 h. The mixture was then slowly warmed to room temperature, with the ammonia bubbling off through a mercury bubbler. After removal of residual volatiles under vacuum for 1 minute, **1** was recovered as a white powder by sublimation under high vacuum (<1mm) at 60°C onto a dry ice cooled cold finger. (2.353g, 7.081mmol, 73%); m.p. 63 – 64°C, lit. 65 – 66°C[78]; $\nu_{max}(CO)/cm^{-1}$ (hexane) 2130m , 2044vs, 2011s, 1979w ; δ_H(400 MHz; $CDCl_3$) 0.05 (6H, s, Os-*Me*). All spectroscopic data is in agreement with the literature.[78]

Synthesis of *fac*-$Os(CO)_3(NCMe)Me_2$ (2)

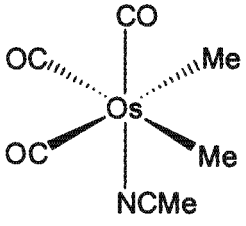

A stirred solution of **1** (316 mg, 0.951 mmol) in acetonitrile (5 ml) was treated with a slight excess of $Me_3NO.2H_2O$ (116 mg, 1.04 mmol) in acetonitrile (6 ml). The mixture was stirred at room temperature for 24 h, after which time the reaction was judged to be complete by IR spectroscopy and TLC (silica, 25% dichloromethane in hexane, R_f = 0.19). The solvents were removed under reduced pressure, and the crude residue was purified by column chromatography (silica gel, 25% dichloromethane in hexane). Upon removal of solvents *in vacuo*, the solid obtained was recrystallised from dichloromethane / hexane to give **2** as white microcrystals. (231 mg, 0.669 mmol, 70%), m.p. 104-107°C; (Found: C, 24.6; H, 2.5; N, 4.0. $C_7H_9NO_3Os$ requires C, 24.3; H, 2.6; N, 4.1%); $\nu_{max}(CO)/cm^{-1}$ (dichloromethane) 2072s, 1980vs; δ_H (400 MHz; $CDCl_3$) 2.45 (3H, s, -NC*Me*), 0.062 (6H, s, Os-*Me*); δ_H (200 MHz; C_6D_6) 0.59 (6H, s, Os-*Me*), 0.20 (3H, s, -NC*Me*); $\delta_{C\{H\}}$ (100 MHz; $CDCl_3$) 180.4 (*C*O), 175.9 (*C*O), 117.9 (Me*C*N) 3.5 (*Me*CN), -16.3 (Os-*Me*); $\delta_{C\{H\}}$ (75 MHz; C_6D_6) 181.1 (*C*O), 176.8 (*C*O), 118.6 (Me*C*N), 0.45 (*Me*CN), -15.4 (Os-*Me*); *m/z* (FAB) 347 (M^+, 26%), 332 (M^+ - Me, 61%), 319 (M^+ - CO, 43%), 304 (M^+ - CO – Me, 100%), 291 (M^+ - 2CO, 35%), 276 (M^+ - 2CO - Me, 30%)

Synthesis of *fac*-$Os(CO)_3(THF)Me_2$ (3)

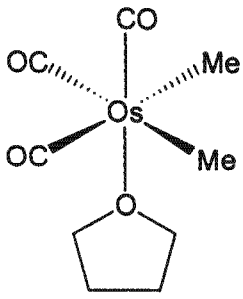

To a stirred solution of **1** (65mg, 0.20mmol) in THF (5ml) was added a solution of $Me_3NO.2H_2O$ (30mg, 0.27mmol) in THF (20ml). The reaction was monitored by IR spectroscopy. After stirring for 16h, the reaction was complete, and the reaction mixture was filtered through silica. Upon removal of the volatiles *in vacuo*, a clear oil was recovered, which decomposed after a short time (c.a. 2 minutes) under high vacuum. **3** was thus characterised by IR spectroscopy and by its analogous reactivity to the isolable compound **2** (see syntheses of **4** and **7** below). $\nu_{max}(CO)/cm^{-1}$ (THF) 2068s, 1969vs

Synthesis of *fac*-$Os(CO)_3(PPh_3)Me_2$ (4)

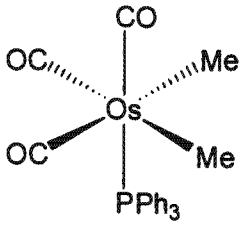

This compound has previously been prepared directly from **1**.[71]

1) Synthesis from 2

A mixture of **2** (152mg, 0.440mmol) and PPh_3 (118mg, 0.450mmol) in toluene (10ml) was stirred at 75°C. The reaction was monitored by infrared spectroscopy, and judged to be complete after 48h. The volatiles were removed *in vacuo*, and after column chromatography (silica, 20% dichloromethane in hexane, R_f = 0.28), **4** was recovered as a white crystalline solid. (192mg, 0.339mmol, 77%); m.p. 119-122°C, (Found: C, 48.8; H, 3.7. $C_{23}H_{21}O_3POs$ requires C, 48.8; H, 3.7); $\nu_{max}(CO)/cm^{-1}$ (toluene) 2068vs, 1994s, 1960s; δ_H (300 MHz; $CDCl_3$) 7.44 – 7.42 (15H, m, H_{aryl}), -0.22 (6H, d, ^3J(PH) 8Hz, Os-*Me*); $\delta_{C\{H\}}$ (75 MHz; $CDCl_3$) 178.8 (*CO trans* to Me), 177.1 (d, ^2J(PC) 9Hz, *CO trans* to PPh_3), 133.9 (d, ^3J(PC) 10Hz, $C_{3,5}$ [PPh_3]), 131.0 (d, ^1J(PC) 50Hz, C_1 [PPh_3]), 130.6 (d, ^4J(PC) 2Hz, C_4 [PPh_3]), 128.3 (d, ^3J(PC) 10Hz, $C_{2,6}$ [PPh_3]), -22.4 (d, ^2J(PC) 8 Hz, Os-*Me*); $\delta_{P\{H\}}$ (120 MHz; $CDCl_3$) 0.89; *m/z* (FAB) 553 (M^+ - Me, 7%), 537 (M^+ - 2Me - H, 100%), 509 (M^+ - 2Me - H - CO, 60%)

2) Synthesis from 3

A solution of **3** was prepared by treatment of **2** (50mg, 0.15mmol) with an excess of $Me_3NO.2H_2O$ in THF and filtration through silica after completion of the reaction. PPh_3 (40mg, 0.15mmol) was added, and the mixture was refluxed for 48h. The reaction was monitored by IR spectroscopy. After removal of the volatiles *in vacuo* and column chromatography (silica, 20% dichloromethane in hexane), a white crystalline solid was recovered and identified as **4** by IR and NMR spectroscopy. (59mg, 0.10mmol, 69%)

Synthesis of $Os(CO)_2(PPh_3)(NCMe)Me_2$ (5)

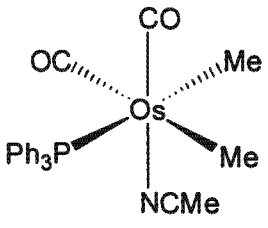

A stirred solution of **4** (100mg, 0.177 mmol) in acetonitrile (5 ml) was treated with $Me_3NO.2H_2O$ (76 mg, 0.68 mmol) in acetonitrile (2 ml), added in 0.5ml aliquots over 48h, after which the reaction was judged to be complete by IR spectroscopy and TLC. After removal of the volatiles *in vacuo* and column chromatography (silica, 40% dichloromethane in hexane, R_f = 0.24), **5** was obtained as a white crystalline material which decomposes in solution or upon standing in air. (69mg, 0.12mmol, 67%); m.p.

133-136°C; ν_{max}/cm^{-1} (dichloromethane) 1992s, 1921s; δ_H (300 MHz; C_6D_6); 7.68 – 6.95 (15H, m, H_{aryl}), 1.25 (3H, d, ^3J(PC) 4Hz, Os-*Me trans* to CO), 0.49 (3H, d, ^3J(PC) 8Hz, Os-*Me trans* to PPh_3), 0.26 (3H, d, ^4J(PC) 1.5Hz, -NC*Me*); $\delta_{P\{H\}}$ (120 MHz; C_6D_6) 9.38; *m/z* (FAB) 582 (M^+ + H, 3%), 542 (M^+ + 2H – MeCN, 11%), 526 (M^+ + H – MeCN – Me, 10%)

Synthesis of $Os(CO)_2(PPh_3)_2Me_2$ (6)

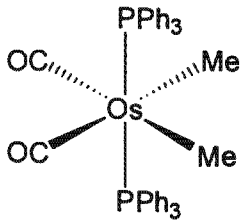

A stirred mixture of **4** (40mg, 0.071mmol) in acetonitrile (5ml) was treated with a solution of $Me_3NO.{}_2H_2O$ (22mg, 0.20mmol) in acetonitrile (5ml). The reaction was monitored by IR spectroscopy. After 16h, the formation of **5** in solution was judged to be complete, and the reaction mixture was filtered through silica to remove excess Me_3NO. The volatiles were removed in vacuo, leaving a solid white residue of crude **5**. PPh_3 (24mg, 0.92mmol) was added, and the solids were dissolved in toluene (10ml). The mixture was stirred and heated to 60°C. The reaction was monitored by IR spectroscopy. After 1h, the bands at 1993 and 1926cm-1 (**5**) were replaced by new bands at 2006 and 1915cm^{-1}, along with a minor band at 1985cm^{-1}. After 3h, bands at bands at 1985 and 1912cm^{-1} were dominant, with the band at 2006 still evident. After 16h, only bands at 1985 and 1911cm^{-1} were apparent. The volatiles were removed *in vacuo*, and after column chromatography (silica, 25% dichloromethane in hexane, R_f = 0.27) and recrystallisation (dichloromethane / hexane), **6** was obtained as a white crystalline solid. (34mg, 0.42mmol, 60%); m.p. 222 – 224°C; (Found: C, 60.2; H, 4.3. $C_{40}H_{36}O_2P_2Os$ requires C, 60.0; H, 4.5%); ν_{max}(CO)/cm^{-1} (dichloromethane) 1985s, 1909s; δ_H (400 MHz; $CDCl_3$) 7.56 – 7.34 (30H, m, H_{aryl}), -0.65 (6H, t, ^3J(PH) 8Hz, Os-*Me*); $\delta_{C\{H\}}$ (100 MHz; $CDCl_3$) 183.6 (t, ^2J(PC) 8Hz, *C*O), 134.2 (C_{aryl}), 132.8 (C_{aryl}), 129.8 (C_{aryl}), 127.8 (C_{aryl}), -13.8 (t, ^2J(PC) 8Hz, Os-*Me*); $\delta_{P\{H\}}$ (120 MHz; $CDCl_3$) 5.84 (s)

Attempted reaction of 6 with Me_3NO / MeCN

A suspension of **6** (24mg, 0.030mmol) in acetonitrile (10ml) was treated with a solution of $Me_3NO.2H_2O$ (15mg, 0.13mmol) in acetonitrile (4ml). IR analysis indicated that the $Os(CO)_2(PPh_3)_2Me_2$ was sparingly soluble in acetonitrile (ν_{max}/cm^{-1} 1982, 1909). The mixture was heated for 40h at 50°C, and then refluxed for an additional 72h. The reaction was monitored by IR spectroscopy. There was no indication of any reaction products, and **6** remained present in the mixture.

Synthesis of $Os(CO)_2$(2,2'-bipy)(COMe)Me (7)

1) Synthesis from 2

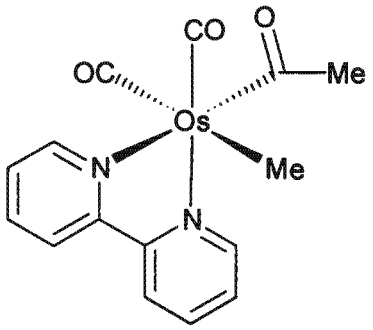

A stirred mixture of **2** (52mg, 0.15mmol) and 2,2'-bipyridyl (27mg, 0.17mmol) in toluene (5ml) was heated to 50°C for 5 days. A bright orange colour developed in the solution, and the reaction was monitored by IR spectroscopy. The volatiles were removed *in vacuo*, and after purification by preparative TLC (alumina, ethyl acetate, $R_f = 0.56$), **7** was obtained as an orange crystalline solid. (61mg, 0.13mmol, 87%); m.p. 169-172°C; (Found: C, 39.0; H, 3.0; N, 6.1. $C_{15}H_{14}N_2O_3Os$ requires C, 39.1; H, 3.1; N, 6.1%); ν_{max}/cm^{-1} (toluene) 1992s (CO), 1916s (CO), 1584w (COMe); δ_H (300 MHz; C_6D_6) 10.34 (1H, m, bipy), 8.61 (1H, m, bipy), 7.06 (2H, m, bipy), 6.87 (2H, m, bipy), 6.58 (1H, m, bipy), 6.27 (1H, m, bipy), 3.15 (3H, s, -CO*Me*), -0.01 (3H, s, Os-*Me*); $\delta_{C\{H\}}$ (75 MHz; $CDCl_3$) 190.5 (*C*OMe), 188.8 (*C*O), 181.7 (*C*O), 155.7 (1-C_{bipy}), 154.9 (1'-C_{bipy}), 153.7 (3-C_{bipy}), 153.4 (3'-C_{bipy}), 137.8 (5-C_{bipy}), 137.2 (5'-C_{bipy}), 126.0 (C_{bipy}), 125.8 (C_{bipy}), 122.6 (C_{bipy}), 122.3 (C_{bipy}), 53.9 (CO*Me*), 1.9 (Os-*Me*); ***m/z*** (EI) 907 ($2M^+$ - Me, 10%), 879 ($2M^+$ - Me - CO, 7%), 461 (M^+ - H, 3%) 447 (M^+ - Me, 40%), 419 (M^+ - Me - CO, 100%), 391 (M^+ - Me – 2CO, 27%)

2) Synthesis from 3

A solution of **3** was prepared by treatment of **1** (50mg, 0.15mmol) with excess $Me_3NO.2H_2O$ in THF and filtration through silica after completion of the reaction. 2,2'-bipyridyl (24mg, 0.15mmol) was added, and the mixture was refluxed for 48h. A dark orange colour formed in solution. The reaction was monitored by IR spectroscopy. After removal of the volatiles *in vacuo* and purification by preparative TLC (alumina, dichloromethane) an orange crystalline solid was recovered and identified as **7** by comparison of its IR and NMR spectra with those of an authentic sample. (44mg, 0.096mmol, 64%)

Synthesis of $Os(CO)_2$(dppm)(COMe)Me (8)

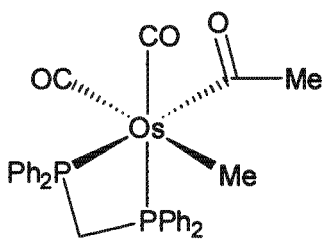

A stirred mixture of **2** (39mg, 0.11mmol) and dppm (43mg, 0.11mmol) in toluene (5ml) was heated to 70°C. The reaction was monitored by IR spectroscopy, and was judged to be complete after 3 days. The volatiles were removed *in vacuo*, and after recrystallisation from dichloromethane/hexane, **8** was obtained as an white crystalline solid. (71mg, 0.10mmol, 91%); m.p. 186-189°C; (Found C, 52.6; H, 3.8. $C_{30}H_{28}P_2O_3Os$ requires C, 52.3; H, 4.1%); ν_{max}/cm^{-1} (dichloromethane) 2003s (CO), 1939s (CO), 1588w (COMe); δ_H (300 MHz; $CDCl_3$) 7.81 – 7.31 (20H, m, H_{aryl}), 4.7 (2H, m, PCH_2P), 2.58 (3H, s, CO*Me*), -0.15 (3H, t, ^3J(PH) 20 Hz, Os-*Me*); $\delta_{C\{H\}}$ (75 MHz; $CDCl_3$) 186.9 (*C*O), 185.6 (d, ^2J(PC) 7Hz, *C*O), 182.9 (d, ^2J(PC) 8Hz, *C*OMe), 135.7 – 127.9, C_{aryl}), 52.9 (d, ^3J(PC) 19Hz, -CO*Me*), 43.3 (dd, ^1J(PC) 29 Hz, ^1J(PC) 24Hz, PCH_2P), -20.6 (dd, ^2J(PC) 9 Hz, ^2J(PC) 6 Hz, Os-*Me*); $\delta_{P\{H\}}$ (75 MHz; $CDCl_3$) -48.2 (d, ^2J(PP) 10Hz), -54.3 (d, ^2J(PP) 10Hz)

Synthesis of $Os(CO)_2(dppe)(COMe)Me$ (9)

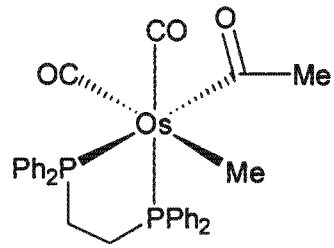

A stirred mixture of $Os(CO)_3(NCMe)Me_2$ (71mg, 0.21mmol) and dppe (83mg, 0.21mmol) in toluene (5ml) was heated to 70°C. The reaction was monitored by IR spectroscopy, and was judged to be complete after 3 days. The volatiles were removed *in vacuo*, and after recrystallisation from dichloromethane/hexane, **9** was obtained as an white crystalline solid. (118mg, 0.168mmol, 81%); m.p. 184-187°C; (Found: C, 53.2; H, 4.0. $C_{31}H_{30}O_3P_2Os$ requires C, 53.0; H, 4.3), ν_{max}/cm^{-1} (dichloromethane) 2005s (CO), 1940s (CO), 1588w (COMe); δ_H (300 MHz; $CDCl_3$) 7.94 – 7.31 (20H, m, H_{aryl}), 2.78 (2H, m, PCH_2CH_2P), 2.49 (3H, s, CO*Me*), 2.41 (2H, m, PCH_2CH_2P), -0.65 (3H, dd, ^3J(PH) 9Hz, ^3J(PH) 9Hz, Os-*Me*) ; $\delta_{C\{H\}}$ (75 MHz; $CDCl_3$); 186.8 (dd, $^2J_{trans}$(PC) 5Hz, $^2J_{cis}$(PC) 4Hz, *C*OMe), 185.6 (dd, $^2J_{trans}$(PC) 5Hz, $^2J_{cis}$(PC) 4Hz, *C*O trans to PPh_2), 181.8 (t, $^2J_{cis}$(PC) 4 Hz, *C*O trans to Me), 135.7 – 127.8 (C_{aryl}), 53.0 (d, $^3J_{trans}$(PC) 18Hz, CO*Me*), 28.2 (dd, ^1J(PC) 33Hz, ^2J(PC) 16Hz, PCH_2CH_2P), 27.5 (dd, ^1J(PC) 28Hz, ^2J(PC) 10 Hz, PCH_2CH_2P), -19.7 (dd, ^2J(PC) 14 Hz, ^2J(PC) 9Hz); *m/z* (FAB) 705 (M^+ + H, 5%), 689 (M^+ - Me, 69%)

Synthesis of $Os(CO)_2(dppp)Me_2$ (10)

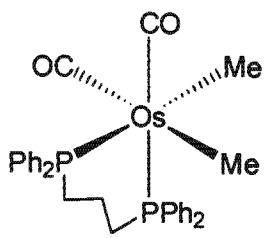

A stirred mixture of **2** (101mg, 0.292mmol) and dppp (121mg, 0.292mmol) in toluene (10ml) was heated to 70°C. The reaction was monitored by IR spectroscopy. After 16 h, $Os(CO)_3(NCMe)Me_2$ was consumed, and new bands at 2068, 1993 and 1960cm^{-1} indicatated formation of a new *fac*-tricarbonyl, presumed to be the pendant dppp intermediate, $Os(CO)_3(dppp)Me_2$, (c.f. **4**: 2068, 1994, 1960cm^{-1}). Simultaneously, new bands at 2013 and 1949cm^{-1} which grew in strength relative to the bands at 2068, 1994, 1960cm^{-1} indicated formation of a dicarbonyl species, presumably $Os(CO)_2(dppp)(COMe)Me$ (c.f. **9** 2002, 1942cm^{-1}). After 72 h the reaction was still incomplete, and the mixture was refluxed for 24h. Significant decomposition was observed, and IR spectroscopy indicated formation of a third product, a dicarbonyl species with bands at 2005 and 1930cm^{-1}, present in solution with both $Os(CO)_3(dppp)Me_2$ and $Os(CO)_2(dppp)(COMe)Me$. After additional reflux for 72h, the bands at 2005 and 1929cm^{-1} dominated. The volatiles were removed *in vacuo*, and the residue was taken up in dichloromethane and filtered through silica. After removal of the volatiles *in vacuo* and two recystallisations from dichloromethane/hexane, a white crystalline solid was recovered and identified as **10**. (55mg, 0.080mmol, 27%); m.p. 242-245°C; (Found: C, 54.2; H, 4.5. $C_{31}H_{32}O_2P_2Os$ requires C, 54.1; H, 4.7%); ν_{max}(CO)/cm^{-1} (dichloromethane) 2001s, 1924s; δ_H (300 MHz; $CDCl_3$) 7.52 – 7.20 (20H, m, H_{aryl}), 2.74 – 1.58 (6H, m, $PCH_2CH_2CH_2P$), -0.14 (3H, dd, $^3J_{cis}$(PC) 8Hz, $^3J_{cis}$(PC) 7Hz, Me *trans* to CO), -0.29 (3H, dd, $^3J_{trans}$(PC) 8Hz, $^3J_{cis}$(PC) 4Hz) Me *trans* to P); $\delta_{C\{H\}}$ (75 MHz; $CDCl_3$) 186.4 (t, ^2J(PP) 7Hz, *CO trans* to Me), 185.3 (m, *CO trans* to P), 136.9 – 127.5 (C_{aryl}), 24.3 (d, ^1J(PC) 26Hz, PCH_2-), 23.4 (dd, ^1J(PC) 30Hz, ^3J(PC) 4Hz, PCH_2-), 19.5 (m, $PCH_2CH_2CH_2P$), -20.1 (dd, $^2J_{cis}$(PC) 10Hz, $^2J_{cis}$(PC) 6Hz, Me *trans* to CO), -23.5 (dd, $^2J_{trans}$(PC) 42Hz, $^2J_{cis}$(PC) 8Hz, Me *trans* to P); $\delta_{P\{H\}}$ (120 MHz; $CDCl_3$) -16.7 (d,

^2J(PP) 24Hz), -24.1 (d, ^2J(PP) 24Hz); *m/z* (FAB) 689 (M^+ - H, 6%), 675 (M^+ - Me, 11%), 658 (M^+ - H - 2Me, 100%), 631 (M^+ - H - 2Me - CO, 34%)

Synthesis of $CH_2[CH_2PPh_2Os(CO)_3Me_2]_2$ (11)

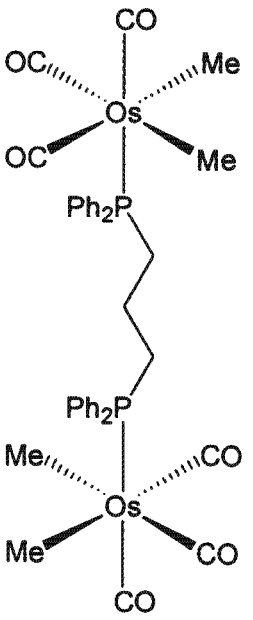

A stirred mixture of **2** (117mg, 0.339mmol) and dppm (68mg, 0.165mmol) in toluene (10ml) was heated to 70°C. A brown colour indicated some decomposition in solution. The reaction was monitored by infrared spectroscopy, and was judged complete after 72h. After removal of the volatiles *in vacuo*, and purification by column chromatography (silica, 25% dichloromethane in hexane, R_f = 0.30) and recrystallisation (dichloromethane / hexane), **11** was obtained as white crystals. (73mg, 0.071mmol, 43%); m.p. 205-208°C; (Found: C, 43.7; H, 3.6. $C_{37}H_{38}O_6P_2Os_2$ requires C, 43.5; H, 3.8%); ν_{max}(CO)/cm^{-1} (toluene) 2069vs, 1993s, 1961s; δ_H (300 MHz; $CDCl_3$) 7.38 – 7.27 (20H, m, H_{aryl}), 2.38 (4H, m, PCH_2CH$_2$CH_2P), 1.01 (2H, m, PCH$_2$CH_2CH$_2$P), -0.46 (12H, d, ^3J(PH) 8 Hz, Os-*Me*); $\delta_{P\{H\}}$ (120 MHz; $CDCl_3$) -7.8 (s); *m/z* (FAB) 1023 (M^+ + H, 20%)

Attempted synthesis of $[Os(CO)_3(NCMe)Me]PF_6$

1) Preparative scale

A solution of CPh_3PF_6 (52mg, 0.13mmol) in dichloromethane (5ml) was added dropwise over 3 hours to a stirred solution of **2** in dichloromethane (5ml). The reaction was monitored by IR spectroscopy (emergence of new peaks at 2114s, 2040s and 2013s cm^{-1} c.f. starting material peaks at 2072, 1981 cm^{-1}) and by the consumption of the orange CPh_3PF_6. Upon completion of the reaction after stirring for 16h, the volatiles were removed *in vacuo* and the residue was washed with pentane (2 x 10ml). ^{1}H NMR analysis indicated a complex array of peaks which could not be identified, suggesting decomposition of the product.

2) NMR observed reaction

To a sample of **2** (30mg, 0.087mmol) in $CDCl_3$ in a Teflon-valved NMR tube was added CPh_3PF_6 (excess). The course of the reaction was monitored by ^{1}H NMR. After 5 min, new peaks at δ_H = 2.65 (s, Os-NC*Me*), 2.19 (s, CPh_3*Me*[119]) and 0.61 (m, unknown) were apparent, along with peaks for unreacted **2**. Decomposition or other by-product peaks was also apparent. After 2h, the reaction was complete (disappearance of peaks from **2**). From the integration, one equivalent of CPh_3Me (δ_H = 2.19) is formed relative to starting **2** (by comparison with the integral of the aryl signals, which do not change during the reaction). However, the presence of significant impurities and the unexplained multiplet (δ_H = 0.61) means that no product can be identified.

Repetition using CD_2Cl_2 instead of $CDCl_3$ as solvent gave similar results.

Synthesis of *cis*-$[Os(CO)_4(NCMe)Me]PF_6$ (12)

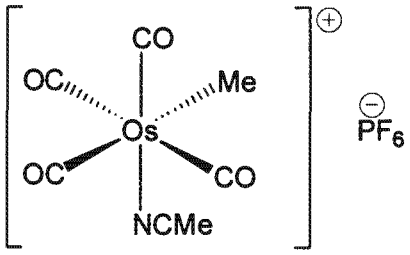

A stirred solution of $Os(CO)_3(NCMe)Me_2$ (28mg, 0.081mmol) in dichloromethane (10ml) was placed under an atmosphere of CO (1 *atm*). A solution of CPh_3PF_6 (31mg, 0.080mmol) in dichloromethane (3 ml) was added dropwise over 5 minutes. The reaction was monitored by IR spectroscopy and by visual observation of consumption of the orange CPh_3PF_6. After stirring for 16h under CO, the reaction was judged to be complete. The volatiles were removed *in vacuo* and the white residue was washed with pentane (3 x 5ml). After drying under high vacuum, a white residue was obtained and identified as impure **12**. (26mg, 0.052mmol, 44%); ν_{max}(CO)/cm^{-1} (CH_2Cl_2) 2113s, 2039vs, 2012vs, 1963w; δ_H (400 MHz; $CDCl_3$) 2.59 (3H, s, Os-NC*Me*), 0.62 (3H, s, Os-*Me*).

Synthesis of *fac*-$[Os(CO)_3(NCMe)_2Me]PF_6$ (13)

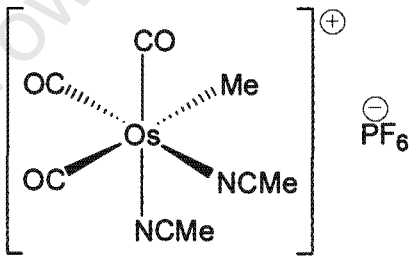

A solution of CPh_3PF_6 (46mg, 0.12mmol) in acetonitrile (5.5ml) was added dropwise over 4h to a stirred solution of $Os(CO)_3(NCMe)Me_2$ (41mg, 0.12mmol) in acetonitrile (5ml). The progress of the reaction was monitored by IR spectroscopy, and by visual observation of the consumption of the orange CPh_3PF_6. After additional stirring for 24h, the volatiles were removed *in vacuo* and the white residue was washed with pentane (3 x 10ml). IR analysis of the pentane washings indicated the presence of trace amounts of unreacted **2**. The remaining white residue was recrystallised from dichloromethane / hexane to give **13** as a white crystalline solid. (48mg, 0.093mmol, 78%); m.p.131-133°C; (Found: C, 18.9; H, 1.6; N, 5.3. $C_8H_9F_6N_2O_3POs$ requires C, 18.6; H, 1.8; N, 5.4%); ν_{max}(CO)/cm^{-1} (dichloromethane) 2123s, 2051vs, 2039vs; δ_H (400 MHz; CD_2Cl_2) 2.59 (6H, s, Os-NC*Me*), 0.52 (3H, s, Os-*Me*); $\delta_{C\{H\}}$ (100 MHz; CD_2Cl_2) 170.9 (*C*O trans to NCMe), 168.4 (*C*O trans to Me), 123.4 (Os-N*C*Me), 3.6 (Os-NC*Me*), -15.9 (Os-*Me*); *m/z* (FAB) 373 ($Os(CO)_3(NCMe)_2Me^+$, 100%), 345 ($Os(CO)_3(NCMe)_2Me^+$ - CO, 66%), 304 ($Os(CO)_3(NCMe)_2Me^+$ - CO - MeCN, 12%)

Attempted Synthesis of $[Os(CO)_3(NCMe)(CH_2{=}CH_2)Me]PF_6$

1) Preparative scale

A solution of **2** (68mg, 0.20mmol) in dichloromethane (5ml) in a thick-walled glass pressure tube was cooled to -78°C and degassed under vacuum three times, replacing the atmosphere with ethene each time. A solution of CPh_3PF_6 (75mg, 0.19mmol) in dichloromethane (5ml) was added against a flow of ethene and the vessel was sealed. The stirred mixture was warmed to room temperature, and the reaction was monitored by IR spectroscopy and by consumption of the yellow CPh_3PF_6. New bands at 2118, 2043 and 2022cm^{-1} formed after 2h, gradually replacing the starting material bands at 2072 and 1981 cm^{-1}. After 16h, consumption of the CPh_3PF_6 was indicated by a colourless solution. IR spectroscopy indicated minor bands

at 2114, 2040 and 2013cm^{-1} overlapping the previously observed bands at 2118, 2043 and 2022cm^{-1}. The volatiles were removed *in vacuo* and the oily residue was washed with pentane (6 x 10ml). The volatiles were removed from the pentane washings, and IR analysis (in dichloromethane) indicated that both excess starting material (2072 and 1981cm^{-1}) and unwanted decomposition product (2114, 2040 and 2013cm^{-1}) had been washed out. After drying the reaction product under high vacuum, a colourless oil was recovered. (85mg); ν_{max}(CO)/cm^{-1} (dichloromethane) 2118s, 2043vs, 2020vs.

NMR analysis indicated a complex array of signals which could not usefully be interpreted.

2) NMR observed reaction

A solution of **2** in dichloromethane (1ml) was transferred into a sealable NMR tube, and the dichloromethane was removed *in vacuo*. The tube was cooled to -78°C. A solution of CPh_3PF_6 (35mg, 0.090mmol) in CD_2Cl_2 (0.6ml) was added to the tube against a flow of argon. The mixture was degassed under vacuum three times, each time replacing the atmosphere with ethene (1atm). The mixture was warmed to 0°C under an atmosphere of ethene, and the tube was then sealed and warmed to room temperature. After twenty minutes a ^{1}H NMR spectrum was run. Consumption of **2** was complete (absence of singlets at 2.45 and 0.06ppm). A singlet at 2.17ppm indicated formation of CPh_3Me. A singlet at 5.40 indicated the presence of free ethene in solution. Complex arrays of peaks at 2.7 - 2.5 and 0.7 - 0.6ppm are respectively assigned to Os-NC*Me* and Os-*Me* signals of several different unknown species. A characteristic multiplet at 4.42ppm could perhaps be assigned as a coordinated ethene. The spectrum however is complex, and no osmium containing products can be clearly identified.

9.3 Experimental details pertaining to Chapter 3

Preparation of Karstedt catalyst solution[137]

A mixture of H_2PtCl_6 (100mg, 0.244mmol), 1,3-divinyltetramethyldisiloxane (1.2ml, 0.97g, 5.2mmol) and $NaHCO_3$ (120mg, 1.43mmol) in ethanol (2ml) was refluxed for 30 min. After cooling to room temperature, the mixture was additionally stirred for 12h. The volatiles were removed *in vacuo* and toluene (5.0ml) was added. After stirring, and then allowing the insoluble material to settle, the clear supernatant was transferred to a storage vial. The catalyst solution (1.1% Pt, theoretical) was used without characterisation in all hydrosilylation reactions in this thesis.

Synthesis of 3-trimethylsilylpropyldimethylphenylsilane (14)

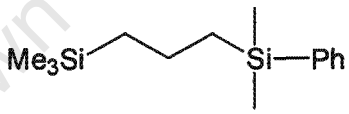

To a stirred mixture of $HSiMe_2Ph$ (465mg, 3.41mmol) and allyltrimethylsilane (475mg, 4.16mmol) was added Karstedt catalyst solution (0.1ml). After one second, a yellow colour formed and an exotherm was observed, and within a few seconds the solution went black. The mixture was additionally stirred for 3 h, taken up in hexane (10ml) and filtered through a short pad of silica. After removal of the volatiles *in vacuo*, **4** was obtained as a clear liquid (760mg, 3.07mmol, 90%); (Found: C, 67.2; H, 10.7 $C_{14}H_{26}Si_2$ requires C, 67.1; H 10.5%); ν_{max}/cm^{-1} (thin film) 3069m, 2954vs, 2912s, 1427s, 1257sh, 1248vs (Si-Me, sym def), 1113s (Si-Ph), 864m, 835m; δ_H(400 MHz; $CDCl_3$) 7.55 – 7.36 (m, 5H, *Ph*), 1.42 (m, 2H, $SiCH_2CH_2CH_2Si$), 0.85 (t ^3J(HH) 8Hz, 2H, $Me_3Si(CH_2)_2CH_2SiMe_2Ph$), 0.59 (t ^3J(HH) 8Hz, 2H, $Me_3SiCH_2(CH_2)_2SiMe_2Ph$), 0.28 (s, 6H, -Si$Me_2$Ph), 0.00 (s, 9H, -Si$Me_3$); $\delta_{C\{H\}}$(75 MHz; $CDCl_3$) 142.7 (*Ph*) 136.4 (*Ph*) 131.5 (*Ph*) 130.5 (*Ph*) 24.1 ($SiCH_2CH_2CH_2Si$) 23.0 ($Me_3Si(CH_2)_2CH_2SiMe_2Ph$) 21.3 ($Me_3SiCH_2(CH_2)_2SiMe_2Ph$) 1.3 (-Si$Me_2$Ph) -0.1 (-Si$Me_3$); *m/z* (EI) 249 ($M^+$ - H, 1%), 235 (M^+ - Me, 5%)

The platinum catalysed reaction of dimethylphenylsilane and allyl bromide: synthesis of bis(dimethylphenylsilyl)ether (15)

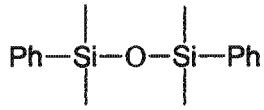

To a stirred mixture of $HSiMe_2Ph$ (711mg, 5.22mmol) and allyl bromide (725mg, 5.99mmol) was added Karstedt catalyst (0.2ml). The mixture was heated to 70°C for 48h. After removing the volatiles under high vacuum, the residual oil was subjected to column chromatography (silica, 10% CH_2Cl_2 in hexane). The solvents were removed *in vacuo* and the major product (R_f = 0.46) was obtained as a clear liquid and identified as **15**. (485mg, 1.69mmol, 65%) δ_H(200 MHz; $CDCl_3$) 7.7 – 7.3 (m, 10H, *Ph*) 0.38 (s, 12H, Si-*Me*); *m/z* (EI) 286 (M^+, 15%), 271 (M^+ - Me, 100%)

The platinum catalysed reaction of dimethylphenylsilane and allyl bromide in the presence of THF: synthesis of 4-bromobutyldimethylphenylsilyl ether (16)

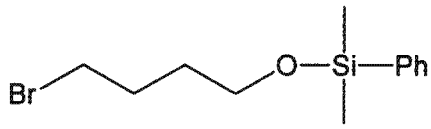

1) To a stirred mixture of $HSiMe_2Ph$ (776mg, 5.69mmol) and allyl bromide (877mg, 7.25mmol) in THF (5ml) was added Karstedt catalyst (0.2ml). The mixture was refluxed for 16h. The volatiles were removed *in vacuo* and the residue was taken up in hexane and filtered through silica. After removal of the hexane *in vacuo*, an impure clear oil was recovered, and identified by ^1H NMR and mass spectrometry to consist predominantly of **16**, with trace amounts of **15**. (1.44g, 5.01mmol, 88%)

2) In a separate experiment to obtain analytically pure **16**, the reaction was repeated and **16** was purified by column chromatography (silica, 10% dichloromethane in hexane, $R_f = 0.15$) in low yield (31%); Found: C, 49.8; H, 6.8. $C_{12}H_{19}BrOSi$ requires C, 50.2; H, 6.7%); ν_{max}/cm^{-1} (thin film) 3069m, 2959s, 2867m, 1590w, 1428s, 1389m, 1298w, 1251vs (Si-Me, sym def), 1116vs (Si-Ph), 1097vs; δ_H(400 MHz; C_6D_6) 7.51 – 7.18 (5H, m, *Ph*), 3.32 (2H, t, ^3J(HH) 6Hz, -C*H*$_2$Br), 2.91 (2H, t, ^3J(HH) 7Hz, -C*H*$_2$O-), 1.58 (2H, q, ^3J(HH) 7Hz, BrCH$_2$C*H*$_2$(CH$_2$)$_2$O-), 1.37 (2H, m, Br(CH$_2$)$_2$C*H*$_2$CH$_2$O-), 0.25 (s, 6H, Si*Me*$_2$Ph); $\delta_{C\{H\}}$ (100 MHz; C_6D_6) 138.1 (*Ph*), 133.6 (*Ph*), 129.7 (*Ph*), 128.0 (*Ph*), 61.8 (-*C*H$_2$O-), 33.3 (-*C*H$_2$Br), 31.1 (Br(CH$_2$)$_2$*C*H$_2$CH$_2$O-), 29.5 (BrCH$_2$*C*H$_2$(CH$_2$)$_2$O-), -1.9 (Si*Me*$_2$Ph); *m/z* (EI) 288 (M^+, 3%) 273 (M^+ - Me, 28%)

Synthesis of *n*-butyldimethylphenylsilane (17)

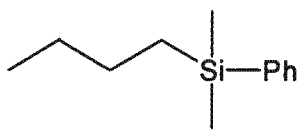

To a stirred mixture of $HSiMe_2Ph$ (350mg, 2.57mmol) and allyl bromide (341mg, 2.82mmol) in pentane (10ml) was added Karstedt catalyst (0.1ml). The mixture was refluxed for 16 h. After cooling to 0°C, a solution of *n*-BuLi in hexane (3.0ml, 1.6M, 4.8mmol) was added dropwise over 2 min. A white precipitate formed immediately. After stirring for 2h at room temperature, the reaction was quenched by the addition of water (20ml). The aqueous and organic phases were separated, and the aqueous phase was extracted with hexane (3 x 20ml). The combined organic fractions were washed with water (3 x 20ml) and brine (1 x 20ml), dried over Na_2SO_4 and filtered. After removal of the volatiles *in vacuo* and purification by column chromatography (silica, hexane, $R_f = 0.50$), **17** was recovered as a clear liquid. (274mg, 1.42mmol, 55%); (Found: C, 75.0; H, 10.6. $C_{12}H_{20}Si$ requires C, 74.9; H, 10.5%); ν_{max}/cm^{-1} (thin film) 3069m, 2956vs, 2921vs, 2872s, 1464m, 1427s, 1248vs (Si-Me, sym. def.), 1113vs (Si-Ph), 836vs; δ_H (300 MHz; $CDCl_3$) 7.55 – 7.36 (5H, m, Si-*Ph*), 1.35 (4H, m, SiCH$_2$C*H*$_2$C*H*$_2$CH$_3$), 0.90 (3H, t, ^3J(HH) 7Hz, Si(CH$_2$)$_3$C*H*$_3$), 0.79 (2H, m, SiC*H*$_2$(CH$_2$)$_2$CH$_3$), 0.28 (6H, s, Si-*Me*); $\delta_{C\{H\}}$ (75 MHz; $CDCl_3$) 139.8 (*Ph*), 133.6 (*Ph*), 128.7 (*Ph*), 127.7 (*Ph*), 26.5 (SiCH$_2$CH$_2$*C*H$_2$CH$_3$), 26.1 (SiCH$_2$*C*H$_2$CH$_2$CH$_3$), 15.4 (Si(CH$_2$)$_3$*C*H$_3$), 13.7 (Si*C*H$_2$(CH$_2$)$_2$CH$_3$), -3.0 (Si-*Me*)

Preparation and NMR-observed hydrolysis of bromodimethylphenylsilane

To a stirred mixture of $HSiMe_2Ph$ (524mg, 3.85mmol) and allyl bromide (740mg, 6.12mmol) in toluene (5ml) was added Karstedt catalyst (0.2ml). The mixture was heated to 65°C for 16h. The volatiles were then removed *in vacuo*, and an NMR sample of the residual liquid was prepared in a Teflon-valved NMR tube. The ^1H NMR spectrum indicated the presence of **$BrSiMe_2Ph$** [δ_H(200 MHz; C_6D_6) 7.7 – 7.1 (5H, m, -*Ph*) 0.56 (3H, s, Si-*Me*)]. A few drops of D_2O were added to the NMR tube, which was shaken. ^1H NMR indicated the gradual hydrolysis of $BrSiMe_2Ph$ to $(PhMe_2Si)_2O$ (singlet at 0.56ppm replaced by singlet at 0.33ppm after 45 min).

Synthesis of 4-bromobutyldimethylphenylsilane (18)

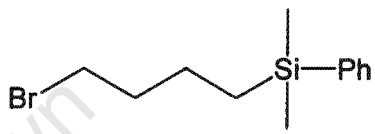

To a stirred mixture of $HSiMe_2Ph$ (441mg, 3.24mmol) and 4-bromo-1-butene (590mg, 4.37mmol) was added Karstedt catalyst (0.1ml). A yellow colour formed immediately, and after 10 min the catalyst decomposed, turning the mixture black. After an additional 4h stirring, the mixture was heated to 50°C and the volatiles were removed under high vacuum. The residue was taken up in hexane and filtered through silica. After removing the hexane *in vacuo*, **18** was recovered as a clear liquid. (827mg, 3.05mmol, 94%); (Found: C, 53.4; H, 7.0 .$C_{12}H_{19}BrSi$ requires C, 53.1; H, 7.1%); ν_{max}/cm^{-1} (thin film) 3068m, 3008m, 2956s, 1589w (Ph), 1487w, 1427s, 1270w, 1249vs (Si-Me, sym def), 1114s (Si-Ph); δ_H(400 MHz; $CDCl_3$) 7.52 – 7.34 (5H, m, Si-*Ph*), 3.39 (2H, t, ^3J(HH) 7Hz, -CH_2Br), 1.88 (2H, m, -CH_2CH_2Br), 1.48 (2H, m, -$CH_2(CH_2)_2$Br), 0.76 (2H, t, ^3J(HH) 8Hz, Si$CH_2(CH_2)_3$Br), 0.28 (6H, s, Si-*Me*); $\delta_{C\{H\}}$ (100 MHz; $CDCl_3$) 142.0 (*Ph*), 136.4 (*Ph*), 131.8 (*Ph*), 130.6 (*Ph*), 39.1 (-CH_2CH_2Br), 36.2 (-CH_2Br), 25.4 (-$CH_2(CH_2)_2$Br), 17.7 (Si$CH_2(CH_2)_3$Br), -0.2 (Si-*Me*); *m/z* (EI) 255 (M^+ - Me, 9%), 135 (M^+ - $(CH_2)_4$Br, 100%)

Synthesis of 4-bromobutyltrichlorosilane (19)

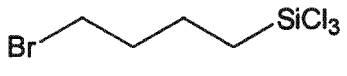

Trichlorosilane (9.0g, 66mmol) was condensed onto a mixture of 4-bromo-1-butene (7.18g, 53.2mmol) and Karstedt catalyst solution (0.2ml) in a thick-walled glass pressure tube. The vessel was sealed, and the stirred mixture was heated to 70°C for 16h. After cooling to room temperature, the volatiles were removed under high vacuum, leaving **19** as a liquid (13.8g, 51.0mmol, 96%); δ_H(300 MHz; C_6D_6) 2.73 (2H, t, ^3J(HH) 6Hz, -CH_2Br), 1.25 (4H, m, -$SiCH_2CH_2CH_2CH_2$Br, 0.69 (2H, t, ^3J(HH) 8Hz, Si$CH_2(CH_2)_3$Br); $\delta_{C\{H\}}$ (75 MHz; C_6D_6) 34.3 (-CH_2CH_2Br), 31.9 (-CH_2Br), 23.0 (-$CH_2(CH_2)_2$Br), 20.9 (Si$CH_2(CH_2)_3$Br)

Synthesis of 4-bromobutyltriallylsilane (20)

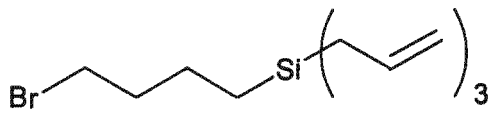

Pentane (10ml) was vacuum transferred onto **19** (1.513g, 5.594mmol). The stirred solution was cooled to 0°C, and an ether solution of allyl magnesium bromide (80ml, 0.25M, 20mmol) was added dropwise over 10 min. The mixture was

stirred at room temperature for 2 h, after which time the reaction was quenched by the addition of saturated aqueous NH_4Cl. The organic and aqueous phases were separated, and the aqueous phase was extracted with ether (3 x 30ml). The combined organic fractions were washed with water (3 x 30ml) and brine (1 x 30 ml). After drying over Na_2SO_4, filtration and removal of the volatiles *in vacuo*, a clear liquid was recovered. This was taken up in hexane and filtered through silica. After removal of the hexane *in vacuo*, **20** was recovered as a colourless liquid. (1.104g, 3.843mmol, 69%); ν_{max}/cm^{-1} (thin film) 3076s, 2995m, 2970s, 2917s, 1630vs (C=C stretch), 1453w, 1392m, 1271m, 991vs, 895vs; δ_H(400 MHz; $CDCl_3$) 5.78 (3H, m, -CH_2CH=CH_2), 4.90 (6H, m, -CH_2CH=CH_2), 3.41 (2H, t, ^3J(HH) 7Hz, -CH_2Br), 1.87 (2H, qn, ^3J(HH) 7Hz, -CH_2CH_2Br), 1.61 (6H, m, -CH_2CH=CH_2), 1.48 (2H, m, -$CH_2(CH_2)_2Br$), 0.59 (2H, m, $SiCH_2(CH_2)_3Br$); $\delta_{C\{H\}}$ (100 MHz; $CDCl_3$) 137.0 (-CH_2CH=CH_2), 116.6 (-CH_2CH=CH_2), 39.0 (-CH_2CH_2Br), 36.1 (-CH_2Br), 24.8 (-$CH_2(CH_2)_2Br$), 22.4 (-CH_2CH=CH_2), 13.4 ($SiCH_2(CH_2)_3Br$); *m/z* (EI) 247 (M^+ - allyl, 13%)

Synthesis of 21

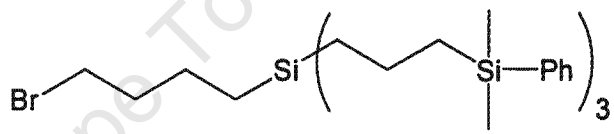

To a stirred mixture of 4-bromobutyltriallylsilane (829mg, 2.89mmol) and $HSiMe_2Ph$ (1.205g, 8.843mmol) was added Karstedt catalyst solution (0.2ml). A yellow colour formed immediately, and the mixture was heated to 90°C. After 15 minutes the solution had turned black as a result of catalyst decomposition. The excess $HSiMe_2Ph$ was removed *in vacuo* at 90°C. The residual oil was taken up in hexane and filtered through silica. After removal of the volatiles *in vacuo*, **21** was recovered as a clear oil. (1.732g, 2.488mmol, 86%); (Found: C, 64.1; H, 8.7. $C_{37}H_{59}BrSi_4$ requires C, 63.8; H, 8.5%); ν_{max}/cm^{-1} (thin film) 3068m, 2954s, 2913vs, 1588w, 1486w, 1449w, 1426s, 1269sh, 1247vs (Si-Me, sym def), 1113vs (Si-Ph), 837vs; δ_H(400 MHz; $CDCl_3$) 7.56 – 7.35 (15H, m, Si-*Ph*), 3.37 (2H, t, ^3J(HH) 7Hz, -CH_2Br), 1.80 (2H, qn, ^3J(HH) 7Hz, -CH_2CH_2Br), 1.33 (8H, m, -$CH_2(CH_2)_2Br$ and -$SiCH_2CH_2CH_2SiMe_2Ph$), 0.81 (6H, t, ^3J(HH) 8Hz, $SiCH_2CH_2CH_2SiMe_2Ph$), 0.54 (6H, t, ^3J(HH) 8Hz, $SiCH_2CH_2CH_2SiMe_2Ph$), 0.40 (2H, m, $SiCH_2(CH_2)_3Br$), 0.27 (18H, s, Si-*Me*); $\delta_{C\{H\}}$ (100 MHz; $CDCl_3$) 139.7 (*Ph*), 133.5 (*Ph*), 128.7 (*Ph*), 127.7 (*Ph*), 36.4 (-CH_2CH_2Br), 33.5 (-CH_2Br), 22.5 (-$CH_2(CH_2)_2Br$), 20.6 ($SiCH_2CH_2CH_2SiMe_2Ph$), 18.5 ($SiCH_2CH_2CH_2SiMe_2Ph$), 17.2 ($SiCH_2CH_2CH_2SiMe_2Ph$), -2.9 (Si-*Me*); $\delta_{Si\{H\}}$ (80 MHz; $CDCl_3$) 2.0 ($SiCH_2CH_2CH_2SiMe_2Ph$), -5.1 ($SiMe_2Ph$); *m/z* (EI) 517 (M^+ - $(CH_2)_3SiMe_2Ph$, 100%)

Synthesis of 22

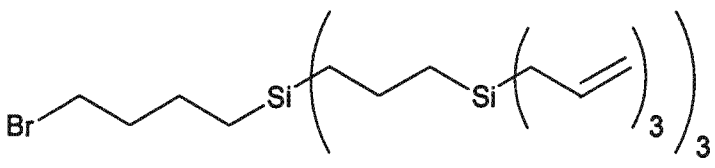

Trichlorosilane (1.3g, 9.6mmol) was condensed onto a mixture of **20** (200mg, 0.696mmol) and Karstedt catalyst solution (0.1ml) in a thick-walled glass pressure tube. The vessel was sealed, and the stirred mixture was heated to 90°C for 48h. After cooling to room temperature, the volatiles were removed *in vacuo*. The vessel was cooled to -10°C, and an ether solution of

allyl magnesium chloride (20ml, 0.41M, 8.2mmol) was added with stirring over 10 minutes. The mixture was stirred at room temperature for 16h, after which time the reaction was quenched by the addition of saturated aqueous NH_4Cl. The organic and aqueous phases were separated, and the aqueous phase was extracted with ether (3 x 20ml). The combined organic fractions were washed with water (3 x 20ml) and brine (1 x 20 ml). After drying over Na_2SO_4, filtration and removal of the volatiles *in vacuo*, a clear liquid was recovered. This was taken up in hexane and filtered through silica. After removal of the hexane *in vacuo*, **22** was recovered as a colourless liquid. (316mg, 0.425mmol, 61%); ν_{max}/cm^{-1} (hexane) 1630s (C=C stretch), 1159m, 1033m, 990m, 895m; δ_H (300 MHz; $CDCl_3$) 5.80 (9H, m, $-CH_2CH=CH_2$), 4.88 (18H, m, $-CH_2CH=CH_2$), 3.42 (2H, t, ^3J(HH) 7Hz, $-CH_2Br$), 1.87 (2H, qn, ^3J(HH) 7Hz, $-CH_2CH_2Br$), 1.61 (18H, m, $-CH_2CH=CH_2$), 1.46 – 1.35 (8H, m, $-CH_2(CH_2)_2Br$ and $SiCH_2CH_2CH_2Si(allyl)_3$), 0.67 (6H, m, $SiCH_2CH_2CH_2Si(allyl)_3$), 0.58 (6H, m, $SiCH_2CH_2CH_2Si(allyl)_3$) 0.50 (2H, m, $SiCH_2(CH_2)_3Br$); δ_C (100 MHz; $CDCl_3$) 134.6($-CH_2CH=CH_2$), 113.8 ($-CH_2CH=CH_2$), 36.6 ($-CH_2CH_2Br$), 33.6 ($-CH_2Br$), 22.7 ($-CH_2(CH_2)_2Br$), 20.0 ($-CH_2CH=CH_2$), 18.5, 17.7, 16.9, 11.8 ($SiCH_2(CH_2)_3Br$); $\delta_{Si\{H\}}$ (80 MHz; $CDCl_3$) 1.8 ($Si(CH_2)_4Br$), -1.6 ($Si(allyl)_3$)

Synthesis of 4-iodobutyldimethylphenylsilane (23)

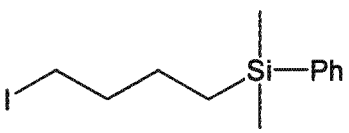

A solution of **18** (677mg, 2.50mmol) in acetone (25ml) was refluxed over KI (8.0g, 48mmol) for 16h. After removal of the volatiles *in vacuo*, the residue was partitioned between hexane (20ml) and water (20ml). The aqueous phase was extracted with hexane (3 x 10ml) and the combined organic fractions were washed with water (3 x 10ml) and brine (1 x 10ml). After drying over Na_2SO_4 and filtration, the volatiles were removed *in vacuo*. The clear liquid residue was taken up in hexane, filtered through silica, and the volatiles were again removed *in vacuo*, leaving **23** as a colourless liquid, which upon standing turns yellow as a result of liberated iodine. (680mg, 2.14mmol, 85%); ν_{max}/cm^{-1} (thin film) 3067m, 2953s, 2925s, 1588w, 1486w, 1426s, 1248vs (Si-Me, sym def), 1199m, 1113vs (Si-Ph); δ_H (400 MHz; $CDCl_3$) 7.56 – 7.36 (5H, m, Si-*Ph*), 3.18 (2H, t, ^3J(HH) 7Hz, $-CH_2I$), 1.84 (2H, qn, ^3J(HH) 7Hz, $-CH_2CH_2I$), 1.45 (2H, m, $-CH_2(CH_2)_2I$), 0.77 (2H, m, $SiCH_2(CH_2)_3I$), 0.29 (6H, s, Si-*Me*); $\delta_{C\{H\}}$ (100 MHz; $CDCl_3$) 139.1 (*Ph*), 133.5 (*Ph*), 128.9 (*Ph*), 127.8 (*Ph*), 36.9 ($-CH_2CH_2I$), 24.8 ($-CH_2(CH_2)_2I$), 14.6 ($SiCH_2(CH_2)_3I$), 6.6 ($-CH_2I$), -3.1 (Si-*Me*); $\delta_{Si\{H\}}$ (80 MHz; $CDCl_3$) -4.0; *m/z* (FAB) 319 (M^+ + H, 2%), 303 (M^+ - Me, 37%), 241 (M^+ - Ph, 36%), 135 (M^+ - $(CH_2)_4I$, 100%)

Synthesis of 24

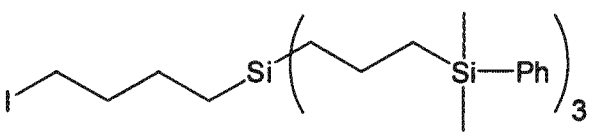

A solution of **21** (453mg, 1.44mmol) in acetone (40ml) was refluxed over KI (8.5g, 51mmol) for 48h. After removal of the volatiles *in vacuo*, the residue was partitioned between hexane (20ml) and water (20ml). The aqueous phase was extracted with hexane (3 x 10ml) and the combined organic fractions were washed with water (3 x 10ml) and brine (1 x 10ml). After drying over Na_2SO_4 and filtration, the volatiles were removed *in vacuo*. The clear liquid residue was taken

up in hexane, filtered through silica, and the volatiles were again removed *in vacuo*, leaving **24** as a clear liquid, which upon standing turns yellow as a result of liberated iodine. (813mg, 1.09mmol, 76%); ν_{max}/cm^{-1} (thin film) 3067w, 2950m, 2911w, 1589m (Ph), 1486w, 1407w), 1326m, 1248vs (Si-Me, sym def), 1197w, 1113s (Si-Ph); δ_H (400 MHz; $CDCl_3$) 7.53 – 7.35 (15H, m, Si-*Ph*), 3.15 (2H, t, ^3J(HH) 7Hz, -CH_2I), 1.76 (2H, qn, ^3J(HH) 7Hz, -CH_2CH$_2$I), 1.33 (8H, m, -CH_2(CH$_2$)$_2$I and -SiCH$_2$CH_2CH$_2$SiMe$_2$Ph), 0.82 (6H, t, ^3J(HH) 8Hz, SiCH$_2$CH$_2$CH_2SiMe$_2$Ph), 0.54 (6H, t, ^3J(HH) 8Hz, SiCH_2CH$_2$CH$_2$SiMe$_2$Ph), 0.39 (2H, m, SiCH_2(CH$_2$)$_3$I), 0.27 (18H, s, Si-*Me*); $\delta_{C\{H\}}$ (100 MHz; $CDCl_3$) 139.7 (*Ph*), 133.5 (*Ph*), 128.7 (*Ph*), 127.7 (*Ph*), 37.1 (-*C*H$_2$CH$_2$I), 24.8 (-*C*H$_2$(CH$_2$)$_2$I), 20.6 (-SiCH$_2$*C*H$_2$CH$_2$SiMe$_2$Ph), 18.5 (-SiCH$_2$CH$_2$*C*H$_2$SiMe$_2$Ph), 17.3 (-Si*C*H$_2$CH$_2$CH$_2$SiMe$_2$Ph), 11.4 (-Si*C*H$_2$CH$_2$(CH$_2$)$_2$I), 6.8 (-*C*H$_2$I) -2.8 (Si-*Me*); $\delta_{Si\{H\}}$ (80 MHz; $CDCl_3$) 1.9 (*Si*CH$_2$CH$_2$CH$_2$SiMe$_2$Ph); -5.1 (*Si*Me$_2$Ph)

Reaction of 4-bromobutyldimethylphenylsilane with *t*-BuLi

A stirred solution of 4-bromobutyldimethylphenylsilane (691mg, 2.55mmol) in ether (10ml) was cooled to -78°C. A solution of *t*-BuLi in pentane (5.0ml, 1.7M, 8.5mmol) was added, and after 2min $ClSiMe_3$ (2.0ml, 1.7g, 16mmol) was added. The mixture was stirred for 20min at -78°C, after which the volatiles were removed *in vacuo*. The residue was extracted with hexane, and filtered through silica. After removal of the volatiles *in vacuo*, a colourless liquid was recovered (936mg).

^{1}H NMR analysis indicated a complex array of peaks, including: δ_H (400 MHz. $CDCl_3$) 7.55 – 7.35 (m, Si-*Ph*), 1.36 (m, -CH$_2$CH_2CH$_2$-), 0.88 (s, -C*Me*$_3$), 0.28 (s, -Si*Me*$_2$Ph), 0.09 (s, -Si*Me*$_3$) , 0.06 (s, -Si*Me*$_3$), 0.01 (s, -Si*Me*$_3$), -0.02 (s, -Si*Me*$_3$)

Synthesis of 4-bromobutylchlorodimethylsilane (25)

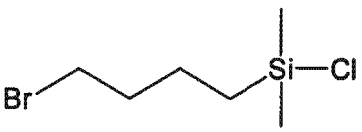

This compound was prepared by a modified literature procedure.[166] $HSiMe_2Cl$ (8.85g, 93.6mmol) was vacuum transferred onto 4-bromo-1-butene (7.57g, 56.1mmol) in a thick-walled glass pressure tube. Karstedt catalyst solution (0.3ml) was added, and the vessel was cooled to –196°C, evacuated and sealed. After warming to room temperature, the stirred mixture was heated to 85°C for 48h. A yellow colour appeared after 10min. The mixture was cooled to 0°C and the volatiles were removed under high vacuum, leaving **25** as a clear liquid. (12.6g, 53.9mmol, 96%); δ_H (300 MHz; C_6D_6) 2.92 (2H. t, ^3J(HH) 7Hz, -CH_2Br), 1.47 (2H, qn, ^3J(HH) 7Hz, -CH_2CH$_2$Br), 1.25 (2H, m, -CH_2(CH$_2$)$_2$Br), 0.41 (2H, t, ^3J(HH) 8Hz, ClSiMe$_2$CH_2(CH$_2$)$_3$Br), 0.16 (6H, s, Si-*Me*); $\delta_{C\{H\}}$ (75 MHz; C_6D_6) 35.7 (-*C*H$_2$CH$_2$Br), 32.8 (-*C*H$_2$Br), 21.7 (-*C*H$_2$(CH$_2$)$_2$Br), 17.9 (ClSiMe$_2$*C*H$_2$(CH$_2$)$_3$Br), 1.4 (Si-*Me*)

Synthesis of 4-bromobutyldimethylsilane (26)

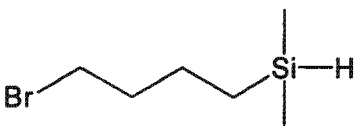

This compound was prepared by a modified literature procedure.[166] **25** (3.788g, 16.49mmol) in pentane (7ml) was added dropwise to a stirred suspension of $LiAlH_4$ (576mg, 15.2mmol) in diethylether (30ml). The mixture was refluxed for 16h. After removing most of the ether and pentane *in vacuo*, the remaining

volatiles were then vacuum distilled into a trap at –196°C, heating the residues to 100°C to volatilise all of the product. After removal of residual ether and pentane under high vacuum, **26** was recovered as a clear liquid which hydrolyses upon standing in air. (2.658g, 13.62mmol, 83%); ν_{max}/cm^{-1} (thin film) 2959s, 2930s, 2112vs (Si-H), 1454w, 1429w, 1250s (Si-Me, sym def), 1220m, 954m, 888s, 836m; δ_H (400 MHz; $CDCl_3$) 3.86 (1H, n, ^3J(HH) 3.5Hz, Si-*H*), 3.42 (2H, t, ^3J(HH) 7Hz, -CH_2Br), 1.89 (2H, qn, ^3J(HH) 7Hz, -CH_2CH$_2$Br), 1.51 (2H, m, -CH_2(CH$_2$)$_2$Br), 0.60 (2H, m, HSiMe$_2$CH_2(CH$_2$)$_3$Br), 0.08 (6H, d, ^3J(HH) 4Hz, Si-*Me*); $\delta_{C\{H\}}$ (75 MHz; C_6D_6) 36.1 (-*C*H$_2$CH$_2$Br), 33.1 (-*C*H$_2$Br), 23.1 (-*C*H$_2$(CH$_2$)$_2$Br), 13.3 (HSiMe$_2$*C*H$_2$(CH$_2$)$_3$Br), -4.6 (Si-*Me*). Spectroscopic data is in agreement with the literature.[166]

Synthesis of 27

To a stirred mixture of tetraallylsilane (206mg, 1.07mmol) and **26** (941mg, 4.82mmol) was added Karstedt catalyst solution (30µl). A yellow colour developed immediately, and the mixture was heated to 150°C for 16h. After removing excess 4-bromobutyldimethylphenylsilane at 120°C *in vacuo*, the residue was taken up in hexane and filtered through silica. The hexane was removed *in vacuo* and **27** was recovered as a viscous colourless oil. (930mg, 0.956mmol, 89%); ν_{max}/cm^{-1} (thin film) 2912vs, 1412m, 1270s, 1247s (Si-Me, sym def), 1142m, 836vs; δ_H (400 MHz; $CDCl_3$) 3.41 (8H, t, ^3J(HH) 7Hz, -CH_2Br), 1.87 (8H, qn, ^3J(HH) 7Hz, -CH_2CH$_2$Br), 1.45 (8H, m, -CH_2(CH$_2$)$_2$Br), 1.32 (8H, m, Si[CH$_2$CH_2CH$_2$SiMe$_2$-]$_4$), 0.56 (16H, m, -SiCH_2(CH$_2$)$_3$Br and Si[CH$_2$CH$_2$CH_2SiMe$_2$-]$_4$), 0.49 (8H, m, Si[CH_2CH$_2$CH$_2$SiMe$_2$-]$_4$), -0.03 (24H, s, Si-*Me*); $\delta_{C\{H\}}$ (100 MHz; $CDCl_3$) 36.3 (-*C*H$_2$CH$_2$Br), 33.5 (-*C*H$_2$Br), 22.5 (-*C*H$_2$(CH$_2$)$_2$Br), 20.1 (-*C*H$_2$-), 18.5 (-*C*H$_2$-), 17.5 (-*C*H$_2$-), 14.4 (-*C*H$_2$-), -3.4 (Si-*Me*); $\delta_{Si\{H\}}$ (80 MHz; $CDCl_3$) 2.3 (-*Si*(CH$_2$)$_4$Br), 0.8 (*Si*[(CH$_2$)$_3$SiMe$_2$-]$_4$); *m/z* (FAB) disintegration under all ionisation conditions occurs, and no identifiable fragments are apparent.

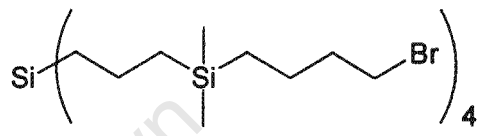

Synthesis of 28

To a stirred mixture of generation 2 allyl terminated dendrimer[140] (270mg, 0.337mmol) and **26** (960mg, 4.92mmol) at 0°C was added Karstedt catalyst solution (50µl). A yellow colour developed after 2min, and the mixture was heated to 120°C for 16h. After removing excess **26** at 120°C under high vacuum and purification by column chromatography (silica, hexane increasing polarity to 30% dichloromethane in hexane, R_f = 0.33 [30% dichloromethane in hexane]), **28** was recovered as a viscous colourless oil. (908mg, 0.289mmol, 86%); ν_{max}/cm^{-1} (thin film) 2952s, 2912vs, 2872m, 1449m, 1411s, 1331m, 1271m, 1247s (Si-Me, sym def), 1143s, 1023m, 950m, 910s, 837vs; δ_H (400 MHz; $CDCl_3$) 3.42 (24H, t, ^3J(HH) 7Hz, -CH_2Br), 1.87 (24H, qn, ^3J(HH) 7Hz, -CH_2CH$_2$Br), 1.45 (24H, m, -CH_2(CH$_2$)$_2$Br), 1.32 (32H, m, Si[CH$_2$CH_2CH$_2$Si[CH$_2$CH_2CH$_2$SiMe$_2$-]$_3$]$_4$), 0.56 (64H, m, -SiCH_2(CH$_2$)$_3$Br and Si[CH_2CH$_2$CH_2Si[CH$_2$CH$_2$CH_2SiMe$_2$-]$_3$]$_4$, 0.50 (24H, m, Si[(CH$_2$)$_3$Si[CH_2CH$_2$CH$_2$SiMe$_2$-]$_3$)]$_4$, -0.02 (72H, s, -Si*Me*$_2$-); $\delta_{C\{H\}}$ (100 MHz; $CDCl_3$) 36.5 (-*C*H$_2$CH$_2$Br),

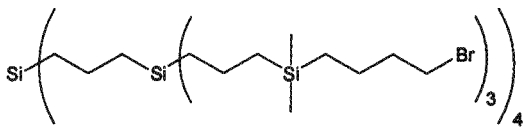

33.6 (-CH_2Br), 22.7 (-$CH_2(CH_2)_2$Br), 20.4 (-CH_2- x 12), 18.8 (-CH_2- x 4), 18.7 (-CH_2- x 12), 18.3 (-CH_2- x 4), 18.0 (-CH_2- x 4), 17.7 (-CH_2- x 12), 14.7 (-CH_2- x 12), -3.1 (-SiMe_2-); $\delta_{Si\{H\}}$ (80 MHz; $CDCl_3$) 2.3 (-$Si(CH_2)_4$Br), 0.7 ($Si[(CH_2)_3Si[(CH_2)_3SiMe_2\text{-}]_3]_4$, coincidental overlap).

Synthesis of 29

To a stirred mixture of generation 3 allyl terminated dendrimer[140] (297mg, 0.113mmol) and **26** (957mg, 4.90mmol) was added Karstedt catalyst solution (50μl). A yellow colour developed after 1min, and the mixture was heated to 120°C for 16h. After removing excess **26** at 100°C under high vacuum, the residual oil was taken up in hexane and filtered through silica. The hexane was removed *in vacuo* and **29** was recovered as a viscous colourless oil. (805mg, 0.0834mmol, 74%); ν_{max}/cm^{-1} (thin film) 3004w, 2951s, 2912vs, 2872s, 2973w, 1449m, 1412s, 1339m, 1269m, 1247vs (Si-Me sym def), 1219m, 1143vs, 1022m, 949m, 909s, 836vs; δ_H (400 MHz, $CDCl_3$) 3.40 (72H, t, ^3J(HH) 7Hz, -CH_2Br), 1.87 (72H, qn, ^3J(HH) 7Hz, -CH_2CH_2Br), 1.45 (72H, m, -$CH_2(CH_2)_3$Br), 1.33 (104H, m, $Si[CH_2CH_2CH_2Si[CH_2CH_2CH_2Si[CH_2CH_2CH_2SiMe_2\text{-}]_3]_3]_4$, 0.59 (208H, m, -Si$CH_2(CH_2)_3$Br and $Si[CH_2CH_2CH_2Si[CH_2CH_2CH_2Si[CH_2CH_2CH_2SiMe_2\text{-}]_3]_3]_4$, 0.50 (72H, m, $Si[(CH_2)_3Si[(CH_2)_3Si[CH_2CH_2CH_2SiMe_2\text{-}]_3]_3]_4$), -0.02 (216H, s, -Si$Me_2$-); $\delta_{C\{H\}}$ (100 MHz, $CDCl_3$) 36.5 (-CH_2CH_2Br), 33.5 (-CH_2Br), 22.7 (-$CH_2(CH_2)_2$Br), 20.5 (-CH_2- x 36), 18.9 (-CH_2- x 12), 18.8 (-CH_2- x 36), 18.6 (-CH_2- x 12), 18.1 (-CH_2- x 12), 17.7 (-CH_2- x 36), 14.7 (-CH_2- x 36), -3.0 (-SiMe_2-). The innermost –CH_2- are not seen as their intensities are too low; $\delta_{Si\{H\}}$ (80 MHz, $CDCl_3$) 2.3 (-$Si(CH_2)_4$Br), 0.7 $Si[(CH_2)_3Si[(CH_2)_3Si[(CH_2)_3SiMe_2\text{-}]_3]_3]_4$, coincidental overlap).

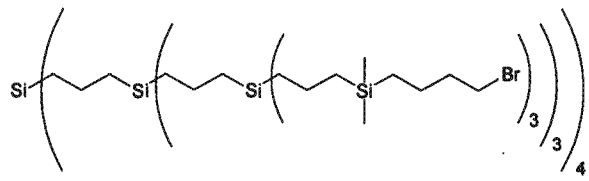

Synthesis of 30

A mixture of **27** (210mg, 0.216mmol) and sodium iodide (4.9g, 33mmol) in acetone (15ml) was refluxed for 20h. After removal of the acetone *in vacuo*, the residue was partitioned between hexane (20ml) and water (20 ml). The aqueous phase was extracted with hexane (3 x 20ml), and the combined organic fractions were washed with water (3 x 20ml). After drying over Na_2SO_4, filtration and removal of the volatiles *in vacuo*, the residue was taken up in hexane and filtered through silica. Upon removal of the solvents *in vacuo*, **30** was recovered as a viscous clear oil. (186mg, 0.160mmol, 74%); ν_{max}/cm^{-1} (dichloromethane) 2914vs, 2875s, 1430w, 1244s (Si-Me, sym def), 1202m; δ_H (400 MHz; $CDCl_3$) 3.20 (8H, t, ^3J(HH) 7Hz, -CH_2I), 1.83 (8H, qn, ^3J(HH) 8Hz, -CH_2CH_2I), 1.40 (8H, m, -$CH_2(CH_2)_2$I), 1.31 (8H, m, $Si[CH_2CH_2CH_2SiMe_2\text{-}]_4$), 0.57 (16H, m, Si$CH_2(CH_2)_3$I and $Si[CH_2CH_2CH_2SiMe_2\text{-}]_4$), 0.48 (8H, m, $Si[CH_2CH_2CH_2SiMe_2\text{-}]_4$), -0.03 (24H, s, Si-*Me*); $\delta_{C\{H\}}$ (100 MHz; $CDCl_3$) 37.0 (-CH_2CH_2I), 24.8 (-$CH_2(CH_2)_2$I), 20.2 (-CH_2-), 18.5 (-CH_2-), 17.5 (-CH_2-), 14.2 (-CH_2-), 6.8 (-CH_2I), -3.3 (Si-*Me*); $\delta_{Si\{H\}}$ (80 MHz; $CDCl_3$) 2.3 (-$Si(CH_2)_4$I), 0.8 ($Si(CH_2)_3SiMe_2$-)

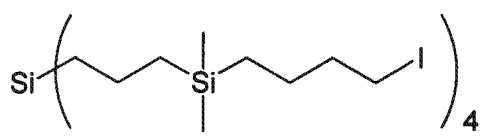

Synthesis of 31

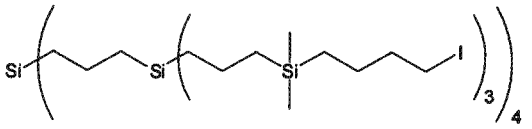

A mixture of **28** (113mg, 0.0359mmol) and potassium iodide (13.0g, 78.3mmol) in acetone (30ml) was refluxed for 48h. After removal of the acetone *in vacuo*, the residue was partitioned between hexane (20ml) and water (20 ml). The aqueous phase was extracted with hexane (3 x 20ml), and the combined organic fractions were washed with water (3 x 20ml). After drying over Na_2SO_4, filtration and removal of the volatiles *in vacuo*, **31** was recovered as a viscous clear oil. (115mg, 0.0310mmol, 86%); ν_{max}/cm^{-1} (thin film) 3003w, 2951s, 2910vs, 2872s, 2793m, 1447m, 1412s, 1334m, 1246vs (Si-Me, sym def), 1200s, 1142s, 1082w, 1021m, 946s, 835m; δ_H (400 MHz; $CDCl_3$) 3.19 (24 H, t, ^3J(HH) 7Hz, -CH_2I), 1.83 (24H, qn, ^3J(HH) 7Hz, -CH_2CH_2I), 1.40 (24H, m, -CH_2(CH_2)$_2$I), 1.32 (32H, m, SiCH$_2$CH_2CH$_2$Si[CH$_2$CH_2CH$_2$SiMe$_2$-]$_3$]$_4$), 0.57 (64H, m, -SiCH_2(CH$_2$)$_3$I and Si[CH_2CH$_2$CH_2Si[CH$_2$CH$_2$CH_2SiMe$_2$-]$_3$]$_4$, 0.48 (24H, m, Si(CH$_2$)$_3$Si[CH_2CH$_2$CH$_2$SiMe$_2$-]$_3$), -0.02 (72H, s, -SiMe_2-); $\delta_{C\{H\}}$ (100 MHz; $CDCl_3$) 37.2 (-CH$_2$CH$_2$I), 25.0 (-CH$_2$(CH$_2$)$_3$I), 20.4 (-CH$_2$- x 12), 18.8 (-CH$_2$- x 4), 18.7 (-CH$_2$- x 12), 18.3 (-CH$_2$- x 4), 18.1 (-CH$_2$- x 4), 17.7 (-CH$_2$- x 12), 14.4 (-CH$_2$- x 12), 6.9 (-CH$_2$I), -3.0 (-SiMe_2-)

Synthesis of 32

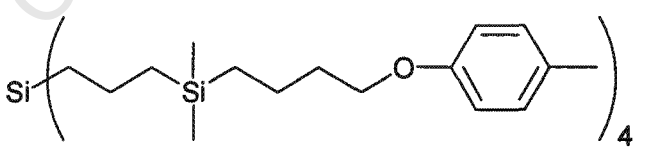

A mixture of **27** (509mg, 0.523mmol), *p*-cresol (265mg, 2.45mmol), K_2CO_3 (424mg, 3.07mmol) and 18-crown-6 (41mg, 0.16mmol) in acetone (20ml) was refluxed for 72h. After removal of the volatiles *in vacuo*, the residue was partitioned between dichloromethane (20ml) and water (20ml). The aqueous phase was extracted with dichloromethane (3 x 20ml), and the combined organic fractions were washed with water (3 x 20ml) and brine (1 x 20ml). After drying over Na_2SO_4, filtration and removal of the volatiles *in vacuo*, the residue was purified by column chromatography (silica, 25% dichloromethane in hexane increasing polarity to 50% dichloromethane in hexane, R_f = 0.09 [25% dichloromethane in hexane]) to give **32** as a viscous cloudy oil. (409mg, 0.378mmol, 72%); (Found: C, 71.2; H, 10.1. $C_{64}H_{108}O_4Si_5$ requires C, 71.1; H, 10.1%); ν_{max}/cm^{-1} (thin film) 2912vs, 2870s, 1615m, 1584m, 1512vs, 1412m, 1292s, 1246vs (Si-Me, sym def), 1175s, 818s; δ_H (400 MHz; $CDCl_3$) 7.08 (8H, d, ^3J(HH) 9Hz, 3,5-H_{Ar}), 6.81 (8H, d, ^3J(HH) 9Hz, 2,6-H_{Ar}), 3.94 (8H, t, ^3J(HH) 7Hz, -CH_2OAr), 2.30 (12H, s, Ar-Me), 1.80 (8H, qn, ^3J(HH) 7Hz, -CH_2CH$_2$OAr), 1.49 (8H, m, -CH_2(CH$_2$)$_2$OAr), 1.35 (8H, m, Si[CH$_2$CH_2CH$_2$SiMe$_2$-]$_4$), 0.59 (24H, m, -SiCH_2(CH$_2$)$_3$OAr and Si[CH_2CH$_2$CH_2SiMe$_2$-]$_4$), -0.01 (24H, s, Si-Me); $\delta_{C\{H\}}$ (100 MHz; $CDCl_3$) 157.1 (1-C_{Ar}), 129.8 (3,5-C_{Ar}), 129.6 (4-C_{Ar}), 114.5 (2,6-C_{Ar}), 67.8 (-CH$_2$OAr), 33.2 (-CH$_2$CH$_2$OAr), 20.5 (Ar-Me), 20.4 (–CH$_2$-), 20.3 (–CH$_2$-), 18.6 (–CH$_2$-), 17.6 (–CH$_2$-), 15.2 (–CH$_2$-), -3.3 (Si-Me); $\delta_{Si\{H\}}$ (80 MHz; $CDCl_3$) 2.2 (-Si(CH$_2$)$_4$OAr), 0.8 (Si(CH$_2$)$_3$SiMe$_2$-)

Synthesis of 33

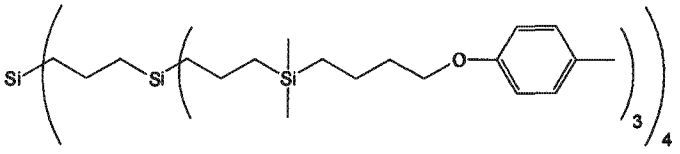

A mixture of **28** (393mg, 0.125mmol), *p*-cresol (245mg, 2.27mmol), K_2CO_3 (355mg, 2.56mmol) and 18-crown-6 (99mg, 0.375mmol) in acetone (40ml) was refluxed for 4 days. After removal of the volatiles *in vacuo*, the residue was partitioned between dichloromethane (20ml) and water (20ml). The aqueous phase was extracted with dichloromethane (3 x 20ml), and the combined organic fractions were washed with water (3 x 20ml) and brine (1 x 20ml). After drying over Na_2SO_4, filtration and removal of the volatiles *in vacuo*, the residue was purified by column chromatography (silica, 30% dichloromethane in hexane increasing polarity to 50% dichloromethane in hexane, R_f = 0.39 [50% dichloromethane in hexane]) to give **33** as a viscous cloudy oil. (195mg, 0.056mmol, 45%); (Found: C, 70.9; H, 10.3. $C_{204}H_{348}O_{12}Si_{17}$ requires C, 70.6; H, 10.1%); ν_{max}/cm^{-1} (thin film) 3029w, 2912vs, 2871s, 1615m, 1585w, 1512vs, 1411m, 1292m, 1246vs (Si-Me, sym def), 1175s, 1142m, 1023s, 909s, 818vs; δ_H (400 MHz; $CDCl_3$) 7.07 (24H, d, ^3J(HH) 8Hz, 3,5-H_{aryl}), 6.80 (24H, d, ^3J(HH) 8Hz, 2,6-H_{aryl}), 3.92 (24H, t, ^3J(HH) 7Hz, -CH_2OAr), 2.29 (36H, s, aryl-*Me*), 1.79 (24H, qn, ^3J(HH) 7Hz, -CH_2CH_2OAr), 1.48 (24H, m, -$CH_2(CH_2)_2$OAr), 1.35 (32H, m, Si[$CH_2CH_2CH_2$Si[$CH_2CH_2CH_2SiMe_2$-]$_3$]$_4$), 0.58 (88H, m, -Si$CH_2(CH_2)_3$OAr and Si$CH_2CH_2CH_2$Si[$CH_2CH_2CH_2SiMe_2$-]$_3$, -0.01 (72H, s, -SiMe_2-); $\delta_{C\{H\}}$ (100 MHz; $CDCl_3$) 157.2 (1-C_{Ar}), 130.0 (3,5-C_{Ar}), 129.7 (4-C_{Ar}), 114.6 (2,6-C_{Ar}), 67.9 (-CH_2OAr), 33.3 (-CH_2CH_2OAr), 20.7 (Ar-*Me*), 20.6 (-CH_2- x 12), 20.5 (-CH_2- x 12), 18.8 (-CH_2- x 4), 18.8 (-CH_2- x 12), 18.3 (-CH_2- x 4), 18.0 (-CH_2- x 4), 17.7 (-CH_2- x 12), 15.4 (-CH_2- x 12), -3.1 (-SiMe_2-); $\delta_{Si\{H\}}$ (80 MHz; $CDCl_3$) 2.2 (-*Si*$(CH_2)_4$OAr), 0.7 (*Si*[$(CH_2)_3$*Si*[$(CH_2)_3SiMe_2$-]$_3$]$_4$, coincidental overlap).

Reaction of tetrakis(3-[-{4-bromobutyl}dimethylsilyl]propyl)silane with *t*-BuLi followed by $ClSiMe_3$ (synthesis of 34)

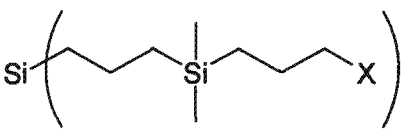

X = 30% CMe_3
70% $SiMe_3$

To a stirred solution of **27** (200mg, 0.206mmol) in ether (5ml) was added a solution of t-BuLi in pentane (1.3ml, 1.7M, 2.2mmol). After 5min $ClSiMe_3$ (1.0ml, 0.85g, 7.9mmol) was added. A white precipitate of LiCl formed immediately. The mixture was stirred for 60min at room temperature, after which the volatiles were removed *in vacuo*. The residue was extracted with hexane, and filtered through silica. After removal of the volatiles *in vacuo*, and drying under high vacuum at 50°C, a colourless oil (**34**) was recovered (160mg). δ_H (200 MHz; $CDCl_3$) 1.4 – 1.2 (m, all -$CH_2CH_2CH_2$-), 0.87 (s, -Si$(CH_2)_3CMe_3$), 0.6 – 0.4 (m, all SiCH_2CH_2-), -0.03 (s, Si$(CH_2)_3SiMe_2(CH_2)_4$X, X = $SiMe_3$ or CMe_3), -0.05 (s, Si$(CH_2)_3SiMe_2(CH_2)_4SiMe_3$)

From the integration, it is approximated that 30% of the terminal groups are -CMe_3, and 70% are –$SiMe_3$. The starting material signal for –CH_2Br (t, 3.41ppm) is absent.

Repetition of the experiment at -78°C gave similar results.

9.4 Experimental details pertaining to Chapter 4

Synthesis of 2,6-bis-[1-(2-methylphenylimino)ethyl]pyridine (35)

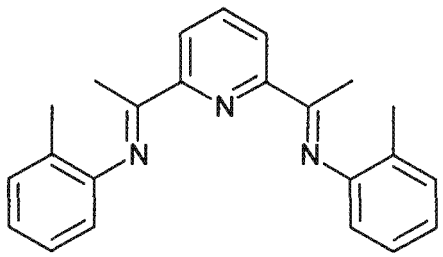

A modified literature procedure was used to prepare this compound.[17] A solution of 2,6-diacetylpyridine (394mg, 2.41mmol) and *o*-toluidine (4.0ml, 4.0g, 37mmol) in dichloromethane (15ml) over sodium sulphate (3g) was brought to reflux for 48 h. After cooling to room temperature, the solution was filtered and the volatiles were removed *in vacuo*, leaving a mixture of product and excess *o*-toluidine as a yellow oil. Addition of methanol and cooling to -20°C resulted in slow formation of pale yellow crystals. After filtration and drying, **35** was obtained as pale yellow crystals (522mg, 1.53mmol, 63%); m.p. 98-101°C; ν_{max}/cm^{-1} (dichloromethane) 3020w, 1644vs (C=N), 1598m, 1569m, 1483s, 1453m, 1366s, 1222s, 1113s; δ_H (400 MHz; $CDCl_3$) 8.42 (2H, d, ^3J(HH) 8Hz, *m*-H_{pyr}), 7.91 (1H, t, ^3J(HH) 8Hz ,*p*-H_{pyr}), 7.23 (4H, m, H_{aryl}), 7.03 (2H, m, H_{aryl}), 6.70 (2H, m, H_{aryl}), 2.36 (6H, s, N=C*Me*), 2.14 (6H, s, aryl-*Me*); $\delta_{C\{H\}}$ (100 MHz; $CDCl_3$) 169.6 (N=*C*Me), 158.3 (2,6-C_{pyr}) , 152.8 (1-C_{aryl}), 139.6 (4-C_{py}), 133.2, 129.2, 126.4, 125.1, 121.0, 20.6 (aryl-*Me*), 19.1 (N=C*Me*). Spectroscopic data is in accordance with the literature.[17])

Synthesis of 2,6-bis-[1-(2,6-dimethylphenylimino)ethyl]pyridine (36)

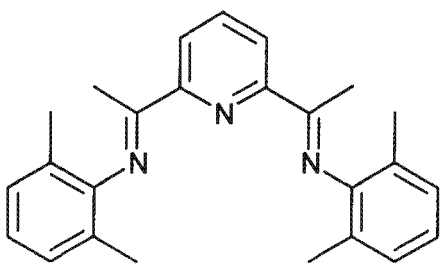

A modified literature procedure was used to prepare this compound.[13] A solution of 2,6-diacetylpyridine (681mg, 4.17mmol) and 2,6-dimethylaniline (2.0ml, 16 ml) in dichloromethane (20ml) over sodium sulphate (3g) was refluxed for 72h. After cooling to room temperature, the mixture was filtered and the volatiles were removed *in vacuo*, leaving a viscous yellow oil. Methanol (10ml) was added and upon cooling to -15°C, pale yellow needles formed. The crystals were isolated by filtration, washed with cold methanol and dried under high vacuum to give **36** as yellow needles. (1.032g, 2.79mmol, 67%); δ_H (300 MHz; $CDCl_3$) 8.51 (2H, d, ^3J(HH) 7.5Hz, *m*-H_{pyr}), 7.93 (1H, t, ^3J(HH) 8.0Hz, *p*-H_{pyr}), 7.10 (4H, m, 3,5-H_{aryl}), 6.96 (2H, t, ^3J(HH) 4.1Hz, 4-H_{aryl}), 2.27 (6H, s, N=C*Me*), 2.08 (6H, s, aryl-*Me*); $\delta_{C\{H\}}$ (75 MHz; $CDCl_3$) 167.1 (N=*C*Me), 155.2 (2,6-C_{pyr}), 148.7 (1-C_{aryl}), 136.8 (4-C_{py}), 127.9, 125.4, 123.0, 122.2, 121.0, 17.9 (aryl-*Me*), 16.4 (N=C*Me*). Spectroscopic data is in accordance with the literature.[13])

Synthesis of 2,6-bis-[1-(4-hydroxy-2-methylphenylimino)ethyl]pyridine (37)

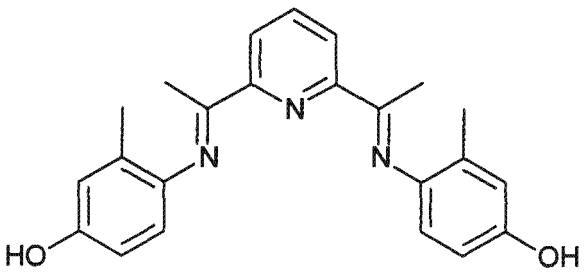

A solution of 2,6-diacetylpyridine (374mg, 2.29mmol), 4-amino-*m*-cresol (1.127g, 9.15mmol) and formic acid (5 drops) in anhydrous methanol (15ml) was heated to 60°C for 4 days. After cooling to room temperature, the dark yellow solution was concentrated *in vacuo* until a yellow precipitate formed. Further precipitation was allowed at -20°C for 15 hours. The precipitate was recovered by filtration and washed with cold methanol. After recrystallisation from hot methanol, **37** was obtained as a yellow crystalline solid. (690mg, 1.85mmol, 81%); m.p. 212-214°C; (Found: C, 74.0; H, 6.2; N, 11.3. $C_{23}H_{23}N_3O_2$ requires: C, 74.0; H, 6.2; N, 11.2%); ν_{max}/cm^{-1} (THF) 3314vs (OH), 1635s (C=N), 1569m, 1494w; δ_H (400 MHz; acetone-d_6) 8.40 (2H, d, ^3J(HH) 8.0Hz, *m*-H_{pyr}), 7.99 (1H, t, ^3J(HH), *p*-H_{pyr}), 7.98 (2H, s, aryl-O*H*), 6.78 (2H, m, H_{aryl}), 6.72 (2H, m, H_{aryl}), 6.57 (2H, d, ^3J(HH) 8.4Hz, H_{aryl}), 2.37 (6H, s, N=*C*Me), 2.08 (6H, s, aryl-*Me*); $\delta_{C\{H\}}$ (100 MHz; $CDCl_3$) 166.3 (N=*C*Me), 156.1 (4-C_{aryl}), 154.1 (2,6-C_{pyr}), 142.4 (1-C_{aryl}), 137.0 (4-C_{py}), 129.2, 122.0, 119.4, 117.2, 113.0, 17.4 (aryl-*Me*), 15.6 (N=C*Me*); *m/z* (FAB) 374 (M^+ + H, 100%), 358 (M^+ - Me, 16%).

Synthesis of 2,6-bis-[1-(4-hydroxyphenylimino)ethyl]pyridine (38)

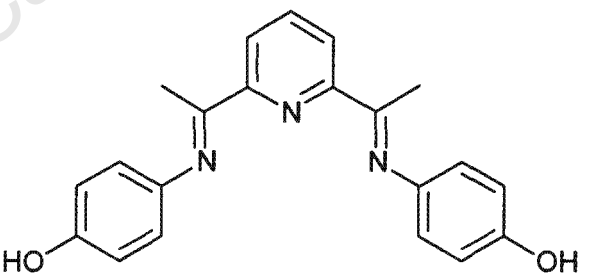

A mixture of 2,6-diacetylpyridine (908mg, 5.56mmol), 4-aminophenol (1.275g, 11.68mmol), toluene (30 ml) and a few crystals of *p*-toluenesulfonic acid was refluxed for 72h, collecting the water by-product in a Dean-Stark condenser. A thick light yellow precipitate formed in the reaction mixture. The mixture was cooled to room temperature and the precipitate was collected by filtration and washed successively with dichloromethane, ether and pentane. After recrystallisation from hot methanol, **38** was recovered as a light yellow powder. (1.812g, 5.24mmol, 84%); m.p. 245 – 247°C; (Found: C, 73.1; H, 5.6; N, 12.0. $C_{21}H_{19}N_3O_2$ requires C, 73.0; H, 5.5; N, 12.1%); ν_{max}/cm^{-1} (THF) 3300vs (OH), 1633m (C=N), 1568m, 1506m; δ_H (300 MHz; DMSO-d_6) 9.11 (2H, br s, aryl-O*H*), 9.29 (2H, d, ^3J(HH) 8Hz, 3,5-H_{py}), 7.99 (1H, t, ^3J(HH) 8Hz, 4-H_{py}), 6.82 – 6.76 (8H, m, H_{aryl}), 2.38 (N=C*Me*); $\delta_{C\{H\}}$ (75 MHz; DMSO-d_6) 166.4 (N=*C*Me), 156.1 (4-C_{aryl}), 154.7 (2,6-C_{py}), 143.7 (1-C_{aryl}), 137.8 (4-C_{py}), 122.4, 121.7, 116.2, 16.4 (N=C*Me*); *m/z* (EI) 345 (M^+, 100%), 330 (M^+ - Me, 5%)

Synthesis of 2,3-bis[2-methyl-4-hydroxylphenylimino]butane (39)

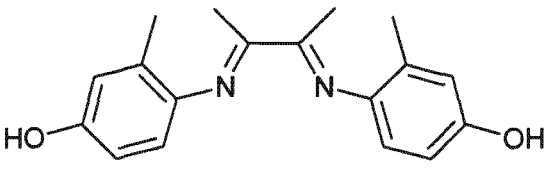

A mixture of 2,3-butadione (912mg, 10.6mmol), 2-methyl-4-hydroxyaniline (3.25g, 26.4mmol) and formic acid (a few drops) was stirred in methanol (35ml) at room temperature for 24h. The mixture was concentrated until a

yellow precipitate formed. Further precipitation was allowed at -20°C for 16h and the precipitate was recovered by filtration. After recrystallisation from hot MeOH, **39** was obtained as a yellow powder. (1.56g, 5.26mmol, 50%); m.p. 122 – 126°C; (Found: C, 73.3; H, 6.7; N. 9.5. $C_{18}H_{20}N_2O_2$ requires C, 73.0; H, 6.8; N, 9.5%); ν_{max}/cm^{-1} (THF) 3310vs (O-H), 1636s (C=N), 1607m, 1583m; δ_H (300 MHz, acetone-d_6) 8.06 (2H, broad s, aryl-O*H*), 6.70 – 6.50 (6H, m, H_{aryl}), 2.12 (6H, s, N=C*Me*), 2.05 (6H, s, aryl-*Me*); $\delta_{C\{H\}}$ (75 MHz, acetone-d_6) 167.6 (N=*C*Me), 154.3 (4-C_{aryl}), 142.1 (1- C_{aryl}), 129.1 (C_{aryl}), 119.1 (C_{aryl}), 117.2 (C_{aryl}), 113.0 (C_{aryl}), 17.3 (aryl-*Me*), 14.8 (N=C*Me*); *m/z* (FAB) 296 (M^+ + H, 93%), 281 (M^+ - Me, 31%)

Synthesis of 2-[1-(2-methylphenylimino)ethyl]pyridine (40)

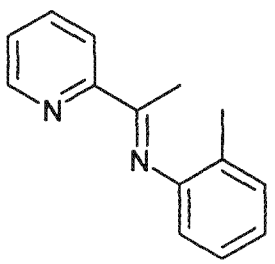

A mixture of 2-acetylpyridine (733mg, 6.05mmol), *o*-toluidine (646mg, 6.04mmol), toluene (30ml) and *p*-toluenesulfonic acid (a few crystals) was refluxed for 18h, collecting the water by-product in a Dean-Stark condenser. After cooling to room temperature, the volatiles were removed *in vacuo*, leaving a yellow oil. This was heated to 100°C under high vacuum to remove residual toluene, leaving **40** as a yellow oil. (1.266g, 6.02mmol, 99%); (Found: C, 79.6; H, 6.7; N, 12.9. $C_{14}H_{14}N_2$ requires C, 80.0; H, 6.7; N, 13.2%); ν_{max}/cm^{-1} (dichloromethane) 2926w, 1645vs (C=N), 1598m, 1568m, 1483s, 1466m, 1423s, 1364s, 1302m, 1222s, 1104m, 1044m; δ_H (300 MHz; $CDCl_3$) 8.67 (1H, d, ^3J(HH) 5Hz, 6-H_{py}), 8.32 (1H, d, ^3J(HH) 8Hz, 3-H_{py}), 7.78 (1H, m, 4-H_{py}), 7.36 (1H, m, 5-H_{py}), 7.24 – 6.67 (4H, m, H_{aryl}), 2.29 (3H, s, N=C*Me*), 2.12 (3H, s, aryl-*Me*); $\delta_{C\{H\}}$ (75 MHz; $CDCl_3$); 166.8 (N=*C*Me), 156.7 (2-C_{py}), 149.9 (6-C_{py}), 148.5 (1-C_{aryl}), 136.3, 130.4, 127.0, 126.4, 124.7, 123.6, 121.3, 118.1, 17.7 (aryl-*Me*), 16.4 (N=C*Me*)

Synthesis of 2-[1-(4-hydroxy-2-methylphenylimino)ethyl]pyridine (41)

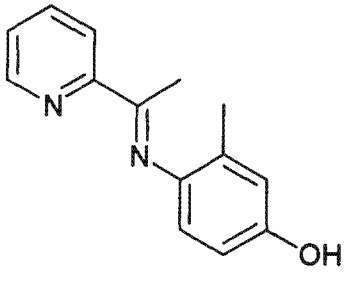

A mixture of 4-amino-*m*-cresol (1.063g, 8.63mmol), toluene (35ml), 2-acetylpyridine (1.05ml, 9mmol) and *p*-toluenesulfonic acid (a few crystals) was refluxed for 18h, collecting the water by-product in a Dean-Stark condenser. A thick yellow precipitate formed in the vessel. The reaction mixture was cooled to room temperature and the precipitate was collected by filtration and washed successively with cold dichloromethane and hexane. After recrystallisation from hot methanol, **41** was obtained as a pale yellow powder (1.367g, 6.04mmol, 70%), m.p. 123 - 127°C; (Found: C, 74.9; H, 6.2; N, 12.3. $C_{14}H_{14}N_2O$ requires C, 74.3; H, 6.2; N, 12.4%); ν_{max}/cm^{-1} (dichloromethane) 3585s (OH), 2922, 1641vs (C=N), 1608m, 1586s, 1566m, 1491vs (Ar), 1466m, 1436m, 1364s, 1209vs, 1180m, 1151m, 1104m, 1045w; δ_H (300 MHz; $CDCl_3$) 8.66 (1H, m, 6-H_{py}), 8.28 (1H, m, 3-H_{py}), 7.79 (1H, td, ^3J(HH) 8Hz, ^4J(HH) 2Hz, 4-H_{py}), 7.37 (1H, m, 5-H_{py}), 6.70 – 6.51 (3H, m, H_{aryl}), 6.0 (1H, br s, -O*H*), 2.31 (3H, s, N=C*Me*), 2.01 (3H, s, aryl-*Me*); $\delta_{C\{H\}}$ (75 MHz; $CDCl_3$) 167.5 (N=*C*Me), 156.9 (4-C_{aryl}), 152.5 (2-C_{py}), 148.4 (6-C_{py}), 142.7 (1-C_{aryl}), 136.6, 129.2, 124.8, 121.5, 119.4, 117.4, 113.1, 17.9 (aryl-*Me*) 16.6 (N=C*Me*); *m/z* (EI) 226 (M^+, 85%), 211 (M^+ - Me, 100%) 148 (M^+ - py, 87%)

Synthesis of 2,6-bis-[1-(4-benzyloxy-2-methylphenylimino)ethyl]pyridine (42)

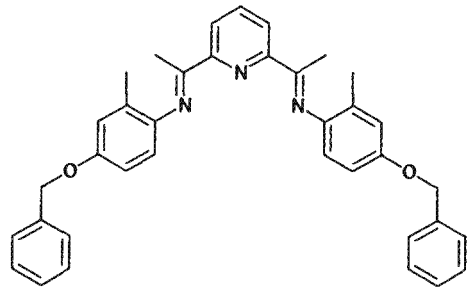

A mixture of **37** (102 mg, 0.273mmol), 18-crown-6 (16mg, 0.061mmol), K_2CO_3 (111mg, 0.80mmol), acetone (10ml) and benzyl bromide (80µl, 0.6mmol) was refluxed for 4 days. A light yellow precipitate formed in the mixture. After concentrating the mixture, and cooling overnight at -15°C, the precipitate was collected by filtration, and partitioned between dichloromethane and slightly alkaline water (c.a. 1ml of 0.1M NaOH added to 250ml water). The aqueous phase was extracted with dichloromethane (20ml x 3), and the combined organic fractions were then washed with slightly alkaline water (20 ml x 3) and slightly alkaline brine (20ml). After drying over Na_2SO_4 and filtration, the volatiles were removed *in vacuo* leaving a yellow crystalline material. This was recrystallised from dichloromethane/methanol to give **42** as a yellow powder (117mg, 0.211mmol, 77%), m.p. 178-180°C; (Found: C, 80.2; H, 6.3; N, 7.5. $C_{37}H_{35}N_3O_2$ requires C, 80.3; H, 6.4; N, 7.6%); ν_{max}/cm^{-1} (dichloromethane) 1637s (C=N), 1570m, 1490vs (Ar), 1454m, 1366m, 1297m, 1207s, 1028m; δ_H (400 MHz; $CDCl_3$) 8.39 (2H, d, ^3J(HH) 8.0Hz, *m*-H_{pyr}), 7.87 (1H, t, ^3J(HH) 7.8Hz, *p*-H_{pyr}), 7.5 - 6.6 (16H, m, H_{aryl} and H_{Ph}), 5.08 (4H, s, OCH_2Ph), 2.38 (6H, s, N=C*Me*), 2.14 (6H, s, aryl-*Me*); $\delta_{C\{H\}}$ (100 MHz; $CDCl_3$) 167.3 (N=*C*Me), 155.8 (4-C_{aryl}), 155.6 (2,6-C_{py}), 143.6 (1-C_{aryl}), 137.6, 136.8, 129.8, 129.2, 128.7, 128.0, 127.7, 122.2, 119.3, 117.2, 112.6, 70.5 (OCH_2Ph), 18.2 (aryl-*Me*), 16.4 (N=C*Me*); *m/z* (FAB) 554 (M^+ + H, 98%), 462 (M^+ - bz, 85%)

Synthesis of 43

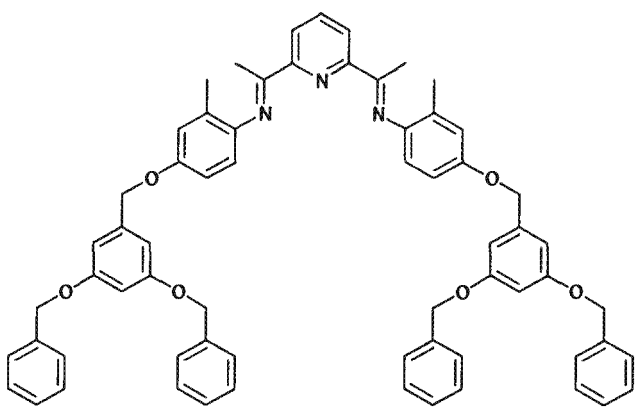

A mixture of **37** (491mg, 1.31mmol), **pbpeG1** (1.026mg, 2.68mmol), K_2CO_3 (456mg, 3.30mmol), 18-crown-6 (78mg, 0.30mmol) and acetone (40ml) was refluxed for 72h. A light yellow precipitate formed in the reaction vessel. After cooling to room temperature, the volatiles were removed *in vacuo* and the residue was partitioned between dichloromethane and slightly alkaline water. The aqueous phase was extracted with dichloromethane (3 x 20 ml), and the combined organic fractions were then washed with slightly alkaline water (3 x 20 ml) and slightly alkaline brine (1x 20 ml). After drying over Na_2SO_4 and filtration, the volatiles were removed *in vacuo*, leaving a yellow foam. This was recrystallised from toluene/hexane to give **43** as an amorphous yellow solid (936mg, 0.956mmol, 73%) m.p. 59-62°C; (Found C, 80.1; H, 6.0; N, 4.2. $C_{65}H_{59}N_3O_6$ requires C, 79.8; H, 6.1; N, 4.3%); ν_{max}/cm^{-1} (dichloromethane) 2924w, 2874w, 1636m (C=N), 1597vs (Ar), 1491s (Ar), 1452s (Ar), 1366s, 1292s, 1210vs, 1160vs, 1122m, 1028s; δ_H (400 MHz; $CDCl_3$) 8.40 (2H, d, ^3J(HH) 8Hz, *m*-H_{py}), 7.87 (1H, t, ^3J(HH) 8Hz, *p*-H_{py}), 7.46 – 6.59 (32H, m, H_{aryl} and H_{Ph}), 5.06 (8H, s, OCH_2Ph),

5.01 (4H, s, OCH_2-aryl wedge), 2.38 (6H, s, N=C*Me*), 2.14 (6H, s, aryl-*Me*); $\delta_{C\{H\}}$ (75 MHz; $CDCl_3$) 167.1 (N=CMe), 160.2 (3,5-$C_{wedge\ aryl}$), 155.6 (4-$C_{core\ aryl}$), 155.4 (2,6-C_{py}), 143.6, 139.9, 136.9, 136.7, 129.0, 128.6, 128.0, 127.6, 122.1, 119.2, 117.1, 112.5, 106.4, 70.3 (OCH_2-aryl wedge), 70.2 (OCH_2Ph), 18.1 (aryl-*Me*), 16.3 (N=C*Me*); *m/z* (FAB) 978 (M^+ + H, 29%), 886 (M^+ - bz, 2%) 674 (M^+ - pbpeG1, 42%)

Synthesis of 44

A mixture of **37** (87mg, 0.23mmol), **pbpeG2** (367mg, 0.454mmol), K_2CO_3 (81mg, 0.59mmol), 18-crown-6 (12mg, 0.045mmol) and acetone (40ml) was refluxed for 48h. After cooling to room temperature, the volatiles were removed *in vacuo* and the residue was partitioned between dichloromethane and slightly alkaline water. The aqueous phase was extracted with dichloromethane (3 x 20 ml), and the combined organic fractions were then washed with slightly alkaline water (3 x 20 ml) and slightly alkaline brine (1x 20 ml). After drying over Na_2SO_4 and filtration, the volatiles were removed *in vacuo*, leaving a yellow oil. Recrystallisation from several solvent systems was attempted, but in each case oiling out took place. After two purifications by oiling out from dichloromethane/hexane and drying under high vacuum, **44** was recovered as a yellow foam. (350mg, 0.192mmol, 83%); m.p. 52-54°C; (Found: C, 79.5; H, 5.8; N, 2.3%. $C_{121}H_{107}N_3O_{14}$ requires C, 79.5; H, 5.9; N, 2.3%); ν_{max}/cm^{-1} (dichloromethane) 2934w, 2876w, 1698w, 1637w (C=N), 1596vs (Ar), 1492m (Ar), 1453s, 1374s, 1294m, 1210m, 1158vs, 1055m, 1029m; δ_H (400 MHz, $CDCl_3$) 8.40 (2H, d, ^3J(HH) 8Hz, *m*-H_{py}), 7.87 (1H, t, ^3J(HH) 8Hz, *p*-H_{py}), 7.42 – 6.56 (64H, m, H_{aryl}), 5.05 (16H, s, OCH_2Ph), 5.01 (4H, s, OCH_2-aryl wedge), 5.00 (8H, s, OCH_2-aryl wedge), 2.37 (6H, s, N=C*Me*), 2.14 (6H, s, aryl-*Me*); $\delta_{C\{H\}}$ (100 MHz; $CDCl_3$) 167.4 (N=CMe), 160.5 (3,5-$C_{wedge\ aryl}$ x 8), 160.3 (3,5-$C_{wedge\ aryl}$ x 4), 155.9 (4-$C_{core\ aryl}$), 155.6 (2,6-C_{py}), 143.8, 140.1, 139.6, 137.1, 130.3, 129.3, 128.8, 128.2, 127.9, 127.8, 122.3, 119.4, 117.3, 112.7, 106.7, 101.9, 101.8, 70.5 (OCH_2-aryl wedge x 2), 70.4 (OCH_2Ph), 70.3 (OCH_2-aryl wedge x 4), 18.3 (aryl-*Me*), 16.5 (N=C*Me*)

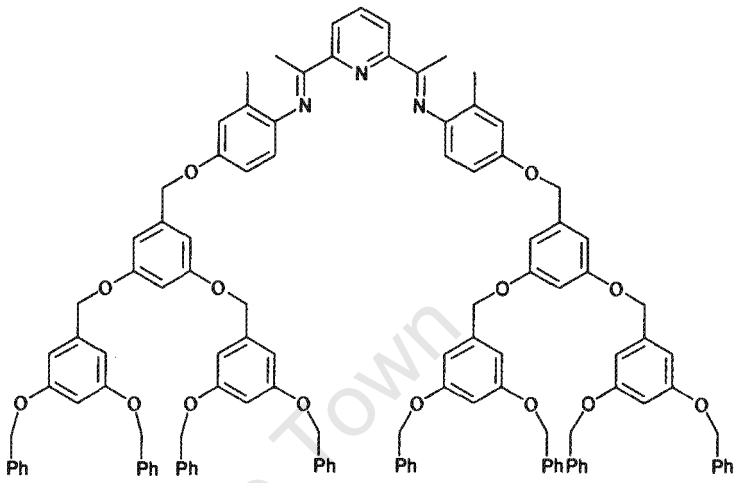

Synthesis of 45

A mixture of **37** (423mg, 1.13mmol), **18** (691mg, 2.55mmol), K_2CO_3 (390mg, 2.83mmol), 18-crown-6 (60mg, 0.23mmol) and acetone (30ml) was refluxed for 48h. After cooling to room temperature, the volatiles were removed *in vacuo*, and the residue was partitioned between dichloromethane and slightly alkaline water. The aqueous phase was extracted with dichloromethane (3 x

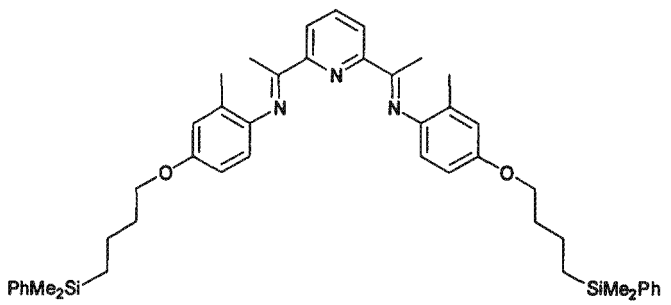

20 ml), and the combined organic fractions were then washed with slightly alkaline water (3 x 20 ml) and slightly alkaline brine (1x 20 ml. After drying over Na_2SO_4 and filtration, the volatiles were removed *in vacuo*, leaving a waxy yellow solid. Recrystallisation from hot methanol gave **45** as an amorphous yellow solid. (500mg, 0.663mmol, 59%); m.p. 62 - 64°C; (Found: C, 74.5; H, 7.9; N, 5.6. $C_{47}H_{59}N_3O_2Si_2$ requires C, 74.8; H, 7.9; N, 5.6%); ν_{max}/cm^{-1} (dichloromethane) 2941s, 2870m, 1636s (C=N), 1604w, 1570w, 1492vs (Ar), 1474m, 1366m, 1288m, 1246vs (Si-Me, sym def), 1210vs, 1163m, 1113s (Si-Ph), 1029m; δ_H (400 MHz; $CDCl_3$) 8.40 (2H, d, ^3J(HH) 8Hz, *m*-H_{py}), 7.87 (1H, t, ^3J(HH) 8Hz, *p*-H_{py}), 7.9 – 6.6 (18H, m, H_{aryl} and H_{Ph}), 3.96 (4H, t, ^3J(HH) 6Hz, $OCH_2(CH_2)_3Si$), 2.38 (6H, s, N=C*Me*), 2.14 (6H, s, aryl-*Me*), 1.83 (4H, qn, ^3J(HH) 6Hz, $OCH_2CH_2(CH_2)_2Si$), 1.55 (4H, m, $O(CH_2)_2CH_2CH_2Si$), 0.85 (4H, t, ^3J(HH) 8.4Hz, $O(CH_2)_3CH_2Si$), 0.31 (12H, s, Si*Me*$_2$Ph); $\delta_{C\{H\}}$ (75 MHz; $CDCl_3$) 167.0 (N=*C*Me), 155.7 (4-C_{aryl}), 155.7 (2,6-C_{py}), 143.1 (1-C_{aryl}), 139.4 (4-C_{py}), 136.6, 133.6, 129.0, 128.8, 127.7, 122.0, 119.1, 116.7, 112.1, 67.8 ($OCH_2(CH_2)_3Si$), 33.1 ($OCH_2CH_2(CH_2)_2Si$), 20.5 ($O(CH)_2CH_2CH_2Si$), 18.1 (aryl-*Me*), 16.2 (N=C*Me*), 15.5 ($O(CH_2)_3CH_2Si$), -3.0 (Si*Me*$_2$Ph); $\delta_{Si\{H\}}$ (80 MHz; $CDCl_3$) -3.7; *m/z* (FAB) 754 (M^+ + H, 68%), 738 (M^+ - Me, 21%), 676 (M^+ - Ph, 5%), 618 (M^+ - $SiMe_2Ph$, 4%)

Synthesis of 46

A mixture of **37** (259mg, 0.693mmol), **21** (1.059g, 1.521mmol), K_2CO_3 (272mg, 1.96mmol), 18-crown-6 (45mg, 0.17mmol) and acetone (20ml) was refluxed for 72h. The volatiles were removed *in vacuo*, and the residue was partitioned between dichloromethane and slightly alkaline water. The aqueous phase was extracted with dichloromethane (3 x 20 ml), and the combined organic fractions were then washed with slightly alkaline water (3 x 20 ml) and slightly alkaline brine (1x 20 ml). After drying over Na_2SO_4 and filtration, the volatiles were removed *in vacuo*, leaving a yellow oil. After recrystallisation from dichloromethane/methanol, **46** was isolated as a yellow oil. (834mg, 0.520mmol, 75%); (Found: C, 72.4; H, 8.5; N, 2.5. $C_{97}H_{139}N_3O_2Si_8$ requires C, 72.6; H, 8.7; N, 2.6%); ν_{max}/cm^{-1} (dichloromethane) 2956s, 2916vs, 2876, 1636s (C=N), 1605w, 1569w, 1492vs (Ph), 1474m, 1450w, 1366m, 1248vs (Si-Me, sym def), 1210vs, 1163w, 1142s, 1112vs (Si-Ph), 1022m; δ_H (400 MHz; C_6D_6) 8.45 (2H, d, ^3J(HH) 8 Hz, *m*-H_{py}), 7.28 (1H, t, ^3J(HH) 8 Hz, *p*-H_{py}), 7.49 – 6.62 (36H, m, H_{aryl} and H_{Ph}), 3.77 (4H, t, ^3J(HH) 6Hz, $OCH_2(CH_2)_3Si$), 2.34 (6H, s, N=C*Me*), 2.14 (6H, s, aryl-*Me*), 1.70 (4H, qn, ^3J(HH) 7Hz, $OCH_2CH_2(CH_2)_2Si$), 1.55 (16H, m, $O(CH_2)_2CH_2CH_2Si$ and $SiCH_2CH_2CH_2SiMe_2Ph$), 0.83 (12H, t, ^3J(HH) 8Hz, $Si(CH_2)_2CH_2SiMe_2Ph$), 0.62 (12H, t, ^3J(HH) 8Hz, $SiCH_2(CH_2)_2SiMe_2Ph$), 0.49 (4H, t, ^3J(HH) 8Hz, $O(CH_2)_3CH_2Si$), 0.28 (36H, s, Si*Me*$_2$Ph); $\delta_{C\{H\}}$ (100 MHz; C_6D_6) 166.4 (N=*C*Me), 156.4 (4-C_{aryl}), 156.0 (2,6-C_{py}), 143.6 (1-C_{aryl}), 139.5 (4-C_{py}), 136.5, 133.8, 129.2, 129.0, 128.1, 122.2, 119.4,

117.1, 112.4, 67.7 ($OCH_2(CH_2)_3Si$), 33.7 ($OCH_2CH_2(CH_2)_2Si$), 20.9, 20.8, 18.9, 18.2 (aryl-*Me*), 17.6, 16.0 (N=C*Me*), 12.6 ($O(CH_2)_3CH_2Si$), -2.9 ($SiMe_2Ph$); $\delta_{Si\{H\}}$ (75 MHz; $CDCl_3$) 1.9 (-*Si*$(CH_2)_3SiMe_2Ph$) -5.1 ($-Si(CH_2)_3SiMe_2Ph$); *m/z* (FAB) 1604 ($M^+ + H$, 30%), 1589 ($M^+ + H$ - Me, 7%), 1469 ($M^+ + H - SiMe_2Ph$, 8%), 1426 ($M^+ - (CH_2)_3SiMe_2Ph$, 9%)

Synthesis of 2,6-bis-[1-(4-benzyloxyphenylimino)ethyl]pyridine (47)

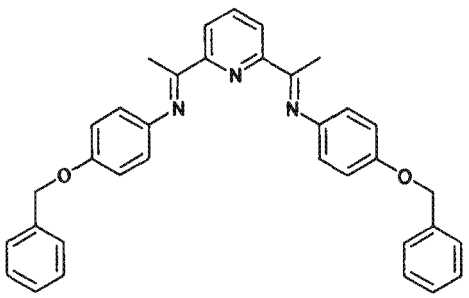

A mixture of **38** (271mg, 0.784mmol), benzyl bromide (0.50 ml, 0.72g, 4.2mmol), K_2CO_3 (325mg, 2.35mmol), 18-crown-6 (40mg, 0.15mmol) and acetone (20ml) was refluxed for 72h. The volatiles were removed *in vacuo*, and the residue was partitioned between dichloromethane and slightly alkaline water. The aqueous phase was extracted with dichloromethane (3 x 20 ml), and the combined organic fractions were then washed with slightly alkaline water (3 x 20 ml) and slightly alkaline brine (1 x 20 ml. After drying over Na_2SO_4 and filtration, the volatiles were removed *in vacuo*, leaving a yellow waxy solid. After recrystallisation from dichloromethane/methanol, **47** was obtained as a yellow crystalline material. (309mg, 0.588mmol, 75%), m.p. 228-229°C; (Found: C, 80.1; H, 5.9; N, 7.9. $C_{35}H_{31}N_3O_2$ requires C, 80.0; H, 5.9; N, 8.0%); ν_{max}/cm^{-1} (dichloromethane) 1636s (C=N), 1604w, 1569w, 1502vs (Ar), 1455m, 1366m, 1211m, 1167w, 1121m, 1024m; δ_H (300 MHz; $CDCl_3$) 8.33 (2H, d, ^3J(HH) 8Hz, *m*-H_{py}), 7.84 (1H, t, ^3J(HH) 8Hz, *p*-H_{py}), 7.48 – 6.80 (18H, m, H_{aryl} and H_{Ph}), 5.09 (4H, s, OCH_2Ph), 2.44 (6H, s, N=C*Me*); $\delta_{C\{H\}}$ (75 MHz; $CDCl_3$) 167.3 (N=*C*Me), 155.9 (4-C_{aryl}), 155.7 (2,6-C_{py}), 144.9 (1-C_{aryl}), 137.4, 136.7, 128.6, 127.9, 127.5, 122.2, 120.9, 115.6, 70.7 (OCH_2Ph), 16.1 (N=C*Me*); *m/z* (EI) 525 (M^+, 41%), 434 (M^+ - bz, 100%) 342 (M^+ - ArObz, 14%)

Synthesis of 48

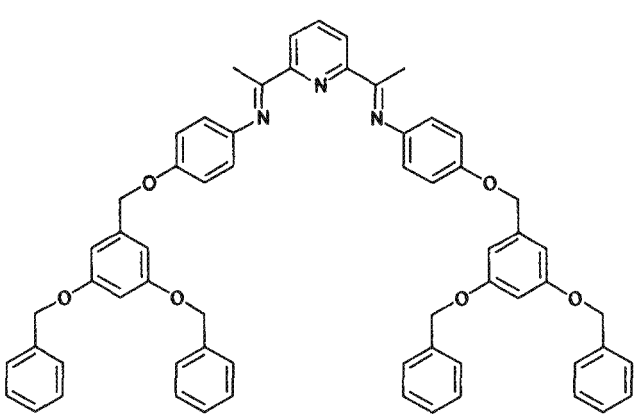

A mixture of **38** (251mg, 0.726mmol), **pbpeG1** (559mg, 1.46mmol), K_2CO_3 (257mg, 1.86mmol), 18-crown-6 (56mg, 0.21mmol) and acetone (40ml) was refluxed for 72h. After cooling to room temperature, the volatiles were removed *in vacuo* and the residue was partitioned between dichloromethane and slightly alkaline water. The aqueous phase was extracted with dichloromethane (3 x 20 ml), and the combined organic fractions were then washed with slightly alkaline water (3 x 20 ml) and slightly alkaline brine (1x 20 ml). After drying over Na_2SO_4 and filtration, the volatiles were removed *in vacuo*, leaving a yellow oil. Recrystallisation from several solvent systems was attempted, but in each case oiling out took place. After two purifications by oiling out from dichloromethane/hexane and drying under high vacuum, **48** was recovered as a yellow foam. (369mg, 0.399mmol, 55%); m.p. 47 – 49°C; (Found: C, 80.0; H, 5.7; N, 4.3.

$C_{63}H_{55}N_3O_2$ requires C, 79.6; H, 5.8; N, 4.4%); ν_{max}/cm^{-1} (dichloromethane) 2923w, 2876w, 1936w (C=N), 1596vs (Ar), 1501vs, 1452s, 1367m, 1343m, 1321m, 1212s, 1159vs, 1122w, 1028m; δ_H (400 MHz, $CDCl_3$) 8.34 (2H, d, ^3J(HH) 8Hz, *m*-H_{py}), 7.86 (1H, t, ^3J(HH) 8Hz, *p*-H_{py}), 7.43 – 6.60 (32H, m, H_{aryl} and H_{Ph}), 5.07 (8H, s, OCH_2Ph), 5.03 (4H, s, OCH_2-aryl wedge), 2.46 (6H, s, N=C*Me*); $\delta_{C\{H\}}$ (100 MHz; $CDCl_3$) 167.6 (N=*C*Me), 160.3 (3,5-$C_{wedge\ aryl}$), 155.8 (4-$C_{core\ aryl}$), 155.6 (2,6-C_{py}), 144.8, 139.8, 137.0, 136.9, 128.8, 128.2, 127.7, 122.3 121.0, 115.5, 106.5, 101.7, 70.4 (O*C*H_2-aryl wedge), 70.3 (O*C*H_2Ph), 16.4 (N=C*Me*); *m/z* (FAB) 950 (M^+ + H, 15%)

Synthesis of 49

A mixture of **38** (462mg, 1.36mmol), **18** (794mg, 2.93mmol), K_2CO_3 (492mg, 3.56mmol), 18-crown-6 (77mg, 0.29mmol) and acetone (30ml) was refluxed for 72h. The volatiles were removed *in vacuo* and the residue was partitioned between dichloromethane and slightly alkaline water. The aqueous phase was extracted with dichloromethane (3 x 20 ml), and the combined organic fractions were then washed with slightly alkaline water (3 x 20 ml) and slightly alkaline brine (1 x 20 ml). After drying over Na_2SO_4 and filtration, the volatiles were removed *in vacuo*, leaving a yellow waxy solid. Recrystallisation from hot methanol gave **49** as an amorphous yellow solid. (933mg, 1.28mmol, 94%); m.p.68-69°C; (Found: C, 74.5; H, 7.6; N, 5.7. $C_{45}H_{55}N_3O_2Si_2$ requires C, 74.4; H, 7.6; N, 5.8%); ν_{max}/cm^{-1} (dichloromethane) 2940m, 2870m, 1635s (C=N), 1605w, 1568w, 1502vs (Ar), 1471m, 1366m, 1288w, 1241s (Si-Me, sym def), 1213s, 1167w, 1113s (Si-Ph), 1022m; δ_H (400 MHz; $CDCl_3$) 8.33 (2H, d, ^3J(HH) 8Hz, *m*-H_{py}), 7.85 (1H, t, ^3J(HH) 8Hz, *p*-H_{py}), 7.55 – 6.80 (18H, m, H_{aryl} and H_{Ph}), 3.97 (4H, t, ^3J(HH) 7Hz, OCH_2(CH$_2$)$_3$Si), 2.44 (6H, s, N=C*Me*), 1.83 (4H, qn, ^3J(HH) 7Hz, OCH$_2$CH_2(CH$_2$)$_2$Si), 1.54 (4H, m, O(CH$_2$)$_2$CH_2CH$_2$Si), 0.84 (4H, m, O(CH$_2$)$_3$CH_2Si), 0.30 (12H, s, -Si*Me*$_2$Ph); $\delta_{C\{H\}}$ (100 MHz; $CDCl_3$) 167.2 (N=*C*Me), 155.8 (4-C_{aryl}), 155.7 (2,6-C_{py}), 144.2 (1-C_{aryl}), 139.3 (4-C_{py}), 136.6, 133.5, 128.8, 127.7, 122.0, 120.8, 114.9, 67.8 (O*C*H_2(CH$_2$)$_3$Si), 33.0 (OCH$_2$*C*H$_2$(CH$_2$)$_2$Si), 20.4 (O(CH)$_2$*C*H$_2$CH$_2$Si), 16.1 (N=C*Me*), 15.5 (O(CH$_2$)$_3$*C*H$_2$Si), -3.1 (-Si*Me*$_2$Ph); $\delta_{Si\{H\}}$ (80 MHz; $CDCl_3$) -4.1; *m/z* (FAB) 726 (M^+ + H, 9%), 590 (M^+ - SiMe$_2$Ph, 2%)

Synthesis of 50

A mixture of **38** (84mg, 0.24mmol), **21** (352mg, 0.506mmol), K_2CO_3 (90mg, 0.65mmol), 18-crown-6 (12mg, 0.045mmol) and acetone (20ml) was refluxed for 72h. The volatiles were removed *in vacuo* and the residue was partitioned between dichloromethane and slightly alkaline water. The aqueous phase was extracted with dichloromethane (3 x 20 ml), and the combined organic fractions were then washed with slightly alkaline water (3 x 20 ml) and slightly alkaline brine (1 x 20 ml). After drying over Na_2SO_4 and filtration, the volatiles were removed *in vacuo*, leaving a yellow oil. Two purifications by oiling out from dichloromethane/methanol gave **50** as a yellow oil. (355mg, 0.223mmol, 94%); δ_H (400 MHz; C_6D_6) 8.53 (2H, d, ^3J(HH) 8Hz, *m*-H_{py}), 7.34 (1H, t, ^3J(HH) 8Hz, *p*-H_{py}), 7.58 – 6.91 (38H, m, H_{aryl} and H_{Ph}), 3.81 (4H, t, ^3J(HH) 6Hz, $OCH_2(CH_2)_3Si$), 2.49 (6H, s, N=C*Me*), 1.76 (4H, qn, ^3J(HH) 7Hz, $OCH_2CH_2(CH_2)_2Si$), 1.53 (16H, m, $O(CH_2)_2CH_2CH_2Si$ and $SiCH_2CH_2CH_2SiMe_2Ph$), 0.92 (12H, t, ^3J(HH) 8Hz, $Si(CH_2)_2CH_2SiMe_2Ph$), 0.70 (12H, t, ^3J(HH) 8Hz, $SiCH_2(CH_2)_2SiMe_2Ph$), 0.56 (4H, m, $O(CH_2)_3CH_2Si$), 0.34 (36H, s, -Si*Me*$_2$Ph); $\delta_{C\{H\}}$ (100 MHz; C_6D_6) 166.3 (N=*C*Me), 156.2 (4-C_{aryl}), 155.9 (2,6-C_{py}), 144.7 (1-C_{aryl}), 139.3 (4-C_{py}), 136.7, 133.6, 128.8, 127.4, 122.1, 121.0, 115.0, 67.6 ($OCH_2(CH_2)_3Si$), 33.4 ($OCH_2CH_2(CH_2)_2Si$), 20.7, 20.6, 18.7, 17.4, 15.6 (N=C*Me*), 12.5 ($O(CH_2)_3CH_2Si$), -3.0 (Si*Me*$_2$Ph); $\delta_{Si\{H\}}$ (75 MHz; $CDCl_3$) 1.8 (-*Si*$(CH_2)_3SiMe_2Ph$) -5.4 ($-Si(CH_2)_3SiMe_2Ph$); *m/z* (FAB) 1575 (M^+ + H, 31%), 1440 (M^+ - $SiMe_2Ph$, 6%)

Synthesis of 2-[1-(4-benzyloxy-2-methylphenylimino)ethyl]pyridine (51)

A mixture of **41** (257mg, 1.14mmol), benzyl bromide (0.15 ml, 0.22g, 1.3mmol), K_2CO_3 (215mg, 1.56mmol), 18-crown-6 (32mg, 0.12mmol) and acetone (20ml) was refluxed for 48h. The volatiles were removed *in vacuo*, and the residue was partitioned between dichloromethane and slightly alkaline water. The aqueous phase was extracted with dichloromethane (3 x 20 ml), and the combined organic fractions were then washed with slightly alkaline water (3 x 20 ml) and slightly alkaline brine (1 x 20 ml. After drying over Na_2SO_4 and filtration, the volatiles were removed *in vacuo*, leaving a yellow oil, which was soluble in a wide range of solvents. After three recrystallisations by concentration of a hexane solution, **51** was obtained as a pale yellow powder. (206mg, 0.651mmol, 57%); m.p. 64 – 67°C; (Found: C, 79.8; H, 6.4; N, 8.6. $C_{21}H_{20}N_2O$ requires C, 79.7; H, 6.4; N, 8.9%); ν_{max}/cm^{-1} (dichloromethane) 2924w, 1641s (C=N), 1585m, 1566w, 1491vs (Ar), 1467w, 1379w, 1364m, 1300m, 1207s, 1161m, 1104m, 1028m; δ_H (300 MHz; $CDCl_3$) 8.67 (1H, m, ^3J(HH) 5Hz, 6-H_{py}),

8.32 (1H, m, ^3J(HH) 8Hz, 3-H_{py}), 7.78 (1H, td, ^3J(HH) 8Hz, ^4J(HH) 2Hz, 4-H_{py}), 7.45 – 7.33 (6H, m, 5-H_{py} and H_{Ph}), 6.91 (1H, d, ^4J(HH) 3Hz, 3-H_{aryl}), 6.83 (dd, ^3J(HH) 8Hz, ^4J(HH) 3Hz, 5-H_{aryl}), 6.61 (1H, d, ^3J(HH) 8Hz, 6-H_{aryl}), 5.06 (2H, s, OCH_2Ph), 2.32 (3H, s, N=C*Me*), 2.12 (3H, s, aryl-*Me*); $\delta_{C\{H\}}$ (75 MHz; $CDCl_3$) 167.1 (N=*C*Me), 157.0 (4-C_{aryl}), 155.4 (2-C_{py}), 148.5 (6-C_{py}), 143.5 (1-C_{aryl}), 137.4, 136.3, 129.0, 128.5, 127.8. 127.5, 124.6, 121.3, 119.1, 117.1, 112.4, 70.3 (O*C*H_2Ph), 18.1 (aryl-*Me*), 16.4 (N=C*Me*); *m/z* (EI) 316 (M^+, 34%), 225 (M^+ - bz, 100%)

Synthesis of 2,3-bis[2-methyl-4-benzyloxyphenylimino]butane (52)

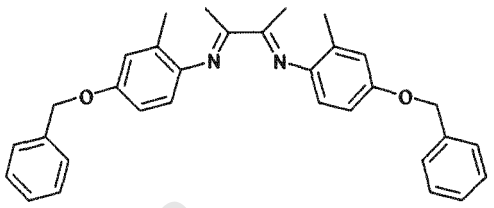

A mixture of **39** (490mg, 1.66mmol), 18-crown-6 (90mg, 0.34mmol), K_2CO_3 (580mg, 4.20mmol), acetone (30ml) and benzyl bromide (0.50ml, 4.2mmol) was refluxed for 48h. The volatiles were removed *in vacuo* and the residue was partitioned between dichloromethane and slightly alkaline water. The aqueous phase was extracted with dichloromethane (20ml x 3), and the combined organic fractions were then washed with slightly alkaline water (20 ml x 3) and slightly alkaline brine (20ml). After drying over Na_2SO_4 and filtration, the volatiles were removed *in vacuo* leaving a yellow crystalline material. This was recrystallised from dichloromethane/methanol to give **52** as a yellow powder. (341mg, 0.715mmol, 43%); m.p. 130 – 134°C; (Found: C, 80.1; H, 6.9; N, 6.0. $C_{32}H_{32}N_2O_2$ requires C, 80.6; H, 6.8; N, 5.9%); ν_{max}/cm^{-1} (dichloromethane) 2922w, 2869w, 1640s (C=N), 1604m, 1576w, 1490vs (Ar), 1379w, 1362m, 1241s, 1200vs (Ar-O), 1162m, 1119s, 1028s (CH_2-O); δ_H (300 MHz, $CDCl_3$) 7.46 – 6.58 (16H, m, H_{aryl}), 5.07 (4H, s, O*C*H_2Ph), 2.16 (6H, s, *Me*), 2.14 (6H, s, *Me*); $\delta_{C\{H\}}$ (75 MHz, $CDCl_3$) 168.0 (N=*C*Me), 155.6 (4-C_{aryl}), 143.1 (1-C_{aryl}), 137.3 (1-C_{Ph}), 129.0, 128.5, 127.9, 127.5, 118.8, 117.1, 112.4, 70.3 (O*C*H_2Ph), 18.1 (aryl-*Me*) 15.5 (N=C*Me*)

Synthesis of 53

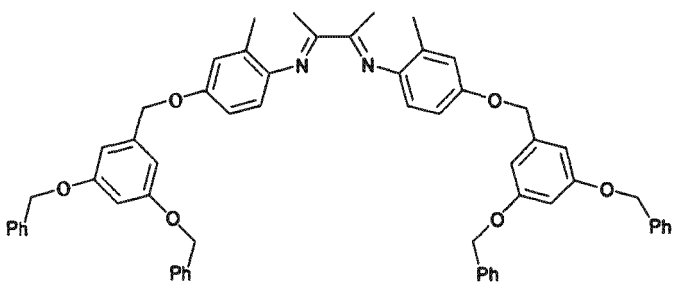

A mixture of **39** (219mg, 0.739mmol), **pbpeG1** (559mg, 1.46), 18-crown-6 (40mg, 0.15mmol), K_2CO_3 (261mg, 1.90mmol) in acetone (20ml) was refluxed for 48h. The volatiles were removed *in vacuo* and the residue was partitioned between dichloromethane and slightly alkaline water. The aqueous phase was extracted with dichloromethane (20ml x 3), and the combined organic fractions were then washed with slightly alkaline water (20 ml x 3) and slightly alkaline brine (20ml). After drying over Na_2SO_4 and filtration, the volatiles were removed *in vacuo* leaving a yellow solid. This was recrystallised from dichloromethane / methanol to give **53** as a yellow powder. (380mg, 0.422mmol, 57%); m.p. 143 – 146°C; (Found: C, 79.6; H, 6.0; N, 3.5. $C_{60}H_{56}N_2O_6$ requires C, 80.0; H, 6.3; N, 3.1%); ν_{max}/cm^{-1} (dichloromethane) 2922w, 2876w, 1639m (C=N), 1597vs (Ar), 1490s

(Ar), 1452m, 1376m, 1202s, 1160vs, 1119m, 1028m; δ_H (300 MHz, $CDCl_3$) 7.42 – 6.64 (32H, m, H_{aryl}), 5.05 (8H, s, OCH_2Ph), 5.00 (4H, s, OCH_2-aryl wedge), 2.14 (6H, s, *Me*), 2.12 (6H, s, *Me*); $\delta_{C\{H\}}$ (100 MHz, $CDCl_3$) 167.9 (N=*C*Me), 160.2 (3,5-$C_{aryl\ wedge}$), 155.5 (4-$C_{aryl\ core}$), 143.1, 139.8, 136.9, 136.7, 128.9, 128.5, 127.9, 127.4, 118.7, 117.8, 112.4, 106.4, 70.2 (OCH_2-aryl wedge), 70.1 (OCH_2Ph), 17.9 (aryl-*Me*), 15.4 (N=C*Me*)

Synthesis of [2,6-bis-[1-(2-methylphenylimino)ethyl]pyridine]iron dichloride (54)

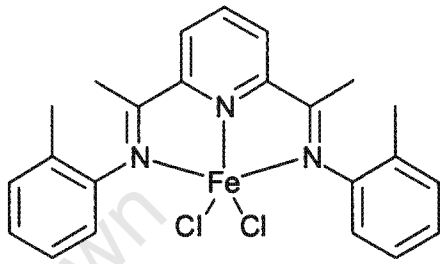

This compound was prepared by a modified literature method.[17] A mixture of **35** (200mg, 0.586mmol) and $FeCl_2.4H_2O$ (112mg, 0.564mmol) was stirred in THF (15ml). A deep blue colour formed immediately. The mixture was stirred for 4h, after which diethyl ether (15ml) was added, resulting in the precipitation of a blue powder. After centrifuging the mixture, the supernatant was removed, and the precipitate was washed with ether (3 x 15ml) and pentane (3 x 15ml), centrifuging and removing the supernatant each time. After drying under high vacuum, **54** was obtained as a dark blue powder. (258mg, 0.551mmol, 98%); m.p. decomposes without melting above 200°C; (Found: C, 59.6; H, 5.6; N, 7.8. $C_{23}H_{23}Cl_2N_3Fe$ requires C, 59.0; H, 5.0; N, 9.0%); ν_{max}/cm^{-1} (dichloromethane) 3682m, 3600w, 2867m, 1602m, 1592w (C=N), 1487m, 1374m, 1229w, 1063m

Synthesis of [2,6-bis-[1-(2,6-dimethylphenylimino)ethyl]pyridine]iron dichloride (55)

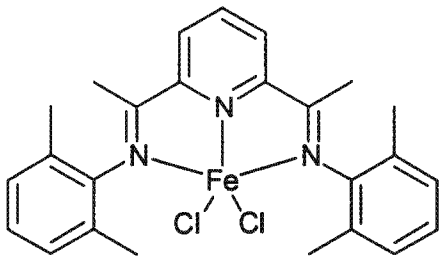

This compound was prepared by a modified literature method.[13] A mixture of **36** (331mg, 0.896mmol) and $FeCl_2.4H_2O$ (175mg, 0.880mmol) was stirred in THF (15ml). A deep purple colour formed immediately. The mixture was stirred for 4h, after which diethyl ether (15ml) was added, resulting in the precipitation of a purple powder. The mixture was centrifuged, the supernatant was removed, and the precipitate was washed with ether (2 x 15ml) and pentane (2 x 15ml), centrifuging and removing the supernatant each time. After drying under high vacuum, **55** was obtained as a purple powder. (478mg, 0.41mmol, 96%); m.p. decomposes without melting above 200°C; ν_{max}/cm^{-1} (dichloromethane) 3688m, 3600w, 2867m, 1606m, 1591w (C=N), 1469w, 1373w, 1214w, 1064s

Synthesis of 56

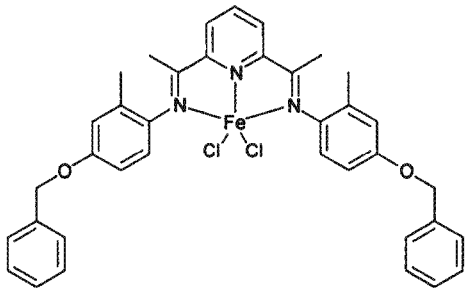

A mixture of **42** (128mg, 0.231mmol) and $FeCl_2.4H_2O$ (44mg, 0.22mmol) was stirred in THF (10ml). A dark green colour formed immediately. The mixture was stirred for 16h, after which diethyl ether (20ml) was added, resulting in the precipitation of a green solid. The mixture was centrifuged, the supernatant was removed and the precipitate was washed with ether (3 x 15ml) and pentane (1 x 15ml), centrifuging and removing the supernatant each time. After drying under high vacuum, **56** was obtained as a green powder. (142mg, 0.209mmol, 95%); m.p. decomposes without melting above 200°C; (Found: C, 65.1; H, 5.0; N, 6.0. $C_{37}H_{35}Cl_2N_3O_2Fe$ requires C, 65.3; H, 5.2; N, 6.2%); ν_{max}/cm^{-1} (dichloromethane) 3685w, 3599w, 2873w, 1590m (C=N), 1494s (Ph), 1421s, 1374m, 1220s (Ar-O), 1167m, 1096w, 1039m, 1028m; *m/z* (FAB) 679 (M^+, 21%), 644 (M^+ - Cl, 98%)

Synthesis of 57

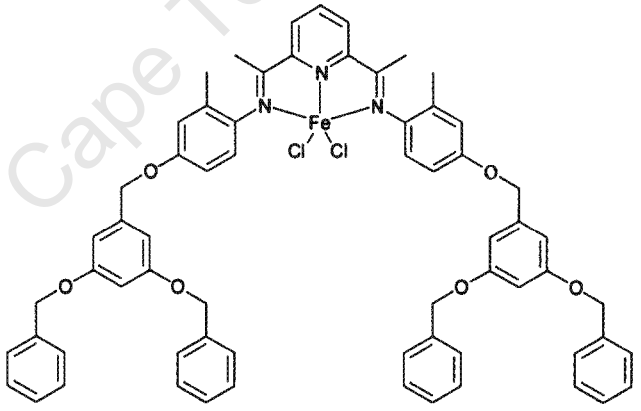

A mixture of **43** (368mg, 0.376mmol) and $FeCl_2.4H_2O$ (73mg, 0.37mmol) was stirred in THF (15ml). A dark green colour formed immediately. The mixture was stirred for 7h, after which diethyl ether (20ml) was added, resulting in the precipitation of a green solid. The mixture was centrifuged, the supernatant was removed and the precipitate was washed with ether (3 x 15ml) and pentane (2 x 15ml), centrifuging and removing the supernatant each time. After drying under high vacuum, **57** was obtained as an olive green powder. (373mg, 0.338mmol, 90%); m.p. 164 – 166°C; (Found: C, 70.7; H, 5.3; N, 3.8. $C_{65}H_{59}Cl_2N_3O_6Fe$ requires C, 70.7; H; 5.4; N, 3.8); ν_{max}/cm^{-1} (dichloromethane) 3690w, 3599w, 2922w, 2875w, 1597vs (Ar), 1495s (Ar), 1450m, 1374s, 1293m, 1219s, 1159vs, 1028m; *m/z* (FAB) 1103 (M^+, 3%), 1068 (M^+ - Cl, 8%)

Synthesis of 58

A mixture of **44** (223mg, 0.122mmol) and $FeCl_2.4H_2O$ (20mg, 0.10mmol) was stirred in THF (10ml). A dark green colour formed immediately. The mixture was stirred for 5h, after which the mixture was concentrated to approximately 5ml and diethylether (15ml) was added, resulting in the precipitation of a green solid. The mixture was centrifuged, the supernatant was removed and the residue was redissolved in THF (5ml) and precipitated out by the addition of diethylether (15ml). The mixture was centrifuged and the supernatant was removed. This procedure was repeated two further times. After drying under high vacuum, **58** was obtained as an dark green powder. (186mg, 0.0952mmol, 95%); m.p. 83 – 85°C; (Found: C, 73.6; H, 5.3; N, 2.2. $C_{121}H_{107}Cl_2N_3O_{14}Fe$ requires C, 74.4; H, 5.5; N, 2.2%); ν_{max}/cm^{-1} (dichloromethane) 2925w, 2874w, 1595s (Ar), 1495m, 1454m, 1448m, 1374m, 1217w, 1158s, 1054m, 1029m

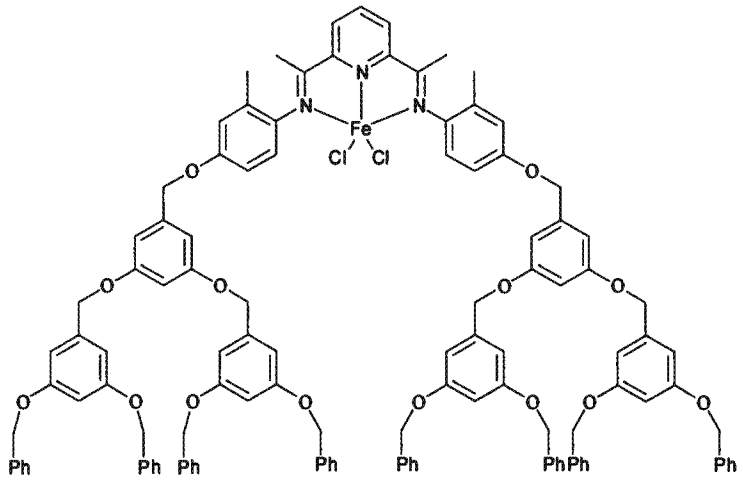

Synthesis of 59

A mixture of **45** (202mg, 0.268mmol) and $FeCl_2.4H_2O$ (50mg, 0.25mmol) was stirred in THF (15ml). A dark green colour formed immediately. The mixture was stirred for 16h, after which diethyl ether (20ml) was added, resulting in the precipitation of a dark green solid. The mixture was centrifuged, the supernatant was removed and the precipitate was washed with ether (3 x 15ml) and pentane (2 x 15ml), centrifuging and removing the supernatant each time. After drying under high vacuum, **59** was obtained as a dark green amorphous solid, which decomposes upon standing in air. (215mg, 0.244mmol, 98%); (Found: C, 62.3; H, 6.3; N, 4.5. $C_{47}H_{59}Cl_2N_3O_2Si_2Fe$ requires C, 64.1; H, 6.8; N, 4.5%); ν_{max}/cm^{-1} (dichloromethane) 3686m, 3601w, 2938m, 2871w, 1605m, 1590w (C=N), 1495s, 1374w, 1248s (Si-Me, sym def), 1220s, 1169w, 1112m (Si-Ph); *m/z* (FAB) 879 (M^+, 3%), 844, (M^+ - Cl, 31%)

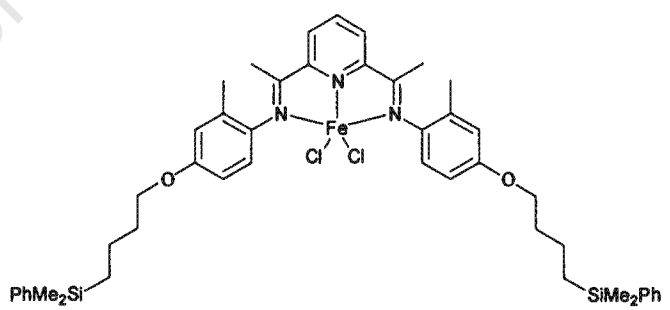

Synthesis of 60

A mixture of **46** (66mg, 0.041mmol) and $FeCl_2.4H_2O$ (20mg, 0.10mmol) was stirred in THF (10ml). A dark blue colour formed immediately. The mixture was stirred for 2h. The dark blue supernatant was separated from the excess $FeCl_2.4H_2O$, and the volatiles were removed *in vacuo* to give **60** as an air-sensitive dark blue/green oil. (57mg, 0.033mmol, 80%); *m/z* (FAB) 1730 (M^+ + H, 2%), 1694 (M^+ - Cl, 9%), 1659 (M^+ - 2Cl, 4%)

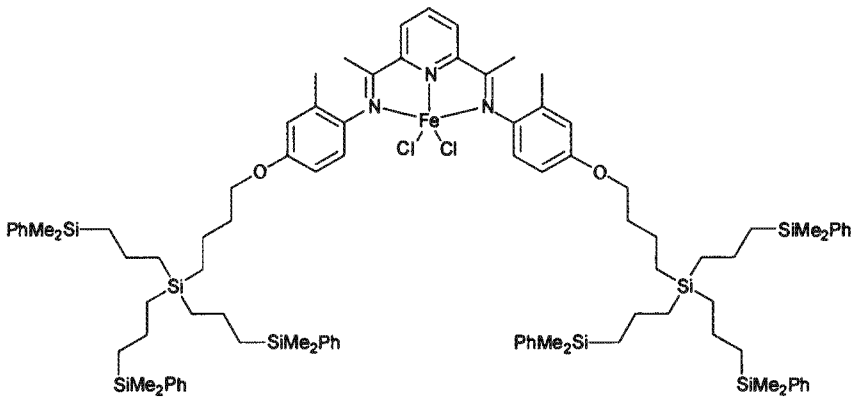

Synthesis of 61

A mixture of **47** (163mg, 0.310mmol) and $FeCl_2.4H_2O$ (53mg, 0.27mmol) was stirred in THF (15ml). A dark purple colour formed immediately. The mixture was stirred for 6h, after which diethyl ether (20ml) was added, resulting in the precipitation of a dark purple solid. The mixture was centrifuged, the supernatant was removed and the precipitate was washed with 40% THF in ether (5 x 15ml) and ether (1 x 15ml), centrifuging and removing the supernatant each time. After drying under high vacuum, **61** was obtained as a dark purple powder. (154mg, 0.236mmol, 89%); m.p. decomposes without melting above 200°C; (Found: C, 63.5; H, 4.8; N, 6.2. $C_{35}H_{31}Cl_2N_3O_2Fe$ requires C, 64.4; H, 4.8; N, 6.4%); ν_{max}/cm^{-1} (dichloromethane) 1582w (C=N), 1503vs (Ar), 1465w, 1454w, 1379m, 1238s, 1171m, 1110m, 1014m; *m/z* (FAB) 652 (M^+ + H, 3%), 616 (M^+ - Cl, 29%)

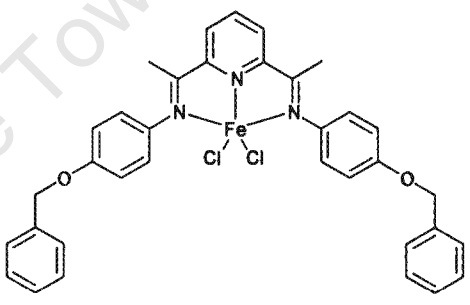

Synthesis of 62

A mixture of **48** (170mg, 0.179mmol) and $FeCl_2.4H_2O$ (26mg, 0.13mmol) was stirred in THF (20ml). A dark purple colour formed immediately. The mixture was stirred for 12h, after which it was concentrated and diethyl ether (20ml) was added, resulting in the precipitation of a dark purple solid. The mixture was centrifuged, the supernatant was removed and the precipitate was washed with 20% THF in ether (5 x 15ml), centrifuging and removing the supernatant each time. After drying under high vacuum, **62** was obtained as a dark purple powder. (134mg, 0.124mmol, 96%); m.p.115 – 119°C; (Found: C, 69.6; H, 4.8; N, 3.9. $C_{63}H_{55}Cl_2N_3O_6$ requires C, 70.3; H, 5.1; N, 3.9); ν_{max}/cm^{-1} (dichloromethane)

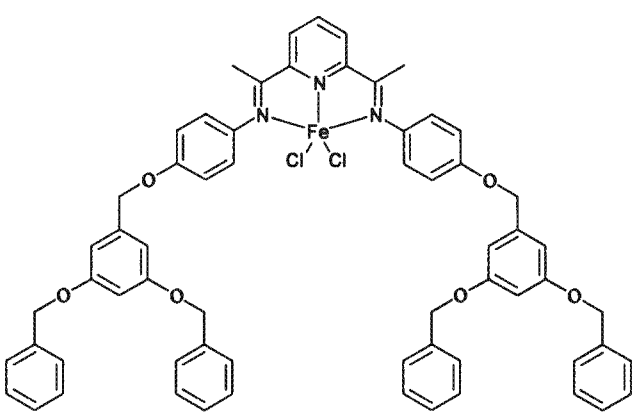

2948w, 2875w, 1598vs (Ar), 1583sh, 1500s (Ar), 1453m, 1378m, 1344w, 1321w, 1161s, 1111w, 1028m; *m/z* (FAB) 1040 (M^+ - Cl, 22%), 1005 (M^+ - 2Cl, 7%)

Synthesis of 63

A mixture of **49** (154mg, 0.212mmol) and $FeCl_2.4H_2O$ (38mg, 0.19mmol) was stirred in THF (10ml). A dark purple colour formed immediately. The mixture was stirred for 16h, after which diethyl ether (20ml) was added, resulting in the precipitation of a dark purple solid. The mixture was centrifuged, the supernatant was removed and the precipitate was washed with 20% THF in ether (3 x 15ml), centrifuging and removing the supernatant each time. After drying under high vacuum, **63** was obtained as a purple powder. (156mg, 0.183mmol, 95%); (Found: C, 61.6; H, 6.3; N, 4.8. $C_{45}H_{55}Cl_2N_3O_2Si_2Fe$ requires C, 63.4; H, 6.5; N, 4.9%); ν_{max}/cm^{-1} (dichloromethane) 2954m, 2872w, 1604m, 1580w (C=N), 1502s, 1469m, 1401m, 1378m, 1322w, 1166m, 1112m (Si-Ph), 1016m

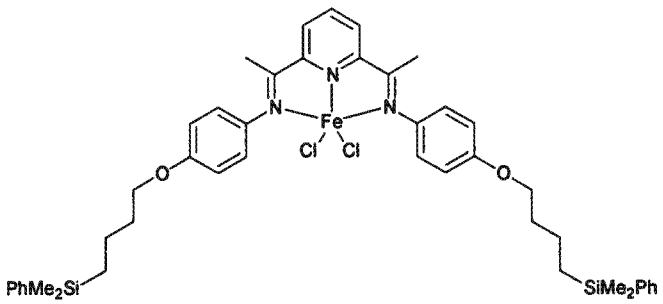

Synthesis of 64

A solution of **40** (328mg, 1.56mmol) in dichloromethane (10ml) was added to a stirred suspension of $(COD)PdCl_2$ (403mg, 1.41mmol) in dichloromethane (20ml). A thick yellow precipitate formed within 10min. The mixture was stirred for 18h. After filtration, washing with dichloromethane and pentane and drying under high vacuum, **64** was obtained as a yellow powder. (488mg, 1.26mmol, 89%); m.p. 311 – 315 (decomposes without melting); (Found: C, 43.6; H, 3.4; N, 6.7. $C_{14}H_{14}Cl_2N_2Pd$ requires C, 43.4; H, 3.6; N, 7.2%); ν_{max}/cm^{-1} (nujol mull) 1590w (C=N), 1330w, 1297w, 1263w, 1167w; δ_H (400 MHz; DMSO-d_6) 9.17 (1H, d, ^3J(HH) 5Hz, 6-H_{py}), 8.39 (1H, t, ^3J(HH) 8Hz, 4-H_{py}), 8.26 (1H, d, ^3J(HH) 8Hz, 3-H_{py}), 7.95 (1H, t, ^3J(HH) 7Hz, 5-H_{py}), 2.26 (N=C*Me*), 2.24 (aryl-*Me*); $\delta_{C\{H\}}$ (100 MHz; $CDCl_3$) 180.6 (N=*C*Me), 157.4 (2-C_{py}), 150.5 (6-C_{py}), 145.5 (1-C_{aryl}), 141.8, 131.1, 130.8, 130.0, 129.0, 128.0, 126.9, 123.0, 19.0 (aryl-*Me*), 18.7 (N=C*Me*); *m/z* (FAB) 739 ($2M^+$ - Cl, 25%), 704 ($2M^+$ - 2Cl, 14%), 353 (M^+ - Cl, 12%) , 315 (M^+ - 2Me - H, 100%)

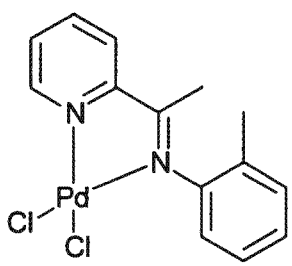

Synthesis of 65

A mixture of **41** (556mg, 2.46mmol) and $(COD)PdCl_2$ (635mg, 2.22mmol) in dichloromethane (20ml) was stirred under reflux for 16h. A thick dark yellow precipitate formed. After cooling to room temperature, the precipitate was collected by filtration and washed with dichloromethane and pentane. After drying under high vacuum, **65** was obtained as a dark yellow powder. (830mg, 2.06mmol, 93%); m.p. 310 – 315°C (decomposes without melting); (Found: C, 42.1; H, 3.5; N, 6.9. $C_{14}H_{14}Cl_2N_2OPd$ requires C, 41.7; H, 3.5; N, 6.9%);

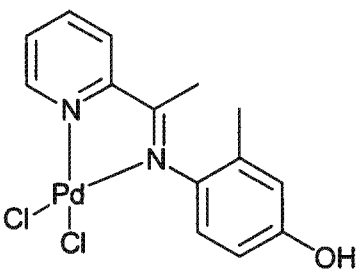

ν_{max}/cm^{-1} (nujol mull) 3316s (OH), 1584w (C=N); δ_H (400 MHz; DMSO-d_6) 9.44 (1H, s, -O*H*), 9.14 (1H, dd, ^3J(HH) 6Hz, ^5J(HH) 1.4Hz, 6-H_{py}), 8.38 (1H, td, ^3J(HH) 8Hz, ^5J(HH) 1.5Hz, 4-H_{py}), 8.24 (1H, dd, ^3J(HH) 8Hz, ^5J(HH) 0.8Hz, 3-H_{py}), 7.92 (1H, m, ^3J(HH) 7Hz, 5-H_{py}), 6.81 – 6.59 (3H, m, H_{aryl}), 2.23 (3H, s, N=C*Me*), 2.16 (3H, s, aryl-*Me*); $\delta_{C\{H\}}$ (100 MHz; DMSO-d_6) 180.9 (N=*C*Me), 157.4 (4-C_{aryl}), 156.9 (2-C_{py}), 150.4 (6-C_{py}), 141.8 (1-C_{aryl}), 137.7, 132.3, 129.8, 128.9, 124.0, 117.1, 113.5, 19.0 (aryl-*Me*), 18.9 (N=C*Me*); *m/z* (FAB) 331 (M^+ - 2Me - H, 25%)

Synthesis of 66

A mixture of **52** (261mg, 0.548mmol) and (COD)$PdCl_2$ (113mg, 0.396mmol) was stirred in dichloromethane (15ml) for 24h. The thick yellow precipitate that had formed was recovered by filtration and washed with dichloromethane and hexane to give **66** as a yellow-orange powder. (142mg, 0.217mmol, 55%); m.p. decomposes without melting above 220°C; (Found: C, 58.6; H, 4.8; N, 4.2. $C_{32}H_{32}Cl_2N_2O_2Pd$ requires C, 58.8; H, 4.9; N, 4.3%); ν_{max}/cm^{-1} (dichloromethane) 2929w, 2856w, 1602s, 1579w (C=N), 1495s (Ar), 1352m, 1233m, 1170m; δ_H (300 MHz, DMSO-d_6) 7.45 – 6.91 (16H, m, H_{aryl}), 5.09 4H, s, OCH_2Ph), 2.30 (6H, s, N=C*Me*), 2.06 (6H, s, aryl-*Me*); $\delta_{C\{H\}}$ (75 MHz, DMSO-d_6) 181.2 (N=*C*Me), 157.2 (6-C_{aryl}), 138.1 (1-C_{aryl}), 136.8 (1-C_{Ph}), 131.6, 128.2, 127.6, 127.5, 122.7, 115.9, 111.9, 69.4 (OCH_2Ph), 20.0 (*Me*), 17.9 (*Me*)

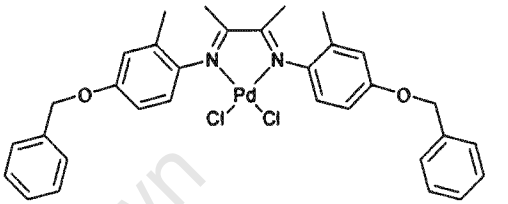

Synthesis of 67

A mixture of **53** (50mg, 0.055mmol) and (COD)$PdCl_2$ (12mg, 0.042mmol) was stirred in dichloromethane (10ml) for 24h. The volatiles were removed *in vacuo* and the residue was recrystallised from dichloromethane/hexane to give **67** as a glassy yellow solid (30mg, 0.028mmol, 66%); m.p. 170-173°C decomposes without melting; (Found: C, 66.5; H, 5.1; N, 2.6. $C_{60}H_{56}Cl_2N_2O_6$ requires C, 66.8; H, 5.2; N, 2.6%); ν_{max}/cm^{-1} (KBr disk) 2360w, 1670w, 1570w (C=N), 1474s (Ar), 1445m, 1360m, 1022m; δ_H (300 MHz, $CDCl_3$) 7.34 – 6.81 (32H, m, H_{aryl}), 4.97 (8H, s, OCH_2Ph), 4.83 (4H, s, OCH_2-aryl wedge), 2.38 (6H, s, N=C*Me*), 2.09 (6H, s, aryl-*Me*); $\delta_{C\{H\}}$ (75 MHz, $CDCl_3$) 181.0 (N=*C*Me), 160.1 (3,5-$C_{aryl\ wedge}$), 158.1 (4-$C_{aryl\ core}$), 139.3, 138.5, 136.9, 131.7, 128.5, 127.9, 127.6, 123.0, 116.9, 106.5, 101.7, 70.1(OCH_2-aryl wedge), 69.9 (OCH_2Ph), 20.3 (N=C*Me*), 18.0 (aryl-*Me*)

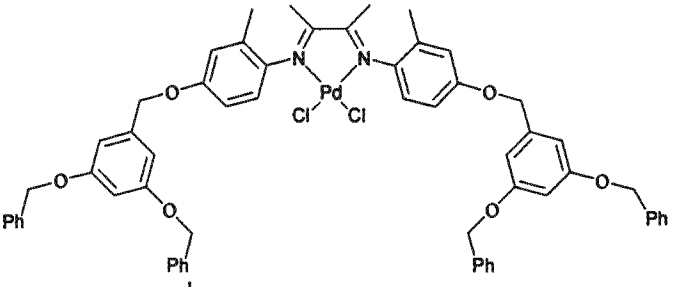

The reaction between 27 and 41

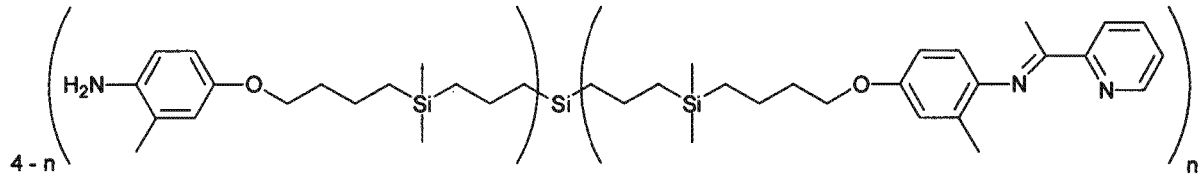

n = 4, 3, 2, 1

A mixture of **41** (205mg, 0.906mmol), **27** (202mg, 0.208mmol), K_2CO_3 (184mg, 1.33mmol) and 18-crown-6 (40mg, 0.15mmol) in acetone (20ml) was refluxed for 72h. The volatiles were removed *in vacuo*, and the residue was partitioned between dichloromethane (20ml) and slightly alkaline water (20ml). The aqueous phase was extracted with dichloromethane (3 x 20ml), and the combined organic fractions were washed with slightly alkaline water (3 x 20ml) and slightly alkaline brine (1 x 20ml). After drying over Na_2SO_4 and filtration, the volatiles were removed *in vacuo*, leaving a dark yellow oil (310mg). Purification was not possible, as this material was soluble in a wide range of solvents. ^{1}H NMR analysis indicated the absence of unreacted –C*H*$_2$Br (t, 3.41). Some characteristic peaks of the expected products were observed: δ_H (200 MHz; C_6D_6) 8.49 (m, H_{py}), 7.2 – 6.5 (m, H_{py} and H_{aryl}), 3. 83 (t, ^3J(HH) 7Hz, -Si(CH$_2$)$_3$C*H*$_2$O-), 2.44 (s, N=C*Me*), 2.14 (s, aryl-*Me*), 1.9 – 1.5 (m, all -CH$_2$C*H*$_2$CH$_2$-), 0.9 – 0.5 (all –SiC*H*$_2$CH$_2$-), 0.13 (s, Si(CH$_2$)$_3$Si*Me*$_2$(CH$_2$)$_4$-). However, other peaks indicated a degree of hydrolysis of the imine: δ_H 3.50 (br s, aryl-N*H*$_2$), 2.08 (s, aryl-*Me*), 0.11 (s, Si(CH$_2$)$_3$Si*Me*$_2$(CH$_2$)$_4$-).

The reaction between 27 and 65

A mixture of **65** (383mg, 0.949mmol), **27** (225mg, 0.231mmol), K_2CO_3 (160mg, 1.16mmol) and 18-crown-6 (30mg, 0.12mmol) in acetone (30ml) was refluxed for 48h. The solution went black after a few hours. The volatiles were removed *in vacuo*, leaving an intractable black tar. No attempts were made to analyse this decomposed product.

9.5 Experimental details pertaining to chapter 5

Synthesis of 2,6-bis-[1-(4-ethoxy-2-methylphenylimino)ethyl]pyridine (68)

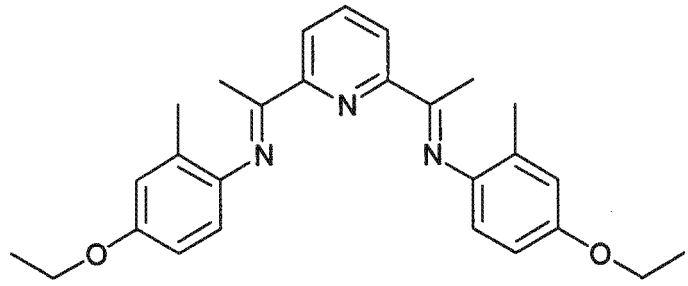

A stirred mixture of **37** (421mg, 1.13mmol), ethyl bromide (5.0ml, 7.3g, 67mmol), K_2CO_3 (397mg, 2.87mmol) and 18-crown-6 (60mg, 0.23mmol) in acetone (30ml) was refluxed (b.p. ethyl bromide: 37 - 40°C) for 48h. The volatiles were removed *in vacuo* and the residue was partitioned between dichloromethane and slightly alkaline water. The aqueous phase was extracted with dichloromethane (3 x 20 ml), and the combined organic fractions were then washed with slightly alkaline water (3 x 20 ml) and slightly alkaline brine (1 x 20 ml). After drying over Na_2SO_4 and filtration, the volatiles were removed *in vacuo*, leaving a waxy yellow solid. Recrystallisation from dichloromethane/hexane gave **68** as a bright yellow crystalline solid. (412mg, 0.960mmol, 85%); m.p. 148 – 150°C; (Found: C, 75.1; H, 7.1; N, 9.5. $C_{27}H_{31}N_3O_2$ requires C, 75.5; H, 7.3; N, 9.8%); ν_{max}/cm^{-1} (dichloromethane) 3064w, 3056w, 3046w, 2990w, 1636s (C=N), 1569m, 1492s (Ar), 1478s, 1429s, 1366m, 1210vs; δ_H (400 MHz. $CDCl_3$) 8.39 (2H, d, ^3J(HH) 8Hz, *m*-H_{py}), 7.86 (1H, t, ^3J(HH) 8Hz, *p*-H_{py}), 6.83 – 6.61 (6H, m, H_{aryl}), 4.04 (4H, q, ^3J(HH) 7Hz, OCH_2CH_3), 2.37 (6H, s, N=C*Me*), 2.13 (6H, s, aryl-*Me*), 1.42 (6H, t, ^3J(HH) 7Hz, OCH_2CH_3); $\delta_{C\{H\}}$ (100 MHz; $CDCl_3$) 167.0 (N=*C*Me), 155.6 (4-C_{aryl}), 155.5 (2,6-C_{py}), 143.1 (1-C_{aryl}), 136.6 (4-C_{py}), 128.9, 122.0, 119.1, 116.6, 112.0, 63.6 (OCH_2CH_3), 18.0 (aryl-*Me*), 16.1 (N=C*Me*), 14.9 (OCH_2CH_3); *m/z* (FAB) 430 (M^+ + H, 100%), 414 (M^+ - Me, 31%)

Synthesis of 2,6-bis-[1-(4-bromo-2-methylphenylimino)ethyl]pyridine (69)

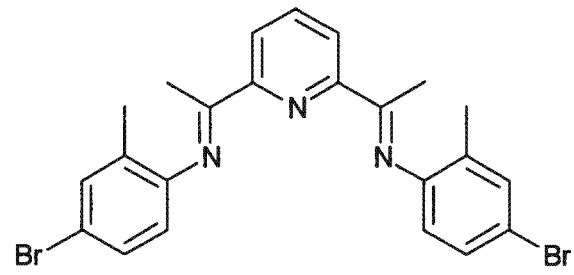

A mixture of 2,6-diacetylpyridine (412mg, 2.52mmol), 4-bromo-2-methylaniline (948mg, 5.10mmol) and *p*-toluenesulfonic acid (a few crystals) in toluene (35ml) was refluxed for 4h, collecting the water by-product in a Dean Stark condenser. The mixture was cooled to room temperature and concentrated. Precipitation of the crude product was induced by addition of pentane (15ml). After allowing completion of precipitation at -15°C, the precipitate was recovered by filtration, and recrystallised from dichloromethane / methanol to give **69** as a pale yellow crystalline solid. (1.030g, 2.063mmol, 82%); m.p. 149 – 151°C; (Found: C, 55.5; H, 4.1; N, 8.3. $C_{23}H_{21}Br_2N_3$ requires C, 55.3; H, 4.2; N, 8.4%); ν_{max}/cm^{-1} (dichloromethane) 1644vs (C=N), 1569m, 1474vs, 1367m, 1223m, 1120s; δ_H (400 MHz; C_6D_6) 8.34 (2H, d, ^3J(HH) 8Hz, *m*-H_{py}), 7.28 – 7.20 (5H, m, *p*-H_{py} and 3,5-H_{aryl}), 6.32 (2H, d, ^3J(HH) 8Hz, 6-H_{aryl}), 2.18 (6H, s, N=C*Me*), 1.89 (6H, s, aryl-*Me*); $\delta_{C\{H\}}$ (100 MHz; $CDCl_3$) 167.0 (N=*C*Me), 155.5 (2,6-C_{py}), 149.3 (1-C_{aryl}), 136.9 (4-C_{aryl}), 133.6, 129.8, 129.7, 122.7, 120.0, 116.8, 17.5 (aryl-*Me*), 16.1 (N=C*Me*); *m/z* (FAB) 500 (M^+ + H, 100%), 484 (M^+ - Me, 27%)

Synthesis of 2,6-bis-[1-(2-methyl-4-nitrophenylimino)ethyl]pyridine (70)

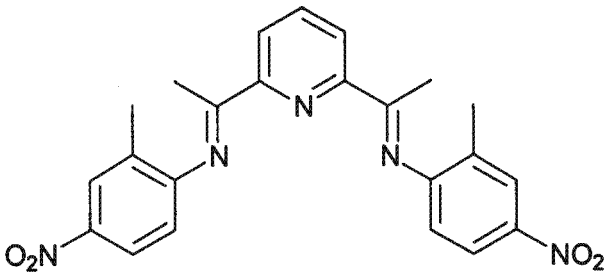

A mixture of 2,6-diacetylpyridine (533mg, 3.27mmol), 2-methyl-4-nitroaniline (994mg, 6.53mmol) and *p*-toluenesulfonic acid (a few crystals) in toluene (50ml) was refluxed for 16h, collecting the water by-product in a Dean Stark condenser. Some decomposition was apparent. The yellow solution was filtered to remove insoluble decomposition products, and hexane was added to induce precipitation. After allowing completion of precipitation at -15°C, the yellow precipitate was recovered by filtration, washing with pentane. Recrystallisation from dichloromethane/hexane gave **70** as a yellow crystalline solid. (1.053g, 2.44mmol, 75%); m.p. 221 – 223°C; (Found: C, 63.7; H, 4.7; N, 15.9. $C_{23}H_{25}N_5O_4$ requires C, 64.0; H, 4.9; N, 16.2%); ν_{max}/cm^{-1} (dichloromethane) 2925w, 1652s (C=N), 1606m, 1582vs, 1515vs (NO_2), 1478m, 1343vs (NO_2), 1225vs; δ_H (300 MHz; $CDCl_3$) 8.42 (2H, d, ^3J(HH) 8Hz, *m*-H_{py}), 8.16 – 8.08 (4H, m, 3,5-H_{aryl}), 7.96 (1H, t, ^3J(HH) 8Hz), 6.79 (2H, d, ^3J(HH) 8Hz, 6-H_{aryl}), 2.36 (6H, s, N=C*Me*), 2.20 (6H, s, aryl-*Me*); $\delta_{C\{H\}}$ (75 MHz; $CDCl_3$) 167.3 (N=*C*Me), 155.9 (2,6-C_{aryl}), 154.5 (1-C_{aryl}), 144.0 (4-C_{aryl}), 137.2, 128.2, 125.9, 123.1, 122.6, 118.3, 17.8 (aryl-*Me*), 16.8 (N=C*Me*); *m/z* (FAB) 432 (M^+ + H, 37%), 416 (M^+ - Me, 10%)

Synthesis of 2,6-bis-[1-(2,4-dimethylphenylimino)ethyl]pyridine (71)

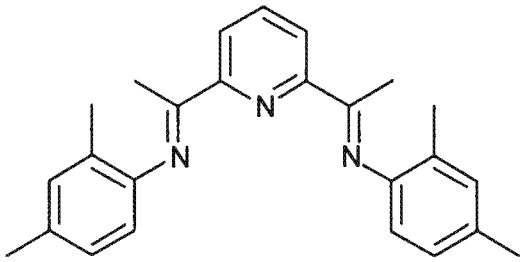

This compound has been prepared by another method in the literature.[18] A mixture of 2,6-diacetylpyridine (465mg, 2.85mmol), 2,4-dimethylaniline (1.0ml, 980mg, 8.1mmol) and *p*-toluenesulfonic acid (a few crystals) in toluene (40ml) was refluxed for 12h, collecting the water by-product in a Dean Stark condenser. A yellow colour formed. The volatiles were removed *in vacuo*, leaving a yellow oil. Addition of methanol resulted in the immediate precipitation of a yellow solid, which was collected by filtration and washed with methanol. After recrystallisation from dichloromethane/methanol, **71** was obtained as a yellow crystalline material (815mg, 2.21mmol, 77%); m.p. 121 – 123°C; (Found: C, 80.8; H, 7.4; N, 11.2. $C_{27}H_{25}N_3$ requires C, 81.3; H, 7.4; N, 11.4%); ν_{max}/cm^{-1} (dichloromethane) 2923w, 1640vs (C=N), 1610w, 1569m, 1491s, 1452w, 1366s, 1323w, 1218s, 1119s, 1077w; δ_H (400 MHz; $CDCl_3$) 8.41 (2H, d, ^3J(HH) 8Hz, *m*-H_{py}), 7.88 (1H, t, ^3J(HH) 8Hz, *p*-H_{py}), 7.07 – 6.59 (6H, m, H_{aryl}), 2.36 (6H, s, aryl-*Me*), 2.35 (6H, s, aryl-*Me*), 2.12 (6H, s, N=C*Me*); $\delta_{C\{H\}}$ (100 MHz; $CDCl_3$) 167.0 (N=*C*Me), 155.7 (2,6-C_{py}), 147.6 (1-C_{aryl}), 136.8 (4-C_{aryl}), 133.0 (4-C_{py}), 127.2, 127.0, 122.3, 118.2, 20.9 (4-aryl-*Me*), *17.8* (2-aryl-*Me*), 16.3 (N=C*Me*). Spectroscopic data is in agreement with the literature.[18]

Attempted synthesis of {2,6-bis-[1-(4-hydroxy-2-methylphenylimino)ethyl]pyridine}iron dichloride

A mixture of **37** (198mg, 0.530mmol) and $FeCl_2.4H_2O$ (101mg, 0.508mmol) was stirred in THF (10ml). A dark green colour formed almost immediately. The mixture was stirred for 4h, after which diethyl ether (15ml) was added, resulting in the precipitation of a dark green complex. After centrifuging the mixture, the supernatant was removed, and the precipitate was washed with ether (3 x 15ml) and pentane (1 x 15ml), centrifuging and removing the supernatant each time. During this work-up procedure, the colour darkened significantly due to apparent decomposition. After drying under high vacuum a dark green powder was recovered. (240mg); *m/z* (EI) 499 (M^+, 3%), 464 (M^+ - Cl, 25%), 429 (M^+ - 2Cl, 10%)

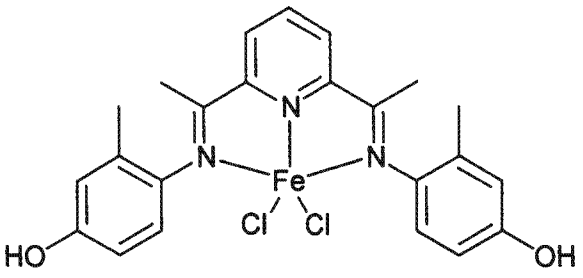

Synthesis of 72

A mixture of **68** (92mg, 0.21mmol) and $FeCl_2.4H_2O$ (39mg, 0.20mmol) was stirred in THF (10ml). A dark green precipitate formed almost immediately. The mixture was stirred for 6h, after which diethyl ether (15ml) was added, resulting in complete precipitation of the dark green complex. The mixture was centrifuged, the supernatant was removed and the precipitate was washed with ether (3 x 15ml) and pentane (1 x 15ml), centrifuging and removing the supernatant each time. After drying under high vacuum, **72** was obtained as a dark green powder. (105mg, 0.189mmol, 96%); m.p. decomposes without melting above 200°C; (Found: C, 58.3; H, 5.7; N, 6.6. $C_{27}H_{31}Cl_2N_3O_2Fe$ requires C, 58.3; H, 5.6; N, 7.8%); ν_{max}/cm^{-1} (dichloromethane) 1592w (C=N), 1577w, 1495m, 1477w, 1393w, 1374w, 1220s; *m/z* (EI) 555 (M^+, 17%), 520 (M^+ - Cl, 100%), 485 (M^+ - 2Cl, 23%)

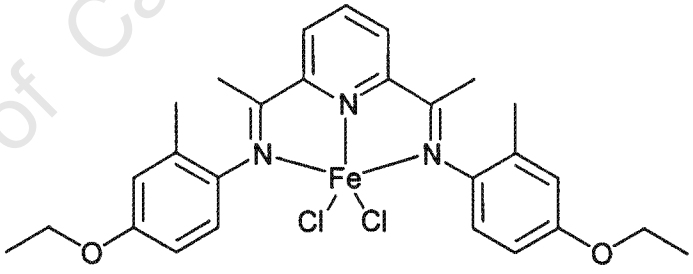

Synthesis of 73

A mixture of **69** (54mg, 0.108mmol) and $FeCl_2.4H_2O$ (18mg, 0.091mmol) was stirred in THF (10ml). A dark purple precipitate formed almost immediately. The mixture was stirred for 6h, after which diethyl ether (15ml) was added, resulting in complete precipitation of the purple complex. The mixture was centrifuged, the supernatant was removed and the precipitate was washed with ether (3 x 15ml) and pentane (1 x 15ml),

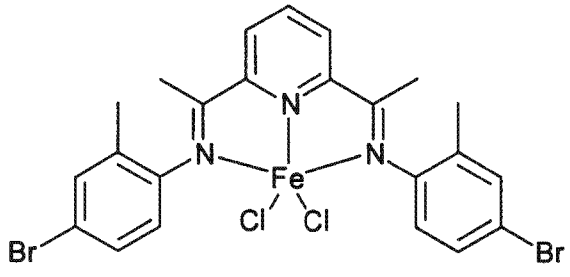

centrifuging and removing the supernatant each time. After drying under high vacuum, **73** was obtained as a flaky purple solid. (46mg, 0.73mmol, 81%); m.p. decomposes without melting above 200°C; (Found: C, 45.0; H, 3.5; N, 6.3. $C_{23}H_{21}Br_2Cl_2N_3Fe$ requires C, 44.1; H, 3.4; N, 6.7%); ν_{max}/cm^{-1} (dichloromethane) 1622w, 1589w (C=N), 1478m, 1375m; *m/z* (EI) 625 (M^+, 20%), 590 (M^+ - Cl, 100%)

Synthesis of 74

A mixture of **70** (323mg, 0.748mmol) and $FeCl_2.4H_2O$ (140mg, 0.704mmol) was stirred in THF (15ml). A dark green precipitate formed almost immediately. The mixture was stirred for 16h, after which diethyl ether (15ml) was added, resulting in complete precipitation of the dark green complex. The mixture was centrifuged, the supernatant was removed and the precipitate was washed with ether (3 x 15ml) and pentane (1 x 15ml), centrifuging and removing the supernatant each time. After drying under high vacuum, **74** was obtained as a dark green powder. (370mg, 0.663mmol, 94%); m.p. decomposes without melting above 200°C; (Found: C, 50.4; H, 3.9; N, 10.7. $C_{23}H_{21}Cl_2N_5O_4Fe$ requires C, 49.5; H, 3.8; N, 11.6%); ν_{max}/cm^{-1} (dichloromethane) 1585w (C=N), 1523s, 1482w, 1374s; *m/z* (EI) 557 (M^+, 2%), 522 (M^+ - Cl, 10%)

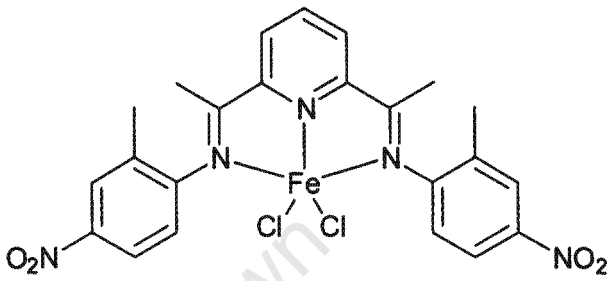

Synthesis of 75

This compound has been prepared by by a modified literature procedure.[18] **71** (524mg, 1.42mmol) and $FeCl_2.4H_2O$ (233mg, 1.17mmol) was stirred in THF (15ml). A dark blue colour formed almost immediately. The mixture was stirred for 6h, after which diethyl ether (15ml) was added, resulting in the precipitation of a dark green complex. The mixture was centrifuged, the supernatant was removed and the precipitate was washed with 20% THF in ether (5 x 15ml), centrifuging and removing the supernatant each time. After drying under high vacuum, **75** was obtained as a blue powder. (565mg, 1.14mmol, 97%); m.p. decomposes without melting above 200°C; (Found: C, 60.6; H, 5.7; N, 7.4. $C_{25}H_{27}Cl_2N_3Fe$ requires C, 60.5; H, 5.5; N, 8.5%); ν_{max}/cm^{-1} (dichloromethane) 2864w, 1593w (C=N), 1494m, 1374w, 1223w, 1063w

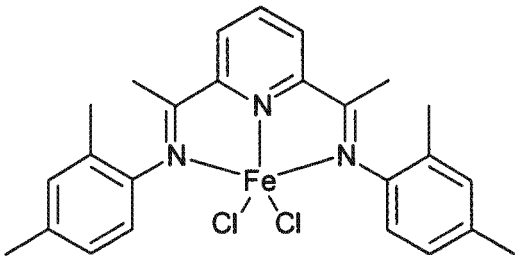

9.6 Experimental details pertaining to chapter 6

Catalytic conditions

Ethene pressure:	1atm
Catalyst loading:	20μmol
Al : Fe	400 : 1
Initial temperature:	30°C
Solvent:	toluene
Total volume:	30ml

Catalytic procedure

The reaction vessel (a 100ml glass 2-necked round bottomed flask) was connected *via* a three-way tap to the Schlenk line and the ethene line. The ethene line was connected to a mercury bubbler so as to release the pressure at just above 1 atmosphere ethene. The vessel was placed in a large oil bath (1.5litre), the temperature of which was maintained at close to 30°C by a thermocouple connected to the stirrer/hot plate. The vessel was opened, and toluene (22.7ml) was added against a flow of argon. In a separate Schlenk tube, a suspension of the precatalyst was prepared such that 20μmol was present in 2.0ml toluene. This was stirred vigorously to ensure uniform distribution of the precatalyst through the suspension. MAO (5.3ml of a 10% solution in toluene) was added to the reaction vessel, and the mixture was stirred (the same stirrer bar and rate of stirring was used in each catalytic run). The ethene pressure was increased so that the gas started bubbling through the mercury bubbler. The MAO/toluene mixture was then placed under ethene pressure (1 atm) and degassed under vacuum three times, refilling with ethene each time. This was done by using the three-way tap to switch between vacuum (Sclenk-line) and ethene (ethene line). The precatalyst (20μmol in 2.0ml toluene) was then added against a flow of ethene. The catalyst is activated immediately by the MAO, as indicated by the formation of an orange colour. The catalytic reaction was then allowed to proceed for the desired time (60 or 20 minutes), during which time the ethene pressure was maintained such that a constant release through the bubbler was observed. The reaction was then quenched by the addition of isopropanol (5.0ml) and HCl (20ml, 1.0M).

Work-up procedure and analysis

After quenching the reaction, the aqueous and organic phases were separated. The aqueous phase was extracted with toluene (3 x 30ml) and the combined organic fractions were washed with water (3 x 30ml) and brine (1 x 30 ml). The organic fractions were then dried over Na_2SO_4. The mixture was then filtered into a 250ml volumetric flask, washing the Na_2SO_4 with more toluene to ensure all the oligomers had been transferred to the flask. Any insoluble products (low molecular weight polymers) were scraped off the filter paper, dried, and weighed. A known quantity of 1-undecene (100mg in 5.00ml) was transferred to the volumetric flask, and the volume was made up to 250ml with toluene. After thoroughly shaking up the

flask, gas chromatography was used to analyse the oligomers. The volatiles were then removed *in vacuo*, leaving the involatile oligomers and some residual toluene. The mass was recorded (isolated yield), and the oligomers were redissolved in hexane (100ml). This solution was again analysed by gas chromatography.

Calculation of yield and TON

From the GC data, the yield was determined by using a TRUE BASIC program to calculate the mass of volatile oligomers lost and the mass of residual toluene included in the isolated yield. The code for the program is shown in appendix C.

9.7 Experimental details pertaining to chapter 7

Synthesis of literature compounds

Trimethylsilylbis(diphenylphosphino)methane[198] (**76**), $Mo(CO)_4(COD)$[209], $Mo(CO)_4(dppm)$[209] and (dimethylsilylbis[diphenylphosphino]methane)molybdenum tetracarbonyl[212] were prepared as described in the literature.

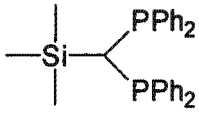

$Mo(CO)_4(COD)$

$Mo(CO)_4(dppm)$

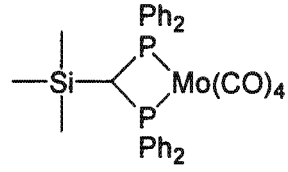

COD = 1,5-cyclooctadiene

dppm = bis(diphenylphosphino)methane

Synthesis of dimethylsilylbis(diphenylphosphino)methane (77)

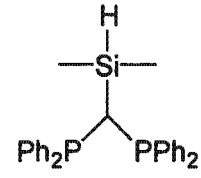

A solution of BuLi in hexane (1.9ml, 1.6M, 3.0mmol) was added over 5 min to a stirred solution of dppm (1.076g, 2.80mmol) and TMEDA (0.43ml, 2.9mmol) in toluene (20ml). The mixture was stirred for 3h. $ClSiMe_2H$ (0.36ml, 3.2mmol) was then added, resulting in the immediate formation of a white precipitate of LiCl. After additional stirring for 1h, the mixture was centrifuged, and the clear supernatant was separated from the LiCl. After removal of the volatiles *in vacuo*, a clear oil remained. After trituration with pentane, a white powder was recovered and recrystallised from toluene/pentane to give **77**, contaminated with a small amount of free dppm, as a white powder. (781mg, 1.76mmol, 63%); δ_H (300 MHz, C_6D_6) 7.65 – 6.98 (20H, m, H_{aryl}), 4.26 (1H, m, Si-*H*), 2.80 (1H, m, $[Ph_2P]_2CHSi$), -0.19 (6H, d, ^3J(HH) 4Hz, Si-*Me*); $\delta_{C\{H\}}$ (75 MHz, C_6D_6) 134.7 – 127.6 (C_{aryl}), 16.8 (t, ^1J(PC) 79Hz, $[Ph_2P]_2CHSi$), -3.2 (t, ^3J(PC) 4Hz, Si-*Me*), $\delta_{P\{H\}}$ (120 MHz, C_6D_6) -11.1 (s)

Reactions of deprotonated dppm with Me_3SiCH_2X (X = Cl, I)

1) A solution of BuLi in hexane (0.80ml, 1.6M, 1.3mmol) was added over 5 min to a stirred solution of bis(diphenylphosphino)methane (398mg, 1.04mmol) and TMEDA (0.20ml, 0.15mg, 1.3mmol) in toluene (10ml). The mixture was stirred for 3h. (Chloromethyl)trimethylsilane (0.40ml, 0.35g, 2.8mmol) was added. No immediate formation of a precipitate was observed. After stirring for 24h, a small amount of white precipitate was observed. The mixture was filtered and the volatiles were removed *in vacuo*, leaving an oily residue (302mg). ^1H NMR analysis indicated that this residue was predominantly bis(diphenylphosphino)methane (c.a. 70% of total diphosphine species by integration). δ_H (200MHz, C_6D_6) 7.47 – 7.03 (H_{aryl}), 2.79 (t, ^2J(PH) 1.9Hz, PCH_2P), in agreement with the spectrum of an authentic sample.

2) In a similar experiment, (iodomethyl)trimethylsilane was used instead of (chloromethyl)trimethylsilane. After a similar work-up, bis(diphenylphosphino)methane was again recovered as the major component of the reaction residue.

3) A stirred mixture of bis(diphenylphosphino)methane (550mg, 1.43mmol) and KO^{t}Bu (161mg, 1.43mmol) in toluene (10ml) was cooled to -78°C. A solution of BuLi in hexane (1.25ml, 1.6M, 2.0mmol) was added over 5 min. The mixture was allowed to warm to room temperature. A voluminous yellow precipitate formed in the mixture, which was additionally stirred for 2h. After centrifuging, the supernatant solution was removed, and toluene (15ml) was added. The mixture was stirred briefly, and after centrifuging, the supernatant solution was again removed. Toluene (10ml) and (iodomethyl)trimethylsilane (0.70ml, 1.0g, 4.7mmol) were added, and the mixture was stirred for 16h at room temperature and then at 50°C for 4h. The yellow precipitate slowly went into solution and was replaced by a smaller mass of white precipitate. After cooling to room temperature and centrifuging, the supernatant solution was removed and the volatiles were removed *in vacuo*, leaving a yellow oil. This was recrystallised from hot ethanol to give a white solid (168mg). ^{1}H NMR analysis suggested that this material was a 65:35 mixture of dppm and the desired product (1,1'-bis(diphenylphosphino)-2-trimethylsilylethane). δ_H (200 MHz, C_6D_6) 7.49 – 7.00 (20H, m, H_{aryl}), 3.42 (1H, t, ^3J(HH) 7Hz, PCH(CH_2SiMe_3)P), 1.24 (2H, d, ^3J(HH) 7Hz, PCH(CH_2SiMe$_3$)P), -0.01 (9H, s, PCH(CH_2SiMe_3)P).

Attempted platinum catalysed reaction between allyltrimethylsilane and 77

To a stirred solution of 77 (507mg, 1.14mmol) and allyltrimethylsilane (0.30ml, 0.21g, 1.8mmol) in THF (4ml) was added Karstedt catalyst solution (0.1ml). A yellow colour was observed to form. The reaction was stirred at room temperature for 24 h and then under reflux for a further 24h. The reaction was monitored by IR spectroscopy, and no reaction was observed. In particular, the characteristic C=C stretch of the allyltrimethylsilane at ν_{max}/cm^{-1} = 1630 persisted. The volatiles were removed *in vacuo*, and the ^{1}H NMR spectrum confirmed the presence of unreacted 77.

Synthesis of 3-trimethylsilylpropyl(chloromethyl)dimethylsilane (78)

To a stirred mixture of (chloromethyl)dimethylsilane (597mg, 5.50mmol) and allyltrimethylsilane (0.72ml, 0.50g, 4.4mmol) in THF (5ml) was added Karstedt catalyst solution (0.2ml). After 10s a yellow colour formed and an exotherm was observed. The mixture was stirred for 2h, during which time a black colour formed due to catalyst decomposition. The volatiles were removed *in vacuo*, and the residual oil was taken up in hexane and filtered though silica. After removal of the volatiles *in vacuo*, **78** was recovered as a colourless liquid (743mg, 3.33mmol, 76%); δ_H (300 MHz, $CDCl_3$) 2.78 (2H, s, -CH_2Cl), 1.38 (2H, m, $Me_3SiCH_2CH_2CH_2SiMe_2CH_2Cl$), 0.74 (2H, m, ^3J(HH) 8Hz, $Me_3SiCH_2CH_2CH_2SiMe_2CH_2Cl$), 0.60 (2H, m, ^3J(HH) 8Hz, $Me_3SiCH_2CH_2CH_2SiMe_2CH_2Cl$), 0.11 (6H, s, -Si$Me_2CH_2$Cl), -0.01 (9H, s, -Si$Me_3$); $\delta_{C\{H\}}$ (75

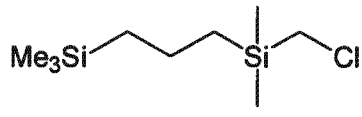

MHz, $CDCl_3$) 30.5 (-CH_2Cl), 21.2 ($Me_3SiCH_2CH_2CH_2SiMe_2CH_2Cl$), 18.2 ($SiCH_2$-), 18.1 ($SiCH_2$-), -1.6 (-$SiMe_2CH_2Cl$), -4.5 (-$SiMe_3$)

Inhibition of platinum catalysed hydrosilylation reaction by bis(diphenylphosphino)methane

To a stirred mixture of (chloromethyl)dimethylsilane (466mg, 4.29mmol), allyltrimethylsilane (0.64ml, 0.46g, 4.0mmol) and dppm (20mg, 0.052mmol) in THF (5ml) was added Karstedt catalyst solution (0.1ml). A yellow colour formed in the solution. The mixture was stirred for 20h. No reaction was apparent, as indicated by IR spectroscopy (persistence of C=C stretch of allyltrimethylsilane at ν_{max}/cm^{-1} = 1630). After removal of the volatiles *in vacuo* a light yellow solid was recovered which was identified by ^1H NMR spectroscopy to be dppm.

Synthesis of chlorodimethyl(3-trimethylsilyl)propylsilane (79)

To a stirred mixture of allyltrimethylsilane (1.24g, 10.8mmol) and chlorodimethylsilane (4.0ml, 3.4g, 36mmol) was added Karstedt catalyst solution (0.1ml). A yellow colour formed after 5 minutes. The mixture was stirred at room temperature for 16h. The mixture was cooled to 0°C and the volatiles were removed under high vacuum, leaving **79** as an air-sensitive liquid. (2.08g, 10.0mmol, 92%); δ_H (300 MHz, C_6D_6) 1.46 (2H, m, $Me_3SiCH_2CH_2CH_2SiMe_2Cl$), 0.76 (2H, m, $Me_3SiCH_2CH_2CH_2SiMe_2Cl$), 0.54 (2H, m, $Me_3SiCH_2CH_2CH_2SiMe_2Cl$), 0.24 (6H, s, $Me_3SiCH_2CH_2CH_2SiMe_2Cl$), 0.00 (9H, s, $Me_3SiCH_2CH_2CH_2SiMe_2Cl$); $\delta_{C\{H\}}$ (75 MHz, C_6D_6) 23.5 (CH_2), 20.8 (CH_2), 18.0 (CH_2) 1.7 (Me_3Si-), -1.6 (-$SiMe_2Cl$)

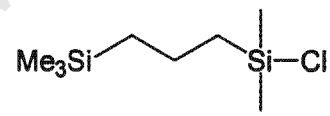

Synthesis of 80

A solution of BuLi in hexane (2.0ml, 1.6M, 3.2mmol) was added over 5 min to a stirred solution of dppm (1.16g, 3.02mmol) and TMEDA (0.53ml, 0.41mg, 3.5mmol) in toluene (10ml). The mixture was stirred for 3h. A solution of **79** (793mg, 3.80mmol) in toluene (5ml) was added, and the mixture was stirred at 45°C for 16h. A cloudy precipitate formed in the solution. After cooling to room temperature and centrifuging, the clear supernatant was separated from the precipitate and the volatiles were removed *in vacuo*. The mixture was taken up in pentane (20ml) and separated from a small amount of insoluble white powder, which is assumed to be unreacted bis(diphenylphosphino)methane. After concentration to approximately 10ml and cooling to -78°C, a white powder crystallised out, and the supernatant was removed and discarded. This material were again recrystallised from pentane at -78°C, and after drying under high vacuum, **80** was obtained as a white powder (1.532g, 2.75mmol, 91%). m.p. 55-59°C; (Found: C, 70.6; H, 7.6. $C_{33}H_{42}P_2Si_2$ requires C, 71.2; H, 7.6%); δ_H (300 MHz, C_6D_6) 7.67 – 6.84 (20H, m, H_{aryl}), 3.09 (1H, s, -$SiMe_2CH(PPh_2)_2$), 1.41 (2H, m, $Me_3SiCH_2CH_2CH_2SiMe_2$-), 0.64 (2H, m, $Me_3SiCH_2CH_2CH_2SiMe_2$-), 0.51 (2H, m, $Me_3SiCH_2CH_2CH_2SiMe_2$-), 0.05 (6H, s,

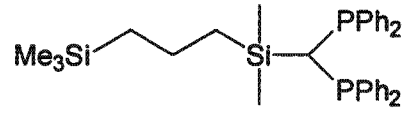

$Me_3SiCH_2CH_2CH_2Si\mathit{Me}_2$-), 0.02 (9H, s, $\mathit{Me}_3SiCH_2CH_2CH_2SiMe_2$-); $\delta_{C\{H\}}$ (75 MHz, C_6D_6) 139.5 – 126.9 (C_{aryl}), 21.4 (s, $Me_3SiCH_2\mathit{C}H_2CH_2SiMe_2$-), 21.1 (t, ^3J(PC) 5Hz, $Me_3SiCH_2CH_2\mathit{C}H_2SiMe_2CH(PPh_2)_2$), 19.1 (s, $Me_3Si\mathit{C}H_2CH_2CH_2SiMe_2$-), 17.6 (t, ^1J(PC) 47Hz, $Me_3SiCH_2CH_2CH_2SiMe_2\mathit{C}H(PPh_2)_2$), -0.8 (t, ^3J(PC) 6Hz, $-Si\mathit{Me}_2CH(PPh_2)_2$), -1.4 (s, $\mathit{Me}_3SiCH_2CH_2CH_2SiMe_2$-); $\delta_{P\{H\}}$ (120 MHz, C_6D_6) -12.8; *m/z* (EI) 556 (M^+, 47%), 541 (M^+ - Me, 7%), 483 (M^+ - $SiMe_3$, 2%), 441 (M^+ - $(CH_2)_3SiMe_3$, 5%)

Synthesis of tetrakis(3-[chlorodimethylsilyl]propyl)silane (81)

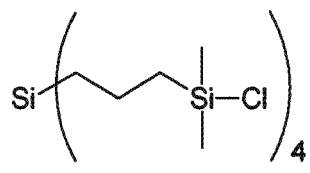

This compound was prepared by a modified literature preparation.[204] To a stirred mixture of tetraallylsilane (435mg, 2.26mmol) and chlorodimethylsilane (2.0ml, 1.7g, 18mmol) in a thick-walled glass pressure tube was added Karstedt catalyst solution (0.1ml). The mixture was cooled to -78°C and the vessel was evacuated and sealed. After warming to room temperature, the mixture was heated to 100°C. A yellow colour and an exotherm were observed after 10 minutes. The reaction mixture was stirred at 100°C for 48h. After cooling to room temperature, the volatiles were removed under high vacuum, leaving **81** as an air-sensitive viscous oil. (1.277g, 2.24mmol, 99%); δ_H (300 MHz, C_6D_6) 1.51 (8H, m, $Si[CH_2C\mathit{H}_2CH_2SiMe_2Cl]_4$), 0.76 (8H, m, $Si[CH_2CH_2C\mathit{H}_2SiMe_2Cl]_4$), 0.62 (8H, m, $Si[C\mathit{H}_2CH_2CH_2SiMe_2Cl]_4$), 0.25 (24H, s, $Si[CH_2CH_2CH_2Si\mathit{Me}_2Cl]_4$); $\delta_{C\{H\}}$ (75 MHz, C_6D_6) 23.7 ($Si[CH_2\mathit{C}H_2CH_2SiMe_2Cl]_4$), 18.2 ($Si\mathit{C}H_2$-), 17.0 ($Si\mathit{C}H_2$-), 1.8 ($Si[CH_2CH_2CH_2Si\mathit{Me}_2Cl]_4$). Spectroscopic data is in agreement with the literature.[204]

Reaction of deprotonated dppm with 81

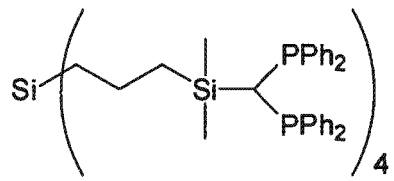

A solution of BuLi in hexane (1.5ml, 1.6M, 2.4mmol) was added to a stirred solution of dppm (1.018g, 2.65mmol) and TMEDA (0.50ml, 0.39mg, 3.3mmol) in toluene (20ml). The mixture was stirred for 3h. A solution of **81** (325mg, 0.569mmol) in toluene (8ml) was added. A cloudy precipitate formed in the solution. The mixture was stirred at 40°C for 18h, after which time the yellow colour had disappeared. The mixture was stirred additionally at 55°C for 3h and then cooled to room temperature. After centrifuging, the clear supernatant was separated from the precipitate and the volatiles were removed *in vacuo*, leaving an off-white oil. Numerous attempts were made to purify this product by recrystallisation. After oiling out of toluene/pentane at -50°C and drying under high vacuum, a white oil was recovered (305mg) ^{1}H NMR analysis indicated that impurities remained, including dppm. Although this product could not be obtained in pure form, the ^{1}H NMR suggests the probable formation of the desired product **tetrakis[3-(dimethylbis(diphenylphosphino)methylsilyl)propyl]silane**. δ_H (200 MHz, C_6D_6) 7.69 - 6.89 (80H, m, H_{aryl}), 3.13 (4H, s, $Si[CH_2CH_2CH_2SiMe_2C\mathit{H}\{PPh_2\}_2]_4$), 1.51 (8H, m, $Si[CH_2C\mathit{H}_2CH_2SiMe_2CH\{PPh_2\}_2]_4$), 0.72 (16H, m, $Si[C\mathit{H}_2CH_2C\mathit{H}_2SiMe_2CH\{PPh_2\}_2]_4$), 0.09 (24H, s, $Si[CH_2CH_2CH_2Si\mathit{Me}_2CH\{PPh_2\}_2]_4$)

This experiment was repeated with minor modifications several times, and similar results were obtained.

Synthesis of 82

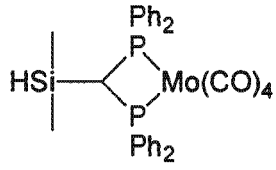

A solution of BuLi in hexane (0.94ml, 1.6M, 1.5mmol) was added to a stirred mixture of $Mo(CO)_4$(dppm) (0.842g, 1.42mmol) and TMEDA (0.25ml, 0.19g, 1.7mmol) in toluene (20ml). A yellow precipitate formed after 5 minutes. The mixture was additionally stirred for 2h. $ClSiMe_2H$ (2.0ml, 1.7g, 18mmol) was added, and after 5 minutes some of the precipitate appeared to be going into solution. The mixture was heated to 50°C for 16h, after which time the yellow colour had completely disappeared and a white precipitate had formed. The excess chlorodimethylsilane was removed *in vacuo*. 0.1M HCl (20ml) was added, and the organic and aqueous phases were separated. The aqueous fraction was extracted with diethylether (3 x 20ml) and the combined organic fractions were washed with 0.1M HCl (2 x 30ml) and acidified brine (1 x 30ml). After drying over $MgSO_4$ and filtration, the volatiles were removed *in vacuo*, leaving a light yellow solid which was recrystallised from dichloromethane/methanol to give **82** as a light yellow crystalline solid. (0.731g, 1.12mmol, 79%); (Found: C, 57.5; H, 4.2. $C_{31}H_{28}O_4P_2SiMo$ requires C, 57.2; H, 4.3%); δ_H (300 MHz, $CDCl_3$) 7.70 – 7.38 (20H, m, H_{aryl}), 4.81 (1H, td, ^2J(PH) 10Hz, ^3J(HH) 2.5Hz, $[Ph_2P]_2CHSiMe_2H$), 3.79 (1H, m, $[Ph_2P]_2CHSiMe_2H$), -0.44 (6H, d, ^3J(HH) 4Hz, $[Ph_2P]_2CHSiMe_2H$); $\delta_{C\{H\}}$ (75 MHz, $CDCl_3$) 219.1 (m, 2 x *CO trans* to P), 215.6 (t, $^3J_{cis}$(PC) 9Hz, 1 x *CO cis* to P), 208.9 (t, $^3J_{cis}$(PC) 8Hz, 1 x *CO cis* to P), 137.3 – 128.1 (C_{aryl}), 44.9 (t, ^2J(PC) 6Hz, $[Ph_2P]_2CHSiMe_2H$), -3.4 (s, $[Ph_2P]_2CHSiMe_2H$); $\delta_{P\{H\}}$ (120 MHz, $CDCl_3$) 14.4 (s); *m/z* (EI) 652 (M^+, 9%), 596 (M^+ - 2CO, 38%), 568 (M^+ - 3CO, 7%), 540 (M^+ - 4CO, 100%)

Attempted platinum catalysed reaction between allyltrimethylsilane and 82

To a stirred mixture of **82** (90mg, 0.14mmol) and allyltrimethylsilane (0.5ml, 0.36mg, 3.1mmol) in THF (5ml) was added Karstedt catalyst solution (0.1ml). The mixture was stirred at room temperature for 5h, and then at 50°C for 12h. The volatiles were removed under high vacuum, leaving a yellow solid (85mg). ^{1}H NMR analysis indicated that this residue consisted of unreacted **82**, with some $Mo(CO)_4$(dppm) also present. No indication of any hydrosilylation products could be observed.

Inhibition of platinum catalysed hydrosilylation reaction by $Mo(CO)_4$(dppm)

To a stirred mixture of (chloromethyl)dimethylsilane (462mg, 4.25mmol), allyltrimethylsilane (309mg, 2.70mmol) and $Mo(CO)_4$(dppm) (20mg, 0.034mmol) in THF (3ml) was added Karstedt catalyst (0.2ml). The mixture was stirred for 16h. No reaction was apparent, as indicated by IR spectroscopy (persistence of C=C stretch of allyltrimethylsilane at ν_{max}/cm^{-1} = 1630). After removal of the volatiles *in vacuo* a solid residue, presumably of $Mo(CO)_4$(dppm) was recovered (23mg)

Reaction of deprotonated $Mo(CO_4)$(dppm) with 79

A solution of BuLi in hexane (0.52ml, 1.6M, 0.83mmol) was added to a stirred mixture of $Mo(CO)_4$(dppm) (490mg, 0.827mmol) and TMEDA (0.15ml, 0.12g, 0.99mmol) in toluene (15ml). A yellow precipitate

formed after 5 minutes. The mixture was additionally stirred for 1.5h. A solution of **78** (190mg, 0.910mmol) in toluene (5ml) was added. The mixture was heated to 50°C for 16h. After cooling to room temperature, water (20ml) was added, and the organic and aqueous phases were separated. The aqueous fraction was extracted with diethylether (3 x 20ml) and the combined organic fractions were washed with water (2 x 30ml) and brine (1 x 30ml). After drying over $MgSO_4$ and filtration through a pad of silica, the volatiles were removed *in vacuo*, leaving a waxy yellow solid (483mg). ^{1}H NMR analysis indicated that a mixture of products was present, including $Mo(CO)_4$(dppm) and the desired product **83** (see below) in a 65:35 ratio.

Synthesis of 83

A mixture of **80** (347mg, 0.623mmol) and $Mo(CO)_4$(COD) (256mg, 0.80mmol) in toluene was stirred at 45°C for 48h. The solution became darker yellow and the reaction was monitored by IR spectroscopy. New peaks at 2018, 1929 and 1892cm^{-1} indicated the formation of the desired product. After 48h the reaction was judged to be complete, and the mixture was filtered through a pad of silica and concentrated to the point of crystallisation. Crystallisation was allowed to complete at -15°C, and the crystals were collected by filtration and washed with cold hexane. After drying under high vacuum, **83** was obtained as a yellow crystalline solid. (362mg, 0.473mmol, 76%); m.p.147 – 151°C; (Found: C, 57.7; H, 5.4. $C_{37}H_{42}O_4P_2Si_2Mo$ requires C, 58.1; H, 5.5%); ν_{max}/cm^{-1} (toluene) 2018s, 1928m, 1893vs; δ_H (300 MHz, $CDCl_3$) 7.72 – 7.36 (20H, m, H_{aryl}), 4.94 (1H, t, ^2J(PH) 10Hz, -$SiMe_2CH[PPh_2]_2$), 0.91 (2H, m, $Me_3SiCH_2CH_2CH_2SiMe_2$-), 0.25 (2H, m, $Me_3SiCH_2CH_2CH_2SiMe_2$-), 0.07 (2H, m, $Me_3SiCH_2CH_2CH_2SiMe_2$-), -0.10 (9H, s, $Me_3SiCH_2CH_2CH_2SiMe_2$-), -0.42 (6H, s, $Me_3SiCH_2CH_2CH_2SiMe_2$-); $\delta_{P\{H\}}$ (120MHz, $CDCl_3$) 16.2 (s); *m/z* (EI) 766 (M^+, 5%), 710 (M^+ - 2CO, 33%), 682 (M^+ - 3CO, 7%), 654 (M^+ - 4CO, 100%)

Chapter 10:

References

1 K. Ziegler, E. Holtzkamp, H. Breil, and H. Martin, *Angewandte Chemie*, 1955, **67**, 541.

2 G. Natta, *Angewandte Chemie*, 1956, **68**, 393.

3 S. D. Ittel, L. K. Johnson, and M. Brookhart, *Chemical Reviews*, 2000, **100**, 1169.

4 M. Bochman, *Journal of the Chemical Society, Dalton Transactions*, 1996, 255.

5 S. Mecking, *Angewandte Chemie, International Edition*, 2001, **40**, 534.

6 H. H. Brintzinger, D. Fischer, R. Mulhaupt, B. Rieger, and R. M. Waymouth, *Angewandte Chemie, International Edition in English*, 1995, **34**, 1143.

7 R. Brull, W. H. Meyer, and H. G. Raubenheimer, *South African Journal of Chemistry*, 1998, **51**, 73.

8 J. Skupinska, *Chemical Reviews (Washington, DC, United States)*, 1991, **91**, 613.

9 P. J. Flory, *Journal of the American Chemical Society*, 1940, **62**, 1561.

10 L. K. Johnson, C. M. Killian, and M. Brookhart, *Journal of the American Chemical Society*, 1995, **117**, 6414.

11 G. J. P. Britovsek, V. C. Gibson, B. S. Kimberley, P. J. Maddox, S. J. McTavish, G. A. Solan, A. J. P. White, and J. Williams, *Chemical Communications*, 1998, 849.

12 G. J. P. Britovsek, M. Bruce, V. C. Gibson, B. S. Kimberley, P. J. Maddox, S. Mastroianni, S. J. McTavish, C. Redshaw, G. A. Solan, S. Stroemberg, A. J. P. White, and D. J. Williams, *Journal of the American Chemical Society*, 1999, **121**, 8728.

13 B. L. Small, M. Brookhart, and A. M. A. Bennett, *Journal of the American Chemical Society*, 1998, **120**, 4049.

14 G. J. P. Britovsek, G. K. B. Clentsmith, V. C. Gibson, D. M. L. Goodgame, S. J. McTavish, and Q. A. Pankhurst, *Catalysis Communications*, 2002, **3**, 207.

15 S. A. Svejda and M. Brookhart, *Organometallics*, 1999, **18**, 65.

16 C. M. Killian, L. K. Johnson, and M. Brookhart, *Organometallics*, 1997, **16**, 2005.

17 B. L. Small and M. Brookhart, *Journal of the American Chemical Society*, 1998, **120**, 7143.

18 G. J. P. Britovsek, S. Mastroianni, G. A. Solan, S. P. D. Baugh, C. Redshaw, V. C. Gibson, A. J. P. White, D. J. Williams, and M. R. J. Elsegood, *Chemistry--A European Journal*, 2000, **6**, 2221.

19 P. Cossee, *Journal of Catalysis*, 1964, **3**, 80.

20 D. J. Tempel, L. K. Johnson, R. L. Huff, P. S. White, and M. Brookhart, *Journal of the American Chemical Society*, 2000, **122**, 6686.

21 D. P. Gates, S. A. Svejda, E. Onate, C. M. Killian, L. K. Johnson, P. S. White, and M. Brookhart, *Macromolecules*, 2000, **33**, 2320.

22 T. Schleis, T. P. Spaniol, J. Okuda, J. Heinemann, and R. Mulhaupt, *Journal of Organometallic Chemistry*, 1998, **569**, 159.

23 L. Deng, T. K. Woo, L. Cavallo, P. M. Margl, and T. Ziegler, *Journal of the American Chemical Society*, 1997, **119**, 6177.

24 L. H. Shultz and M. Brookhart, *Organometallics*, 2001, **20**, 3975.

25 T. K. Woo and T. Ziegler, *Journal of Organometallic Chemistry*, 1999, **591**, 204.

26 A. S. Abu-Surrah, K. Lappalainen, U. Piironen, P. Lehmus, T. Repo, and M. Leskela, *Journal of Organometallic Chemistry*, 2002, **648**, 55.

27 L. Deng, P. M. Margl, and T. Ziegler, *Journal of the American Chemical Society*, 1997, **119**, 1094.

28 S. A. Svejda, L. K. Johnson, and M. Brookhart, *Journal of the American Chemical Society*, 1999, **121**, 10634.

29 D. J. Tempel and M. Brookhart, *Organometallics*, 1998, **17**, 2290.

30 T. M. Kooistra, Q. Knijnenburg, J. M. M. Smits, A. D. Horton, P. H. M. Budzelaar, and A. W. Gal, *Angewandte Chemie, International Edition*, 2001, **40**, 4719.

31 V. C. Gibson, M. J. Humphries, K. P. Tellmann, D. F. Wass, A. J. P. White, and D. J. Williams, *Chemical Communications (Cambridge, United Kingdom)*, 2001, 2252.

32 V. C. Gibson, K. P. Tellman, M. J. Humphries, and D. F. Wass, *Chemical Communications*, 2002.

33 G. J. P. Britovsek, V. C. Gibson, S. K. Spitzmesser, K. P. Tellmann, A. J. P. White, and D. J. Williams, *Journal of the Chemical Society, Dalton Transactions*, 2002, 1159.

34 T. Schleis, J. Heinemann, T. P. Spaniol, R. Mulhaupt, and J. Okuda, *Inorganic Chemistry Communications*, 1998, **1**, 431.

35 T. J. J. Kinnunen, M. Haukka, T. T. Pakkanen, and T. A. Pakkanen, *Journal of Organometallic Chemistry*, 2000, **613**, 257.

36 G. J. P. Britovsek, V. C. Gibson, B. S. Kimberley, S. Mastroianni, C. Redshaw, G. A. Solan, A. J. P. White, and D. J. Williams, *Journal of the Chemical Society, Dalton Transactions*, 2001, 1639.

37 G. J. P. Britovsek, V. C. Gibson, S. Mastroianni, D. C. H. Oakes, C. Redshaw, G. A. Solan, A. J. P. White, and D. J. Williams, *European Journal of Inorganic Chemistry*, 2001, 431.

38 Z. Guan and W. J. Marshall, *Organometallics*, 2002, **21**, 3580.

39 S. P. Meneghetti, P. J. Lutz, and J. Kress, *Organometallics*, 1999, **18**, 2734.

40 A. Koppl and H. G. Alt, *Journal of Molecular Catalysis A: Chemical*, 2000, **154**, 45.

41 L. Wang, W.-H. Sun, L. Han, H. Yang, Y. Hu, and X. Jin, *Journal of Organometallic Chemistry*, 2002, **658**, 62.

42 G. J. P. Britovsek, S. P. D. Baugh, O. Hoarau, V. C. Gibson, D. F. Wass, A. J. P. White, and D. J. Williams, *Inorganica Chimica Acta*, 2002, **345**, 279.

43 Y. Chen, C. Qian, R. Chen, and Y. Tang, in 'Halogen-substituted bis(phenyliminoethyl)pyridine transition metal complexes as catalysts for ethylene polymerization', Cn, 2001.

44 R. Souane, F. Isel, F. Peruch, and P. J. Lutz, *Comptes Rendus Chimie*, 2002, **5**, 43.

45 V. C. Gibson, A. Tomov, D. F. Wass, A. J. P. White, and D. J. Williams, *Journal of the Chemical Society, Dalton Transactions*, 2002, 2261.

46 D. Reardon, F. Conan, S. Gambarotta, G. Yap, and Q. Wang, *Journal of the American Chemical Society*, 1999, **121**, 9318.

47 S. Milione, G. Cavallo, C. Tedesco, and A. Grassi, *Journal of the Chemical Society, Dalton Transactions*, 2002, 1839.

48 D. Reardon, G. Aharonian, S. Gambarotta, and G. P. A. Yap, *Organometallics*, 2002, **21**, 786.

49 M. Bruce, V. C. Gibson, C. Redshaw, G. A. Solan, A. J. P. White, and D. J. Williams, *Chemical Communications (Cambridge)*, 1998, 2523.

50 D. Pappalardo, C. Tedesco, and C. Pellecchia, *European Journal of Inorganic Chemistry*, 2002, 621.

51 E. L. Dias, M. Brookhart, and P. S. White, *Organometallics*, 2000, **19**, 4995.

52 A. Held, F. M. Bauers, and S. Mecking, *Journal of the Chemical Society, Chemical Communications*, 2000, 301.

53 L. K. Johnson, S. Mecking, and M. Brookhart, *Journal of the American Chemical Society*, 1996, **118**, 267.

54 H. W. Boone, P. S. Athey, M. J. Mullins, D. Philipp, R. Muller, and W. A. Goddard, *Journal of the American Chemical Society*, 2002, **124**, 8790.

55 M. Kang, A. Sen, L. Zakharov, and A. L. Rheingold, *Journal of the American Chemical Society*, 2002, **124**, 12080.

56 B. L. Small and A. J. Marcucci, *Organometallics*, 2001, **20**, 5738.

57 S. J. McLain, J. Feldman, E. F. McCord, K. H. Gardner, M. F. Teasley, E. B. Coughlin, K. J. Sweetman, L. K. Johnson, and M. Brookhart, *Macromolecules*, 1998, **31**, 6705.

58 M. D. Leatherman and M. Brookhart, *Macromolecules*, 2001, **34**, 2748.

59 B. L. Small and M. Brookhart, *Macromolecules*, 1999, **32**, 2120.

60 J. A. Ewan, *Journal of the American Chemical Society*, 1984, **106**, 6355.

61 E. F. McCord, S. J. McLain, L. T. J. Nelson, S. D. Arthur, E. B. Coughlin, S. D. Ittel, L. K. Johnson, D. Tempel, C. M. Killian, and M. Brookhart, *Macromolecules*, 2001, **34**, 362.

62 C. M. Killian, D. J. Tempel, L. K. Johnson, and M. Brookhart, *Journal of the American Chemical Society*, 1996, **118**, 11664.

63 F. Peruch, H. Cramail, and A. Deffieux, *Macromolecules*, 1999, **32**, 7977.

64 C. Elschenbroich and A. Salzer, 'Organometallics: a concise introduction', VCH Publishers, 1989.

65 F. A. Cotton and G. Wilkinson, 'Advanced Inorganic Chemistry: a Comprehensive Text', John Wiley and Sons, 1980.

66 P. S. Braterman, 'Metal Carbonyl Spectra', New York Academic Press, 1975.

67 G. Wilkinson, F. G. A. Stone, and E. W. Abel, 'Comprehensive Organometallic Chemistry', Pergamon Press, 1982.

68 J. R. Moss, *Journal of Molecular Catalysis A: Chemical*, 1996, **107**, 169.

69 P. C. Ford and W. T. Boese, *Advances in Chemistry Series*, 1997, **253**, 221.

70 F. L'Eplattenier, *Inorganic Chemistry*, 1969, **8**, 965.

71 W. J. Carter, J. W. Kelland, S. J. Okrasinski, K. E. Warner, and J. R. Norton, *Inorganic Chemistry*, 1982, **21**, 3955.

72 J. Evans, S. J. Okrasinski, A. J. Pribula, and J. R. Norton, *Journal of the American Chemical Society*, 1977, **99**, 5835.

73 F. L'Eplattenier and C. Pelichet, *Helvetica Chimica Acta*, 1970, **53**, 1091.

74 N. J. Bristow, B. D. Moore, M. Poliakoff, G. Ryott, and J. J. Turner, *Journal of Organometallic Chemistry*, 1984, **260**, 181.

75 P. J. Harris, J. A. K. Howard, S. A. R. Knox, R. P. Phillips, F. G. A. Stone, and P. Woodward, *Journal of the Chemical Society, Dalton Transactions: Inorganic Chemistry (1972-1999)*, 1976, 377.

76 W. J. Carter, S. J. Okrasinski, and J. R. Norton, *Organometallics*, 1985, **4**, 1376.

77 S. A. Brewer, L. A. Buggey, J. H. Holloway, and E. G. Hope, *Journal of the Chemical Society, Dalton Transactions: Inorganic Chemistry*, 1995, 2941.

78 R. D. George, S. A. R. Knox, and F. G. A. Stone, *Journal of the Chemical Society, Dalton Transactions: Inorganic Chemistry (1972-1999)*, 1973, 972.

79 D. J. Blumer, K. W. Barnett, and T. L. Brown, *Journal of Organometallic Chemistry*, 1979, **173**, 71.

80 U. Koelle, *Journal of Organometallic Chemistry*, 1977, **133**, 53.

81 Y. Shvo and E. Hazum, *Journal of the Chemical Society, Chemical Communications*, 1976, 829.

82 'Inorganic Syntheses', ed. H. D. Kaesz, John Wiley and Sons, 1989.

83 D. S. C. Black, G. B. Deacon, and N. C. Thomas, *Inorganica Chimica Acta*, 1982, **65**, L75.

84 G. Bellachioma, G. Cardaci, A. Macchioni, and C. Zuccaccia, *Journal of Organometallic Chemistry*, 2001, **628**, 255.

85 G. Bellachioma, G. Cardaci, A. Macchioni, and P. F. Zanazzi, *Inorganic Chem*, 1993, **32**, 547.

86 E. A. V. Ebsworth, D. W. H. Rankin, and S. Cradock, 'Structural methods in inorganic chemistry', Blackwell Scientific Publications, 1987.

87 P. G. Jackson, *Personal Communication*, 2003.

88 F. Calerazzo, *Angewandte Chemie, International Edition English*, 1977, **16**, 299.

89 E. J. Kuhlmann and J. J. Alexander, *Coordination Chemistry Reviews*, 1980, **33**, 195.

90 H. Berke and R. Hoffmann, *Journal of the American Chemical Society*, 1978, **100**, 7224.

91 C. S. Kraihanzel and P. K. Maples, *Journal of Organometallic Chemistry*, 1969, **20**, 269.

92 C. S. Kraihanzel and P. K. Maples, *Journal of Organometallic Chemistry*, 1976, **117**, 159.

93 F. J. G. Alonso, A. Llamazares, V. Riera, M. Vivanco, M. R. Diaz, and S. G. Granda, *Journal of the Chemical Society, Chemical Communications*, 1991, 1058.

94 M. Green and D. C. Wood, *Journal of the American Chemical Society*, 1966, **88**, 4106.

95 E. G. Lundquist, K. Folting, J. C. Huffman, and K. G. Caulton, *Organometallics*, 1990, **9**, 2254.

96 C. F. J. Barnard, J. A. Daniels, and R. J. Mawby, *Journal of the Chemical Society, Dalton Transactions*, 1979, 1331.

97 R. W. Glyde and R. J. Mawby, *Inorganica Chimica Acta*, 1971, **5**, 317

98 M. A. Bennet, J. C. Jeffery, and G. B. Robertson, *Inorganic chemistry*, 1981, **20**, 330

99 G. Cardaci, G. Reichenbach, G. Bellachioma, B. Wassink, and M. C. Baird, *Organometallics*, 1988, **7**, 172

100 R. W. Marshman and P. A. Shapley, *Journal of the American Chemical Society*, 1990, **112**, 8369.

101 G. Reichenbach, G. Cardaci, and G. Bellachioma, *Journal of the Chemical Society, Dalton Transactions: Inorganic Chemistry (1972-1999)*, 1982, 847.

102 D. R. Saunders, M. Stephenson, and R. J. Mawby, *Journal of the Chemical Society, Dalton Transactions: Inorganic Chemistry (1972-1999)*, 1983, 2473.

103 D. R. Saunders, M. Stephenson, and R. J. Mawby, *Journal of the Chemical Society, Dalton Transactions: Inorganic Chemistry (1972-1999)*, 1984, 1153.

104 D. R. Saunders and R. J. Mawby, *Journal of the Chemical Society, Chemical Communications*, 1984, 140.

105 M. Pankowski and M. Bigorgne, *Journal of Organometallic Chemistry*, 1983, **251**, 333.

106 R. J. Puddephat, *Chemical Society Reviews*, 1983, **12**, 99.

107 A. Sanders, L. Cohen, W. P. Giering, D. Kenedy, and C. V. Magatti, *Journal of the American Chemical Society*, 1973, **95**, 5430.

108 M. L. H. Green and P. L. Nagy, *Journal of Organometallic Chemistry*, 1963, **1**, 58.

109 L. Cohen, W. P. Giering, D. Kenedy, C. V. Magatti, and A. Sanders, *Journal of Organometallic Chemistry*, 1974, **65**, C57

110 A. T. Patton, C. E. Strouse, C. B. Knobler, and J. A. Gladysz, *Journal of the American Chemical Society*, 1983, **105**, 5804

111 K. Roder and H. Werner, *Angewandte Chemie, International Edition English*, 1987, **26**, 686.

112 J. C. Hayes, P. Jernakoff, G. A. Miller, and N. J. Cooper, *Pure and Applied Chem*, 1984, **56**, 25.

113 W. A. Kiel, G.-Y. Lin, and J. A. Gladysz, *Journal of the American Chemical Society*, 1980, **102**, 3299.

114 H. Werner, H. Kletzen, A. Hohn, W. Paul, and W. Knaup, *Journal of Organometallic Chemistry*, 1986, **306**, 227.

115 D. A. Straus, C. Zhang, and T. D. Tilly, *Journal of Organometallic Chemistry*, 1989, **369**, C13.

116 L. Jia, X. Yang, A. Ishihara, and T. J. Marks, *Organometallics*, 1995, **14**, 3135.

117 X. Yang, C. L. Stern, and T. J. Marks, *Journal of the American Chemical Society*, 1994, **116**, 10015.

118 G. S. Hill, L. M. Rendina, and R. J. Puddephatt, *Journal of the Chemical Society, Dalton Transactions: Inorganic Chemistry*, 1996, 1809.

119 R. E. Dixon and A. Streitwieser, *Journal of Organic Chemistry*, 1992, **57**, 6125.

120 H. Werner and U. Wecker, *Journal of Organometallic Chemistry*, 2000, **593-594**, 192.

121 M. A. Bennet, I. J. McMahon, and S. Pelling, *Journal of Organometallic Chemistry*, 1990, **382**, 175.

122 D. A. Tomalia, H. Baker, J. Dewald, M. Hall, G. Kallos, S. Martin, Roeck, J. Ryder, and P. Smith, *Polymer*, 1985, **17**, 177.

123 G. R. Newkome, C. N. Moorefield, and G. R. Baker, *Aldrichimica Acta*, 1992, **25**, 31.

124 E. Buhleier, W. Wehner, and F. Vogtle, *Synthesis*, 1978, 155.

125 F. Zeng and S. C. Zimmerman, *Chemical Reviews*, 1997, **97**, 1681.

126 T. M. Miller and T. X. Neenan, *Chem. Mat.*, 1990, **2**, 346.

127 C. J. Hawker and J. M. J. Frechet, *Journal of the American Chemical Society*, 1990, **112**, 7638.

128 H.-F. Chow, Y.-K. Chan, C. C. Mak, and M.-K. Ng, *Tetrahedron*, 1996, **52**, 4277.

129 G. R. Newkome and X. Lin, *Macromolecules*, 1991, **24**, 1443.

130 K. Lorentz, R. Mulhaupt, and H. Frey, *Macromolecules*, 1995, **28**, 6657.

131 T. M. Miller, T. X. Neenan, R. Zayas, and H. E. Bair, *Journal of the American Chemical Society*, 1992, **114**, 1018.

132 L.-L. Zhou and J. Roovers, *Macromolecules*, 1992, **26**, 963.

133 A. W. Van der Made and P. W. N. M. Van Leeuwen, *Journal of the Chemical Society, Chemical Communications*, 1992, 1400.

134 D. Seyferth, D. Y. Son, A. L. Rheingold, and R. L. Ostrander, *Organometallics*, 1994, **13**, 2682.

135 C. S. Cundy, B. M. Kingston, and M. F. Lappert, *Advances in Organometallic Chemistry*, 1973, **11**, 330.

136 J. L. Speier, *Advances in Organometallic Chemistry*, 1979, **17**, 407.

137 D. N. Willing, *U.S. patent*, 1968, 3 419 593.

138 B. D. Karstedt, *U.S. patent*, 1973, 3.

139 M. F. Lappert and F. P. A. Scott, *Journal of Organometallic Chemistry*, 1995, **492**, C11.

140 R. Meijboom, *PhD thesis*, 2001.

141 R. Roesler, B. J. N. Har, and W. E. Piers, *Organometallics*, 2002, **21**, 4300.

142 M. Benito, O. Rossell, M. Seco, and G. Segales, *Inorganica Chimica Acta*, 1999, **291**, 247.

143 M. Benito, O. Rossell, M. Seco, G. Muller, J. I. Ordinas, M. Font-Bardia, and X. Solans, *European Journal of Inorganic Chemistry*, 2002, 2477.

144 D. de Groot, J. C. de Wilde, R. J. van Haaren, J. N. H. Reek, P. C. J. Kamer, P. W. N. M. van Leeuwen, E. B. Eggeling, D. Vogt, H. Kooijman, A. L. Spek, and A. W. van der Made, *Chemical Communications (Cambridge)*, 1999, 1623.

145 D. de Groot, P. G. Emmerink, C. Coucke, J. N. H. Reek, P. C. J. Kamer, and P. W. N. M. van Leeuwen, *Inorganic Chemistry Communications*, 2000, **3**, 711.

146 P. I. Coupar, P.-A. Jaffres, and R. E. Morris, *Journal of the Chemical Society, Dalton Transactions: Inorganic Chemistry*, 1999, 2183.

147 I. Sato, R. Kodaka, K. Hosoi, and K. Soai, *Tetrahedron: Asymmetry*, 2002, **13**, 805.

148 N. J. Hovestad, A. Ford, J. T. B. H. Jastrzebski, and G. van Koten, *Journal of Organic Chemistry*, 2000, **65**, 6338.

149 M. Benito, O. Rossell, M. Seco, and G. Segales, *Journal of Organometallic Chemistry*, 2001, **619**, 245.

150 I. Cuadrado, M. Moran, A. Moya, C. M. Casado, M. Barranco, and B. Alonso, *Inorganica Chimica Acta*, 1996, **251**, 5.

151 H. I. Beerens, P. Wijkens, J. T. B. H. Jastrzebski, F. Verpoort, L. Verdonck, and G. Van Koten, *Journal of Organometallic Chemistry*, 2000, **603**, 244.

152 N. J. Hovestad, E. B. Eggeling, H. J. Heidbuchel, J. T. B. H. Jastrzebski, U. Kragl, W. Keim, D. Vogt, and G. Van Koten, *Angewandte Chemie, International Edition*, 1999, **38**, 1655.

153 A. W. Kleij, R. A. Gossage, R. J. M. K. Gebbink, N. Brinkmann, E. J. Reijerse, U. Kragl, M. Lutz, A. L. Spek, and G. van Koten, *Journal of the American Chemical Society*, 2000, **122**, 12112.

154 S. W. Krska and D. Seyferth, *Journal of the American Chemical Society*, 1998, **120**, 3604.

155 Z. Wu and K. Biemann, *International Journal of Mass Spectrometry and Ion Processes*, 1997, **165**, 349.

156 D. De Groot, J. N. H. Reek, P. C. J. Kamer, and P. W. N. M. Van Leeuwen, *European Journal of Organic Chemistry*, 2002, 1085.

157 R. Meijboom, M. J. Overett, and J. R. Moss, *manuscript in preparation*, 2003.

158 R. Van Heerbeek, J. N. H. Reek, P. C. J. Kamer, and P. W. N. M. Van Leeuwen, *Tetrahedron Letters*, 1999, **40**, 7127.

159 G. E. Oosterom, J. N. H. Reek, P. C. J. Kamer, and P. W. N. M. Van Leeuwen, *Angewandte Chemie, International Edition*, 2001, **40**, 1828.

160 L. J. Twyman, A. S. H. King, and I. K. Martin, *Chemical Society Reviews*, 2002, **31**, 69.

161 J. Laane, *Journal of the American Chemical Society*, 1967, **89**, 1144.

162 J. Pikies and W. Wojnowski, *Journal of Organometallic Chemistry*, 1990, **393**, 187.

163 P. W. Jolly and G. Wilke, 'The organic chemistry of nickel', Academic Press, 1974.

164 N. M. Boag, M. Green, J. L. Spencer, and F. G. A. Stone, *Journal of Organometallic Chemistry*, 1977, **127**, C51.

165 H. Kurosawa and G. Yoshida, *Journal of Organometallic Chemistry*, 1976, **120**, 297.

166 J. V. Swisher and H.-H. Chen, *Journal of Organometallic Chemistry*, 1974, **69**, 93.

167 J. Ryan, M. G., and J. Speier, *Journal of the American Chemical Society*, 1960, **82**, 3601.

168 U. Kruerke, *Chem. Ber.*, 1962, **95**, 174.

169 J. Ohshita, A. Iwata, F. Kanetani, A. Kunai, Y. Yamamoto, and C. Matui, *Journal of Organic Chemistry*, 1999, **64**, 8024.

170 V. D. Tyurin, N. V. Ushakov, S. P. Gubin, and N. S. Nametkin, *Izvestiya Akademii Nauk SSSR, Seriya Khimicheskaya*, 1968, 1407.

171 P. E. Rakita and L. S. Worsham, *Journal of Organometallic Chemistry*, 1977, **137**, 145.

172 J. March, 'Advanced organic chemistry: reactions, mechanisms and structure', John Wiley and Sons, 1992.

173 R. Meijboom, A. T. Hutton, and J. R. Moss, *Organometallics*, 2003, **22**, 1811.

174 'Organometallics in synthesis', ed. M. Schlosser, John Wiley and Sons, 1994.

175 H. Neumann and D. Seebach, *Tetrahedron Letters*, 1976, **17**, 4839.

176 M. Schlosser, J. H. Choi, and S. Tagagishi, *Tetrahedron*, 1990, **46**, 5633.

177 S. E. Thomas, 'Organic synthesis: the roles of boron and silicon', Oxford University Press, 1991.

178 S. Zhang, X.-M. Zhang, and F. G. Bordwell, *Journal of the American Chemical Society*, 1995, 117.

179 P. Schleyer, T. Clark, A. Kos, G. W. Spitznagel, C. Rhode, D. Arad, K. N. Houk, and N. G. Rondan, *Journal of the American Chemical Society*, 1984, **106**, 6467.

180 M. A. Cook, C. Eaborn, and D. R. M. Walton, *Journal of Organometallic Chemistry*, 1971, **29**, 389.

181 C. Eaborn and J. C. Jeffrey, *Journal of the Chemical Society*, 1957, 137.

182 C. Eaborn and J. C. Jeffrey, *Journal of the Chemistry Society*, 1954, 137.

183 R. D. Walkup, R. R. Kane, and N. U. Obeyesekere, *Tetrahedron Letters*, 1990, **31**, 1531.

184 Y.-H. Liao and J. R. Moss, *Journal of the Chemical Society, Chemical Communications*, 1993, 1774.

185 Y.-H. Liao and J. R. Moss, *Organometallics*, 1995, **14**, 2130.

186 Y.-H. Liao and J. R. Moss, *Organometallics*, 1996, **15**, 4307.

187 M. Schlosser, 'Organometallics in synthesis', John Wiley and Sons, 1994.

188 H. B. Friedrich and J. R. Moss, 'Advances in Organometallic Chemistry', ed. F. G. A. Stone and R. West, Academic Press, 1991.

189 I. Gitsov, P. T. Ivanova, and J. M. J. Frechet, *Macromolecular Rapid Communications*, 1994, **15**, 387.

190 E. G. Oosterom, R. J. van Haaren, J. N. H. Reek, P. C. J. Kamer, and P. W. N. M. van Leeuwen, *Chemical Communications (Cambridge)*, 1999, 1119.

191 J. A. Dean, 'Lange's Handbook of Chemistry', McGraw-Hill, Inc., 1992.

192 B. Cornils and W. A. Herrmann, 'Applied homogeneous catalysis with organometallic compounds: a comprehensive handbook', Wiley-VCH, 2000.

193 L. Ropartz, K. J. Haxton, D. F. Foster, R. E. Morris, A. M. Z. Slawin, and D. J. Cole-Hamilton, *Journal of the Chemical Society, Dalton Transactions*, 2002, 4323.

194 M. T. Reetz, G. Lohmer, and R. Schwickardi, *Angewandte Chemie, International Edition in English*, 1997, **36**, 1526.

195 S. C. Bourque, F. Maltais, W.-J. Xiao, O. Tardif, H. Alper, P. Arya, and L. E. Manzer, *Journal of the American Chemical Society*, 1999, **121**, 3035.

196 R. A. Findeis and L. H. Gade, *Journal of the Chemical Society, Dalton Transactions*, 2002, 3952.

197 K. Issleib and H. P. Abicht, *Journal fuer Praktische Chemie (Leipzig)*, 1970, **312**, 456.

198 R. Appel, K. Geisler, and H. F. Schaeler, *Chemische Berichte*, 1979, **112**, 648.

199 C. L. Lee, Y. P. Yang, S. J. Rettig, B. R. James, D. A. Nelson, and M. A. Lilga, *Organometallics*, 1986, **5**, 2220.

200 H. Schmidbaur, J. R. Mandl, J. M. Bassett, G. Blaschke, and B. Zimmer-Gasser, *Chemische Berichte*, 1981, **114**, 433.

201 M. Lusser and P. Peringer, *Journal of Organometallic Chemistry*, 1986, **312**, C61.

202 J. W. J. Knapen, A. W. van der Made, J. C. de Wilde, P. W. N. M. van Leeuwen, P. Wijkens, D. M. Grove, and G. van Koten, *Nature (London)*, 1994, **372**, 659.

203 M. Schlosser, *Pure and Applied Chemistry*, 1988, **60**, 741.

204 B. Alonso, I. Cuadrado, M. Moran, and J. Losada, *Journal of the Chemical Society, Chemical Communications*, 1994, 1400.

205 I. Cuadrado, M. Moran, J. Losada, C. M. Casado, C. Pascual, B. Alonso, and F. Lobete, *Advances in dendritic macromolecules*, 1996, **3**, 151.

206 J. Chatt and H. R. Watson, *J. Chem. Soc.*, 1961, 4980.

207 S. O. Grim, W. L. Briggs, R. C. Barth, C. A. Tolman, and J. P. Jesson, *Inorganic Chemistry*, 1974, **13**, 1095.

208 C. Kayran, F. Kozanoglu, S. Ozkar, S. Saldamli, A. Tekkaya, and C. G. Kreiter, *Inorganica Chimica Acta*, 1999, **284**, 229.

209 A. Tekkaya, C. Kayran, S. Ozkar, and C. G. Kreiter, *Inorganic Chemistry*, 1994, **33**, 2439.

210 A. Tekkaya and S. Ozkar, *Journal of Organometallic Chemistry*, 1999, **590**, 208.

211 S. Al-Jibori and B. L. Shaw, *Journal of Organometallic Chemistry*, 1984, **273**, 213.

212 S. Al-Jibori and B. L. Shaw, *Journal of the Chemical Society, Chemical Communications*, 1982, 286.

213 S. Al-Jibori and B. L. Shaw, *Inorganica Chimica Acta*, 1983, **74**, 235.

214 J. Villieras, C. Bacquet, D. Masure, and J. F. Normant, *Journal of Organometallic Chemistry*, 1973, **50**, C7.

215 R. W. Hoffmann, H.-C. Stiasny, and J. Krueger, *Tetrahedron*, 1996, **52**, 7421.

216 D. D. Perrin and W. L. F. Armarego, 'Purification of Laboratory Chemicals', Pergamon Press, 1988.

217 J. Dixon, *personal communication*, 2003.

Acknowledgements

Any task as daunting as completing a PhD cannot be achieved without the participation, encouragement and support of others, and I am particularly indebted to the following people:

- My supervisor, Prof John Moss, for his enthusiasm, encouragement and academic direction, and also for his kindness, hospitality and for appreciating that his students are more than just fixtures in front of the fumehoods.

- Other members of the Organometallic Research Group who have had intellectual input and given practical advice towards this work. In particular Dr Reinout Meijboom, for teaching me most of what I know about organometallic laboratory techniques, and who deserves much credit for the improvements in laboratory infrastructure and techniques over the last 6 years. Also Dr Paul Beagley, for his excellent and selfless role as laboratory supervisor, and for providing practical advice and encouragement in moments of despair. The work on substituted palladium α-diimine complexes was done in collaboration with Burgert Blom. Other members of the group have contributed to a generally good atmosphere in Lab A111, and have been a part of the PhD experience, through good times and bad. They include Dr Ipe Mavunkal, Dr Meredith Hearshaw, Dr Margaret Blackie, Dr Jaisheila Rajput, Mazwi Ndlovu and Burgert Blom.

- The technical and support staff in the chemistry department, without whom none of this would have been possible, including Pete Roberts and Noel Hendricks for the NMR's, Pierro Benincasa for the microanalysis, Dr Philip Boshoff of Cape Technicon for the mass spectrometry, Dr Hong Su for the crystal structure, and also Andre, Denise, Sweetness, Arthur, John, Marilyn, Sean, Gerald and Klaus for their valuable and often unappreciated roles.

- Sasol, for the financial support that made these studies possible.

- Dr Johntho Dixon of Sastech R&D, for his enthusiasm and support, and most especially for the FID GC analysis done at the last minute when it transpired that the dinosaur at UCT was not going to do the trick. You saved the day!

- My parents, for investing so much in me while I was growing up, and for providing a wonderful home right to the end of my studies.

- My friends, in particular Rory, Belinda, Roy, Gareth, James and Rosie, for their faithful support and genuine friendship for many years.

- My fiancée, Rosalie, for your love. In the toughest times, you made it all seem worthwhile.

- Yahweh, who knew this chemistry a long time ago (but didn't give any of it away)

Appendix A: Numbered Compounds

Note: All new compounds and some literature compounds described in this thesis have been numbered. In the interests of readability, the numbers are only used in the discussion where the length of the compound's IUPAC name make this necessary. Where concise molecular formulae or names accurately describe the compound under discussion, these are preferred.

<table>
<tr><th colspan="4">Chapter 2</th></tr>
<tr><td>1</td><td> 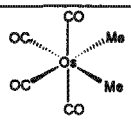 </td><td>9</td><td> 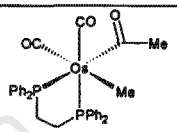 </td></tr>
<tr><td>2</td><td> 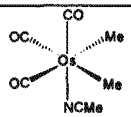 </td><td>10</td><td> 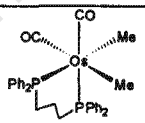 </td></tr>
<tr><td>3</td><td> 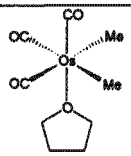 </td><td>11</td><td> 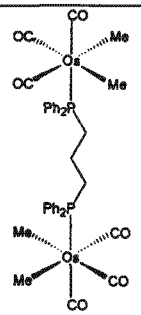 </td></tr>
<tr><td>4</td><td> 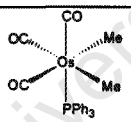 </td><td>12</td><td> 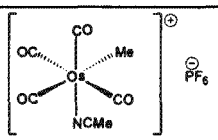 </td></tr>
<tr><td>5</td><td> 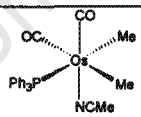 </td><td>13</td><td> 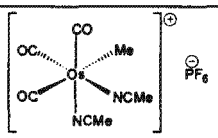 </td></tr>
<tr><td>6</td><td> 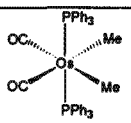 </td><td></td><td></td></tr>
<tr><td>7</td><td> 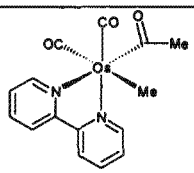 </td><td></td><td></td></tr>
<tr><td>8</td><td> 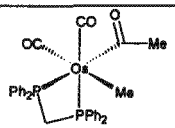 </td><td></td><td></td></tr>
</table>

Chapter 3

14	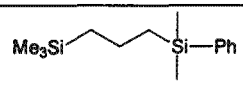	25	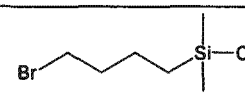
15	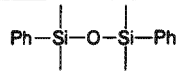	26	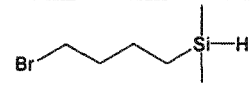
16	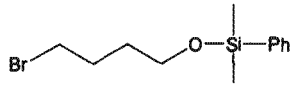	27	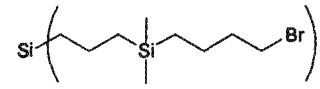
17	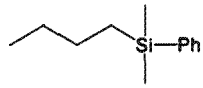	28	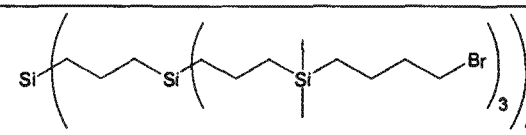
18	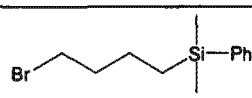	29	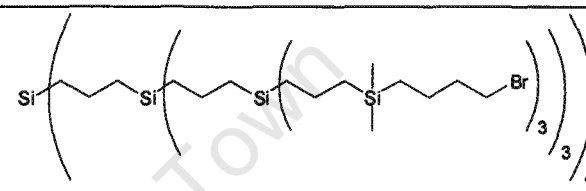
19	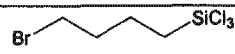	30	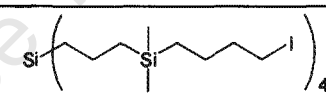
20	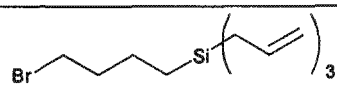	31	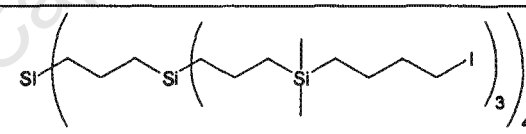
21	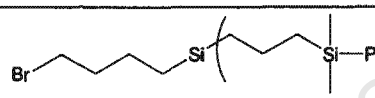	32	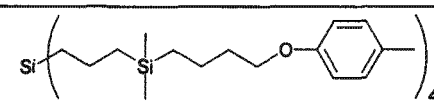
22	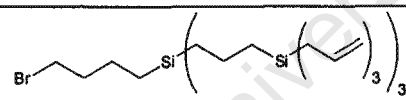	33	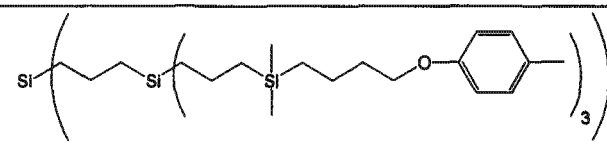
23	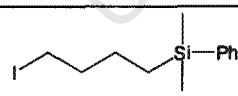	34	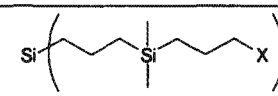 X = 30% CMe_3 70% $SiMe_3$
24	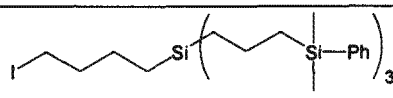		

Chapter 4

35	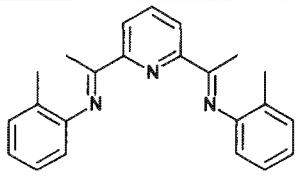	41	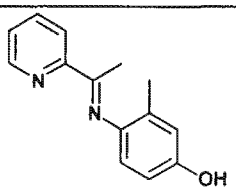
36	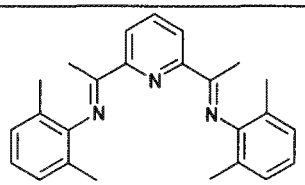	42	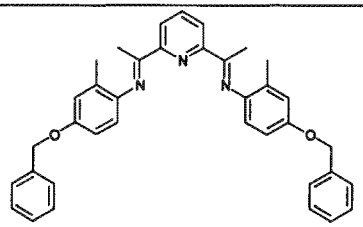
37	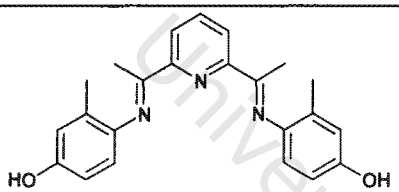	43	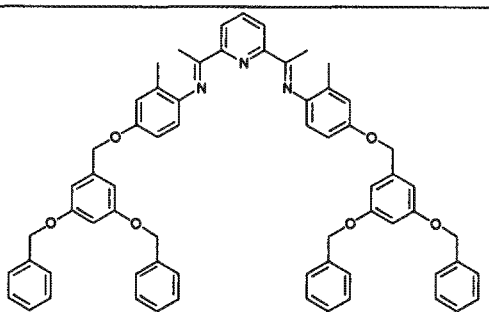
38	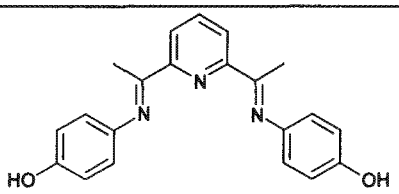	44	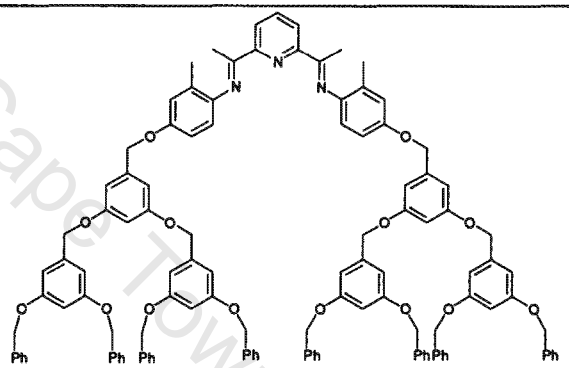
39	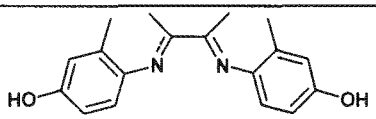	45	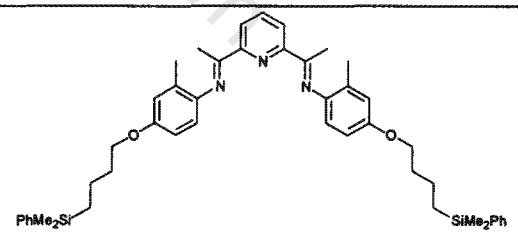
40	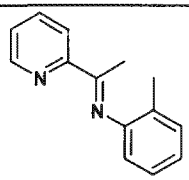	46	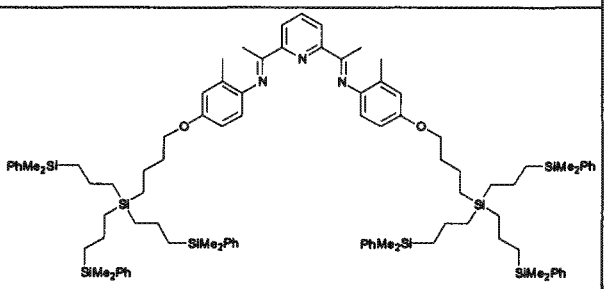

47	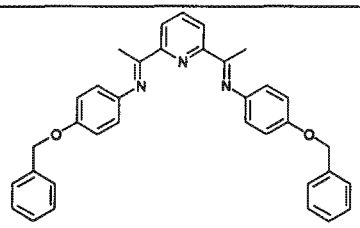	53	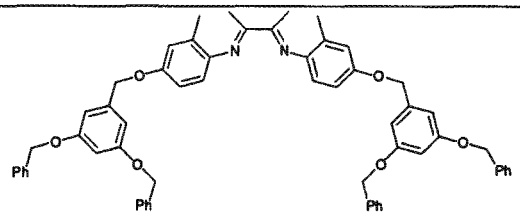
48	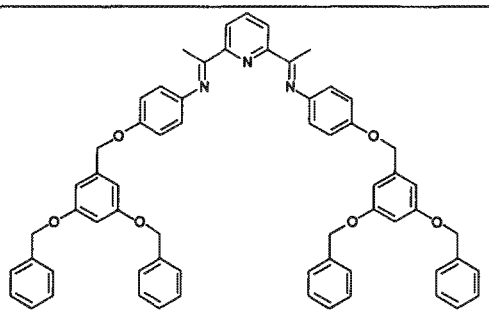	54	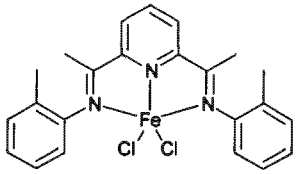
49	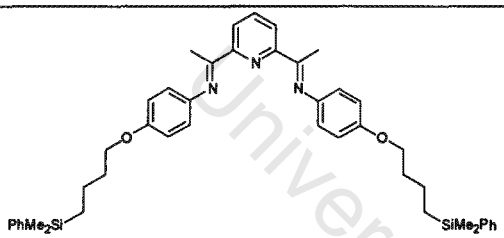	55	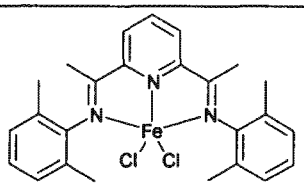
50	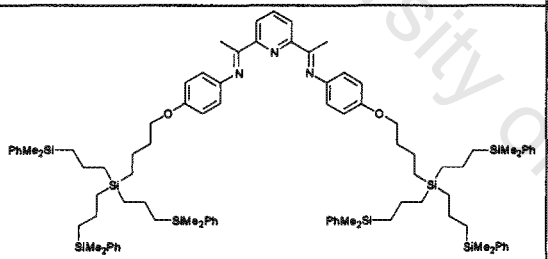	56	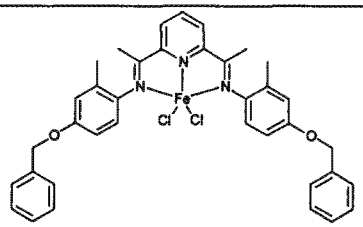
51	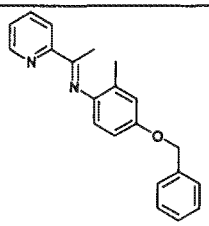	57	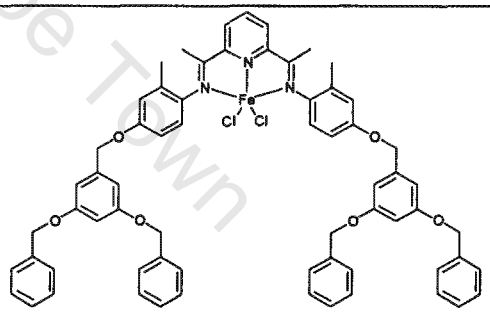
52	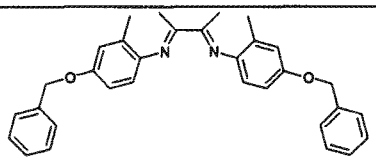	58	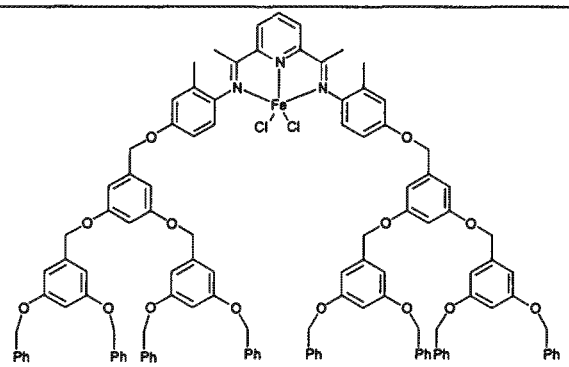

59	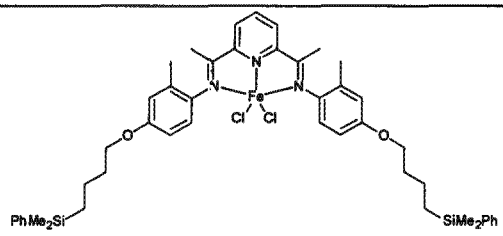	64	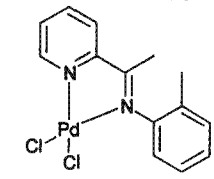
60	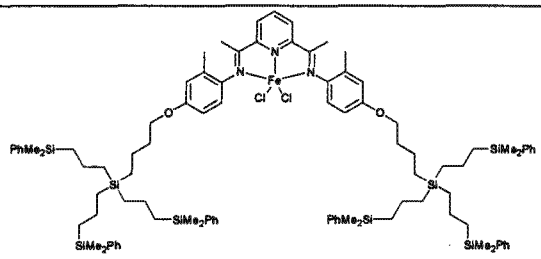	65	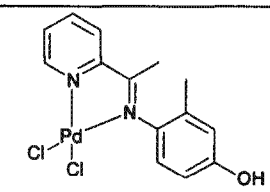
61	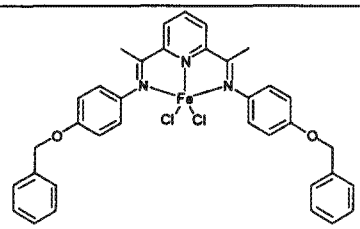	66	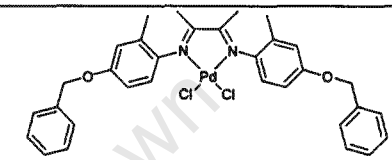
62	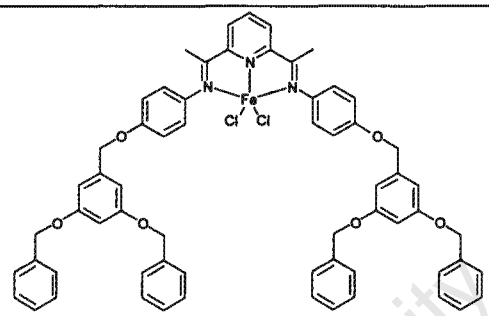	67	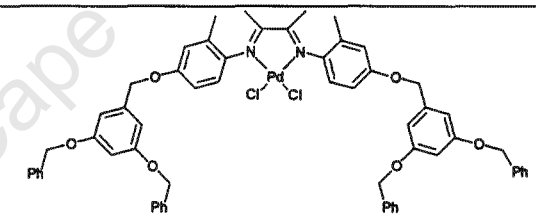
63	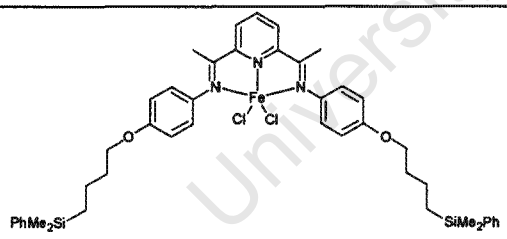		

Chapter 5

68	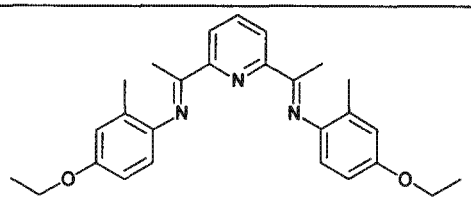	72	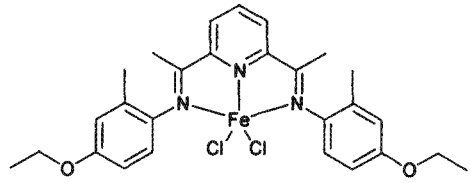
69	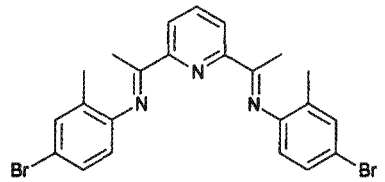	73	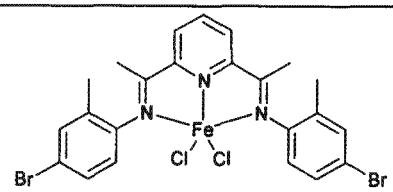
70	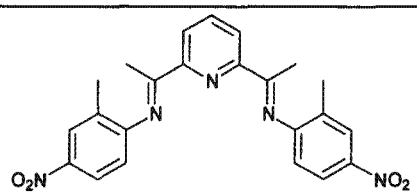	74	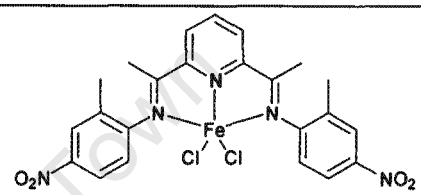
71	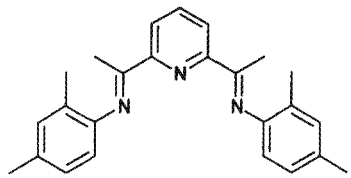	75	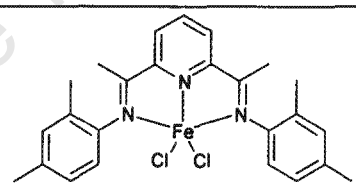

Chapter 7

76	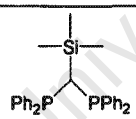	80	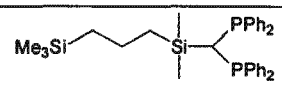
77	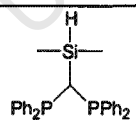	81	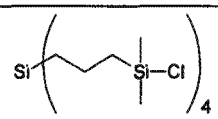
78	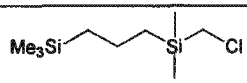	82	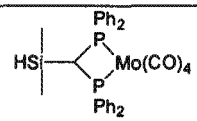
79	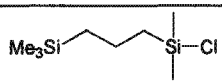	83	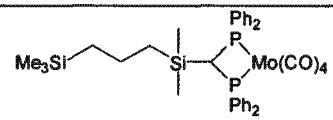

Appendix B: Data for X-ray crystal structure of compound 8

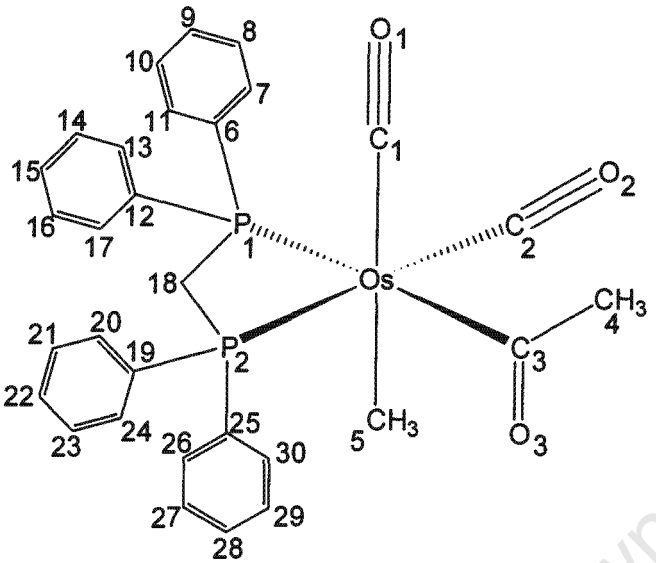

Numbering scheme for **8**

Table 1. Crystal data and structure refinement for **8**.

Identification code	c:\struct~1\mtd193\final\c2c	
Empirical formula	C30 H28 O3 Os P2	
Formula weight	688.66	
Temperature	298(2) K	
Wavelength	0.71070 A	
Crystal system, space group	Monoclinic, C2/c	
Unit cell dimensions	a = 20.0449(2) A	alpha = 90 deg.
	b = 12.03100(10) A	beta = 110.35 deg.
	c = 25.3155(2) A	gamma = 90 deg.
Volume	5724.01(9) A^3	
Z, Calculated density	8, 1.598 Mg/m^3	
Absorption coefficient	4.595 mm^-1	
F(000)	2704	
Crystal size	0.10 x 0.06 x 0.04 mm	
Theta range for data collection	3.55 to 27.87 deg.	
Limiting indices	-26<=h<=26, -15<=k<=15, -33<=l<=33	
Reflections collected / unique	69954 / 6810 [R(int) = 0.0528]	
Completeness to theta = 27.87	99.6 %	
Max. and min. transmission	0.8375 and 0.6565	

Refinement method	Full-matrix least-squares on F^2
Data / restraints / parameters	6810 / 0 / 327
Goodness-of-fit on F^2	1.186
Final R indices [I>2sigma(I)]	R1 = 0.0397, wR2 = 0.1185
R indices (all data)	R1 = 0.0843, wR2 = 0.1974
Largest diff. peak and hole	1.513 and -2.636 e.A^-3

Table 2. Atomic coordinates (x 10^4) and equivalent isotropic displacement parameters (A^2 x 10^3) for **8**. U(eq) is defined as one third of the trace of the orthogonalized U^{ij} tensor.

	x	y	z	U(eq)
Os(1)	5855(1)	7499(1)	6350(1)	35(1)
P(1)	6248(1)	9336(1)	6214(1)	32(1)
P(2)	6980(1)	7907(2)	7079(1)	35(1)
C(3)	5720(4)	5966(6)	6710(3)	52(2)
C(6)	5701(3)	10562(5)	6135(3)	35(1)
C(19)	7800(4)	7378(5)	7015(3)	39(2)
C(18)	6945(3)	9412(5)	6915(2)	38(2)
C(1)	6224(4)	6700(6)	5867(3)	50(2)
C(12)	6715(3)	9557(5)	5719(2)	35(1)
C(25)	7152(4)	7797(6)	7831(3)	39(2)
C(5)	5368(4)	8327(6)	6918(3)	55(2)
C(10)	5535(6)	12477(5)	6328(5)	60(3)
C(21)	9025(6)	7592(8)	7053(6)	69(3)
C(15)	7397(4)	9814(9)	4938(3)	62(3)
C(30)	6819(5)	7074(9)	8061(4)	67(2)
C(17)	7238(4)	8829(6)	5703(3)	47(2)
C(9)	4847(6)	12458(5)	5924(5)	58(3)
C(13)	6540(4)	10418(6)	5335(3)	44(2)
C(29)	6988(6)	7011(10)	8650(4)	80(3)
C(20)	8417(4)	8012(7)	7120(3)	52(2)
C(7)	5006(4)	10553(6)	5736(3)	49(2)
C(14)	6882(4)	10536(6)	4930(3)	55(2)
C(23)	8437(4)	5838(7)	6806(3)	59(2)
C(24)	7816(4)	6289(5)	6857(3)	46(2)
C(28)	7483(7)	7704(9)	8996(4)	73(3)
C(27)	7849(5)	8437(7)	8786(3)	67(2)

C(11)	5956(4)	11536(5)	6437(3)	47(2)
C(16)	7589(4)	8970(7)	5327(3)	62(2)
C(26)	7678(4)	8482(6)	8199(3)	51(2)
C(8)	4591(4)	11497(6)	5624(3)	61(2)
C(22)	9031(4)	6500(8)	6910(3)	63(2)
O(1)	6388(4)	6207(6)	5546(3)	88(2)
C(2)	4921(6)	7488(5)	5787(5)	57(3)
O(2)	4383(5)	7480(4)	5473(5)	90(3)
O(3)	6201(3)	5380(4)	6973(3)	76(2)
C(4)	4975(5)	5578(8)	6661(5)	101(4)

Table 3. Bond lengths [A] and angles [deg] for **8**.

Os(1)-C(1)	1.895(7)
Os(1)-C(2)	1.918(11)
Os(1)-C(3)	2.116(7)
Os(1)-C(5)	2.235(7)
Os(1)-P(1)	2.4111(16)
Os(1)-P(2)	2.4160(18)
P(1)-C(6)	1.808(6)
P(1)-C(12)	1.825(6)
P(1)-C(18)	1.839(6)
P(2)-C(25)	1.817(7)
P(2)-C(19)	1.821(8)
P(2)-C(18)	1.854(6)
C(3)-O(3)	1.193(8)
C(3)-C(4)	1.527(11)
C(6)-C(11)	1.395(9)
C(6)-C(7)	1.408(9)
C(19)-C(24)	1.373(9)
C(19)-C(20)	1.397(11)
C(1)-O(1)	1.143(8)
C(12)-C(17)	1.377(9)
C(12)-C(13)	1.380(9)
C(25)-C(30)	1.347(12)
C(25)-C(26)	1.406(10)
C(10)-C(11)	1.382(10)

C(10)-C(9)	1.402(16)
C(21)-C(22)	1.364(11)
C(21)-C(20)	1.383(14)
C(15)-C(14)	1.342(11)
C(15)-C(16)	1.372(12)
C(30)-C(29)	1.411(12)
C(17)-C(16)	1.377(10)
C(9)-C(8)	1.381(10)
C(13)-C(14)	1.425(9)
C(29)-C(28)	1.358(17)
C(7)-C(8)	1.378(9)
C(23)-C(22)	1.381(11)
C(23)-C(24)	1.404(10)
C(28)-C(27)	1.367(14)
C(27)-C(26)	1.406(10)
C(2)-O(2)	1.096(13)

C(1)-Os(1)-C(2)	90.9(4)
C(1)-Os(1)-C(3)	88.4(3)
C(2)-Os(1)-C(3)	94.3(3)
C(1)-Os(1)-C(5)	175.6(3)
C(2)-Os(1)-C(5)	87.1(4)
C(3)-Os(1)-C(5)	87.8(3)
C(1)-Os(1)-P(1)	98.8(2)
C(2)-Os(1)-P(1)	100.6(2)
C(3)-Os(1)-P(1)	163.3(2)
C(5)-Os(1)-P(1)	85.5(2)
C(1)-Os(1)-P(2)	97.2(2)
C(2)-Os(1)-P(2)	168.3(2)
C(3)-Os(1)-P(2)	94.2(2)
C(5)-Os(1)-P(2)	85.3(2)
P(1)-Os(1)-P(2)	70.01(6)
C(6)-P(1)-C(12)	104.0(3)
C(6)-P(1)-C(18)	107.1(3)
C(12)-P(1)-C(18)	104.9(3)
C(6)-P(1)-Os(1)	123.2(2)
C(12)-P(1)-Os(1)	120.2(2)
C(18)-P(1)-Os(1)	94.8(2)

C(25)-P(2)-C(19)	102.7(4)
C(25)-P(2)-C(18)	106.5(3)
C(19)-P(2)-C(18)	106.7(3)
C(25)-P(2)-Os(1)	124.9(3)
C(19)-P(2)-Os(1)	119.5(3)
C(18)-P(2)-Os(1)	94.3(2)
O(3)-C(3)-C(4)	116.3(7)
O(3)-C(3)-Os(1)	123.7(6)
C(4)-C(3)-Os(1)	120.0(6)
C(11)-C(6)-C(7)	118.8(6)
C(11)-C(6)-P(1)	122.2(5)
C(7)-C(6)-P(1)	119.0(5)
C(24)-C(19)-C(20)	117.9(7)
C(24)-C(19)-P(2)	118.2(6)
C(20)-C(19)-P(2)	124.0(5)
P(1)-C(18)-P(2)	97.2(3)
O(1)-C(1)-Os(1)	174.3(7)
C(17)-C(12)-C(13)	117.8(6)
C(17)-C(12)-P(1)	120.3(5)
C(13)-C(12)-P(1)	121.9(5)
C(30)-C(25)-C(26)	117.5(7)
C(30)-C(25)-P(2)	124.0(7)
C(26)-C(25)-P(2)	118.5(6)
C(11)-C(10)-C(9)	120.7(7)
C(22)-C(21)-C(20)	118.3(10)
C(14)-C(15)-C(16)	120.8(7)
C(25)-C(30)-C(29)	121.3(9)
C(12)-C(17)-C(16)	121.2(7)
C(8)-C(9)-C(10)	119.8(7)
C(12)-C(13)-C(14)	120.9(7)
C(28)-C(29)-C(30)	120.2(10)
C(21)-C(20)-C(19)	122.5(8)
C(8)-C(7)-C(6)	121.2(6)
C(15)-C(14)-C(13)	118.9(7)
C(22)-C(23)-C(24)	119.5(7)
C(19)-C(24)-C(23)	120.5(7)
C(29)-C(28)-C(27)	121.0(9)
C(28)-C(27)-C(26)	118.0(9)

C(10)-C(11)-C(6)	119.8(7)
C(15)-C(16)-C(17)	120.3(7)
C(25)-C(26)-C(27)	122.0(8)
C(7)-C(8)-C(9)	119.7(7)
C(21)-C(22)-C(23)	121.3(9)
O(2)-C(2)-Os(1)	178.9(13)

Table 4. Anisotropic displacement parameters (A^2 x 10^3) for **8**. The anisotropic displacement factor exponent takes the form: -2 pi^2 [h^2 a*^2 U11 + ... + 2 h k a* b* U12]

	U11	U22	U33	U23	U13	U12
Os(1)	34(1)	30(1)	44(1)	0(1)	18(1)	2(1)
P(1)	34(1)	31(1)	33(1)	2(1)	14(1)	2(1)
P(2)	36(1)	34(1)	36(1)	4(1)	14(1)	3(1)
C(3)	55(5)	36(4)	72(5)	4(4)	29(4)	3(4)
C(6)	41(4)	31(3)	40(3)	-2(3)	22(3)	-1(3)
C(19)	37(4)	45(5)	37(4)	3(3)	15(3)	2(3)
C(18)	38(4)	39(4)	36(3)	2(3)	10(3)	1(3)
C(1)	51(4)	47(4)	52(4)	-7(4)	19(4)	8(3)
C(12)	37(4)	38(4)	30(3)	3(3)	12(3)	2(3)
C(25)	46(4)	36(3)	38(4)	9(3)	18(3)	7(3)
C(5)	59(5)	49(4)	72(5)	4(4)	39(4)	11(4)
C(10)	56(7)	33(5)	80(8)	-18(3)	10(5)	1(3)
C(21)	44(6)	82(8)	83(8)	-1(5)	23(6)	-2(4)
C(15)	74(6)	62(6)	73(6)	7(4)	55(5)	11(4)
C(30)	75(6)	77(6)	57(5)	7(5)	33(5)	-9(5)
C(17)	51(4)	50(4)	49(4)	12(3)	27(3)	13(3)
C(9)	51(5)	45(5)	75(7)	-2(3)	17(5)	15(3)
C(13)	46(4)	46(4)	43(4)	0(3)	17(3)	-3(3)
C(29)	101(8)	95(8)	59(6)	35(6)	46(6)	16(7)
C(20)	40(4)	47(5)	64(5)	-9(4)	12(4)	-2(4)
C(7)	46(4)	38(4)	53(4)	-8(3)	5(3)	7(3)
C(14)	72(5)	55(5)	49(4)	10(3)	35(4)	-7(4)
C(23)	60(5)	53(5)	71(5)	4(4)	32(4)	15(4)
C(24)	44(4)	37(4)	60(4)	10(3)	21(3)	3(3)
C(28)	94(9)	90(7)	37(5)	14(5)	26(5)	41(7)
C(27)	96(7)	56(5)	49(5)	2(4)	24(5)	22(5)

C(11)	43(4)	31(4)	59(4)	-3(3)	8(3)	3(3)
C(16)	57(5)	66(5)	79(6)	15(4)	44(4)	23(4)
C(26)	64(5)	42(4)	50(4)	6(3)	23(4)	13(4)
C(8)	43(4)	55(5)	68(5)	-7(4)	-4(4)	12(4)
C(22)	39(4)	81(7)	74(6)	3(5)	27(4)	16(4)
O(1)	95(5)	94(5)	85(4)	-26(4)	43(4)	19(4)
C(2)	43(5)	47(6)	73(7)	5(3)	12(5)	0(3)
O(2)	59(6)	85(7)	96(8)	9(3)	-11(5)	3(3)
O(3)	77(4)	45(3)	111(5)	35(3)	39(4)	14(3)
C(4)	66(6)	60(6)	186(12)	31(6)	56(7)	-15(5)

Table 5. Hydrogen coordinates (x 10^4) and isotropic displacement parameters (A^2 x 10^3) for **8**

	x	y	z	U(eq)
H(18A)	6800	9854	7177	46
H(18B)	7392	9689	6899	46
H(5A)	4893	8558	6703	83
H(5B)	5647	8965	7091	83
H(5C)	5356	7815	7205	83
H(10)	5709	13129	6525	72
H(21)	9419	8043	7104	83
H(15)	7625	9887	4677	74
H(30)	6472	6606	7828	80
H(17)	7356	8231	5951	57
H(9)	4563	13091	5859	70
H(13)	6194	10929	5341	53
H(29)	6760	6493	8801	96
H(20)	8419	8743	7239	62
H(7)	4824	9899	5544	59
H(14)	6751	11103	4664	66
H(23)	8447	5098	6703	70
H(24)	7412	5848	6782	55
H(28)	7574	7680	9382	87
H(27)	8200	8893	9025	81

H(11)	6408	11552	6710	56
H(16)	7957	8492	5337	74
H(26)	7920	8980	8050	61
H(8)	4140	11486	5348	74
H(22)	9444	6196	6882	75
H(4A)	4719	5355	6280	151
H(4B)	4727	6175	6763	151
H(4C)	5012	4959	6909	151

Table 6. Torsion angles [deg] for **8**.

C(1)-Os(1)-P(1)-C(6)	138.2(3)
C(2)-Os(1)-P(1)-C(6)	45.6(4)
C(3)-Os(1)-P(1)-C(6)	-107.0(8)
C(5)-Os(1)-P(1)-C(6)	-40.6(3)
P(2)-Os(1)-P(1)-C(6)	-127.2(3)
C(1)-Os(1)-P(1)-C(12)	2.6(3)
C(2)-Os(1)-P(1)-C(12)	-90.0(4)
C(3)-Os(1)-P(1)-C(12)	117.4(8)
C(5)-Os(1)-P(1)-C(12)	-176.2(3)
P(2)-Os(1)-P(1)-C(12)	97.2(2)
C(1)-Os(1)-P(1)-C(18)	-107.7(3)
C(2)-Os(1)-P(1)-C(18)	159.7(4)
C(3)-Os(1)-P(1)-C(18)	7.1(8)
C(5)-Os(1)-P(1)-C(18)	73.5(3)
P(2)-Os(1)-P(1)-C(18)	-13.1(2)
C(1)-Os(1)-P(2)-C(25)	-136.7(4)
C(2)-Os(1)-P(2)-C(25)	89.2(18)
C(3)-Os(1)-P(2)-C(25)	-47.7(4)
C(5)-Os(1)-P(2)-C(25)	39.7(4)
P(1)-Os(1)-P(2)-C(25)	126.6(3)
C(1)-Os(1)-P(2)-C(19)	-2.1(3)
C(2)-Os(1)-P(2)-C(19)	-136.3(18)
C(3)-Os(1)-P(2)-C(19)	86.9(3)
C(5)-Os(1)-P(2)-C(19)	174.3(3)
P(1)-Os(1)-P(2)-C(19)	-98.9(3)
C(1)-Os(1)-P(2)-C(18)	109.8(3)

C(2)-Os(1)-P(2)-C(18)	-24.4(18)
C(3)-Os(1)-P(2)-C(18)	-161.2(3)
C(5)-Os(1)-P(2)-C(18)	-73.8(3)
P(1)-Os(1)-P(2)-C(18)	13.0(2)
C(1)-Os(1)-C(3)-O(3)	65.5(7)
C(2)-Os(1)-C(3)-O(3)	156.3(8)
C(5)-Os(1)-C(3)-O(3)	-116.8(7)
P(1)-Os(1)-C(3)-O(3)	-50.7(12)
P(2)-Os(1)-C(3)-O(3)	-31.7(7)
C(1)-Os(1)-C(3)-C(4)	-117.1(8)
C(2)-Os(1)-C(3)-C(4)	-26.3(8)
C(5)-Os(1)-C(3)-C(4)	60.6(8)
P(1)-Os(1)-C(3)-C(4)	126.7(8)
P(2)-Os(1)-C(3)-C(4)	145.7(7)
C(12)-P(1)-C(6)-C(11)	-86.4(6)
C(18)-P(1)-C(6)-C(11)	24.3(6)
Os(1)-P(1)-C(6)-C(11)	132.2(5)
C(12)-P(1)-C(6)-C(7)	90.5(6)
C(18)-P(1)-C(6)-C(7)	-158.8(5)
Os(1)-P(1)-C(6)-C(7)	-51.0(6)
C(25)-P(2)-C(19)-C(24)	97.9(7)
C(18)-P(2)-C(19)-C(24)	-150.3(6)
Os(1)-P(2)-C(19)-C(24)	-45.3(7)
C(25)-P(2)-C(19)-C(20)	-81.9(7)
C(18)-P(2)-C(19)-C(20)	29.9(8)
Os(1)-P(2)-C(19)-C(20)	135.0(6)
C(6)-P(1)-C(18)-P(2)	143.3(3)
C(12)-P(1)-C(18)-P(2)	-106.7(3)
Os(1)-P(1)-C(18)-P(2)	16.3(3)
C(25)-P(2)-C(18)-P(1)	-144.6(3)
C(19)-P(2)-C(18)-P(1)	106.3(4)
Os(1)-P(2)-C(18)-P(1)	-16.3(3)
C(2)-Os(1)-C(1)-O(1)	-8(7)
C(3)-Os(1)-C(1)-O(1)	86(7)
C(5)-Os(1)-C(1)-O(1)	55(9)
P(1)-Os(1)-C(1)-O(1)	-109(7)
P(2)-Os(1)-C(1)-O(1)	180(100)
C(6)-P(1)-C(12)-C(17)	173.6(5)

C(18)-P(1)-C(12)-C(17)	61.4(6)
Os(1)-P(1)-C(12)-C(17)	-43.4(6)
C(6)-P(1)-C(12)-C(13)	-9.1(6)
C(18)-P(1)-C(12)-C(13)	-121.4(6)
Os(1)-P(1)-C(12)-C(13)	133.8(5)
C(19)-P(2)-C(25)-C(30)	-110.9(8)
C(18)-P(2)-C(25)-C(30)	137.2(8)
Os(1)-P(2)-C(25)-C(30)	29.7(9)
C(19)-P(2)-C(25)-C(26)	67.2(6)
C(18)-P(2)-C(25)-C(26)	-44.7(6)
Os(1)-P(2)-C(25)-C(26)	-152.3(5)
C(26)-C(25)-C(30)-C(29)	0.5(14)
P(2)-C(25)-C(30)-C(29)	178.5(7)
C(13)-C(12)-C(17)-C(16)	1.6(11)
P(1)-C(12)-C(17)-C(16)	179.0(6)
C(11)-C(10)-C(9)-C(8)	-1.2(19)
C(17)-C(12)-C(13)-C(14)	1.1(10)
P(1)-C(12)-C(13)-C(14)	-176.2(5)
C(25)-C(30)-C(29)-C(28)	1.5(17)
C(22)-C(21)-C(20)-C(19)	-3.8(16)
C(24)-C(19)-C(20)-C(21)	2.0(13)
P(2)-C(19)-C(20)-C(21)	-178.2(8)
C(11)-C(6)-C(7)-C(8)	2.7(11)
P(1)-C(6)-C(7)-C(8)	-174.2(6)
C(16)-C(15)-C(14)-C(13)	0.4(14)
C(12)-C(13)-C(14)-C(15)	-2.2(11)
C(20)-C(19)-C(24)-C(23)	0.3(11)
P(2)-C(19)-C(24)-C(23)	-179.5(6)
C(22)-C(23)-C(24)-C(19)	-0.8(11)
C(30)-C(29)-C(28)-C(27)	-3.0(17)
C(29)-C(28)-C(27)-C(26)	2.4(15)
C(9)-C(10)-C(11)-C(6)	1.3(17)
C(7)-C(6)-C(11)-C(10)	-2.0(12)
P(1)-C(6)-C(11)-C(10)	174.9(8)
C(14)-C(15)-C(16)-C(17)	2.3(15)
C(12)-C(17)-C(16)-C(15)	-3.4(13)
C(30)-C(25)-C(26)-C(27)	-1.0(12)
P(2)-C(25)-C(26)-C(27)	-179.2(6)

C(28)-C(27)-C(26)-C(25)	-0.4(12)
C(6)-C(7)-C(8)-C(9)	-2.7(13)
C(10)-C(9)-C(8)-C(7)	1.9(16)
C(20)-C(21)-C(22)-C(23)	3.2(16)
C(24)-C(23)-C(22)-C(21)	-1.0(13)
C(1)-Os(1)-C(2)-O(2)	144(32)
C(3)-Os(1)-C(2)-O(2)	56(32)
C(5)-Os(1)-C(2)-O(2)	-32(32)
P(1)-Os(1)-C(2)-O(2)	-117(32)
P(2)-Os(1)-C(2)-O(2)	-81(32)

Appendix C: TRUE BASIC program for calculating α and yield for ethene oligomerisation reactions

This programme is specific for the catalytic conditions and work-up described in sections 6.1 and 6.2. It assumes i) all 1-alkene response factors are the same, i.e. 1, ii) toluene response factor is 0.9[217], iii) catalyst loading is 20μmol, iv) 100mg undecene is added as internal standard.

```
Print "Input total involatile mass"
Input M
Print "Input C10 integral, from worked-up reaction mixture in toluene"
Input C10
Print "Input C11 integral, from worked-up reaction mixture in toluene"
Input C11
Print "Input C12 integral, from worked up reaction mixture in toluene"
Input C12
Print "Input C14 integral, from worked-up reaction mixture in toluene"
Input C14
Print "Input C16 integral (as above)"
Input C16
Print "Input C18 integral (as above)"
Input C18
Print "Input C20 integral (as above)"
Input C20
Print "Input C22 integral (as above)"
Input C22
Print "Input toluene integral, from hexane sample"
Input tol
Print "Input C10 integral from hexane sample"
Input C10hex
Print "Input C11 integral from hexane sample"
Input C11hex
Print "Input C12 integral from hexane sample"
Input C12hex
Print "Input C14 integral from hexane sample"
Input C14hex
let A1012 = C12 / C10 * 140 / 168
let A1214 = C14 / C12 * 168 / 196
let A1416 = C16 / C14 * 196 / 224
let A1618 = C18 / C16 * 224 / 252
let A1820 = C20 / C18 * 252 / 280
let A2022 = C22 / C20 * 280 / 308
Print "Alpha values"; A1012; A1214; A1416; A1618; A1820; A2022
let aav = (A1012 * A1214 * A1416 * A1618 * A1820)^(1/5)
Print "Average alpha value, C10 to C20"; aav
let NC14 = C14 / C11 * 154 / 196 * 0.000649
let NC12 = C12 / C11 * 154 / 168 * 0.000649
let NC10 = C10 / C11 * 154 / 140 * 0.000649
let NC8 = NC10 / aav
let NC6 = NC8 / aav
let NC4 = NC6 / aav
let NC10hex = C10hex / C14hex * 196 / 140 * NC14
let NC10diff = NC10 - NC10hex
let NC11hex = C11hex / C14hex * 196 / 154 * NC14
let NC12hex = C12hex / C14hex * 196 / 168 * NC14
let NC12diff = NC12 - NC12hex
let mvololig = NC4 * 56 + NC6 * 84 + NC8 * 112 + NC10diff * 140 + NC12diff *
168
```

```
let ntol = tol / 0.9 / C14hex * 196 / 92 * NC14
let mtol = ntol * 92
let mC11 = NC11hex * 154
let yield = M + mvololig - mtol - mC11
Print "mass involatiles:"; M; "g"
Print "mass volatile oligomers:"; mvololig; "g"
Print "mass toluene"; mtol; "g"
Print "mass C11"; MC11; "g"
Print "total calculated mass"; yield; "g"
End
```